THE UNIVERSITY OF QUEENSLAND

AUSTRALIA

The role of *Nfix* in the development of the embryonic and postnatal cerebral cortex

Yee Hsieh Evelyn Heng

Bachelor of Science (First Class Honours)

A thesis submitted for the degree of Doctor of Philosophy at

The University of Queensland in 2014

School of Biomedical Science

Abstract

Neurogenesis is an intricate process that is essential for the proper formation of the central nervous system (CNS) during development, which continues into postnatal ages and throughout adulthood within two restricted regions of the rodent brain: the subgranular zone (SGZ) of the hippocampal dentate gyrus and the subventricular zone (SVZ) lining the lateral ventricles. This process relies on a series of events, including progenitor cell proliferation and differentiation, and the subsequent migration of newborn neurons to their ultimate destination within the brain. These events are tightly orchestrated by multiple different transcription factors in a spatially and temporally specific manner. Alteration in any of these events can lead to cognitive, motor and intellectual disabilities, which is why it is critically important to understand how neural progenitor cell proliferation and differentiation is regulated.

This thesis focuses on the role of Nuclear factor one X (NFIX) in regulating neural progenitor cell biology within the developing and postnatal SGZ and SVZ. NFIX belongs to a group of site-specific transcription factors known as the Nuclear factor one (NFI) family. Previous studies have shown that NFI proteins play multiple roles during development of the CNS, including axon guidance, neuronal migration, progenitor cell differentiation, gliogenesis and neurogenesis (Shu T et al. 2003; Steele-Perkins G et al. 2005; Deneen B et al. 2006; Barry G et al. 2008; Piper M et al. 2011; Heng YH et al. 2012). However, much of the focus on this family with relation to neural development has been centred on NFIA and NFIB, as knockout mice for these genes were generated first (das Neves L et al. 1999; Grunder A et al. 2002). However, both *Nfia*$^{-/-}$ and *Nfib*$^{-/-}$ mice die in the early perinatal period, which precludes the use of these mice as models to investigate genesis of the postnatal and adult brain neurogenic niches.

Although the role of NFIX in cortical development has been less intensively investigated, *Nfix*$^{-/-}$ mice survive postnatally (Campbell CE et al. 2008), making this strain a valuable model in which to investigate the transcriptional control of stem cell biology within the SVZ and SGZ. Preliminary data has revealed that NFIX is expressed by neural progenitor cells within the CNS, and that mice lacking this gene possess abnormal phenotypes within the hippocampus and the SVZ postnatally (Campbell CE et al. 2008). However, these preliminary findings did not investigate the cellular or molecular mechanisms by which NFIX exert its effects. As such, the goal of this thesis was to expand these findings, and to elucidate the role of NFIX during the development of the hippocampus and the SVZ, and, moreover, to identify the downstream targets via which this transcription factor regulates progenitor cell proliferation and differentiation within these regions.

The first component of this thesis involved investigating of the role of NFIX in the embryonic and postnatal hippocampus. Here, I analysed the expression pattern of NFIX within the hippocampus, and found that neural progenitor cells within the hippocampus ventricular zone expressed this transcription factor. Furthermore, the absence of *Nfix* was shown to result in delays in the differentiation of neural progenitor cells, indicating that NFIX plays an important role in promoting their differentiation. The differentiation of neural stem cells in *Nfix*-deficient mice did eventually occur, albeit 2-3 days later than in wild-type controls, suggestive of other factors ultimately promoting neural stem cell differentiation in these knockout mice, perhaps other NFI family members. I also revealed that postnatal *Nfix*$^{-/-}$ mice display abnormal hippocampal morphology, including a reduction in the number of neural progenitor cells within the subgranular zone. Mechanistically, we demonstrated that the cortical progenitor cell maintenance factor *Sry-related HMG box 9 (Sox9)* was significantly upregulated in the hippocampus of the mutant mice, and that NFIX was able to repress *Sox9* promoter-driven transcriptional activity *in vitro*. This work, published in *Cerebral Cortex* (Heng YH et al. 2014) is indicative of the critical role of NFIX in mediating stem cell biology. This is also supported by two recent manuscripts, where I contributed data to help reveal that

NFIX regulates stem cell differentiation within the nascent cerebellum (Piper M et al. 2011), and that, at a functional level, *Nfix* is involved in hippocampal-dependent learning and memory (Harris L et al. 2013).

Furthermore, this thesis also focussed on the role of NFIX in the olfactory system, including the olfactory bulb, rostral migratory stream (RMS) and the SVZ during development, postnatally and within the adult. Firstly, I extensively mapped the expression of NFIX within these areas at a cell-type specific level using confocal microscopy. These data have revealed that NFIX is expressed by neural stem cells, transit amplifying cells and neuroblasts within the SVZ, as well as by periglomerular neurons within the olfactory bulb. These expression patterns suggest that NFIX might play a role in regulating neurogenesis within the SVZ, a hypothesis I was able to support by demonstrating that *Nfix*$^{-/-}$ mice display multiple abnormalities within this neurogenic niche. These included a significant increase in the number of PAX6-expressing progenitor cells within the SVZ, as well as an increased level of proliferation within the SVZ, as assayed both *in vivo* and *in vitro*. In addition, the migration of SVZ-derived neuroblasts to the olfactory bulb was impaired in mutant mice, suggesting that NFIX regulates this process *in vivo*. These findings were recently published in the prestigious international journal *Cerebral Cortex* (Heng YHE et al, 2014). Collectively, this work highlights the important role played by NFIX in the biology of the SVZ, and reveals that NFIX mediates multiple processes within this region of the brain.

In conclusion, the expression, cellular and molecular data presented in this thesis highlights NFIX as a key regulator of multiple key processes including driving progenitor cell proliferation, mediating migration and promoting differentiation in the embryonic and postnatal brain. Future work will need to focus on the neurogenic niches of the adult brain, to investigate how the NFI family regulates stem cell biology in the mature brain.

Declaration by author

This thesis is composed of my original work, and contains no material previously published or written by another person except where due reference has been made in the text. I have clearly stated the contribution by others to jointly-authored works that I have included in my thesis.

I have clearly stated the contribution of others to my thesis as a whole, including statistical assistance, survey design, data analysis, significant technical procedures, professional editorial advice, and any other original research work used or reported in my thesis. The content of my thesis is the result of work I have carried out since the commencement of my research higher degree candidature and does not include a substantial part of work that has been submitted to qualify for the award of any other degree or diploma in any university or other tertiary institution. I have clearly stated which parts of my thesis, if any, have been submitted to qualify for another award.

I acknowledge that an electronic copy of my thesis must be lodged with the University Library and, subject to the General Award Rules of The University of Queensland, immediately made available for research and study in accordance with the *Copyright Act 1968*.

I acknowledge that copyright of all material contained in my thesis resides with the copyright holder(s) of that material. Where appropriate I have obtained copyright permission from the copyright holder to reproduce material in this thesis.

Publication during candidature

Research Publication

1. **Heng YH,** Barry G, Richards LJ, Piper M. (2012). "Nuclear Factor I Genes regulate neuronal migration." NeuroSignals **20**:159-167

2. **Heng YH**, McLeay RC, Harvey TJ, Smith AG, Barry G, Cato K, Plachez C, little E, Mason S, Dixon C, Gronostajski RM, Bailey TL, Richards LJ, Piper M. "NFIX regulates neural progenitor cell differentiation during hippocampal morphogenesis." (2014) Cerebral Cortex **24**:261-279

3. Plachez C, Cato K, McLeay RC, **Heng YH**, Bailey TL, Gronostasjki RM, Richards LJ, Puche AC, Piper M. (2012). " Expression of nuclear Factor One Gene A and -B in the Olfactory Bulb." J Comp Neurol **520**:3135-3149

4. Piper M, Harris L, Barry G, **Heng YH**, Plachez C, Grnonstajski RM, Richards LJ. (2011). "Nuclear factor one X regulates the development of multiple cellular populations in the postnatal cerebellum." J Comp Neurol **519**: 3532-3548.

5. Harris L, Dixon C, Cato K, **Heng YHE**, Kurniawan ND, Ullmann, JFP, Janke AL, Gronostajski RM, Richards LJ, Burne THJ, Piper M (2013). "Heterozygosity for Nuclear factor one X affects hippocampal-dependent behaviour in mice." PLoS One, **8**: e65478.

6. **Heng YHE**, Zhou B, Harris L, Harvey T, Smith A, Martynoga B, Anderson J, Achimastou A, Cato K, Richards LJ, Gronostajski RM, Yeo GS, Guillemot F, Bailey TL, Piper M. "NFIX regulates proliferation and migration within the murine SVZ neurogenic niche." Cereb Cortex. 1-21; doi:10.1093/cercor/bhu253

Conference Abstract

***Poster**:* NFIX regulates the differentiation of neural progenitor cells through the repression of Sox9. **Yee Hsieh Evelyn Heng**, Guy Barry, Sharon Mason, Robert McLeay, Richard M. Gronostajski, Timothy L. Bailey, Linda J Richard and Michael Piper.
Brisbane Cell and Development Biology Meeting, University of Queensland, Australia (2011)

***Poster*:** NFIX regulates the differentiation of neural progenitor cells through the repression of Sox9. **Yee Hsieh Evelyn Heng**, Guy Barry, Sharon Mason, Robert McLeay, Richard M. Gronostajski, Timothy L. Bailey, Linda J Richard and Michael Piper.
Australian Neuroscience Society, Gold Coast, Australia (2012)

***Poster*:** NFIX regulate neurogenesis within the SVZ of the postnatal mouse brain. **Yee Hsieh Evelyn Heng**, Richard M. Gronostajski, Linda J Richard and Michael Piper.
Australian Neuroscience Society, Melbourne, Australia (2013)

***Poster*:** NFIX regulate neurogenesis within the SVZ of the postnatal mouse brain. **Yee Hsieh Evelyn Heng**, Richard M. Gronostajski, Linda J Richard and Michael Piper.
Brisbane Cell and Development Biology Meeting, University of Queensland, Australia (2013)

***Poster*:** NFIX regulates the differentiation of neural progenitor cells through the repression of Sox9. **Yee Hsieh Evelyn Heng**, Guy Barry, Sharon Mason, Robert McLeay, Richard M. Gronostajski, Timothy L. Bailey, Linda J Richard and Michael Piper.
Molecular and Cellular Neurobiology (Gordon Research Conference), Hong Kong (2014)

Publication included in this thesis

1. Chapter 3- **Heng YH**, McLeay RC, Harvey TJ, Smith AG, Barry G, Cato K, Plachez C, little E, Mason S, Dixon C, Gronostajski RM, Bailey TL, Richards LJ, Piper M. "NFIX regulates neural progenitor cell differentiation during hippocampal morphogenesis." (2014) Cerebral Cortex **24**(1):261-279

Contributor	**Statement of contribution**
Heng YH (Candidate)	Designed experiments (60%) Wrote the paper (65%) Edit paper (50%)
Piper M	Designed experiments (40%) Wrote paper (35%) Edit paper (30%)
Gronostajski RM	Edited paper (10%)
Richards LJ	Edited paper (10%)
Harvey TJ	qPCR and Luciferase assay were done in association with candidate in for Figure 3.11D and 3.11H
Smith AG	Electrophoretic mobility shift assay (EMSA) and supershift assays in Figure 3.11F
Bailey TL and McLeay RC	Identified Potential NFI binding sites in Figure 3.11E
Mason S	Contributed to Microarray data in table 3.1
Dixon C, little E, Barry G, Cato K and Plachez C	Contributed to experiments

2. Chapter 5- **Heng YHE**, Zhou B, Harris L, Harvey T, Smith A, Martynoga B, Anderson J, Achimastou A, Cato K, Richards LJ, Gronostajski RM, Yeo GS, Guillemot F, Bailey TL, Piper M. "NFIX regulates proliferation and migration within the murine SVZ neurogenic niche." Cereb Cortex. 1-21, doi:10.1093/cercor/bhu253

Contributor	**Statement of contribution**
Heng YHE (Candidate)	Designed experiments (60%) Wrote paper (65%) Edit paper (50%)

Piper M	Designed experiments (40%) Wrote Paper (35%) Edit paper (30%)
Gronostajski RM	Edited paper (10%)
Richards LJ	Edited paper (10%)
Harvey TJ	qPCR and Luciferase assay were done in association with candidate in for Figure 5.9G
Smith AG	Electrophoretic mobility shift assay (EMSA) and supershift assays in Figure 5.9E and F
Bailey TL and Piper M	Identified putative NFI binding sites within the promotes of genes misregulated in the SVZ of *Nfix*$^{-/-}$ mice in Table 5.3
Yeo GS	Ingenuity Pathway Analysis in Figure 5.9C
Harris L	Ki67 and DCX Immunofluorescence and cell counts of wild type and *Nfix*$^{-/-}$ mice presented in figure 5.8A-F

Contributions by others to the thesis

Chapter 3

- Microarray analysis of E16 *Nfix*$^{-/-}$ mice and wild type hippocampus were performed by Dr. Sharon Mason.
- DAVID analysis of functional classification of gene misregulated within the hippocampus of E16 was performed by Dr. Michael Piper.
- Potential NFI binding sites were identified by Dr. Timothy Bailey and Dr. Robert McLeay (IMB, University of Queensland).
- Electrophoretic mobility shift assay (EMSA) and supershift assays were conducted by Dr. Aaron Smith (SBMS, University of Queensland).
-qPCR and Luciferase assay were done in association Dr. Tracey Harvey (SBMS, University of Queensland).

Chapter 4

- The immunofluorescence analysis and confocal imaging were performed together with Dr. Kathleen Cato and Dr. Michael Piper (SBMS, University of Queensland).
- The immunofluorescence analysis and confocal imaging of Ki67 and DCX was performed by Mr Lachlan Harris (PhD student under the supervisor Dr. Michael Piper, SBMS, University of Queensland).
- Putative NFI binding sites within the promoters of genes central to SVZ progenitor and periglomerular interneuron function were identified by Dr. Michael Piper (SBMS, University of Queensland) and Dr. Timothy Bailey (IMB, University of Queensland).

Chapter 5

- Ki67 and DCX immunofluroscence and cell counts of wild type and *Nfix*$^{-/-}$ mice SVZ were performed by Mr Lachlan Harris (PhD student under the supervisor of Dr. Michael Piper, SBMS, University of Queensland).
- EMSA and supershift assays were conducted by Dr. Aaron Smith (SBMS, University of Queensland).
- Microarray analyses were performed by Dr. Michael Piper (SBMS, University of Queensland), and analysis using Ingenuity Pathway Analysis (IPA) was performed by Dr. Giles Yeo (CIMR, Cambridge, UK).
- Luciferase assays were conducted in association with Dr. Tracey Harvey (SBMS, University of Queensland).
- Putative NFI binding sites within the promoters of genes misregulated in the SVZ of *Nfix*$^{-/-}$ mice were identified by Dr. Michael Piper (SBMS, University of Queensland) and Dr. Timothy Bailey (IMB, University of Queensland).

Statements of parts of the thesis submitted to qualify for the award of another degree

None.

Acknowledgements

First and foremost, I would like to thank my principal supervisor Dr. Michael Piper for this opportunity to work under him, as well as for his wonderful guidance, generous support and encouragement. I am also grateful for the patience you had with me all this while. Thank you for always being so supportive where I can always come up to you and clear my doubts regarding my projects. Furthermore, no matter how busy you were, you will always try to help me out. You have taught me so many things, and provided me with the best training that transformed me from an international student who do not write or speak very well to an independent and confident researcher. I am very blessed to have you as my supervisor and mentor for the past few years. I would not have come so far without your guidance and support. THANK YOU SO MUCH.

This thesis would not have been possible without the support and scientific contribution from my co-supervisor Professor Linda Richards, and everyone from the Piper laboratory: Dr. Tracey Harvey, Lachlan Harris, Kathleen Cato, Diana Vidovic and Chantelle Reid. My gratitude also extends to people outside my lab: Kelvin Yin, Mitchell Fane and Swati Iyer. Thank you all so much for your friendship, support, guidance, intellectual discussions and all the lovely time we spent in and out of the lab. I thank all of you for making the lab such an interesting and happy environment that it feels like a second home to me. Thanks Lockie, for being such a good friend for picking and dropping me at the airport countless times. In addition, I would also like to express my gratitude to the financial support provided by the University of Queensland International scholarship during my candidature.

I would also like to thank my beloved family and friends who have supported me and encouraged me throughout this entire time. Thanks mum for always believing in me and loving me. You stood by me all this time and provided me with all you have. THANK YOU.

Alvin, my fiancé, thank you for always being there for me.

Lastly, but most importantly, I would like to thank God for leading me through every phase of my life and providing for my needs. Every challenge that you have provided me helped to mold me to who I am today.

Keywords

Neural Progenitor cells, proliferation, differentiation, development, postnatal neurogenesis, NFIX, NFI

Australia and New Zealand Standard Research Classification (ANZSRC)

060103 Cell development, Proliferation and death 100%

Field of Research (FoR) Classification

FoR code: 1109, Neuroscience, 100%

TABLE OF CONTENTS

LIST OF FIGURES AND TABLES

Chapter 1

Chapter 2

Chapter 3

Chapter 4

Chapter 5

LIST OF ABBREVIATION

Apcdd1: *Adenomaosis polysis coli down-regulated 1*
ANE: Ammonic neuroepithelium
BAC: Bacterial artificial chromosome
BP: Base pair
BrdU: Bromodeoxyuridine
BMP: Bone morphogenetic protein
BV: Blood vessel
ChIP-seq: Chromatin immunoprecipitation-sequencing
CA: *cornu ammonis*
CA1: *cornu ammonis 1*
CA2: *cornu ammonis 2*
CA3 *cornu ammonis 3*
CC3: Cleave caspase-3
CDK5: Cyclin dependent kinase 5
CNS: Central nervous system
CP: Cortical Plate
DAB: 3,3'-Diaminobenzidine
DCX: Doublecortin
E: Embryonic
EMSA: Electrophoretic mobility shift assay
EPL: External plexiform layer
EMX2: Empty spiracles homeobox 2
EGF: Epidermal growth factor
EGFR: Epidermal growth receptor
FGFR: Fibroblast growth factor receptor
FGF: Fibroblast growth factor
FGE: Fimbrial glioepithelium
FIMO: Find individual motif occurrence
GLAST: Astrocyte-specific glutamate/aspartate transporter
CGNs: Cerebellar granule neurons
GABAa: γ-aminobutyric acid type A
GABRA6: γ-aminobutyric acid type A receptor
GAD65: Glutamate decarboxylase 65
GAD67: Glutamic acid decarboxylase 67
GFP: Green fluorescent protein
GFAP: Glial fibrillary acidic protein
GL: Glomerular layer
GCL: Granule cell layer
Gapdh: Glyceraldehyde 3-phosphate dehydrogenase
GDNF: glial derived neurotrophic factor
Hsp90: heat shock protein
HES1: Hairy and enhancer of split-1
HES5: Hairy and enhancer of split-5
IML: Inner molecular layer
IF: Immunofluorescence
IHC: Immunohistochemistry
IPL: Internal plexiform layer
IZ: Intermediate zone
KO: Knockout
Lhx2: LIM homeobox gene
MZ: Marginal zone
mRNA seq: mRNA sequencing
MCL: Mitral cell layer

NFI: Nuclear Factor One
NFIA: Nuclear Factor One-A
NFIB: Nuclear Factor One-B
NFIC: Nuclear Factor One-C
NFIX: Nuclear Factor One-X
NSC: Neural stem cell
Ngn: Neurogenin
Ngn1: Neurogenin 1
Ngn2: Neurogenin 2
NCAM1: Neural cell adhesion molecule 1
NDEL1: Nude neurodevelopment protein 1-like 1
PROX1: Prospero-related homeobox 1
PAX6: Paired box gene 6
P: Postnatal
PDNE: Dentate neuroepithelium
PHH3: Phospho-histone H3
PFA: Paraformaldehyde
PCR: Polymerase chain reaction
PBS: Phosphate buffered saline
PSA-NCAM: Polysialylated-neural cell adhesion molecule
qPCR: Quantitative real-time PCR
RNA: Ribonucleic acid
RMS: Rostral migratory stream
SHH: Sonic hedgehog
SGZ: Subgranular zone
SVZ: Subventricular zone
SDM: Secondary dentate matrix
SOX: Sry-related HMG box
SOX2: Sry-related HMG box-2
SOX9: Sry-related HMG box-9
Tag1: Transient axonal glycoprotein-1
TSS: Transcription Start Site
TBR1: T-box, brain, 1
TBR2: T-box transcription factor Eomes
TDM: Tertiary dentate matrix
VZ: Ventricular Zone

CHAPTER 1

Literature review

1.0 Introduction: development of the subventricular zone and hippocampus

The CNS is one of the most complex and highly organised structures within the body, and comprises of four major differentiated cell types: neurons, astrocytes, oligodendrocytes and ependymal cells. All of these cells originally derive from a single layer of neuroepithelial cells that forms the neural plate within the early developing embryo at E7.5 in mice. As development continues, the lateral edge of the neural plate curls up and meets at the dorsal midline forming the neural tube, which contains a fluid filled center that later forms the ventricular system and spinal canal of the CNS. Within the neural tube, neuroepithelial cells span the inner ventricular surface to the pial surface of the neural tube. They divide and proliferate at the ventricular surface, forming a germinal area known as the ventricular zone (Waterston RH et al. 2002). Within the VZ, neuroepithelial cells initially divide symmetrically to expand the progenitor cell pool and subsequently begin to divide asymmetrically to generate daughter cells that migrate radially away from the VZ from E11 (Takahashi T et al. 1994; Chenn A and SK McConnell 1995).

At the most rostral end of the neural tube, two lateral vesicles are formed early in development. These vesicles ultimately give rise to the telencephalon, the dorsal regions of which produce the cerebral hemispheres. At the onset of neurogenesis (E11.5) within the developing cerebral hemispheres, neuroepithelial cells give rise to radial glia that reside in the VZ while maintaining contact with the pial surface via a radially projecting basal process (Huttner WB and M Brand 1997; Gotz M and WB Huttner 2005; Kriegstein A and A Alvarez-Buylla 2009). Radial glia largely divide asymmetrically in the VZ, producing one daughter cell that is a radial glial cell, and another fated to become a basal progenitor cell (also known as intermediate progenitor cell). Basal progenitors form a secondary germinal zone known as the SVZ, and, at least within rodents, these SVZ progenitors divide once symmetrically to produce two daughter cells that become neurons. As cortical development continues, the cell population within the SVZ expands, while the proliferative fraction of the VZ declines. By E16 within the mouse cortex, progenitor cells within the SVZ proliferate

actively, while the majority of the proliferative cells within the VZ begin to leave the cell cycle (Figure 1.1). By the early postnatal period, the cortical VZ becomes fully depleted and the majority of cells within the SVZ also differentiate.

After development, neurogenesis continues to occur postnatally and throughout adulthood within two discrete neurogenic niches, the SVZ lining the lateral ventricles and the SGZ of the hippocampus dentate gyrus. These two neurogenic niches harbor self-renewing multipotent neural stem cells, which give rise to differentiated neurons and glial cells. Within the SVZ, neural stem cells are derived from the neuroepithelial progenitor cells, the radial glia, from all parts of the telencephalic neuroepithelium, including the lateral ganglionic eminence, cortex and medial ganglionic eminence (Merkle FT et al. 2004; Young KM et al. 2007). Contrastingly, the pool of adult neural stem cells found within the SGZ are derived from the ventral hippocampus during development (Li G et al. 2013). Despite advances in our understanding of postnatal neurogenesis, little is known about the mechanisms that regulate the development of these neurogenic niches. This gap in knowledge formed the basis of the research performed during my candidature, where I aimed to elucidate the mechanisms that are involved in the development of these niches.

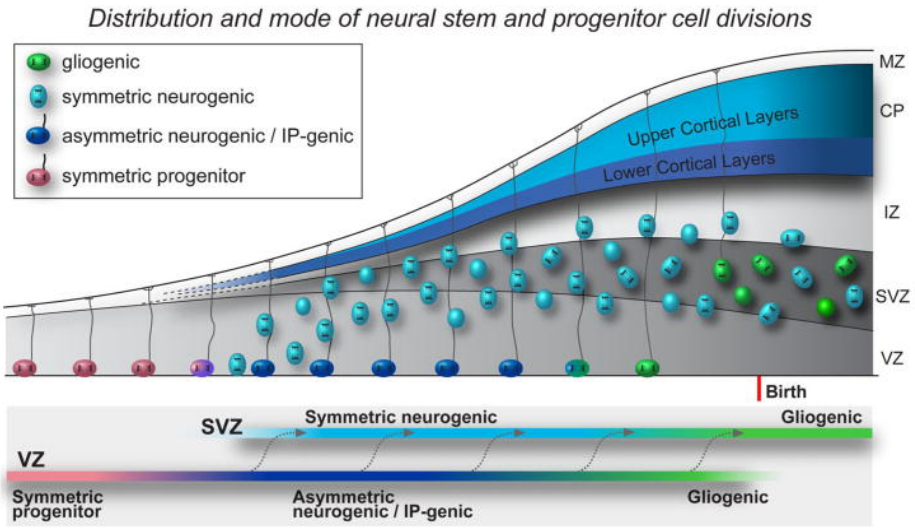

Figure 1.1. Neural progenitor cell differentiation within the embryonic cortex.

Radial glial cells within the VZ divide at the apical surface of the brain during development. Before neurogenesis begins, most radial glial cells divide symmetrically (red cells), expanding the VZ progenitor cell pool. Subsequently, at the onset of neurogenesis, radial glial cells begin to undergo asymmetric divisions (dark blue cells). These divisions give rise to one radial glial daughter cell and one intermediate progenitor cell. Intermediate progenitor cells (light blue cells) exit the apical VZ and form a second germinal niche above the VZ, known as the SVZ. Most intermediate progenitor cells divide asymmetrically and produce two daughter cells that give rise to the neurons of the cortical plate (Waterston RH et al. 2002). Towards the end of embryogenesis, progenitors within the VZ and SVZ begin to produce glia (green cells). IZ, intermediate zone; MZ, marginal zone. Image adapted from (Noctor SC et al. 2008).

1.1 Postnatal neurogenesis

As discussed above, the production of neurons within the cortex does not cease at birth, but rather neural progenitor cells continue to generate neurons during postnatal life and throughout adulthood in two specific regions of the rodent cerebral cortex: the SVZ lining the lateral ventricles and the SGZ of the hippocampal dentate gyrus (Alvarez-Buylla A and DA Lim 2004; Mu Y et al. 2010).

1.1.1 SVZ neurogenesis

In the postnatal rodent SVZ, proliferating radial glia like stem cells (called Type B cells; Figure. 1.2) stationed in the wall of the lateral ventricles give rise to transit amplifying progenitor cells (called Type C cells). These intermediate progenitor cells then give rise to neuroblasts (called Type A cells) that migrate tangentially along a long, relatively restricted pathway known as the rostral migratory stream (RMS) into the olfactory bulb (Hinds JW 1968; Bayer SA 1983). The RMS contains specialized surrounding glial cells that form a tube-like structure (glial tube), which acts as a scaffold for the migrating neuroblasts. Once the neuroblasts reach the center of the olfactory bulb, they migrate radially into the granular and periglomerular cell layers, where they differentiate into mature granule and periglomerular interneurons respectively (Ming GL and H Song 2005; Mu Y et al. 2010; Ming GL and H Song 2011). During migration along the RMS, migrating neuroblasts form long chain like structures and migrate closely to one another, using homophilic adhesion to facilitate this process. In rodents, neuroblasts first begin to form this chain like structure in the early postnatal period (Peretto P et al. 2005) and the RMS is structurally mature by P20 (Peretto P et al. 1997; Law AK et al. 1999; Peretto P et al. 1999). The process of adult neurogenesis within the SVZ is critical for odour discrimination and olfactory memory (Sakamoto M et al. 2011; Kageyama R et al. 2012), as well as innate olfactory behaviours (Sakamoto M et al. 2011). However, although our understanding of the molecules regulating SVZ neurogenesis has improved dramatically over the past decade, it is still unclear as to how the development of this neurogenesis niche is controlled, and our comprehension of the genes that regulate ongoing neurogenesis is far from complete.

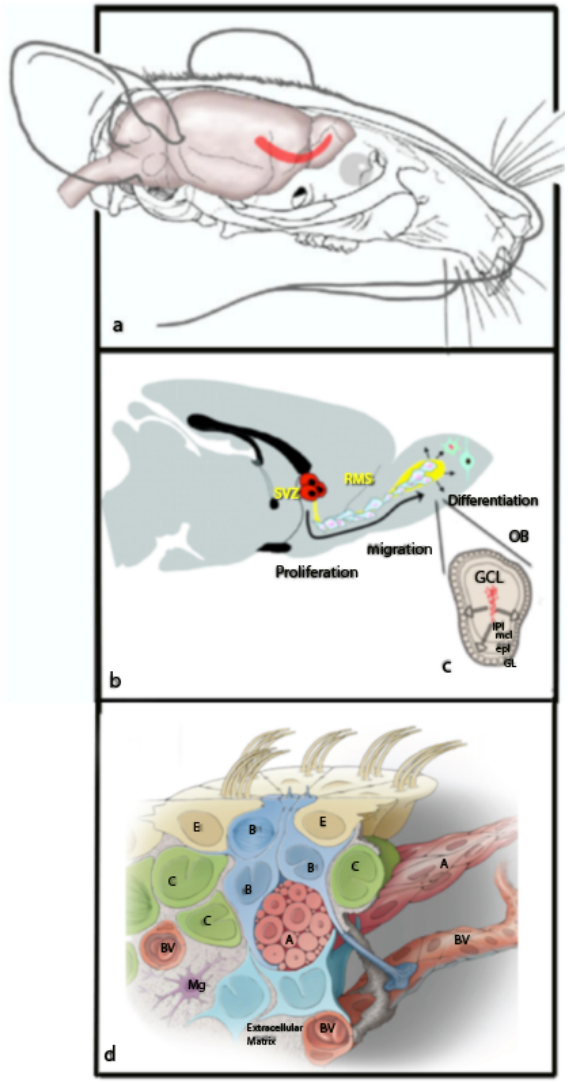

Figure 1.2. Adult neurogenesis in the SVZ.

(A) The head of an adult rodent displaying the location of the RMS (highlighted in red). ***(B)*** Mid-sagittal section of an adult rodent brain. Within the SVZ, progenitor cells proliferate and differentiate into the neuroblasts that migrate tangentially through the RMS into the main olfactory bulb (OB) where they differentiate into interneurons (Altman J 1969; Luskin MB 1993). ***(C)*** A coronal section of the olfactory bulb. When the migrating neuroblasts reach the olfactory bulb they migrate radially outward across multiple layers of the olfactory bulb toward the granule cell layer (GCL) and glomerular layer (GL), where they differentiate into mature interneurons (O'Rourke NA 1996; Luskin MB 1998). ***(D)*** Schematic of the wall of the lateral ventricles, revealing the position of neural stem cells (Type B cells), transit amplifying cells (Type C cells) and neuroblasts (Type A cells). Type B stem cells maintain contact with the ventricular space via a primary cilium, and are also in close contact with the vascular environment (Ming GL and H Song 2005; Ihrie RA and A Alvarez-Buylla 2011). Granule cell layer (GCL), external plexiform layer (EPL), mitral cell layer (mcl), internal plexiform layer (IPL), glomerular layer (GL), Blood vessel (BV), Image modified from (Lennington JB et al. 2003; 2005; Ihrie RA and A Alvarez-Buylla 2011).

1.1.2 Postnatal SGZ neurogenesis

Another region of the dorsal telencephalon that contains neural progenitor cells that continue to generate neurons throughout life is the SGZ of the hippocampal dentate gyrus. The mature hippocampus consists of the dentate gyrus, *cornu ammonis* (*CA*) 1, *CA2* and *CA3* regions, and the subiculum. In mice, the development of this structure begins at E10.5 from cells within the most caudomedial portion of the cortex (Grove EA and S Tole 1999; Li G and SJ Pleasure 2005; O'Leary DD and S Sahara 2008). The pyramidal neurons that comprise the *CA* 1 to 3 regions are derived from the radial glial progenitor cells within the ammonic neuroepithelium of the nascent hippocampus between E10 and E18 (Angevine JB, Jr. 1965; Kriegstein AR and SC Noctor 2004; Rakic P 2007). Another region of the hippocampal VZ, the dentate neuroepithelium, contains progenitor cells that will give rise to both dentate granule neurons embryonically, and also to progenitor cells that will ultimately populate the SGZ of the mature dentate gyrus. The migration of dentate granule cells from the dentate neuroepithelium towards the presumptive dentate gyrus begins at approximately E16 (Altman J and SA Bayer 1990; Tatsunori Seki KS et al. 2011). These migratory cells form what is called the secondary dentate matrix. Cells migrating through this matrix take one of two routes. The first route follows a subpial route; these cells become neurons within the granule cell layer (GCL) of the dentate gyrus. The second population of cells take a more direct route to the prospective hilus. Postnatally, the hilus, also known as the tertiary dentate matrix, become the main proliferative zone of the hippocampus, and ultimately gives rise to the neural stem cells that reside within the SGZ neurogenic niche within the adult brain (Figure 1.3).

In the postnatal hippocampal dentate gyrus, a population of radially projecting cells (Type 1 cells) act as quiescent neural stem cells that reside in the SGZ give rise to self-renewing non-radial progenitors (Type 2 cells; Figure 1.4). These Type 2 progenitors in turn give rise to neuroblasts that migrate from the SGZ into the granule cell layer, where they differentiate into local glutamatergic dentate granule cells that are integrated into the existing hippocampal circuitry (Suh H et al. 2007; Mu Y et al. 2010). This process of neurogenesis in the SGZ

continues to take place throughout adulthood and is critical for a number of key processes, including memory, learning and spatial navigation (Grant SG et al. 1992; Lemaire V et al. 2012).

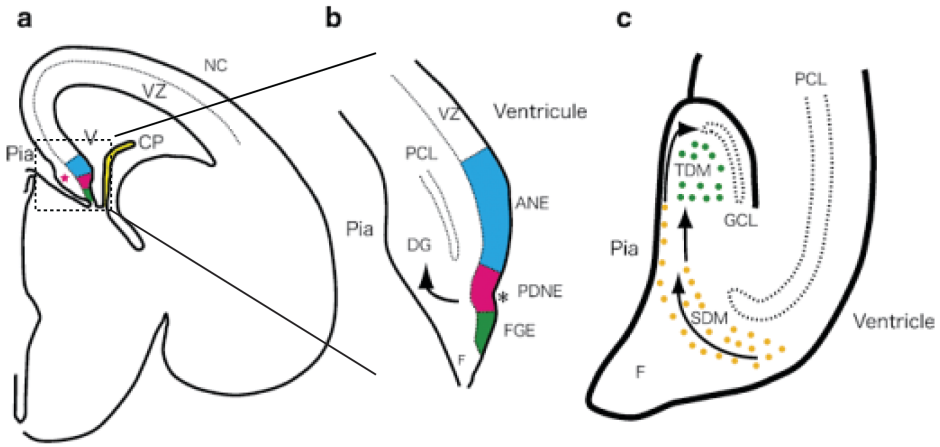

Figure 1.3. Schematic drawings detailing hippocampal development.

(A) Coronal section of a rat forebrain during late embryonic development. The hippocampus is generated from the caudomedial portion of the cortex (boxed region in ***A***). ***(B)*** The hippocampal VZ is divided into three sections: the ammonic neuroepithelium (ANE) (in blue), the dentate neuroepithelium (PDNE) (in red) and the fimbrioglial neuroepithelium (FGE) (in green). The arrow indicates the early path taken by cells derived from the dentate neuroepithelium as they migrate towards the presumptive dentate gyrus. ***(C)*** As development continues, these cells form the secondary dentate matrix (SDM) (yellow dots). Some cells from the SDM travel subpially to form the granule cell layer (GCL) of the dentate gyrus, whereas progenitor cells travel towards the hilus to form the tertiary dentate matrix (TDM), which become the main proliferative zone of the hippocampus in the postnatal period (Green dots). Ultimately, progenitor cells within the TDM will become confined to the SGZ of the adult dentate gyrus. CP: choroid plexus, DG: dentate gyrus, F: fimbria, NC: neocortex, PCL: pyramidal cell layer. V: ventricle. Picture adopted from (Tatsunori Seki KS, Jack M. Parent, Arturo Alvarez-Buylla 2011).

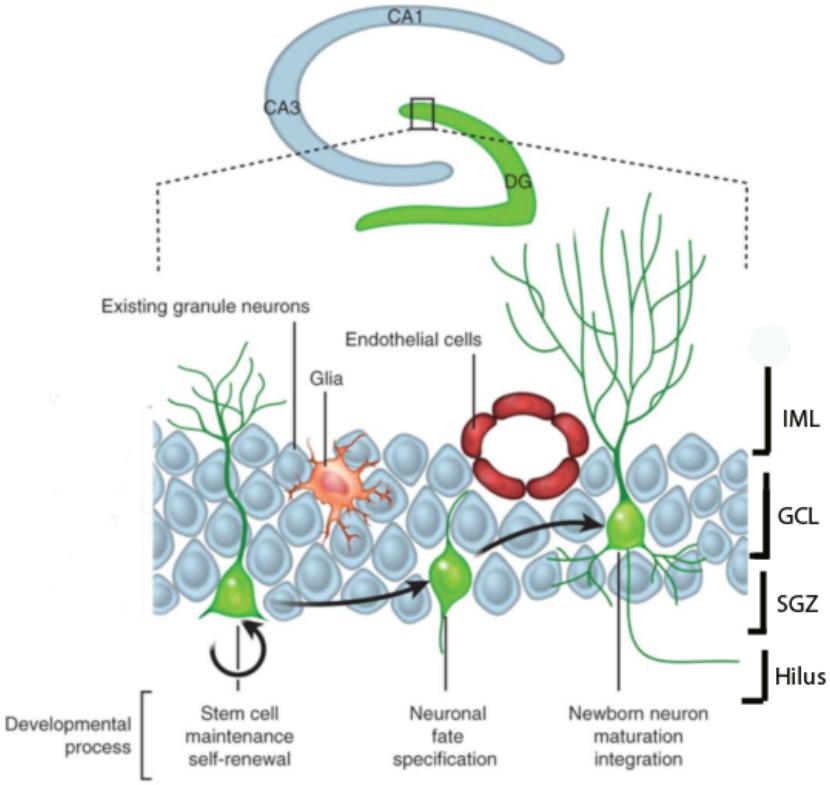

Figure 1.4. Adult neurogenesis in the SGZ.

Within the SGZ of the hippocampal dentate gyrus, neural stem cells self renew and proliferate. These progenitor cells give rise to immature neurons that migrate into the granule cell layer where they mature into mature granule cells and integrate into the existing hippocampal circuitry (Kempermann G et al. 2004; Duan X et al. 2008). IML: inner molecular layer; GCL; granule cell layer; SGZ; subgranular zone. Image altered from (Ma DK et al. 2010).

Adult neurogenesis has now been demonstrated in a variety of species, including humans (Eriksson PS et al. 1998; Quinones-Hinojosa A et al. 2006), and has further been revealed to play a key functional role in a variety of situations, including sex-specific innate olfactory responses, learning, memory and spatial navigation(Alvarez-Buylla A and DA Lim 2004; Sakamoto M et al. 2011; Kageyama R et al. 2012). Despite this understanding, we are still a long way from fully understanding the cellular and molecular mechanisms regulating neural stem cell self-renewal and differentiation, nor from knowing the factors that regulate how these neurogenic niches form in the postnatal period. Interestingly, preliminary data has revealed that transcription factors from the NFI family are expressed within VZ neural stem

cells during embryogenesis(Campbell CE et al. 2008), and that mice lacking NFIs exhibit deficits in the formation of the postnatal neurogenic niches. As such, this thesis aimed to investigate the role of one of these genes, *Nfix*, in mediating the formation of the SVZ and SGZ (Campbell CE et al. 2008),

1.2 *Nfi* genes: Key regulators of nervous system development

Extensive studies have shown that transcription factors play critical roles in regulating neurogenesis within the embryonic, postnatal and adult CNS (Mu Y et al. 2010). Given the importance of progenitor cell proliferation and differentiation during the development and maintenance of the CNS, it is essential to understand how transcription factors control these processes. Some examples of transcription factors that play a role in the regulation of neural progenitor cell self-renewal include the Sry-related HMG box (SOX) family, which have been shown to play an important role in maintaining progenitor cell identity throughout the neuraxis (Graham V et al. 2003). For example, SOX2 is expressed strongly by Type 1 progenitor cells within the adult SGZ (Ferri AL et al. 2004). Furthermore, conditional deletion of *Sox2* in the adult hippocampus results in a significant reduction in the number of progenitor cells within the SGZ and a corresponding decrease of immature granule neurons, which is consistent with the important role played by SOX2 in the maintenance of the progenitor cell pool within the dentate gyrus of the hippocampus (Ferri AL et al. 2004). SOX2 has also been implicated in the regulation of stem cell biology within the adult SVZ (Andreu-Agullo C et al. 2012).

The Notch signalling pathway also plays a central role in stem cell biology by promoting the maintenance of neural progenitor cell self-renewal in both the embryonic and adult brain (Imayoshi I et al. 2010). Major transcriptional targets of the Notch signalling pathway include the basic helix-loop-helix transcription factors *Hes1* and *Hes5* (hairy and enhancer of split homologs-1 and -5), (Ohtsuka T et al. 1999). Studies have shown that *Hes1* is expressed by neural stem cells within the embryonic brain and within the adult neurogenic niches (Kumar

DU et al. 2012). In the absence of *Hes1*, mice exhibit premature neural stem cell differentiation and depletion of neural stem cell pool within the embryonic cortex, suggesting that *Hes1* plays a critical role in maintaining neural stem cell maintenance. Similar functions have been described for *Hes5*. Mechanistically, HES1 has been shown to repress proneural genes such as *Mash1* and *Neurogenin*2 in progenitor cells, thereby inhibiting their differentiation (Kageyama R et al. 2007; Kumar DU et al. 2012). Interestingly, these factors have also been implicated in regulating the self-renewal of progenitor cells within the adult neurogenic niches (Furukawa T et al. 2000; Ohtsuka T et al. 2001; Kageyama R et al. 2005).

One suite of transcription factors that have also been found to play an important role in the regulation of cortical development are the NFI proteins, which are expressed by cells within the embryonic, postnatal and adult brain (Chaudhry AZ et al. 1997). Extensive studies have shown that this family of transcription factors plays an essential role in a variety of CNS processes during development, including axonal guidance and outgrowth (Shu T et al. 2003; Piper M et al. 2011; Heng YH et al. 2012), glial development (Shu T et al. 2003; Steele-Perkins G et al. 2005; Barry G et al. 2008), and neuronal differentiation and migration (Wang W et al. 2007; Mason S et al. 2009) in multiple regions of the CNS. These regions include the olfactory bulb (Plachez C et al. 2012), neocortex (Plachez C et al. 2008), hippocampus (Barry G et al. 2008), cerebellum (Wang W et al. 2004), pons (Steele-Perkins G et al. 2005) and spinal cord (Deneen B et al. 2006).

NFI transcription factors were first identified as host-encoded proteins required for the initiation of adenoviral replication *in vitro* (Nagata K et al. 1982). A single *Nfi* gene is present in the nematode *Caemorhabditis elegans*, in *Drosophila* and in the cephalochordate *Amphioxus* (Fletcher CF et al. 1999; Gronostajski RM 2000; Strausberg RL et al. 2002). Subsequently, four *Nfi* family members were isolated in the vertebrate lineage, including *Nfia*, *Nfib*, *Nfic* and *Nfix* (Rupp RA et al. 1990; Kruse U et al. 1991). As yet, no *Nfi* genes have been found in plants, bacteria or single cell eukaryotes, and the comparative role of NFIs

through evolution has received little attention. The NFI proteins are site-specific transcription factors that have a modular structure, consisting of a conserved N-terminal DNA-binding/dimerization domain and C-terminal transcriptional activation and/or repression domain (Nagata K et al. 1983; Mason S et al. 2009). All four NFI members share a conserved sequence of 220 amino acids in the DNA-binding N-terminal domain. Multiple alternative splicing of individual *Nfi* genes generate different isoforms (Santoro C et al. 1988; Inoue T et al. 1990; Apt D et al. 1994), although the role of specific splice variants *in vivo* is poorly defined. NFIs bind to the dyad symmetric consensus sequence TTGGC(N5)GCCAA as either homo- or hetero- dimers with high affinity (Gronostajski RM et al. 1985; Gronostajski RM 1986; Kruse U and AE Sippel 1994). They can also bind to consensus half site (TTGGC or GCCAA) with reduced affinity (Meisterernst M et al. 1988). NFI proteins have been shown to either activate or repress gene expression, according to the promoter and cellular context in which they are expressed (Gronostajski RM 2000; Murtagh J et al. 2003).

1.2.1 Expression of *Nfi* genes during nervous system development

NFI proteins are expressed by cells in multiple organs during development, including the lung, liver, heart, nervous system and other tissues (Gronostajski RM 2000). In the developing nervous system, *Nfi* genes display distinct, yet partially overlapping expression patterns (Chaudhry AZ et al. 1997). *Nfia, Nfib* and *Nfix* are highly expressed within the CNS and studies using knockout mice have revealed that both *Nfia* and *Nfib* play important roles in the development of many regions of the CNS including the neocortex (Plachez C et al. 2008), hippocampus (Barry G et al. 2008), cerebellum (Wang W et al. 2004), pons (Steele-Perkins G et al. 2005) and spinal cord (Deneen B et al. 2006).

Within the forebrain, NFIA and NFIB are expressed in the developing and postnatal olfactory bulb, as well as by cells within the RMS. In addition, radial glia within the VZ express NFIA and NFIB, as do cells within the marginal zone and the cortical plate during embryogenesis, as well as the embryonic and postnatal SVZ. At the developing telencephalic midline, glial

cells within the indusium griseum and the glial wedge also express NFIA and NFIB, as do the cells that form the subcallosal sling (Shu T et al. 2003; Piper M et al. 2009). Within the developing hippocampus, NFIA is expressed by multiple cellular populations, including radial glia within the VZ, glia within the fimbria and postmitotic neurons within the ammonic neuroepithelium and dentate gyrus (Piper M et al. 2010). The expression of NFIB within the embryonic hippocampus overlaps with the expression of NFIA with the exception that progenitor cells within the fimbrioglial neuroepithelium do not express *Nfib* during embryogenesis (Barry G et al. 2008). Furthermore, within the cerebellum, NFIA and NFIB are expressed within cerebellar granule neurons as they become postmitotic within the premigratory zone of the external granular layer. This expression persists throughout the migration of cerebellar granule neurons through the molecular layer to the internal granule cell layer (Wang W et al. 2007). Finally, in the developing spinal cord, both NFIA and NFIB are expressed by early astrocyte precursor and in a subset of differentiated motorneurons (Deneen B et al. 2006).

The expression pattern of *Nfix* overlaps substantially with the expression of *Nfia* and *Nfib,* which will be discussed in further detail below (section 1.2.3).

Unlike the other *Nfi* mutant mice, *Nfic*$^{-/-}$ mice do not exhibit aberrant brain development, which corresponds to the relatively low level of *Nfic* expressed within the developing forebrain (Chaudhry AZ et al. 1997). However, *Nfic*$^{-/-}$ mice display abnormal molar root formation and exhibit severe incisor defects postnatally (Steele-Perkins G et al. 2003) as a result of the disruption of odontoblast differentiation (Park JC et al. 2007). *Nfic*$^{-/-}$ mice have a tooth development defect but display a normal life span when their diet is supplemented with soft dough to reduce the need for chewing (Steele-Perkins G et al. 2003).

1.2.2 *Nfia* and *Nfib* mutant mice exhibit deficits in CNS development

Nfia$^{-/-}$ mice were generated through the deletion of the 3' splice acceptor site and 219 base pairs of exon 2 (das Neves L et al. 1999). On a stable C57Bl/6J background, *Nfia*$^{-/-}$ mice exhibit a range of neurological deficits, including dysgenesis of the corpus callosum, enlarged lateral ventricles, cerebellar and hippocampal malformation, hydrocephalus, urinary tract defects and malformation of midline glial populations that are required to guide axons of the corpus callosum across the telencephalic midline of the developing brain (das Neves L et al. 1999; Shu T et al. 2003; Lu W et al. 2007). *Nfia*$^{-/-}$ mice also exhibit perinatal lethality, likely as a result of renal developmental deficits (das Neves L et al. 1999; Lu W et al. 2007).

Nfib$^{-/-}$ mice also die at birth but as a result of lung hypoplasia (Steele-Perkins G et al. 2005). *Nfib*$^{-/-}$ mice were generated through the replacement of the 523 base pairs of the 3' portion of exon 2 and the first 177 base pairs of intron 2 with a translational-fusion beta-gal reporter gene and a neomycin resistance gene (lacZ and Neo) (Steele-Perkins G et al. 2005). On a C57B1/6J background *Nfib*$^{-/-}$ mice display a variety of defects in nervous system development, including dygenesis of the corpus callosum, enlarged lateral ventricles, cerebellar and hippocampal defects, abnormal pons formation and a failure of glial maturation at the telencephalic midline (Barry G et al. 2008; Kumbasar A et al. 2009; Piper M et al. 2009). Interestingly, both *Nfia*$^{-/-}$ and *Nfib*$^{-/-}$ mice die prenatally, thereby preventing the analysis of these genes in the postnatal development of the brain using these full knockout strains. For this reason, the work in my thesis, which centred on the development of the postnatal neurogenic niches, focussed on the role of NFIX, as mice lacking this gene survive postnatally (Campbell CE et al. 2008).

1.2.3 *Nfix*

1.2.3.1 *Nfix* expression

Within the developing telencephalon, *Nfix* is expressed by cells within the VZ from E11 (Campbell CE et al. 2008). By E13, *Nfix* expression is more widespread, encompassing cells within the preplate, the septum, the piriform cortex and the ganglionic eminences, as well as within the VZ. By E17 and P0, cells within all of the layers of the cortical plate express *Nfix*. By P7, *Nfix* expression is stronger within layer II/III and V as compared to P0, and remains in layers II/III at P14 (Campbell CE et al. 2008).

Nfix is also detected within the VZ and the differentiating cell layers within the developing hippocampal primordium at E13 (Campbell CE et al. 2008). This expression pattern continues until E15. By E17, *Nfix* is no longer expressed in the stratum radiatum but is highly expressed in the differentiating layers of the hippocampus. By the early postnatal period, *Nfix* is highly expressed in the dentate gyrus and also expressed in the stratum oriens, stratum pyramidale and within the VZ. In the adult brain, *Nfix* expression is detected by cells within the *CA3* and *CA1* regions, as well as by neural progenitor cells within the SGZ of the dentate gyrus. This expression pattern of *Nfix* within the hippocampus suggests that *Nfix* plays a role in regulating the development and maintenance of the hippocampus (Campbell CE et al. 2008).

1.2.3.2 Aberrant brain development in *Nfix*$^{-/-}$ mice

Nfix$^{-/-}$ mice were generated through the deletion of exon 2 (Campbell CE et al. 2008). In contrast to *Nfia*$^{-/-}$ and *Nfib*$^{-/-}$ mice, *Nfix*$^{-/-}$ mice survive postnatally, until weaning around P20, after which they die from causes that are as yet unknown. After P8, these mice fail to thrive, and by P14, *Nfix*$^{-/-}$ mice are obviously smaller than their wild type littermates (Campbell CE et al. 2008). Furthermore, *Nfix*$^{-/-}$ mice open their eyelids and develop ear canals 3 days later than their wild type and heterozygous littermates (Campbell CE et al. 2008). *Nfix*$^{-/-}$ mice also display a deformation of the spine (Driller K et al. 2007). *Nfix*$^{-/-}$ mice display a number of

telencephalic defects, including dysgenesis of the corpus callosum and hydrocephalus (Driller K et al. 2007), as well as expansion of the cingulate cortex and the entire brain along its dorsoventral axis (Campbell CE et al. 2008).

One of the most interesting phenotypes of mice lacking this gene, however, is that the postnatal neurogenic niches are aberrantly formed (Figure. 1.5; 1.6). *Nfix*$^{-/-}$ mice exhibit severe distortions within the hippocampus, including a shorter dentate gyrus and an expansion of the *CA* regions (Campbell CE et al. 2008). This malformation, coupled with the expression pattern of *Nfix* in the developing and postnatal hippocampus, suggests that *Nfix* may play an important role in the development of the hippocampus. Indeed, the distortion of the hippocampus may be a result of aberrant progenitor cell proliferation and differentiation during morphogenesis of this structure. My investigations into the causes underlying the dysmorphic hippocampus in *Nfix*$^{-/-}$ mice form Chapter 3 of this thesis. Within the SVZ, an accumulation of PAX6-positive progenitor cells and doublecortin (DCX)-expressing neuroblasts within the lateral ventricles of the postnatal forebrain is present in *Nfix*$^{-/-}$ mice (Campbell CE et al. 2008). The accumulation of progenitor cells within the SVZ of *Nfix*$^{-/-}$ mice suggests that *Nfix* may play a role in repressing progenitor cell proliferation within the neurogenic niche. Moreover, the accumulation of neuroblasts within the SVZ suggests that *Nfix* may also play a role in regulating the migration of the SVZ-derived neuroblasts toward the olfactory bulb. These hypotheses, which are not necessarily mutually exclusive, were addressed in chapters 4 and 5 of this thesis.

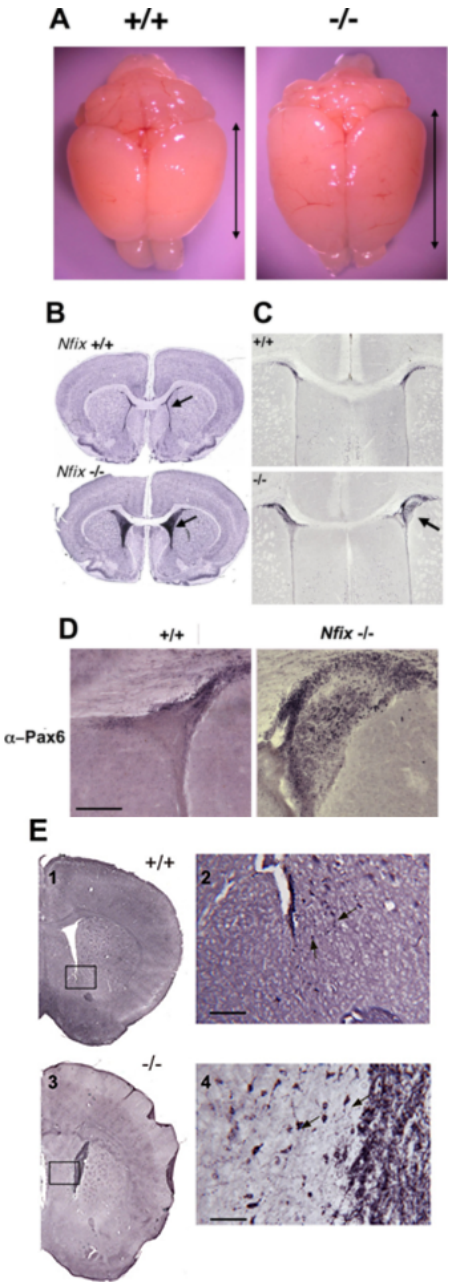

Figure 1.5. Aberrant cells observed in the SVZ of postnatal *Nfix*$^{-/-}$ mice.

(A) Gross structure of the P22 brains of *Nfix* wild type and *Nfix*$^{-/-}$ mice. *Nfix*$^{-/-}$ mice exhibit an increase in the anterior-posterior length of the telencephalon as compared to wild type mice. ***(B, C)*** Cresyl violet-stained coronal sections of the *Nfix*$^{-/-}$ and wild type mice. *Nfix*$^{-/-}$ mice display more cells within the SVZ of the lateral ventricles (arrows). ***(D)*** PAX6 staining reveals extensive expression of this neural progenitor cell marker within the SVZ of the P16 *Nfix*$^{-/-}$ mice compared to controls. **(*E*)** DCX immunostaining in the SVZ of P69 wild type and *Nfix*$^{-/-}$ mice. The panels on the right are magnified views of the boxed regions on the left. There are markedly more DCX-expressing cells within the SVZ of the mutant mice (Campbell CE et al. 2008). Image obtained from (Campbell CE et al. 2008).

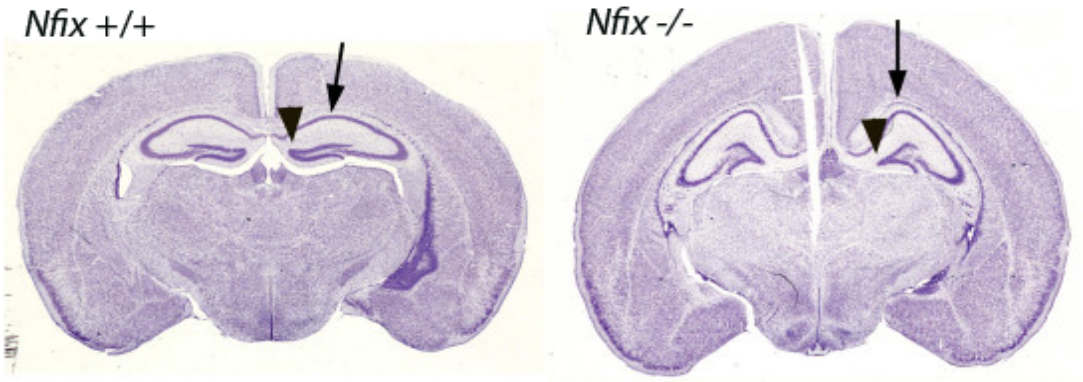

Figure 1.6. Distorted hippocampal morphogenesis in *Nfix*$^{-/-}$ mice.

Coronal sections of P22 wild type and *Nfix*$^{-/-}$ mice stained with haematoxylin. The dentate gyrus of the mutant is shortened (compare arrowheads), whereas the *CA* regions of the mutant are distorted dorsoventrally (compare arrows) (Campbell CE et al. 2008). Image obtained from (Campbell CE et al. 2008).

Taken together, these preliminary data reveal that *Nfix* plays a major role in the morphological development of the forebrain (Campbell CE et al. 2008), in particular the SVZ and the hippocampus, with mice lacking this gene displaying morphological abnormalities in these neurogenic niches of the postnatal brain. However, much remains to be learned regarding the cell-type specific expression of NFIX, especially within the developing and adult cerebral cortex, as well as the molecular mechanisms by which NFIX mediates the development of the SVZ and the hippocampal dentate gyrus. Understanding these questions forms the basis of this thesis.

1.2.4 NFI mediated regulation of neural development

1.2.4.1 Downstream targets of NFI transcription factors

The wide range of nervous system abnormalities observed in the *Nfix*$^{-/-}$ mice has led to intensive research into the transcriptional targets of the NFI proteins. Putative targets of the NFI transcription factors have primarily been identified through the use of candidate based approaches *in vitro*. NFI binding sites have been identified in the promoter regions of many glial and neuronal genes, including the *astrocyte-specific glutamate/aspartate transporter* (*Glast*), *tenascin C* (Barry G et al. 2008), *neurofilament M* (Elder GA et al. 1992), *myelin basic protein* (Tamura T et al. 1988) and *glial fibrillary acidic protein* (*Gfap)* (Miura M et al. 1990). The analysis of *Nfia*$^{-/-}$ *and Nfib*$^{-/-}$ mice has also provided further evidence to support these genes as being direct downstream targets of *Nfi*-mediated transcriptional activation, as knockout mice display downregulated expression of GLAST, GFAP and tenascin C within the cortex and hippocampus (Barry G et al. 2008). Furthermore, *Gfap* has been shown to be a direct downstream target of NFI in the undifferentiated cortical progenitor cells prior to astrocyte differentiation using chromatin immunoprecipitation (Cebolla B and M Vallejo 2006).

Within the developing CNS, other studies have also confirmed that *Nfia* is required to drive the expression of *Gfap*. An insight into one of the mechanisms underlying this process has been recently provided by a study of the embryonic mouse cortex (Namihira M et al. 2009). In this study, the authors used cultured embryonic cortical neural progenitors to demonstrate that the induction of the Notch signalling pathway resulted in the activation of *Nfia* expression. Furthermore, *Nfia* expression was correlated with the dissociation of the methyltransferase, DNMT1, from the STAT3 binding site within the *Gfap* promoter, culminating in demethylation, and hence activation, of this promoter region (Namihira M et al. 2009). As JAK/STAT signalling is required for gliogenesis (Deneen B et al. 2006), these findings place *Nfia* within the molecular cascade required to drive gliogenesis and further

suggest that *Nfia* drives the transcription of glial-specific genes, at least in part, via suppression of repressive DNA methylation.

As mentioned above (section 1.2), the Notch signalling pathway is also a key component required for the maintenance of neural progenitor cell identity. Recent research from our laboratory has demonstrated that *Nfia* promotes gliogenesis through the repression of the key Notch effector gene, *Hes1*. *Nfia*$^{-/-}$ mice display significant upregulation of *Hes1* expression within the telencephalic VZ during late embryogenesis (Piper M et al. 2010). Furthermore, *in silico* promoter analyses, gel shift assays and chromatin immunoprecipitation demonstrated that the promoter of the *Hes1* gene contains a cluster of conserved NFI binding sites that are bound by NFIA both *in vitro* and *in vivo*, and that *Nfia* can repress transcription under the control of the *Hes1* promoter in luciferase assays (Piper M et al. 2010).

Furthermore, *Nfi* genes also have been shown to regulate other processes during CNS development, including granule neuron maturation and migration within the cerebellum. In the cerebellum, the *Nfi* genes are expressed by immature neurons within the premigratory zone, and by cerebellar granule neurons (CGNs) within the internal granule cell layer (Wang W et al. 2004; Wang W et al. 2010; Piper M et al. 2011). Using a dominant negative repressor construct that represses all *Nfi* genes, NFI proteins were implicated in the transcriptional regulation of the α6 subunit of the γ-aminobutyric acid type A (GABAa) receptor (*Gabra6*). GABRA6 is primarily expressed by CGNs within the cerebellum and is part of an intrinsic program that directs their differentiation (Wang W et al. 2004). This suggests that NFI plays a role in directing the CGN differentiation via regulating *Gabra6*. Furthermore, NFI proteins were also recently shown to regulate the expression of the cell adhesion molecules, *N-cadherin*, *Ephrin-B1 and transient axonal glycoprotein-1 (Tag-1)* in CGNs (Wang W et al. 2007; Wang W et al. 2010). These cell adhesion molecules play a critical role in promoting axon formation, migration, and dendrite formation in CGNs. *Nfi* mutant mice display a significant reduction in the expression of these genes within the cerebellum (Wang W et al.

2007; Wang W et al. 2010). These data suggest that NFIs play an important role in neuronal migration through the regulation of cell adhesion molecules.

Collectively, these findings suggest that the NFI family plays an essential role in regulating the development of multiple regions within the developing CNS through the transcriptional regulation of multiple genes that are required for processes including progenitor cell differentiation, neural migration and maturation, and gliogenesis.

Importantly, most studies on the role of *Nfi* genes during CNS development have focused on *Nfia* and *Nfib*, primarily because the knockout strains for these genes were generated first. Although *Nfia*$^{-/-}$ and *Nfib*$^{-/-}$ mice have provided information pertaining to how *Nfi*s regulate cortical development, the drawback of these mutant lines as models to probe ongoing development of the CNS is that both knockout mouse lines exhibit perinatal lethality due to defects in renal development (Lu W et al. 2007) and lung hypoplasia (Steele-Perkins G et al. 2005). As such, these models are unable to provide insights into how NFIs regulate postnatal development of the brain.

Furthermore, our current understanding of how NFIX regulate stem cell biology remains limited. Interestingly, NFIX deletions or nonsense mutations have recently been identified as one of the causative factors for multiple cases of Sotos-like overgrowth and Marshall-Smith syndrome, which are conditions in humans that are characterized by advanced bone age, overgrowth, musculoskeletal abnormalities and abnormal behaviours, as well as learning difficulties. Magnetic resonance imaging analyses revealed that these patients display similar gross defects as observed in homozygous *Nfix*$^{-/-}$ mice, including hypoplasia of the corpus callosum and ventricular dilation. This highlights the key role played by *Nfix* in the development of the brain and thus, this project may be able to provide insights into the human congenital disorders caused by *Nfix* (Malan V et al. 2010; Priolo M et al. 2012; Yoneda Y et al. 2012). The focus of this thesis is, therefore, to investigate the role of NFIX in regulating

stem cell biology within the SGZ and SVZ during both embryonic and postnatal development using *Nfix*$^{-/-}$ mice as a model system.

1.3 Hypothesis and aims

This PhD thesis will address the hypothesis that Nfix controls the subventricular zone and subgranular zone development through regulating the biology of neural stem cells located within these neurogenic niches.

The three main aims that will address this hypothesis are:

Aim 1: To determine if NFIX is required for the development of the hippocampus both embryonically and postnatally, in particular the role played by NFIX in regulating progenitor cell differentiation.

Aim 2: To determine the cell type specific expression of NFIX in the SVZ, RMS and olfactory bulb.

Aim 3: To determine whether NFIX is essential for the proliferation and differentiation of progenitor cells within the SVZ and for the migration of neuroblasts to the olfactory bulb.

CHAPTER 2

Materials and methods

2.1 Animals

2.1.1 General animal care and handling

The animals used in this thesis include wild type C57BL/6J mice, wild type CD1 mice, as well as *Nfix* wild type and *Nfix*$^{-/-}$ mice (Campbell CE et al. 2008) maintained on a C57BL/6J background. Timed-pregnant females were obtained by placing *Nfix*$^{+/-}$ male and *Nfix*$^{+/-}$ female together overnight. The following day designated as embryonic day (E)0 if the female had vaginal plug, and the day of birth was designated postnatal day (0). Mice were gentoyped by polymerase chain reaction (Campbell CE et al. 2008). Transgenic mice expressing green fluorescent protein (GFP) under the control of the glutamic acid (*Gad67*) promoter were also used (Tamamaki N et al. 2003), as were mice expressing GFP under the control of the *Dcx* promoter (Walker TL et al. 2007) mice. The former mice have GFP knocked into the *Gad67* locus, and expression of GFP has previously been shown to co-localise with GAD67 expression (Tamamaki N et al. 2003), The latter strain (*Dcx*-GFP/bacterial artificial chromosome [BAC]) were originally obtained from the Mutant Mouse Regional Resource Center and the Gene Expression Nervous System Atlas BAC transgenic project. The pattern of GFP expression in these animals matches previously reported expression of DCX(Gleeson JG et al. 1999). Finally, we used another BAC transgenic line expressing GFP under the control of the *Hes5* promoter. These mice have been show previously to express GFP in neural stem cells within the adult brain (Jhaveri DJ et al. 2010). All animals were bred at the University of Queensland under approval from the Institutional Animal Ethics Committee. Embryos were obtained from time–mated wild type C57BL/6J mice in majority of the experiments and wild type CD1 mice were used in *in utero* electroporation in chapter 3. A minimum of 3 animals was analysed for each separate phenotypic analysis.

2.1.2 *Nfix* wild type and *Nfix*$^{-/-}$ mice

Nfix wild type and *Nfix*$^{-/-}$ littermate mice were maintained on a C57Bl/6J background. The *Nfix* allele was generated as a conditional line. Initial breedings indicated that mice homozygous or heterozygous for the targeted conditional allele had no obvious phenotypes. The knockout (KO) allele was generated through cre-mediated recombination, using a strain under which cre recombinase expression was controlled by the promoter from the *ZP3* promoter. *ZP3* in expressed in the developing oocyte prior to the first meiotic division, ensuring germline deletion of the targeted gene (Figure 2.1) (Campbell CE et al. 2008). The *Nfix* targeting vector was constructed with a 4.2kb 5' homology arm containing all of exon 2 and 633 bp of intro 2, with a loxP site inserted ~400 bp 5' to the start of exon 2 (Campbell CE et al. 2008).

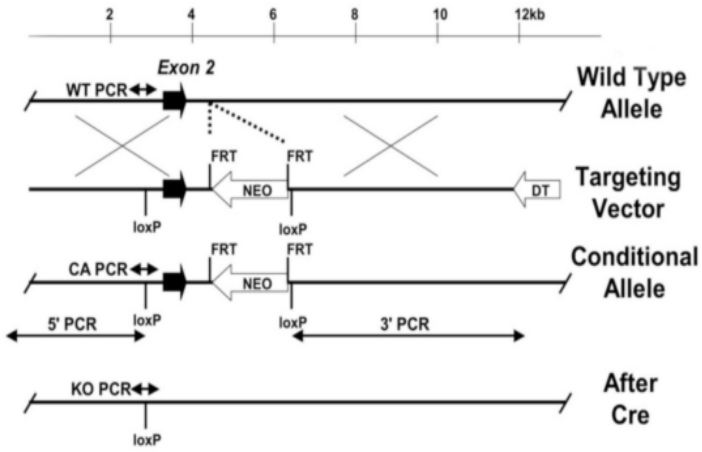

Figure 2.1. Disruption of the *Nfix* gene.

The *Nfix* targeting vector construction and predicted PCR products are shown. The wild type allele containing exon 2 of the wild type *Nfix* gene was used to construct the targeting vector. The targeting vector has a loxP site inserted into the ~400 nucleotides 5' to exon 2 and a FRT flanked PGK-Neo cassette with a second 3' loxP site ~600 nucleotides 3' to the end of exon 2 (white arrow). The arrows indicate the location of PCR primers within genomic DNA used to detect the wild type allele; Conditional Allele and the knockout allele. Males with conditional allele were bred with females expressing Cre recombinase in oocytes from the *ZP3* promoter to generate the knockout allele (after Cre) that lack exon 2. Image adopted from (Campbell CE et al. 2008)

Once the *Nfix*$^{-/-}$ allele was generated, this strain was maintained on a C57Bl/6J background by breeding heterozygous males to wild type females. For experimental work, *Nfix*$^{+/-}$ sires were placed with *Nfix*$^{+/-}$ dams to obtain litters of *Nfix* wild type (*Nfix*$^{+/+}$), *Nfix* heterozygous (*Nfix*$^{+/-}$), *Nfix* knockout (*Nfix*$^{-/-}$), which were generated in Mendelian ratios. Embryos were genotyped by polymerase chain reaction (PCR) (Campbell CE et al. 2008) using primers that flanked the 5' -most loxP site yielding products of 214 bp for the wild type allele and 415bp for the knockout allele.

PCR primers:

Nfix forward primer: 5'-ATGGACATGTCATGGGTGCGACAG-3'

Nfix reverse primer: 5'-AACCAGAGGCACGAGAGCTTGTC-3'

2.1.3 *Gad67-GFP* mice

Adult transgenic mice expressing green fluorescent protein (GFP) under control of the glutamic acid decarboxylase 67 (*Gad67*) promoter were also used (Tamamaki N et al. 2003). These mice have GFP knocked into the *Gad67* locus, and expression of GFP has previously been shown to co-localise with GAD67 expression (Tamamaki N et al. 2003). These mice were kindly provided by by Prof. Pankaj Sah (Queensland Brain Institute) and originated from Dr Yuchio Yanagawa (Gunma University Graduate School of Medicine, Maebashi, Japan).

2.1.4 *Dcx-GFP* mice

Transgenic mice expressing GFP under the control of the doublecortin (*Dcx*) promoter were also used in the study (Walker et al., 2007) and these mice (*Dcx-GFP*/bacterial artificial

chromosome [BAC]) were originally obtained from the Mutant Mouse Regional Resource Center, The Gene Expression Nervous System Atlas BAC transgenic project (Gong S et al. 2002). The pattern of GFP expression in these mice match previously reported expression of DCX (Gleeson et al., 1999). These mice were kindly provided by Prof. Perry Bartlett (Queensland Brain Institute).

2.2 Histological Techniques

2.2.1 Fixation of Tissue

Embryos under E14 were drop-fixed in 4% paraformaldehyde (PFA). Embryonic and postnatal pups that were between E15 to postnatal day (P) P20 were transcardially perfused with 0.9% saline, followed by 4% PFA. The perfused head was be then removed, postfixed in 4% PFA and kept at 4°C. Adult mice were similarly transcardially perfused with saline, then 4% PFA.

2.2.2 Hematoxylin staining

Brains from wild type and *Nfix*$^{-/-}$ embryos and postnatal pups were dissected from the skull, blocked in 3% noble agar (Difco, Sparks, MS), and sectioned at 50 μm on a vibratome (Leica, Nussloch, Germany). Sections were then mounted and stained with Mayer's hematoxylin using standard protocols.

2.2.3 Immunohistochemistry

Immunohistochemistry using the chromogen 3,3' diaminobenzidine was performed throughout this thesis. This was done by firstly blocking floating sections in blocking solution of 2% normal goat serum (Vector Laboratories, Burlingame, CA) or donkey serum (Jackson Laboratories, West Grove, PA) with 0.2% Triton-X 100 in PBS for an hour. The sections were then incubated in a solution containing the primary antibody (listed in Table

2.1) diluted with the blocking solution overnight, then sections were washed three times (each for 20 minutes) with PBS. The sections were then incubated with the secondary antibody (listed in Table 2.2) diluted in the blocking solution for 1 hour. The sections were washed three times with PBS, each for 20 minutes, and incubated with avidin-biotin amplification solution (Vector Laboratories). After three washes with PBS (each for 10 minutes), the sections were transferred into a Ni-DAB chromogen solution (DAB-sigma-Aldrich) and 175 mM of sodium acetate in water. 0.01% of hydrogen peroxide was added into the Ni-DAB chromogen solution and colour reaction was terminated by transferring the sections into PBS. Sections were then mounted on gelatinized slides, air dried for an hour and coverslipped using DPX mounting medium.

2.2.4 Immunohistochemistry on paraffin sections

Brains were perfused as above, embedded in paraffin and sectioned coronally at 6 μm. Hematoxylin staining and immunohistochemistry were performed as described previously (Barry G et al. 2008).

2.2.5 Antibodies parameters

2.2.5.1 Primary antibodies

Table 2.1. Primary antibodies

Primary antibodies	Host	Company	Dilution
BrdU	Mouse monoclonal	G3G4, Developmental Studies Hybridoma Bank	1/5000 (IHC)
Calbindin	Rabbit polyclonal	SWANT, Marly, Switzerland	1/50,000 (IHC)
Calretinin	Rabbit polyclonal	SWANT, Marly, Switzerland	1/50,000 (IHC)
NFIX	Rabbit polyclonal	Abcam, ab101341	1/1000 (IHC) 1/100 (IF)
GFAP	Rabbit polyclonal	Dako, Glostrup, Denmark	1/10,000 (IHC)
GFAP	Mouse monoclonal	Millipore MAB360	1/1000 (IF)
Tuj1	Mouse monoclonal	R&D systems, MAB1195	1/1000 (IF)
GLAST	Rabbit polyclonal	A gift from Dr. Niels Danbolt, University of Oslo, Oslo, Norway	1/50,000 (IHC)
TBR1	Rabbit polyclonal	A gift from Dr. Robert Hevner	1/100,000 (IHC)
TBR2	Rabbit polyclonal	A gift from Dr Robert Hevner, University of Washington	1/5000 (IHC)
Prox1	Rabbit polyclonal	Millipore Bioscience Research Reagents, Billerica, MA	1/25,000 (IHC)

Reelin	Mouse monoclonal	A gift from Dr. Andre Goffinet, University of Louvain Medical School, Brussels, Belgium	1/100000 (IHC)
SOX2	Rabbit polyclonal	Cell Signaling Technology, Danvers, MA	1/1000 (IHC)
Cleaved Caspase 3	Rabbit polyclonal	Cell Signaling Technology	1/5000 (IHC)
Nestin	Mouse monoclonal	Developmental Studies Hybridoma Bank	1/1500 (IHC)
Tenascin C	Rabbit polyclonal	Millipore Bioscience Research Reagents	1/5000 (IHC)
PAX6	Rabbit polyclonal	Millipore Bioscience Research Reagents	1/5000 (IHC)
Ki67	Mouse monoclonal	550609, BD Pharmingen	1/10000 (IHC) 1/1000 (IF)
Ki67	Rabbit polyclonal	NCL-Ki67p, Novocastra	1/200 (IF)
S100β	Mouse monoclonal	Ab66028, Abcam	1/200 (IF)
DCX	Rabbit polyclonal	Ab18723, Abcam	1/50000 (IHC) 1/1000 (IF)
PSA-NCAM	Rabbit polyclonal	Developmental Studies Hybridoma Bank	1/500 (IHC)
PPH3	Rabbit polyclonal	06-570, Millipore	1/10000 (IHC)

2.2.5.2 Secondary antibodies

Table 2.2 Secondary antibodies

Secondary antibodies	Company	Dilution
Goat-anti-rabbit AlexaFluor546	Invitrogen,	1/1000
Donkey-anti mouse AlexaFluor546	Invitrogen	1/1000
Goat-anti-rabbit AlexaFluor448	Invitrogen	1/1000
Donkey-anti mouse AlexaFluor448	Invitrogen	1/1000
Biotinylated goat anti-rabbit IgG	Vector laboratories	1/2000
Biotinylated donkey anti-mouse IgG	Jackson Immunoresearch	1/2000

2.3 *In situ* hybridization

Embryonic brains (chapter 3) and postnatal brains (chapter 5) were collected and fixed as described above (n = 3 for both wild type and *Nfix*$^{-/-}$ mice). *In situ* hybridization was performed using anti-sense probes as previously described (Piper M et al. 2009) with minor modifications. The hybridization temperature was 70°C. The color reaction solution was BM Purple (Roche). *In situ* probes were kindly provided by Dr. Shubha Tole (*KA1, Scip;* Tata Institute of Fundamental Research, Mumbai, India), Dr. Jane Johnson (*Mash1*; University of Texas, Dallas, TX) and by Dr. Ryoichiro Kageyama (*Hes1, Hes5*; Kyoto Uniersity, Kyoto, Japan).

2.4 Reverse transcription and quantitative real-time PCR

For quantitative real-time PCR (qPCR), hippocampi (chapter 3), and olfactory bulb and SVZ (chapter 5) were dissected and samples were then snap frozen. Total RNA was extracted using an RNeasy Micro Kit (Qiagen). Reverse transcription was performed using Superscript III (Invitrogen). 0.5 µg total RNA was reverse transcribed with random hexamers. qPCR reactions were carried out in a Rotor-Gene 3000 (Corbett Life Science) using the SYBR Green PCR Master Mix (Invitrogen). All the samples were diluted 1/100 with RNase/DNase-free water and 5 µl of these dilutions were used for each SYBR Green PCR reaction containing 10µl SYBR Green PCR Master Mix, 10 µM of each primer, and deionized water. The reactions were incubated for 10 min at 95°C followed by 40 cycles with 15 seconds denaturation at 95°C, 20 seconds annealing at 60°C, and 30 seconds extension at 72°C.

2.5 Generation of gene-specific quantitative qPCR standards

The synthesis of these primers was performed by Sigma-Genosys. The following primer sequences were used:

Table 2.3 Primer sequences used in Chapter 3

Gene	Sequence
Sox9 forward	CTCACATCTCTCCTAATGCT
Sox9 reverse	GACCCTGAGATTGCCCAGA
Hprt forward	GCAGTACAGCCCCAAAATGG
Hprt reverse	AACAAAGTCTGGCCTGTATCCAA

Table 2.4 Primer sequences used in Chapter 5

Gene	Sequence
Gapdh For	GCACAGTCAAGGCCGAGAAT
Gapdh Rev	GCCTTCTCCATGGTGGTGAA
Gdnf For	TGAAGACCACTCCCTCGG
Gdnf Rev	GCTTGTTTATCTGGTGACCTTTTC
Dcx For	TGGAAGCATGGATGAACTGG
Dcx Rev	CATGTTGGCAGATGTCTTTACG
Pax6 For	CTCCTAGTCACATTCCTATCAGC
Pax6 Rev	GCAAAGCACTGTACGTGTTG
Gfap For	AGTGGTATCGGTCTAAGTTTG
Gfap Rev	CGATAGTCGTTAGCTTCGTG

2.6 qPCR data expression and analysis

After completion of the PCR amplification, the data were analyzed with the Rotor-Gene software as described previously (Piper M *et al.* 2009). When quantifying the mRNA expression levels, the housekeeping gene *glyceraldehyde 3-phosphate dehydrogenase (Gapdh)* was used as a relative standard. All the samples were tested in triplicate. By means of this strategy, we achieved a relative PCR kinetic of standard and sample. For all qPCR analyses, RNA from 8 biological replicates for both wild type and *Nfix*$^{-/-}$ mice were interrogated. Statistical analyses were performed using a two-tailed unpaired *t*-test. Error bars represent the standard error of the mean.

2.7 Electrophoretic mobility shift assay

Electrophoretic mobility shift assays (EMSAs) were conducted by Dr Aaron Smith (School of Biomedial Science, University of Queensland) for experiments described in both chapters 3 and chapter 5 Nuclear extracts were isolated from the cortex of E18 brains, or from COS cells overexpressing either NFIX or a non-specific transcription factor, AP2. We used the HA-tagged AP2 construct as a non-specific control in our supershift assays to demonstrate the specificity of NFIX binding to our NFI consensus-containing oligonucleotide probes. EMSAs were performed using radiolabeled annealed oligonucleotides containing a control NFI consensus site or the putative *Sox9* consensus sites, which were designated -675, -183, +415 and +598 (for Chapter 3) and *Gdnf* consensus sites (for Chapter 5) from our bioinformatics promoter screen. EMSA reactions were carried out as described previously using 1 μg of nuclear extract (Piper M et al. 2010).

Oligonucleotide sequences for Chapter 3

NFI control: 5′- ggTTTTGGATTGAAGCCAATATGATAA-3′ (upper strand); 5′ggTTATCATATTGGCTTCAATCCAAAA -3′ (lower strand); Sox9 -675 : 5’-ccgggGCAGAAGCTCCAGTCACCACACCAGCTTCGTTGAAc-3’ (upper strand); 5’-

ccgggTTCAACGAAGCTGGTGTGGTGACTGGAGCTTCTGCc -3'(lower strand); -183 :5'-ccgggCATCCACCCTCTGGCTGAGCTCCCCTCCCTTCTCCc-3' (upper strand); 5'-ccgggGGAGAAGGGAGGGGAGCTCAGCCAGAGGGTGGATGc-3'(lower strand); +415 :5'-ccgggGACCGACGAGCAGGAGAAGGGCCTGTCTGGCGCCCc-3' (upper strand); 5'-ccgggGGGCGCCAGACAGGCCCTTCTCCTGCTCGTCGGTCc-3'(lower strand).+598 :5'-ccgggGTGCATCCGCGAGGCGGTCAGCCAGGTGCTGAAGGc-3' (upper strand); 5'-ccgggCCTTCAGCACCTGGCTGACCGCCTCGCGGATGCACc-3' (lower strand).

Oligonucleotide sequences for Chapter 5:

Gdnf -5 : 5'- CCGGGACCTTCTGGGCGGGGCCCCGCGCTCC -3' (upper strand), 5'-CCGGGGAGCGCGGGGCCCCGCCCAGAAGGTC -3' (lower strand); +44 :5'-CCGGGCTGGATGGGATTCGGGCCACTTGGAC -3' (upper strand), 5'-CCGGGTCCAAGTGGCCCGAATCCCATCCAGC -3' (lower strand).

The bases in lower cases were added to enable end filling with radiolabelled nucleotides. Supershift assays were performed with an anti-HA antibody (Sigma; #H9658).

2.8 Luciferase reporter assay

Luciferase reporter assays were conducted for experiments described in both chapters 3 and 5. The constructs used in the luciferase assay for chapter 3 were a full-length *Nfix* expression construct driven by the chick β-actin promoter (*Nfix* pCAGIG IRES GFP) and a construct containing the putative NFI binding site located at +598 within the *Sox9* promoter region (a gift from Peter Koopman) (Kent J et al. 1996). The *Sox9* construct was 250 base pairs in length, and was generated using the following primers: forward 5'-CTCGAGTCTCCTGGACCCCTTC-3'; reverse 5'-AAGCTTCAGCACCTGGCTGACC-3'. A construct containing a mutated NFI consensus sequence was generated in parallel to the Sox9 construct, using an alternative reverse primer: 5'-AAGCTTCAGCACTGGTATGACCGC-3'. The resulting construct, termed *Sox9ΔNFI,* possessed an NFI binding site that was changed from GAGGCGGTCAGCCAG to GAGGCGGTCATACCA. The amplicons were inserted into the XhoI and HindIII restriction enzyme sites of the pGL4.23 luc2minP vector (Promega, Madison, WI). DNA was

transfected into NSC-34 (Cashman NR et al. 1992) cells using FuGene (Invitrogen). A construct encoding the *Renilla* luciferase gene (pRL SV40; Promega) was added to each transfection as a normalization control. After 24 hours, luciferase activity was assessed using a dual-luciferase system (Promega) according to the manufacturer's instructions. In addition, the constructs used in the luciferase assay for chapter 5 were a full-length *Nfix* expression construct (*Nfix* pCAGIG-IRES-GFP) and a *Renilla* luciferase construct cloned downstream of 575 base pairs of the promoter region of the mouse *Gdnf* gene (*Gdnf* Prom). DNA was transfected into Neuro2A cells using FuGene (Invitrogen). A construct encoding the *Cypridina* luciferase gene was added to each transfection as a normalization control. After 48 hours, luciferase activity was measured using a dual luciferase system (Switchgear Genomics). Within each experiment, each treatment was replicated 6 times. Each experiment was also independently replicated a minimum of three times. The pCAGIG vector alone did not significantly alter *Gdnf*-promoter driven luciferase activity (data not shown). Statistical analyses were performed using an ANOVA in both chapters. Error bars represent the standard error of the mean.

2.9 *In utero* electroporation

E13 CD-1 pregnant mice were anesthetized with 1 mg/ml of zylazine and 15 mg/ml ketamine in sterile phosphate buffered saline at 0.07mg/g body weight [diluted in saline; (Parnell Laboratories Aust. Pty. Ltd., Sydney Australia and Troy Laboratories Pty Ltd., Sydney Australia respectively)] and then placed on a heat pad to maintain the body temperature of the animal. After the induction of anesthesia, the mice were subjected to abdominal incision to expose the uterine horns. A pulled glass microcapillary pipette attached to a Picospritzer II (Parker Hannifin, Hollis, NH) was used to perform the injections. The embryos were visualized through the uterine wall, and ~0.3 µl plasmid mixture containing 1.5 µg/µl plasmid DNA (pCAGIG IRES GFP or *Nfix* pCAGIG IRES GFP) plus 0.025% fast green, diluted in

phosphate buffered saline, was injected into the lateral ventricle of the embryo using a fine glass capillary. Fast Green was added to the plasmid mixture to visualize the distribution of the plasmids during injection. Using forceps-shaped electrodes, five 30 volt electric pulses were applied, each separated by a 1 second interval. The electrodes were placed such that the DNA was targeted for electroporation into the VZ of the neocortex. The uterine horns were repositioned into the abdominal cavity and the abdominal wall and skin were sutured. The electroporated pups were perfused three days later at E16 and the brains were sectioned coronally and visualized under a fluorescence microscope to ensure successful electroporation. The expression of GFAP was then ascertained using the DAB immunohistochemical protocols described above. For the vector only controls (n = 20), no GFAP staining was observed within the neocortex. For those pups successfully electroporated with the *Nfix* expression construct (n = 16), all exhibited precocious expression of GFAP within the region overexpressing NFIX.

2.10 Neurosphere assay

Brains of P15 wild type and *Nfix*$^{-/-}$ mice were isolated and manually sectioned coronally. The SVZ was then carefully removed using forceps, then chopped into fine pieces before enzymatic digestion was performed by incubation in 0.05% trypsin at 37°C for 15 minutes, a process that culminated in a single cell suspension. After centrifugation at 700 rpm for 5 minutes, cells were carefully dissociated and resuspended in 5 ml of pre-warmed neurosphere medium containing 20 ng/ml of epidermal growth factor (EGF), 10 ng/ml of basic fibroblast growth factor (FGF) and 3.5 μg/ml of heparin. The cell suspension was then run through a 50μm filter. The primary tissue was plated at a concentration of 2.5 x10^5 cells in 5 ml of medium in a T-25 flask for 7 days. The total number of spheres that had formed was counted after 7 days, as was sphere diameter. The neurospheres were then dissociated and passaged at

a constant density of 2.5 x10^5 cells in 5 ml of medium and then counted 7 days later. This was then repeated for another 5 more passages.

2.10.1 Neurosphere migration assay

To evaluate the contribution of NFIX during migration, floating *Nfix*$^{-/-}$ and *Nfix* wild type passage 4 neurospheres of similar diameter (100 to 200 μm) were seeded onto cover slip coated with poly-L-ornithine (10 mg/ml) and placed into a 6-well plates containing DMEM-F12 (with 5% FBS and 1% penicillin and streptomycin (gibco, life technology)). The spheres were cultured for 3 days at 37°C. After 3 days, the adherent neurospheres were fixed with 4% PFA, rinsed in PBS and blocked with solution containing 0.02% goat serum and 0.002% triton®X100 (MP Biomedicals) in PBS for 1 hour. The cells were washed three times in PBS and incubated in rabbit anti-DCX antibody (1:1000, Abcam, AB18723) at 4^{O}C overnight. The cells were washed with PBS and incubated with goat anti-rabbit Alexa fluor 488 (1:500, Invitrogen) antibodies at room temperature for 1 hour and washed with PBS again. Cell nuclei were stained in PBS containing DAPI (5 μg/ml). The coverslips were washed, mounted with Dako fluorescent mounting medium and examined under a fluorescence microscope (Zeiss). The migration distance of all the radially migrating cells were measured with ImageJ and averaged (n=5).

2.11 BrdU labelling

2.11.1 *In vivo* BrdU incorporation assay

P8 wild type and *Nfix*$^{-/-}$ mice were intraperitoneally injected with BrdU (Invitrogen) at 100 mg/kg. After 5 days, the animals were transcardially perfused with 0.9% saline, followed by 4% PFA, and then postfixed in 4% PFA at 4°C. Brains were removed and sectioned coronally at 50 μm using a vibratome. Antigen retrieval was performed by incubating

sections in 2N HCl for 45 minutes. Immunohistochemistry was then performed as described above. To quantify BrdU-positive cells in the SVZ, RMS and ependymal cell layer, sections at equivalent rostro-caudal positions were imaged, and the total number of BrdU-positive cells in a 200 μm^2 region was counted for both wild type and *Nfix*$^{-/-}$ mice. To quantify BrdU-positive cells in the granule cell layer of the olfactory bulb, the number of immunopositive cells per 200 μm within the glomerular layer was counted, using representative sections from lateral, medial, dorsal and ventral regions of the respective olfactory bulbs. In all cases, at least 5 wild type and 5 *Nfix*$^{-/-}$ brains were used for quantification. Quantification was performed blind to the genotype of the sample, and statistical analyses were performed using a two-tailed unpaired *t*-test. Error bars represent the standard error of the mean.

2.12 Quantification of SVZ size and cell numbers

To measure the area of the SVZ and RMS in postnatal wild type and *Nfix*$^{-/-}$ brains, coronal sections at equivalent rostro-caudal positions were either immunostained or hematoxylin-stained, and imaged with an upright microscope coupled to AxioVision software (Zeiss). The cross-sectional area of the SVZ, rostral SVZ and RMS in both wild type and *Nfix*$^{-/-}$ samples was then calculated. Similarly, to quantify the number of cleave caspase-3 (CC3)-, phosphor-histone H3 (PHH3)- and 5-bromo-2'-deoxyuridine (BrdU)-positive cells within the SVZ of P10 wild type and *Nfix*$^{-/-}$ mice, sections were immunolabelled with the respective antibodies, then imaged. The total number of immunopositive cells within the SVZ was counted, and are presented here as immunopositive cells per mm^2 of the SVZ. To quantify proliferating neuroblasts within the SVZ, P20 wild type and *Nfix*$^{-/-}$ sections, immunofluorescence staining against the markers DCX and Ki67 was performed. Nuclei were also labelled with DAPI. Sections were then imaged using a confocal microscope at the level of the SVZ. For each frame, the total number of DCX-positive cells was quantified, as was the number of cells positive for both DCX and Ki67. Data are presented as the number of cells expressing both DCX and Ki67 as a proportion of the total number of cells expressing DCX. To quantify

interneuron populations within the olfactory bulb, P20 *Nfix* wild type and *Nfix*$^{-/-}$ olfactory bulbs were sectioned coronally on a vibratome, and immunostaining was used to identify interneurons expressing PAX6, calbindin or calretinin. Sections were then imaged, and the number of immunopositive cells per 100 μm within the glomerular layer and granule cell layer was counted, using representative sections from lateral, medial, dorsal and ventral regions of the respective olfactory bulbs. In all cases, at least 5 wild type and 5 *Nfix*$^{-/-}$ brains were used for quantification. Quantification was performed blind to the genotype of the sample, and statistical analyses were performed using a two-tailed unpaired *t*-test. Error bars represent the standard error of the mean.

2.13 Hippocampal and SVZ/RMS microarrays

Hippocampal and SVZ/RMS tissue samples from E16 and P20 *Nfix*$^{-/-}$ mice (n=3) and wild type littermate controls (n=3) were collected. Total RNA was extracted, and the microarray analysis performed at the Australian Research Council Special Research Centre for Functional and Applied Genomics (The University of Queensland, Australia) as described previously (Piper M *et al.* 2010). Labelled and amplified material (1.5 μg/sample) was hybridized to Illumina's MouseWG-6 v2.0 Expression BeadChip at 55°C for 18 h according to the Illumina BeadStation 500X™ protocol. Arrays were washed and then stained with 1 μg/ml cyanine3-streptavidin (Amersham Biosciences). The Illumina BeadArray™ reader was used to scan the arrays according to the manufacturer's instructions. Samples were initially evaluated using the BeadStudio™ software from Illumina. Quality control reports were satisfactory for all samples. The raw data were then imported into GeneSpring GX v7.3 (Agilent). Data were initially filtered using GeneSpring normalization algorithms. Quality control data filtering was then performed using the Bead detection score *p*-value, and with expression values below background, as determined by the cross-gene error model. Differential expression was determined by the one-way ANOVA-Welch's approximate *t*-test

without a multiple testing correction. A cut-off *p*-value of 0.05 was used for the mean difference between wild type and *Nfix*$^{-/-}$ hippocampal tissue. In addition, a 1.5-fold-change filter was imposed on the genes from the ANOVA data set. The full array data set is listed in Supplementary Table 1. Pathway analysis was performed using the DAVID Bioinformatics Resources 6.7 (http://david.abcc.ncifcrf.gov/) (Huang da W et al. 2009).

2.14 Bioinformatic promoter screen

Potential NFI binding site were identified by Dr Timothy Bailey and Dr Robert McLeay (IMB, University of Queensland) in chapter 3, and Dr Michael Piper (SBMS, University of Queensland) and Dr Timothy Bailey (IMB, University of Queensland) in chapter 4 and 5. The NFI binding motif was generated as reported previously (Heng YH et al. 2012) from published chromatin immunoprecipitation-sequencing (ChIP-seq) data for NFI (pan-NFI antibody used) (Pjanic M et al. 2011). The DNA-binding domains of all NFI proteins are highly similar (Mason et al., 2009). In brief, we performed motif discovery using the MEME algorithm (Bailey TL et al. 2009) on ChIP-seq peaks redeclared using the ChIP-Peak algorithm (Schmid CD and P Bucher 2010) from the published ChIP-seq "tag" data for NFI. We then identified potential NFI binding sites by scanning the complete mouse genome downloaded from the UCSC Genome Browser (mm9, July 2007) (Fujita PA et al. 2011) using the MEME-derived motif and the FIMO motif-scanning program (Grant CE et al. 2011). FIMO was run on the mouse genome (without repeat masking) using a 0-order background generated on the entire mouse genome, and a pseudocount of 0.1. All potential binding sites with *p*-value $\leq 10^{-4}$ were reported in the region of -3000 base pairs to +200 base pairs relative to the transcription start site. Putative NFI binding sites near the promoters of genes were identified by viewing the FIMO output using the UCSC genome browser.

2.15 Microscopy

Bright field and Fluorescence images were acquired with an upright Axio-Imager Z1 ® (Carl Zeiss, Gremany) microscope fitted with a motorized stage, AxioCam® HRc camera, and

AxioVisionTM 4.7 with MosaiX software (Carl Zeiss, Göttingen, Gremany). Confocal images were acquired using an upright Axio-Imager Z1 point scanning laser confocal microscope with spectral detection. Images were then cropped, sized and contrasted for presentation with Adobe Photoshop and Adobe Illustrator softwares.

CHAPTER 3

To determine if *Nfix* is required for the development of the hippocampus both embryonically and postnatally, in particular the role played by *Nfix* in regulating progenitor cell differentiation.

The data contained in the following chapter was published in January 2014 in *Cerebral Cortex*

Yee Hsieh Evelyn Heng, Robert C. McLeay, Tracey J. Harvey, Aaron G. Smith, Guy Barry, Kathleen Cato, Céline Plachez, Erica Little, Sharon Mason, Chantelle Dixon, Richard M. Gronostajski, Timothy L. Bailey, Linda J. Richards and Michael Piper. 2014. NFIX regulates neural progenitor cell differentiation during hippocampal morphorgenesis.
Cerebral Cortex January 2014; 24: 261-279

3.0 Aims of chapter

Preliminary studies have been conducted in *Nfix* knockout mice to investigate the role of *Nfix* in the developing and postnatal brain (Campbell CE et al. 2008). This study revealed that NFIX is expressed in the developing cortex and hippocampus, and within the neurogenic niches of the adult brain. Importantly, expression was observed by neural progenitor cells within the VZ of the embryonic neocortex and hippocampus, the radial glia, suggesting a role for NFIX in mediating radial glial cell biology during neocortical and hippocampal morphogenesis. The phenotype of mice lacking *Nfix* was supportive of this theory, with *Nfix* knockout mice displaying severe morphological abnormalities of the forebrain, including a severely distorted hippocampus (Campbell CE et al. 2008). I hypothesised that the malformation of the hippocampus in these mice could be the result of abnormal radial glial proliferation and differentiation during development. Other NFI members, including NFIA and NFIB, have previously been shown to promote radial glial differentiation within the dorsal telencephalon (Piper M et al. 2010) and to drive the expression of astrocytic genes, but the specific role of NFIX during the formation of the hippocampus had yet to be investigated. The goal of this chapter of my thesis was to investigate the molecular mechanisms by which NFIX regulates the formation of the hippocampus during development of this structure. The findings of this chapter were recently published in *Cerebral Cortex* (Heng YH et al., 2014).

With regards to this work published in this manuscript, I did the majority of the experiments and performed the bulk of the quantification of the phenotype. I also wrote the first draft of the manuscript, and assembled the majority of the data into Figures for the paper. The work that was performed by other researchers for this manuscript is described below:

-**Table 1.** Microarray analysis of E16 *Nfix* knockout and wild type hippocampus were performed by Dr Sharon Mason (Previous PhD student under Prof Linda Richards, QBI, University of Queensland).

-**Figure 10.** DAVID analysis of functional classification of gene misregulated within the hippocampus of E16 was performed by Dr Michael Piper.

-**Figure 11E.** Potential NFI binding sites were identified by Dr Timothy Bailey and Dr. Robert McLeay (IMB, University of Queensland).

-**Figure 11F.** Electrophoretic mobility shift assay (EMSA) and supershift assays were conducted by Dr Aaron Smith (SBMS, University of Queensland).

-**Figure 11D and H**. qPCR and Luciferase assay were done in association Dr Tracey Harvey (SBMS, University of Queensland).

Cerebral Cortex January 2014;24:261–279
doi:10.1093/cercor/bhs307
Advance Access publication October 4, 2012

NFIX Regulates Neural Progenitor Cell Differentiation During Hippocampal Morphogenesis

Yee Hsieh Evelyn Heng[1], Robert C. McLeay[3], Tracey J. Harvey[1], Aaron G. Smith[1], Guy Barry[2], Kathleen Cato[1], Céline Plachez[4], Erica Little[2], Sharon Mason[2], Chantelle Dixon[1], Richard M. Gronostajski[5], Timothy L. Bailey[3], Linda J. Richards[1,2] and Michael Piper[1,2]

[1]The School of Biomedical Sciences, [2]Queensland Brain Institute, [3]Institute for Molecular Bioscience, The University of Queensland, Brisbane, Queensland, Australia, [4]School of Medicine, The University of Maryland, Baltimore, MD, USA and [5]Department of Biochemistry and the Program in Neuroscience, Developmental Genomics Group, New York State Center of Excellence in Bioinformatics and Life Sciences, State University of New York at Buffalo, Buffalo, NY, USA

Address correspondence to M. Piper, The School of Biomedical Sciences and the Queensland Brain Institute, The University of Queensland, Brisbane 4072, Queensland, Australia. Email: m.piper@uq.edu.au

Neural progenitor cells have the ability to give rise to neurons and glia in the embryonic, postnatal and adult brain. During development, the program regulating whether these cells divide and self-renew or exit the cell cycle and differentiate is tightly controlled, and imbalances to the normal trajectory of this process can lead to severe functional consequences. However, our understanding of the molecular regulation of these fundamental events remains limited. Moreover, processes underpinning development of the postnatal neurogenic niches within the cortex remain poorly defined. Here, we demonstrate that Nuclear factor one X (NFIX) is expressed by neural progenitor cells within the embryonic hippocampus, and that progenitor cell differentiation is delayed within *Nfix*$^{-/-}$ mice. Moreover, we reveal that the morphology of the dentate gyrus in postnatal *Nfix*$^{-/-}$ mice is abnormal, with fewer subgranular zone neural progenitor cells being generated in the absence of this transcription factor. Mechanistically, we demonstrate that the progenitor cell maintenance factor Sry-related HMG box 9 (SOX9) is upregulated in the hippocampus of *Nfix*$^{-/-}$ mice and demonstrate that NFIX can repress *Sox9* promoter-driven transcription. Collectively, our findings demonstrate that NFIX plays a central role in hippocampal morphogenesis, regulating the formation of neuronal and glial populations within this structure.

Keywords: glia, glial fibrillary acidic protein, neural progenitor cell, nuclear factor one X, SOX9

Introduction

During nervous system formation, one of the most important developmental events to occur is the differentiation of neural progenitor cells into neurons and glia. The embryonic forebrain provides a cogent example of this, with neural progenitor cells within the proliferative ventricular zone, region executing a program of proliferation, then differentiation, to generate the postmitotic cells of the cortex and hippocampus (Sauvageot and Stiles 2002). The abnormal proliferation or differentiation of cortical neural progenitor cells during development can lead to severe functional consequences, such as lissencephaly and microcephaly, both of which can cause mental retardation (Manzini and Walsh 2011). As such, understanding the regulatory processes controlling whether neural progenitor cells either divide and self-renew or exit the cell cycle and differentiate is critical to our understanding of both normal and pathological cortical development.

A number of recent studies have begun to elucidate some of the key molecules and signaling pathways that control how neural progenitor cell proliferation and differentiation is coordinated during development. Examples include the Notch (Shimojo et al. 2008; Imayoshi et al. 2010), fibroblast growth factor (Sahara and O'Leary 2009; Rash et al. 2011), and Sonic hedgehog (SHH; Komada et al. 2008) signaling pathways, all of which have been implicated in regulating progenitor cell identity during development of the cortex. Transcription factors of the Sry-related HMG box (SOX) family have also been shown to play a role in the maintenance of progenitor cell identity (Stolt and Wegner 2010). For instance, both SOX2 and SOX3 are expressed by neural progenitor cells within the developing and adult forebrain (Avilion et al. 2003; Wang et al. 2006), and SOX2 has been implicated in maintaining progenitor cell identity within the developing neocortex (Bani-Yaghoub et al. 2006) and the adult hippocampus (Suh et al. 2007). Another suite of molecules known to play a role in regulating the differentiation of neural progenitor cells are the transcription factors of the Nuclear factor one (NFI) family (Piper et al. 2007; Mason et al. 2009), which in vertebrates comprises 4 members; *Nfia*, *Nfib*, *Nfic*, and *Nfix* (Rupp et al. 1990; Kruse et al. 1991). Mice lacking either *Nfia* or *Nfib* display neurological phenotypes including dysgenesis of the corpus callosum (Shu, Butz, et al. 2003; Shu, Puche, et al. 2003; Piper, Moldrich, et al. 2009; Piper, Plachez, et al. 2009), hippocampal malformation (Barry et al. 2008; Piper et al. 2010), and delays in cerebellar development (Steele-Perkins et al. 2005; Wang et al. 2007). Mechanistically, *Nfi* genes have been implicated in regulating glial development via promoting the expression of astrocyte-specific genes (Gopalan et al. 2006; Brun et al. 2009), and *Nfia* and *Nfib* were recently shown to promote progenitor cell differentiation in a complementary fashion within the developing telencephalon through the repression of the Notch signaling pathway (Piper et al. 2010).

Nfix$^{-/-}$ mice also display severe neurological phenotypes (Driller et al. 2007; Campbell et al. 2008), and NFIX has previously been implicated in driving the expression of astrocytic genes during neural development (Gopalan et al. 2006; Piper et al. 2011). However, the mechanism by which NFIX regulates morphogenesis of the nervous system in vivo remains undefined. Here, using the developing hippocampus of *Nfix*$^{-/-}$ mice as a model, we reveal that NFIX regulates the differentiation of neural progenitor cells through the transcriptional regulation of progenitor-specific pathways. Our data demonstrate that *Nfix*$^{-/-}$ mice display delayed progenitor cell differentiation, which culminates in deficits in both neuronal and glial formation. Moreover, the formation of progenitor cells within the postnatal dentate gyrus is abnormal in *Nfix*$^{-/-}$

mice. Finally, we show that SOX9, a central mediator of progenitor cell self-renewal that acts downstream of SHH signaling during corticogenesis (Scott et al. 2010), is a target for transcriptional repression by NFIX. Taken together, these data reveal a central role for NFIX in orchestrating the timely differentiation of neural progenitor cells within the embryonic hippocampus and for regulating the development of neural progenitor cells within the subgranular zone of the postnatal dentate gyrus.

Materials and Methods

Mouse Strains

Nfix$^{+/+}$ and *Nfix*$^{-/-}$ littermate mice were used for the majority of this study. These mice were maintained on a C57Bl/6J background. These animals were bred at the University of Queensland under approval from the institutional animal ethics committee. Timed-pregnant females were obtained by placing *Nfix*$^{+/-}$ male and *Nfix*$^{+/-}$ female mice together overnight. The following day was designated as embryonic day (E)0 if the female had a vaginal plug. Embryos were genotyped by polymerase chain reaction (PCR; Campbell et al. 2008). For the in utero electroporation experiments, wild-type CD-1 mice were used.

Hematoxylin Staining

Brains from wild-type or *Nfix*$^{-/-}$ embryos were dissected from the skull, blocked in 3% noble agar (Difco, Sparks, MS), and sectioned coronally at 50 μm on a vibratome (Leica, Nussloch, Germany). Sections were then mounted and stained with Mayer's hematoxylin using standard protocols.

Immunohistochemistry

Embryos and postnatal pups were drop fixed in 4% paraformaldehyde (PFA; E14 and below) or transcardially perfused with 0.9% saline, followed by 4% PFA (E15 to postnatal day [P] P20), and then postfixed in 4% PFA at 4 °C. Brains were removed and sectioned at 50 μm using a vibratome. Immunohistochemistry using the chromogen 3,3′-diaminobenzidine was performed as described previously (Plachez et al. 2008). Biotin-conjugated goat antirabbit IgG (BA-1000, Vector Laboratories, Burlingame, CA, United States of America) and donkey antimouse IgG (715-065-150, Jackson ImmunoResearch Laboratories, West Grove, PA, United States of America) secondary antibodies were used for chromogenic immunohistochemistry at 1/1000. For all immunohistochemical analyses, at least 3 wild-type and *Nfix*$^{-/-}$ brains were analyzed. Sections from comparable positions along the rostrocaudal axis were imaged using an upright microscope (Zeiss upright Axio-Imager Z1) fitted with an Axio-Cam HRc camera.

Immunohistochemistry on Paraffin Sections

Brains were perfused as above, embedded in paraffin, and sectioned coronally at 6 μm. Hematoxylin staining and immunohistochemistry were performed as described previously (Barry et al. 2008).

Antibody Parameters

Primary antibodies used for immunohistochemistry on floating sections were anti-NFIX (rabbit polyclonal, 1/10 000; Active Motif, Carlsbad, CA, United States of America); anti-TBR2 (rabbit polyclonal, 1/10 000, a gift from Dr Robert Hevner, University of Washington, Seattle, WA, United States of America); anti-GLAST (rabbit polyclonal, 1/50 000, a gift from Dr Niels Danbolt, University of Oslo, Oslo, Norway); anti-glial fibrillary acidic protein (GFAP) (rabbit polyclonal, 1/15 000, Dako, Glostrup, Denmark); anti-TBR1 (rabbit polyclonal, 1/100 000, a gift from Dr Robert Hevner); anti-prospero-related homeobox 1 (PROX1; rabbit polyclonal, 1/25 000, Millipore Bioscience Research Reagents, Billerica, MA, United States of America); anti-calbindin (rabbit polyclonal, 1/50 000, SWANT, Marly, Switzerland); anti-calretinin (rabbit polyclonal, 1/50 000, SWANT); anti-reelin (mouse monoclonal, 1/100 000, a gift from Dr Andre Goffinet, University of Louvain Medical School, Brussels, Belgium); anti-SOX2 (rabbit polyclonal, 1/1000; Cell Signaling Technology, Danvers, MA, United States of America); anti-cleaved caspase-3 (rabbit polyclonal, 1/5000, Cell Signaling Technology); anti-nestin (mouse monoclonal, 1/1500, Developmental Studies Hybridoma Bank); and anti-tenascin C (rabbit polyclonal, 1/5000, Millipore Bioscience Research Reagents). Primary antibodies used for immunohistochemistry on paraffin sections were anti-PAX6 (rabbit polyclonal, 1:1000; Millipore Bioscience Research Reagents), anti-SOX2 (1:1000), anti-SOX9 (rabbit polyclonal, 1:1000; a gift from Dr Peter Koopman, Institute for Molecular Bioscience, University of Queensland, Brisbane, Australia), and anti-phosphohistone H3 (rabbit polyclonal, 1:1000; Millipore Bioscience Research Reagents).

Quantification of Ventricular Zone Width/Hippocampal Cell Counts

To measure the ventricular zone width in E14–18 wild-type and *Nfix*$^{-/-}$ brains, sections were hematoxylin-stained and imaged with an upright microscope coupled to AxioVision software (Zeiss). The width of the ventricular zone was measured at 3 points along the hippocampus for each section. Data for both wild-type and knockout hippocampi at each age were then pooled for the comparison of ventricular zone width. For phosphohistone H3-, PAX6-, SOX2-, TBR2-, and SOX9-expressing cell counts, the total number of immunopositive cells per 100 μm in the ventricular zone or subventricular zone of each hippocampus was counted. For PROX1-expressing cell counts performed embryonically, the total number of PROX1-positive cells in the emerging dentate gyrus was counted. For postnatal animals, sections were labeled with fluorescent secondary antibodies and imaged with a confocal microscope (Zeiss LSM 510 META) using Zen software (Zeiss). The number of PROX1-positive cells per 100 μm in the upper and lower blades of the dentate gyrus of wild-type or *Nfix*$^{-/-}$ hippocampi was then counted. For all experiments involving quantification, data represent pooled results from at least 5 wild-type and 5 *Nfix*$^{-/-}$ brains. For all cell counts, we also measured the size of the nucleus to determine whether there was a difference between genotypes (Guillery 2002). As no size differences were noted, we did not apply the Abercrombie correction factor. Quantification was performed blind to the genotype of the sample, and statistical analyses were performed using a 2-tailed unpaired *t*-test. Error bars represent the standard error of the mean.

In Situ Hybridization

Embryos were collected and fixed as described above ($n = 3$ for both wild-type and knockout). In situ hybridization was performed using antisense probes as previously described (Piper, Moldrich, et al. 2009; Piper, Plachez, et al. 2009) with minor modifications. The hybridization temperature was 70 °C. The color reaction solution was BM Purple (Roche). In situ probes were kindly provided by Dr Shubha Tole (Tata Institute of Fundamental Research, Mumbai, India).

Hippocampal Microarrays

Hippocampal samples from E16 *Nfix*$^{-/-}$ mice ($n = 3$) and wild-type littermate controls ($n = 3$) were collected. Total RNA was extracted, and the microarray analysis performed at the Australian Research Council Special Research Centre for Functional and Applied Genomics (The University of Queensland, Australia) as described previously (Piper et al. 2010). Labeled and amplified material (1.5 μg/sample) was hybridized to Illumina's MouseWG-6 v2.0 Expression BeadChip at 55 °C for 18 h according to the Illumina BeadStation 500X™ protocol. Arrays were washed and then stained with 1 μg/mL cyanine3-streptavidin (Amersham Biosciences). The Illumina BeadArray™ reader was used to scan the arrays according to the manufacturer's instructions. Samples were initially evaluated using the BeadStudio™ software from Illumina. Quality control reports were satisfactory for all samples. The raw data were then imported into GeneSpring GX v7.3 (Agilent). Data were initially filtered using

GeneSpring normalization algorithms. Quality control data filtering was then performed using the Bead detection score *P*-value, and with expression values below background, as determined by the cross-gene error model. Differential expression was determined by the 1-way analysis of variance (ANOVA)-Welch's approximate *t*-test without a multiple testing correction. A cut-off *P*-value of 0.05 was used for the mean difference between wild-type and *Nfix*$^{-/-}$ hippocampal tissue. In addition, a 1.5-fold–change filter was imposed on the genes from the ANOVA data set. The full array data set is listed in Supplementary Table 1. Pathway analysis was performed using the DAVID Bioinformatics Resources 6.7 (http://david.abcc.ncifcrf.gov/) (Huang da et al. 2009). The full data sets from this analysis are listed in Supplementary Tables 2 and 3.

Reverse Transcription and Quantitative Real-Time PCR

For quantitative real-time PCR (qPCR), hippocampi were dissected and samples were then snap frozen. Total RNA was extracted using an RNeasy Micro Kit (Qiagen). Reverse transcription was performed using Superscript III (Invitrogen). Total RNA (0.5 μg) was reverse transcribed with random hexamers. qPCR reactions were carried out in a Rotor-Gene 3000 (Corbett Life Science) using the SYBR Green PCR Master Mix (Invitrogen). All the samples were diluted 1:100 with RNase/DNase-free water and 5 μL of these dilutions were used for each SYBR Green PCR reaction containing 10 μL SYBR Green PCR Master Mix, 10 μM of each primer, and deionized water. The reactions were incubated for 10 min at 95 °C followed by 40 cycles with 15 s denaturation at 95 °C, 20 s annealing at 60 °C, and 30 s extension at 72 °C.

Generation of Gene-Specific Quantitative qPCR Standards

The synthesis of these primers was performed by Sigma-Genosys. The following primer sequences were used:

Sox9 forward (CTCACATCTCTCCTAATGCT).
Sox9 reverse (GACCCTGAGATTGCCCAGA).
Hprt forward (GCAGTACAGCCCCAAAATGG).
Hprt reverse (AACAAAGTCTGGCCTGTATCCAA).

qPCR Data Expression and Analysis

After completion of the PCR amplification, the data were analyzed with the Rotor-Gene software. When quantifying the mRNA expression levels, the housekeeping gene *HPRT* was used as a relative standard. By means of this strategy, we achieved a relative PCR kinetic of standard and sample. For all qPCR analyses, RNA from 3 independent replicates for both wild-type and *Nfix*$^{-/-}$ mice or control and treated cells were interrogated. All the samples were tested in triplicate, and each experiment was repeated a minimum of 3 times. Statistical analyses were performed using a 2-tailed unpaired *t*-test. Error bars represent the standard error of the mean.

Electrophoretic Mobility Shift Assay

Total cortex was removed from E18 brains to isolate nuclear extracts. Nuclear extracts were also isolated from COS cells expressing an HA-tagged NFIX expression construct (*Nfix* pCAGIG IRES GFP). Protease inhibitor tablets (Roche) were added to the extraction buffers as previously described (Smith et al. 1998). Electrophoretic mobility shift assays (EMSAs) were performed using radiolabeled annealed oligonucleotides containing a control NFI consensus site or the putative *Sox9* consensus sites, which were designated −675, −183, +415, and +598. EMSA reactions were carried out as described previously using 1 μg of nuclear extract and 1 μg of poly-[dI-dC] as nonspecific competitor per reaction (Smith et al. 1998). Oligonucleotide sequences were: NFI control, 5′-ggTTTTGGATTGAAGCCAATATGATAA-3′ (upper strand), 5′-ggTTATCATATTGGCTTCAATCCAAAA-3′ (lower strand); −675, 5′-ccgggGCAGAAGCTCCAGTCACCACACCAGCTTCGTTGAAc-3′ (upper strand); 5′-ccgggTTCAACGAAGCTGGTGTGGTGACTGGAGCTTCTG Cc-3′(lower strand); −183, 5′-ccgggCATCCACCCTCTGGCTGAGCTCC CCTCCCTTCTCCc-3′ (upper strand); 5′-ccgggGGAGAAGGGAGGGGA GCTCAGCCAGAGGGTGGATGc-3′(lower strand); +415, 5′-ccgggGACC GACGAGCAGGAGAAGGGCCTGTCTGGCGCCCc-3′ (upper strand); 5′-ccgggGGGCGCCAGACAGGCCCTTCTCCTGCTCGTCGGTCc-3′(lower strand). +598, 5′-ccgggGTGCATCCGCGAGGCGGTCAGCCAGGTGCTG AAGGc-3′ (upper strand); 5′-ccgggCCTTCAGCACCTGGCTGACCGCC TCGCGGATGCACc-3′ (lower strand). Additional bases used to generate 5′ overhangs for endfill are indicated in lower case.

Luciferase Reporter Assay

The constructs used in the luciferase assay were a full-length *Nfix* expression construct driven by the chick β-actin promoter (*Nfix* pCAGIG IRES GFP), and a construct containing the +598 site derived from the mouse *Sox9* coding sequence (a gift from Peter Koopman; Kent et al. 1996). This construct was 250 base pairs in length and was generated using the following primers: Forward 5′-CTCGAGTCT CCTGGACCCCTTC-3′; reverse 5′-AAGCTTCAGCACCTGGCTGACC-3′. A construct containing a mutated NFI consensus sequence was generated in parallel, using an alternative reverse primer: 5′-AAGCTTCAG-CACTGGTATGACCGC-3′. The resulting construct, termed *Sox9ΔNFI*, possessed an NFI-binding site that was changed from GAGGCGGT-CAGCCAG to GAGGCGGTCATACCA. The amplicons were inserted into the XhoI and HindIII restriction enzyme sites of the pGL4.23 luc2minP vector (Promega, Madison, WI, United States of America). DNA was transfected into NSC-34 (Cashman et al. 1992) cells using FuGene (Invitrogen). Renilla luciferase (pRL SV40; Promega) was added to each transfection as a normalization control. After 24 h, luciferase activity was assessed using a dual-luciferase system (Promega) as per the manufacturer's instructions. Within each experiment, each treatment was replicated 6 times. Each experiment was also independently replicated a minimum of 3 times. Statistical analyses were performed using an ANOVA. Error bars represent the standard error of the mean.

Bioinformatic Promoter Screen

To obtain an NFI binding site motif, data from a recent study identifying NFI-binding sites in vivo using chromatin immunoprecipitation (ChIP) sequencing (Pjanic et al. 2011) were analyzed. NFI peaks were called using ChIP-Peak (Schmid and Bucher 2010) with the following parameters: Server-resident SGA file: mm9/nf1_wt.sga; strand: Any; centering: 75 bp; repeat masker: Checked; window width: 300 bp; vicinity range: 300 bp; peak threshold: 8; count cut-off: 1; refine peak positions: Checked. The NFI motif was created by running MEME (Bailey et al. 2009) on the sequences of 600 of the 708 peak regions declared by ChIP-Peak. The 600 regions were each trimmed to 100 base pairs in width, and chosen randomly from among the 708. MEME was run with parameters: -dna -minw 6 -maxw 30 -revcomp. Potential NFI binding sites were then identified in the promoter region of *Sox9* using FIMO (Grant et al. 2011). The *Sox9* promoter sequence, which we defined as the region 1000 base pairs either side of the transcription start site (TSS), was downloaded from the UCSC Genome Browser (mm9, July 2007; Fujita et al. 2011). FIMO was run on the *Sox9* promoter sequence using a zero-order background generated on all mouse promoter regions, and a pseudocount of 0.1. All potential binding sites with *P*-value $\leq 10^{-3}$ were reported.

In Utero Electroporation

E13 CD-1 pregnant mice were anesthetized with 1 mg/mL of zylazine and 15 mg/mL ketamine in sterile phosphate-buffered saline. After the induction of anesthesia, the mice were subjected to abdominal incision to expose the uterine horns. The embryos were visualized through the uterus wall, and ∼0.3 μL plasmid mixture containing 1.5 μg/μL plasmid DNA (pCAGIG IRES GFP or *Nfix* pCAGIG IRES GFP) plus 0.025% fast green, diluted in phosphate-buffered saline, was injected into the lateral ventricle using a fine glass capillary. Using forceps-shaped electrodes, five 30 V electric pulses were applied, each separated by a 1-s interval. The electrodes were placed such that the DNA was targeted for electroporation into the ventricular zone of the neocortex. The uterine horns were repositioned into the abdominal cavity, and the abdominal wall and skin were sutured.

The electroporated pups were perfused 3 days later at E16, and the brains were sectioned coronally, then stained with the nuclear marker 4′,6-diamidino-2-phenylindole (DAPI; 1:1000), and visualized under a fluorescence microscope to ensure successful electroporation. The expression of GFAP was then ascertained using the immunohistochemical protocols described above. For the vector only controls ($n = 20$), no GFAP staining was observed within the neocortex. For those pups successfully electroporated with the *Nfix* expression construct ($n = 16$), all exhibited precocious expression of GFAP within the region overexpressing NFIX.

Results

Embryonic Neural Progenitor Cells Within the Hippocampus Express NFIX

During telencephalic development, NFIX is expressed widely within both the cortex and the hippocampus (Campbell et al. 2008). At E13, NFIX was expressed by neural progenitor cells within the ventricular zone of the hippocampus, but not by cells within the cortical hem region (Fig. 1*A*,*B*). This expression pattern was maintained at E14, with progenitors within both the ammonic neuroepithelium and dentate neuroepithelium expressing this transcription factor (Fig. 1*C*,*D*). By E17, expression of NFIX within the hippocampus was widespread, encompassing cells within the *cornu ammonis* (CA) regions and the dentate gyrus, as well neural progenitor cells within the ventricular zone (Fig. 1*E*,*F*). NFIX has previously been linked to the regulation of astrocyte-specific genes including *Gfap*, brain fatty acid-binding protein, and α1-antichymotrypsin (Gopalan et al. 2006; Brun et al. 2009; Piper et al. 2011); however, our findings indicate that NFIX may also regulate transcriptional activity within neural progenitor cells in the developing hippocampus.

Hippocampal Neural Progenitor Cell Differentiation is Delayed in Nfix$^{-/-}$ Mice

We have previously shown that mice lacking *Nfix* display gross morphological abnormalities with regard to postnatal neocortical and hippocampal formation (Campbell et al. 2008), although the underlying mechanism by which *Nfix* regulates neural progenitor cell biology remains undefined. To address this issue, we first analyzed embryonic hippocampal development in *Nfix*$^{-/-}$ mice. Hematoxylin staining of E18 wild-type and *Nfix*$^{-/-}$ mice revealed that the dentate gyrus in the mutant was markedly reduced in size, and, moreover, that the size of the hippocampal ventricular zone in the mutant was significantly enlarged in comparison to that of wild-type controls (Figs 1*G*–*J* and 2*C*). These phenotypes were also evident 2 days earlier at E16, the time at which the dentate gyrus is becoming morphologically recognizable in the hippocampus of wild-type mice (Fig. 2*A*). In *Nfix*$^{-/-}$ mice at E16, the dentate gyrus had yet to develop at a morphological level (Fig. 2*B*), and the hippocampal ventricular zone was significantly wider than that in littermate controls (Fig. 2*C*).

These findings suggested that the balance between neural progenitor cell self-renewal and differentiation was abnormal in the absence of *Nfix*, culminating in the maintenance of progenitor cell proliferation for longer than in wild-type mice. To investigate this, we analyzed the expression of the neural progenitor cell-specific marker PAX6 (Gotz et al. 1998). At E14, there was no difference between hippocampal PAX6 expression in wild-type and *Nfix*$^{-/-}$ mice (data not shown). However, by E16, there were significantly more PAX6-expressing neural progenitor cells within the ventricular zone of *Nfix*$^{-/-}$ mice (Fig. 2*D*,*E*,*L*). Furthermore, the expression of a second marker for neural progenitor cells, SOX2 (Avilion et al. 2003; Suh et al. 2007), also revealed a significant

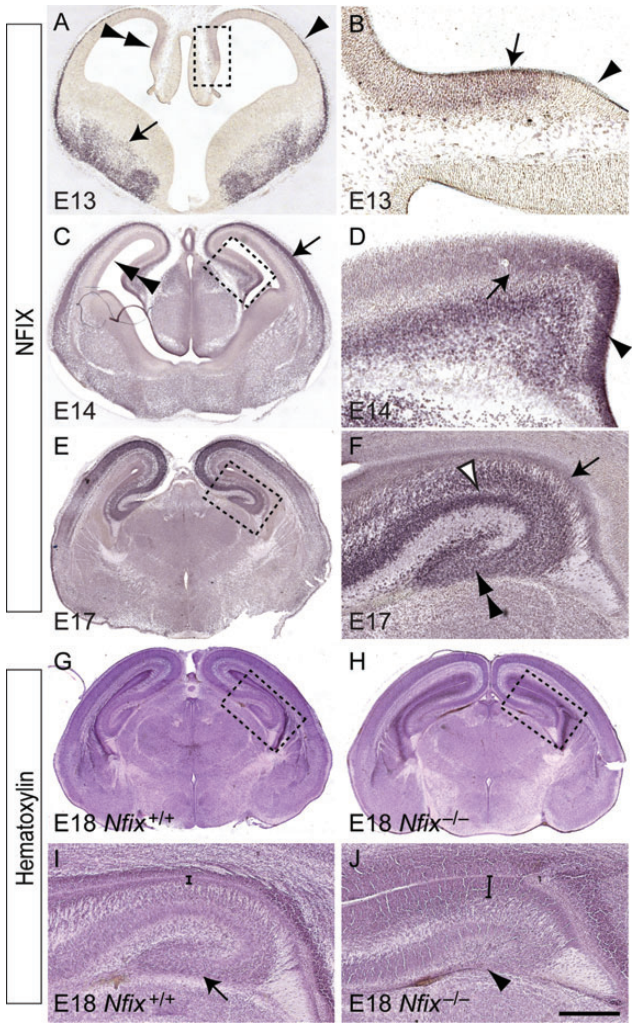

Figure 1. Expression of NFIX in the developing hippocampus. (*A*–*F*) Expression of NFIX in coronal sections of the embryonic hippocampus. (*A*) At E13, NFIX expression was observed within the hippocampus (double arrowhead), the marginal zone of the cortex (arrowhead), and the ventral telencephalon (arrow). (*B*) Higher magnification view of the boxed region in *A*. NFIX was expressed within the ammonic neuroepithelium (arrow), but was not expressed within the cortical hem (arrowhead). (*C*) At E14, NFIX expression was observed within the cortical plate (arrow) and ventricular zone (double arrowhead) of the neocortex. (*D*) Higher magnification view of the boxed region in *C*, showing expression of NFIX by progenitor cells within both the ammonic neuroepithelium (arrow) and the dentate neuroepithelium (arrowhead). (*E*) At E17, NFIX was expressed broadly within the dorsal telencephalon. (*F*) Higher magnification view of the boxed region in *E*. Within the E17 hippocampus, NFIX was expressed by ventricular zone progenitor cells (arrow) and by cells within the CA region (open arrowhead) and the dentate gyrus (double arrowhead). (*G*–*J*) Hematoxylin-stained coronal sections of E18 wild-type (*G*) and *Nfix*$^{-/-}$ (*H*) brains. (*I*) Higher magnification view of the boxed region in *G*, showing the distinctive shape of the dentate gyrus in the wild-type hippocampus (arrow in *I*). (*J*) Higher magnification view of the boxed region in *H*, demonstrating that the hippocampal ventricular zone was markedly wider within *Nfix*$^{-/-}$ brains (compare brackets in *I* and *J*) and that the dentate gyrus was severely reduced in the absence of this transcription factor (arrowhead in *J*). Scale bar (in *J*): *A*, 600 μm; *B*, 75 μm; *C*, 750 μm; *D*, 100 μm; (*E*, *G*, *H*), 1 mm; (*F*, *I*, *J*), 300 μm.

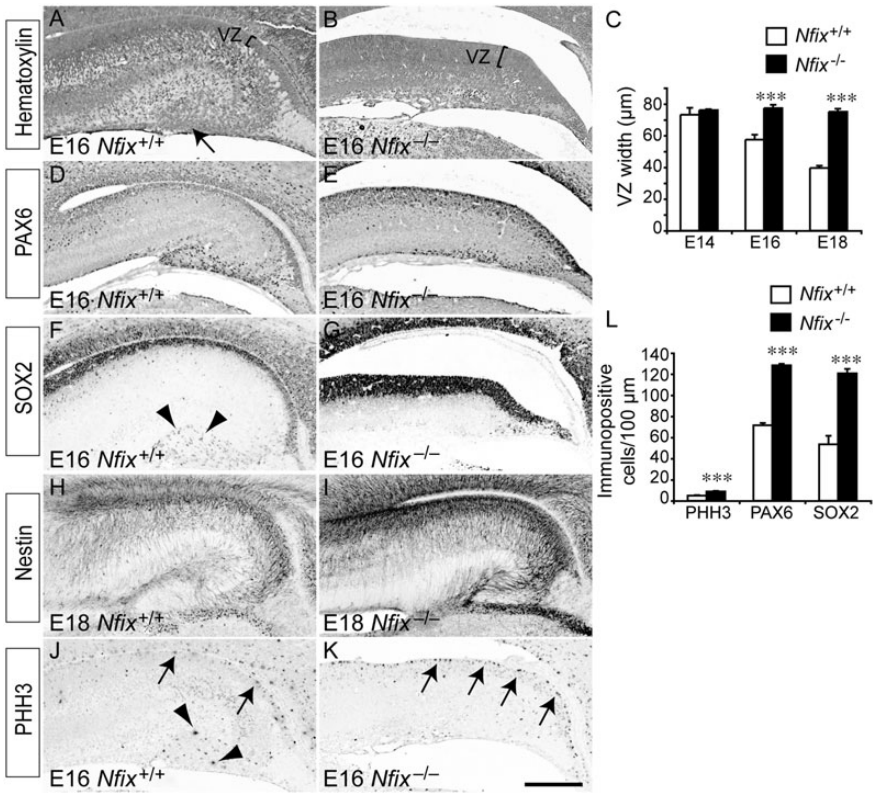

Figure 2. Delayed differentiation of ventricular zone progenitor cells in the *Nfix*$^{-/-}$ hippocampus. (*A* and *B*) Coronal paraffin sections of E16 wild-type and *Nfix*$^{-/-}$ brains stained with hematoxylin. The emerging dentate gyrus can be seen clearly in the wild-type (arrow in *A*), but is absent in the mutant at this age. The brackets delineate the ventricular zone (VZ). (*C*) The ventricular zone was significantly wider in the mutants than the controls at both E16 and E18. (*D–K*) Immunostaining of the progenitor cell markers PAX6 (*D*, *E*), SOX2 (*F*, *G*), and nestin (*H*, *I*), and the mitotic marker phosphohistone H3 (PHH3, *J*, *K*). There were more PAX6- and SOX2-expressing cells within the ventricular zone of E16 *Nfix*$^{-/-}$ mice (*D–G*). There were also markedly higher levels of nestin expression within the hippocampus of *Nfix*$^{-/-}$ mice at E18 (*H*, *I*). There were more mitotically active cells (arrows in *J* and *K*) in the ventricular zone of the *Nfix*$^{-/-}$ hippocampus. However, whereas SOX2-positive and PHH3-positive cells were seen within the dentate gyrus of E16 wild-type mice (arrowheads in *F* and *J*), we did not observe such cells within the presumptive dentate gyrus region of *Nfix*$^{-/-}$ mice. (*L*) Quantification of the number of immunopositive cells revealed that there were significantly more cells expressing PHH3, PAX6, or SOX2 in the hippocampal ventricular zone of the *Nfix*$^{-/-}$ mutant than in the wild-type control at E16. ***$P < 0.001$, Student's *t*-test. Scale bar (in *H*): *A–G*, *J*, *K*, 250 μm; *H*, *I*, 300 μm.

expansion of the neural progenitor cell pool within *Nfix*$^{-/-}$ mice (Fig. 2*F*,*G*,*L*).

Neural progenitor cells within the ventricular zone also express the intermediate filament protein nestin (Lendahl et al. 1990; Dahlstrand et al. 1995). Expression of nestin within the hippocampus of late gestation *Nfix*$^{-/-}$ mice was markedly higher than that within wild-type controls, further emphasizing a delay in the differentiation of neural progenitor cells in the *Nfix* mutants (Fig. 2*H*,*I*). Finally, the expression pattern of phosphohistone H3, a specific marker for cells undergoing mitosis, revealed that there were significantly more mitotically active cells in the hippocampal ventricular zone of *Nfix*$^{-/-}$ mice at E16 than in their littermate controls (Fig. 2*J–L*). Importantly, the delay in the differentiation of ventricular zone progenitors was also observed within the neocortical ventricular zone, suggesting that NFIX regulates the differentiation of neural progenitors throughout the pallium (Supplementary Figs 1 and 2). Collectively, these data indicate a shift in the balance of progenitor cell activity toward self-renewal as opposed to differentiation in the absence of *Nfix*.

Nfix$^{-/-}$ *Mice Display Delays in Basal Progenitor Cell Differentiation*

During development, neural progenitor cells within the ventricular zone give rise to a secondary, transient population of progenitors with limited proliferative capacity, known as intermediate progenitor cells (Gotz and Huttner 2005). These progenitors, which are located within the subventricular zone, express specific markers such as TBR2 (Englund et al. 2005). Given the delay in ventricular zone progenitor differentiation, we postulated that delays in intermediate progenitor cell development may also be evident within the subventricular zone of *Nfix*$^{-/-}$ mice. At E14, there were no significant differences in the number of intermediate progenitor cells between *Nfix*$^{-/-}$ mice and wild-type controls (Fig. 3*E* and data not shown). By E16, however, there were more TBR2-positive cells within the hippocampal subventricular zone of wild-type mice than within *Nfix* mutants (Fig. 3*A*,*B*, *E*), suggestive of a delay in intermediate progenitor cell formation in *Nfix*$^{-/-}$ mice. At E18 in wild-type mice, there were fewer TBR2-positive intermediate progenitors than at E16, consistent with these cells differentiating to form postmitotic neuronal cells. Interestingly, the decline in intermediate progenitor cell numbers observed between E16 and E18 in wild-type mice was not observed in *Nfix*$^{-/-}$ mice between these ages. Instead, at E18, there were significantly more TBR2-positive cells within the hippocampal subventricular zone of the mutant mice in comparison to wild-type controls (Fig. 3*C–E*). These data suggest that intermediate progenitor cell differentiation is delayed in *Nfix*$^{-/-}$ mice, further

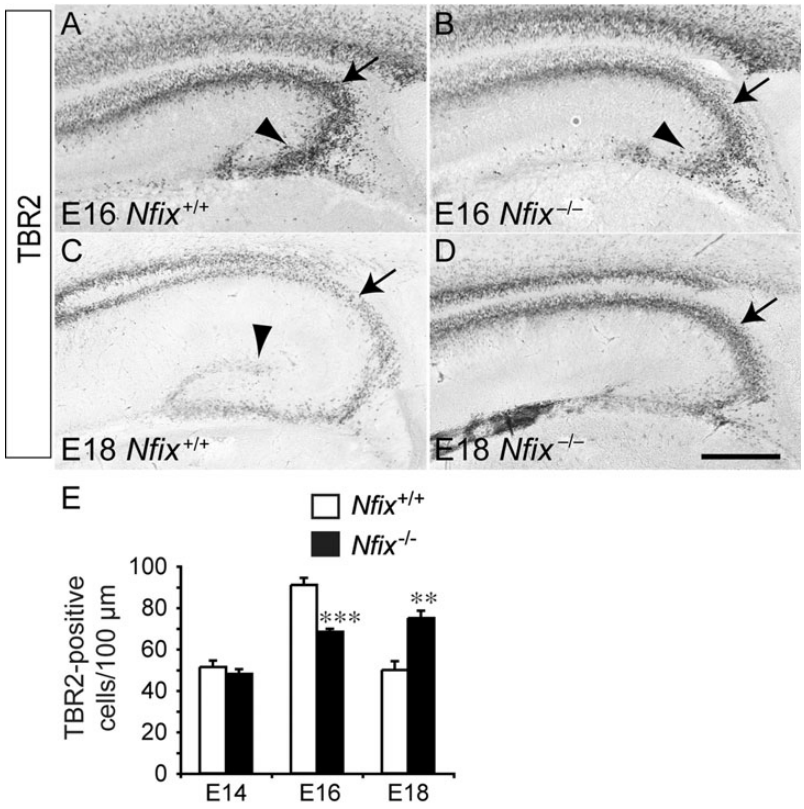

Figure 3. Altered trajectory of basal progenitor cell development in the *Nfix*$^{-/-}$ hippocampus. Expression of TBR2, a basal progenitor cell-specific marker, at E16 (*A*, *B*) and E18 (*C*, *D*). At E16, strong expression of TBR2 in the wild-type was observed in the subventricular zone of the hippocampus (arrow in *A*) and within the emerging dentate migratory stream (arrowhead in *A*). In the mutant, there were fewer TBR2-expressing cells evident within the subventricular zone (arrow in *B*) and the dentate migratory stream (arrowhead in *B*) of the hippocampus. In contrast, at E18, expression of TBR2 was more pronounced in the subventricular zone of the mutant hippocampus (arrow in *D*) than within the wild-type (arrow in *C*). In the wild-type, but not the *Nfix* mutant, TBR2-positive cells also demarcated the dentate gyrus at E18 (arrowhead in *C*). (*E*) Quantification of the number of TBR2-positive cells within the subventricular zone revealed that there were significantly more basal progenitor cells within the subventricular zone of the wild-type at E16, whereas this situation was reversed at E18, when there were more basal progenitor cells within the *Nfix*$^{-/-}$ subventricular zone. $^{**}P < 0.01$, $^{***}P < 0.001$, Student's *t*-test. Scale bar (in *D*): *A*, *B*, 250 µm; *C*, *D*, 300 µm.

demonstrating that this transcription factor plays a central role in regulating the balance of neural progenitor cell proliferation and differentiation during development of the hippocampus.

Glial and Neuronal Development is Delayed in Nfix$^{-/-}$ *Mice*

Given the delay in ventricular zone neural progenitor cell differentiation within the hippocampus of *Nfix*$^{-/-}$ mice, we next sought to analyze the development of postmitotic populations within the hippocampus of these mice. Hippocampal astrocytes are derived from progenitor cells within the ammonic neuroepithelium and the fimbrioglial epithelium of the hippocampal anlage and give rise to the supragranular glial bundle and the fimbrial glial bundle, respectively (Rickmann et al. 1987; Sievers et al. 1992). Analysis of the expression of the astroglial markers astrocyte-specific glutamate transporter GLAST (Shibata et al. 1997) and tenascin C (Gotz et al. 1998) revealed a marked reduction in expression of these proteins within the hippocampal ventricular zone of *Nfix*$^{-/-}$ mice (Fig. 4*A*–*D*), indicating a delay in glial differentiation in the absence of *Nfix*. Delays in astrocytic formation were even more apparent when expression of GFAP was analyzed. In wild-type mice, expression of GFAP within the fimbrial glia was observed at E14 (Fig. 4*E*), and by E16 GFAP expression was also observed within glia derived from the ammonic neuroepithelium (Fig. 4*G*). By E18, GFAP expression within the hippocampus of wild-type mice was extensive, with the supragranular glial bundle and the fimbrial glial bundles clearly delineated, and with GFAP-positive fibers localizing to the hippocampal fissure (Fig. 4*I*). In contrast, no GFAP expression was present within the hippocampus of E14 *Nfix*$^{-/-}$ mice (Fig. 4*F*), and expression was only observed within the fimbrial glia at E16 (Fig. 4*H*). By E18 in the mutant, GFAP expression was localized to both the supragranular glia and the fimbrial glia, but to a far lesser extent than observed within age-matched controls (Fig. 4*J*). Instead, GFAP expression in the mutant at E18 was comparable with that in E16 wild-type hippocampi (compare Fig. 4*G* and *J*). Similarly, the development of mature glia within the neocortex was delayed in the absence of *Nfix* (Supplementary Fig. 3). As mature glia are critical for morphogenesis of the dentate gyrus (Barry et al. 2008), these data indicate that the delayed glial differentiation from ventricular zone neural progenitor cells may, in part, underlie the phenotypic abnormalities present within the hippocampus of *Nfix*$^{-/-}$ mice.

To determine whether the alteration in the balance between neural progenitor cell self-renewal and differentiation within *Nfix*$^{-/-}$ mice also had consequences for neuronal development, we next investigated neurogenesis within

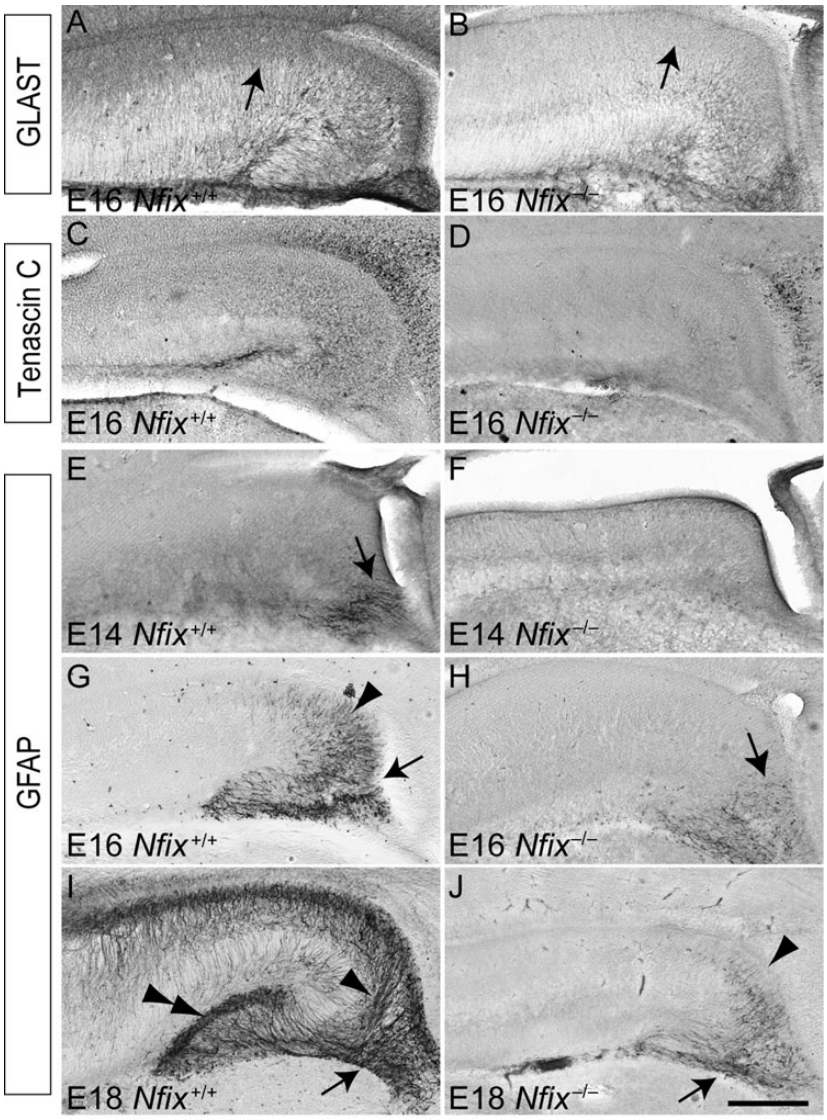

Figure 4. Delayed development of the fimbrial and supragranular glial bundles in the *Nfix*$^{-/-}$ hippocampus. Coronal sections of the hippocampus between E14 and E18 in wild-type (*A*, *C*, *E*, *G*, *I*) and *Nfix*$^{-/-}$ (*B*, *D*, *F*, *H*, *J*) mice, showing expression of the astroglial markers GLAST (*A*, *B*) and tenascin C (*C*, *D*), and the mature astrocytic marker, GFAP (*E*–*J*). At E16, GLAST was expressed strongly by astroglial cells within the ventricular zone of the wild-type hippocampus (arrow in *A*), but was expressed at a much lower level in the *Nfix*$^{-/-}$ hippocampus (arrow in *B*). Tenascin C was also expressed at a lower level in the hippocampus of *Nfix*$^{-/-}$ mice (*C*, *D*). At E14, expression of GFAP was evident within the fimbrial glioepithelium of the wild-type (arrow in *E*), but was absent in the mutant (*F*). At E16, GFAP expression in the wild-type hippocampus was evident within the fimbrial glioepithelium (arrow in *G*) and the ammonic neuroepithelium (arrowhead in *G*). In the *Nfix*$^{-/-}$ hippocampus, GFAP expression was seen within the fimbrial glioepithelium at this age (arrow in *H*). At E18, GFAP was strongly expressed within the wild-type hippocampus, including within the dentate gyrus (double arrowhead in *I*), the supragranular glial bundle (arrowhead in *I*), and the fimbrial glial bundle (arrow in *I*). In the mutant at E18, however, the expression of GFAP within the ammonic neuroepithelium (arrowhead in *J*) and the fimbrial glioepithelium (arrow in *J*) of the hippocampus was markedly reduced. Scale bar (in *J*): *A*–*D*, *G*, *H*, 250 μm; *E*, *F*, 100 μm; *I*, *J*, 300 μm.

these mice. The transcription factor TBR1 is expressed by both pyramidal neurons within the CA regions of the hippocampus and by dentate granule neurons within the emerging dentate gyrus (Englund et al. 2005). In wild-type sections at E16 and E18, TBR1-expressing neurons were present within these 2 loci of the hippocampus (Fig. 5*A*,*C*). In contrast, hippocampal sections from E16 *Nfix*$^{-/-}$ mice revealed delays in the formation of TBR1-positive cells (Fig. 5*B*). Indeed, by E18, TBR1 expression within the hippocampus of *Nfix*$^{-/-}$ mice resembled that within E16 wild-type controls (compare Fig. 5*A* and *D*). Delays in neuronal development were also observed within the neocortex of *Nfix*$^{-/-}$ mice (Supplementary Fig. 4). Furthermore, expression of the hippocampal subfield markers *Ka1* (a CA3 marker) at E16 and *Scip* (a CA1 marker) (Bettler et al. 1990; Frantz et al. 1994) at E18 by in situ hybridization revealed significant developmental delays within *Nfix*$^{-/-}$ mice (Fig. 5*E*–*H*). Taken together, these findings demonstrate that developmental delays are present within both neuronal and glial lineages within the pallium in the absence of *Nfix*.

Dentate Granule Cell Development is Abnormal in the Absence of Nfix

In addition to revealing delays in the formation of pyramidal neurons within the hippocampus of *Nfix*$^{-/-}$ mice, analysis of TBR1 expression also revealed delays in the development of dentate granule neurons (Fig. 5*D*). Together with mature glia,

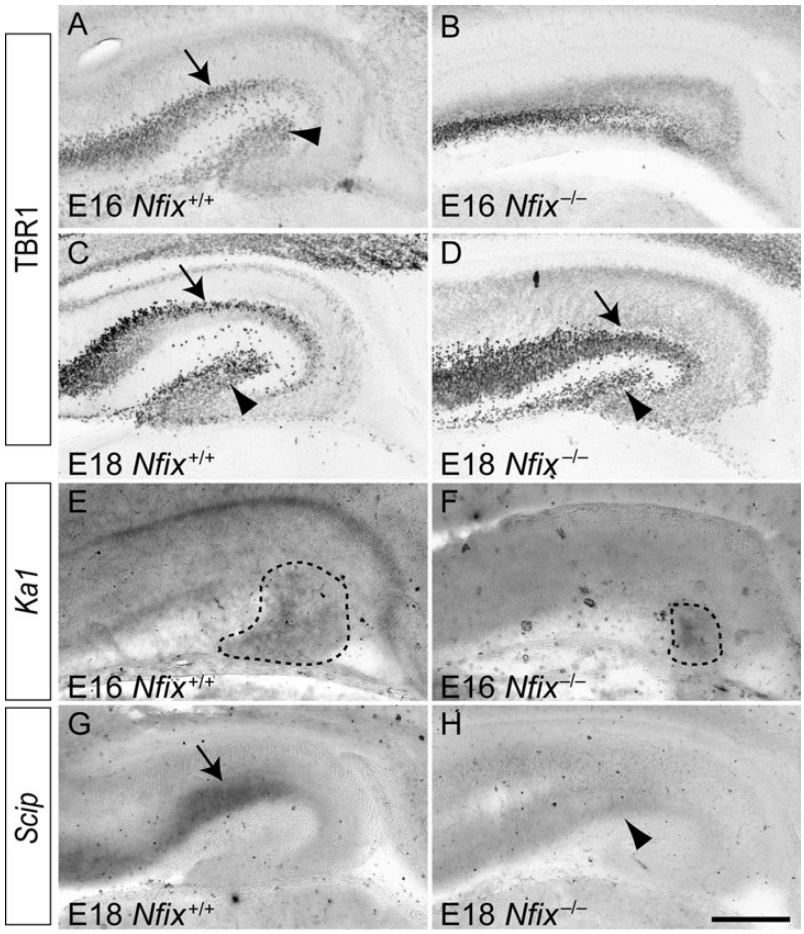

Figure 5. Neuronal development is delayed in the hippocampus of *Nfix*$^{-/-}$ mice. Expression of the neuronal marker TBR1 (*A–D*) and the hippocampal subfield markers *Ka1* and *Scip* (*E–H*) in coronal sections of wild-type (*A*, *C*, *E*, *G*) and *Nfix*$^{-/-}$ (*B*, *D*, *F*, *H*) mice. At E16 (*A*) and E18 (*C*) of the wild-type, expression of TBR1 was evident within the pyramidal cell layer of the hippocampus (arrows in *A* and *C*) and within the emerging dentate gyrus (arrowheads in *A* and *C*). In the mutant at E16, however, the expression of TBR1 within the hippocampus appeared delayed (*B*). By E18, the expression of TBR1 within the hippocampus of *Nfix*$^{-/-}$ mice was evident within the pyramidal cell layer of the hippocampus (arrow in *D*) and within the emerging dentate gyrus (arrowhead in *D*), in a pattern similar to that observed in the E16 wild-type hippocampus (compare *A* and *D*). The expression of the CA3 subfield marker *Ka1* revealed a significantly reduced area of expression in the mutant compared with the wild-type control (*Ka1* expression is delineated by the dashed lines in *E* and *F*). (*G*) In situ hybridization revealed the expression of the CA1 subfield marker *Scip* in the wild-type hippocampus (arrow in *G*). (*H*) The expression of *Scip* mRNA was markedly reduced in the mutant at E18 (arrowhead in *H*). Scale bar (in *H*): *A*, *B*, *E*, *F*, 250 μm; *C*, *D*, *G*, *H*, 300 μm.

dentate granule neurons, are critical for the formation of the dentate gyrus (Zhou et al. 2004). These cells, which can be identified by the expression of the transcription factor PROX1 (Pleasure, Anderson, et al. 2000; Pleasure, Collins, et al. 2000), are derived from neural progenitor cells within the dentate neuroepithelium at approximately E14, and migrate into the granular layer of the emerging dentate gyrus in association with the hippocampal radial glial scaffold (Zhou et al. 2004). The high levels of NFIX expression within the dentate neuroepithelium at E14 (Fig. 1*D*) hinted at a role for NFIX in dentate granule neuron formation. To assess this we analyzed the expression of PROX1 in wild-type and *Nfix*$^{-/-}$ mice. In wild-type hippocampi at E16, PROX1-expressing dentate granule neurons were present within the presumptive dentate gyrus, and by E18, the localization of these cells within the dentate gyrus was beginning to resolve into the V-shape formed by the upper and lower blades of the granular zone (Fig. 6*A*,*C*). In the mutant, however, there were significantly fewer PROX1-expressing cells within the hippocampus at both E16 and E18 (Fig. 6*B*,*D*,*E*), and the dentate granule neurons had not migrated into the dentate gyrus, perhaps due to the delays in the formation of the supragranular and fimbrial glial bundles (Fig. 4*J*). Collectively, these data demonstrate that the production of both pyramidal neurons and dentate granule neurons is delayed within the hippocampus of *Nfix*$^{-/-}$ mice.

Development of Interneurons and Cajal–Retzius Cells Occurs Normally in Nfix$^{-/-}$ *Mice*

During cortical development, interneurons, which are derived from neural progenitor cells within the ventral pallium, migrate tangentially into all regions of the cortex, including the hippocampus (Pleasure, Anderson, et al. 2000; Pleasure, Collins, et al. 2000). NFIX was not expressed within neural progenitor cells within the ventral pallium at E13 (Fig. 1*A*), and in line with this, the production of calbindin-positive and calretinin-positive interneurons, and their subsequent migration into the hippocampus, occurred normally within *Nfix*$^{-/-}$ mice (Fig. 7*A–D*). Furthermore, development of the choroid plexus, which serves as a source for bone

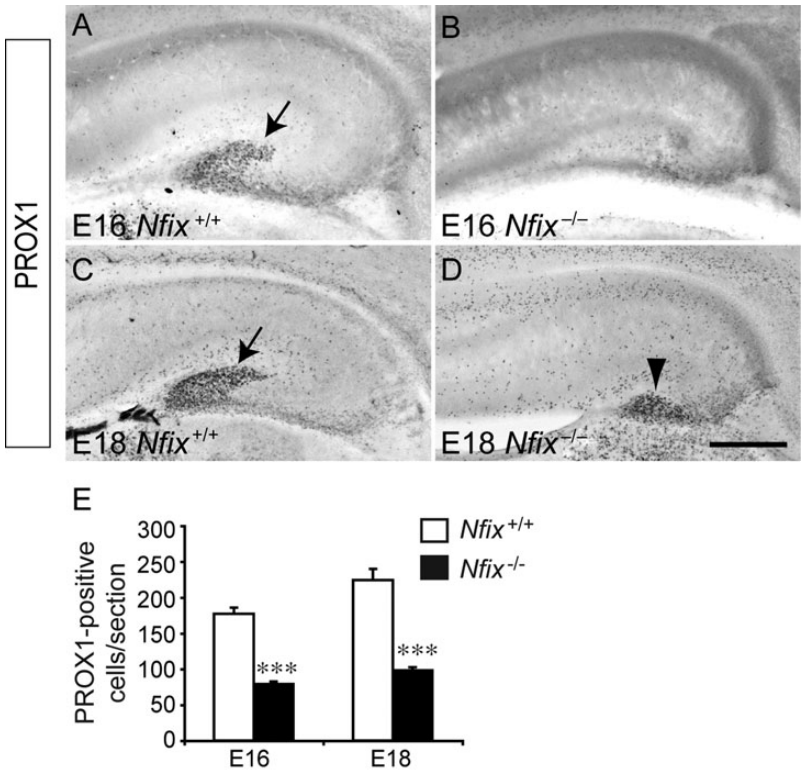

Figure 6. Dentate granule cell development is delayed in the *Nfix*$^{-/-}$ hippocampus. Expression of the dentate granule cell marker PROX1 in the hippocampus of wild-type (*A*, *C*) and *Nfix*$^{-/-}$ (*B*, *D*) mice. At E16, the expression of PROX1 was observed within the developing dentate gyrus of the wild-type (arrow in *A*), but was significantly reduced within the *Nfix* mutant at this age (*B*). By E18, PROX1-expressing cells within the hippocampus of the wild-type clearly demarcated the dentate gyrus (arrow in *C*). In the *Nfix* mutant, PROX1-expressing cells were evident by this age (arrowhead in *D*), although these cells were aberrantly positioned, and did not form the normal chevron shape of the dentate gyrus. (*E*) Quantification of PROX1-expressing cells revealed significantly fewer dentate granule cells within the hippocampus of *Nfix*$^{-/-}$ mice at both E16 and E18. ***$P < 0.001$, Student's *t*-test. Scale bar (in *D*): *A*, *B*, 250 μm; *C*, *D*, 300 μm.

morphogenetic proteins during development (Hebert et al. 2002), was normal within *Nfix*$^{-/-}$ mice (data not shown). Calretinin expression is also evident within Cajal–Retzius neurons. These specialized cells are derived from a variety of areas within the developing pallium, including the cortical hem (Bielle et al. 2005; Garcia-Moreno et al. 2007). Interestingly, expression of reelin, another marker for Cajal–Retzius cells, was normal within *Nfix*$^{-/-}$ mice, with the caveat that reelin-expressing cells did not migrate as far dorsally along the incipient hippocampal fissure in the mutant. Importantly, reelin expression during development has been shown to contribute to hippocampal morphogenesis by regulating the formation of the radial glial scaffold (Frotscher et al. 2003). Thus, the lack of NFIX expression within the cortical hem (Fig. 1*B*), together with the specification and development of Cajal–Retzius cells, suggests that the phenotypic abnormalities within the hippocampus of *Nfix*$^{-/-}$ mice do not arise as a consequence of impairments to the reelin signaling pathway.

Postnatal Nfix$^{-/-}$ *Mice Exhibit Abnormal Hippocampal Morphology*

To this point, our data had implicated *Nfix* in regulating the differentiation of embryonic neural progenitor cells within the emerging hippocampal formation. The hippocampal dentate gyrus is, however, one of the few regions of the postnatal and adult brain in which neural progenitor cells persist, giving rise to new neurons throughout life (Ihrie and Alvarez-Buylla 2008). However, the precise origin of these subgranular zone progenitor cells, and importantly, the molecular mechanisms regulating their development, remain poorly defined. Unlike mice lacking *Nfia* or *Nfib*, which die perinatally (Shu, Butz, et al. 2003; Shu, Puche, et al. 2003; Steele-Perkins et al. 2005), *Nfix*$^{-/-}$ mice survive until approximately P20 on a C57Bl/6J background, enabling the contribution of *Nfix* to the postnatal development of the hippocampus to be investigated. Analysis of the hippocampus in P2 *Nfix*$^{-/-}$ mice revealed that the dentate gyrus had indeed developed by this stage, and, furthermore, that very few PAX6-expressing neural progenitor cells were present within the ventricular zone of either wild-type or *Nfix*$^{-/-}$ mice (Fig. 8*A*–*D*). The expression of GFAP, however, was still markedly reduced in the mutant at this age (Fig. 8*F*). By P20, the morphological consequences of the absence of *Nfix* during development were manifest, with the CA1 region being dorsally enlarged, and both the upper and lower blades of the dentate gyrus being significantly shortened mediolaterally (Fig. 8*G*,*H*,*K*), akin to the earlier descriptions of this mutant (Campbell et al. 2008). Given the decrease in the size of the dentate gyrus, we quantified the number of PROX1-expressing dentate granule neurons within the blades of the dentate gyrus from P20 wild-type and *Nfix*$^{-/-}$ mice. Interestingly, there were significantly fewer dentate granule neurons per unit length within the upper blade of the dentate gyrus (Fig. 8*L*). When considered in light of the decreased length of the dentate gyrus blades within *Nfix*$^{-/-}$

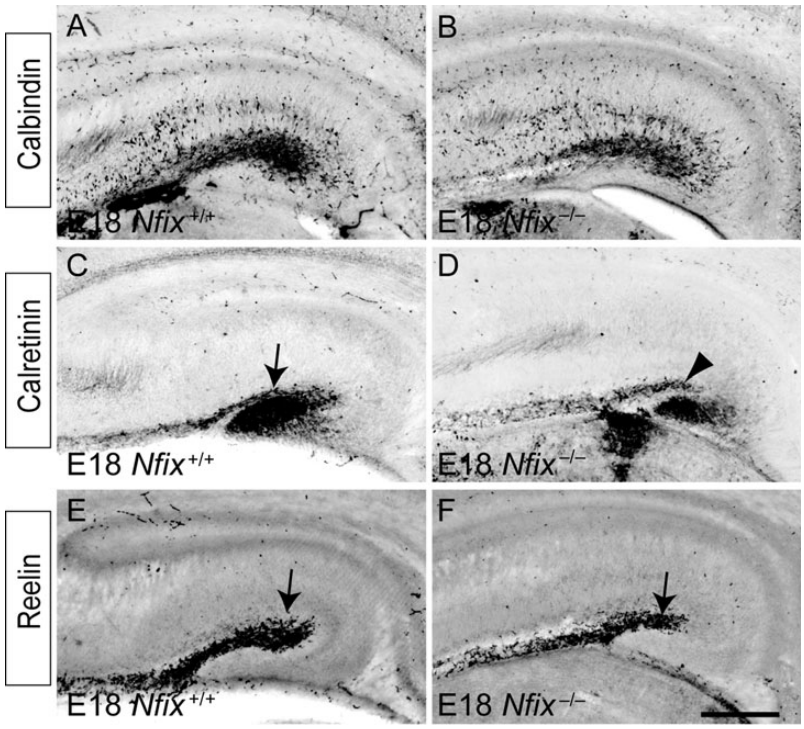

Figure 7. The migration of hippocampal interneurons and Cajal–Retzius neurons occurs normally the absence of *Nfix*. Expression of calbindin (*A*, *B*), calretinin (*C*, *D*), and reelin (*E*, *F*) in coronal sections of wild-type (*A*, *C*, *E*) and *Nfix*$^{-/-}$ (*B*, *D*, *F*) mice at E18. Calbindin-expressing interneurons migrated normally into the hippocampus of *Nfix*$^{-/-}$ mice (*B*). Similarly, calretinin-expressing interneurons migrated normally into the hippocampus of the mutant. Although the hippocampal fissure was evident in the wild-type at this age (arrow in *C*), it was markedly reduced in the mutant (arrowhead in *D*). Reelin-expressing Cajal–Retzius cells migrated normally into the hippocampus of *Nfix*$^{-/-}$ mice, although, due to the reduced size of the hippocampal fissure, these cells did not migrate as far dorsally in the mutant as they did in the wild-type (compare arrows in *E* and *F*). Scale bar (in *F*): 300 μm.

mice, these data suggest that although morphogenesis of the dentate gyrus does eventually occur in these mice, fewer dentate granule neurons ultimately populate this structure postnatally.

Fewer Neural Progenitor Cells are Found Within the Subgranular Zone of Postnatal Nfix$^{-/-}$ *Mice*

Although it is now well established that neural progenitor cells within the subgranular zone of the dentate gyrus generate new dentate granule neurons within the postnatal and adult mammalian brain (Seri et al. 2001), how these cells arise during development remains unclear. It has been suggested that hippocampal radial glia give rise to subgranular zone progenitors (Eckenhoff and Rakic 1988; Seri et al. 2004), but this is yet to be experimentally verified. Furthermore, the molecular mechanisms regulating this developmental event are poorly defined. A number of lines of evidence suggested a role for *Nfix* in this process. First, we have previously shown that cells within the subgranular zone express NFIX (Campbell et al. 2008). Secondly, the reduction in the size of the dentate gyrus, and the number of PROX1-expressing cells within this structure (Fig. 8*K*,*L*), indicated a deficit in the production of dentate granule neurons. Finally, our analysis of E16 wild-type and *Nfix*$^{-/-}$ mice had shown a marked reduction in the number of mitotically active (Fig. 2*K*) and SOX2-positive (Fig. 2*G*) cells within the emerging dentate gyrus of *Nfix* knockouts, illustrative of abnormal development of subgranular zone neural progenitors in *Nfix* mutant mice.

To investigate the role of *Nfix* in the formation of subgranular zone neural progenitor cells, we analyzed the expression of markers for this population within the dentate gyrus of postnatal *Nfix*$^{-/-}$ mice. GFAP is expressed by both astrocytes and neural progenitor cells within the dentate gyrus (Seri et al. 2001), but can be used to identify progenitors within the subgranular zone, as they exhibit radially oriented GFAP-positive fibers that extend into the granular cell layer (Seri et al. 2004). This was readily seen within the dentate gyrus of P15 wild-type mice (Fig. 9*A*,*B*). In *Nfix*$^{-/-}$ mice, however, although the expression of GFAP was evident within the dentate gyrus, there were far fewer radially oriented fibers, and the GFAP-expressing cells appeared to be disorganized with regard to their projection into the granular zone (Fig. 9*C*,*D*).

SOX2 expression can also be used to identify self-renewing cells within the subgranular zone (Suh et al. 2007). In wild-type mice, SOX2-positive cells were aligned beneath the granular zone, but in the mutants these cells appeared more scattered throughout the hilus (Fig. 9*E*–*H*). This decrease was not due to excessive apoptosis, as we did not observe any increase in cleaved caspase-3–positive cells within the dentate gyrus of *Nfix*$^{-/-}$ mice either embryonically or postnatally (data not shown). Finally, we analyzed the expression of doublecortin (DCX), a microtubule-associated protein expressed by immature neurons (Gleeson et al. 1999). The expression of DCX within the dentate gyrus of wild-type postnatal brains revealed that DCX-expressing neuroblasts extended radial processes into the granular zone of the dentate gyrus (Fig. 9*I*,*J*). In the mutant, however, DCX-expressing cells did not exhibit

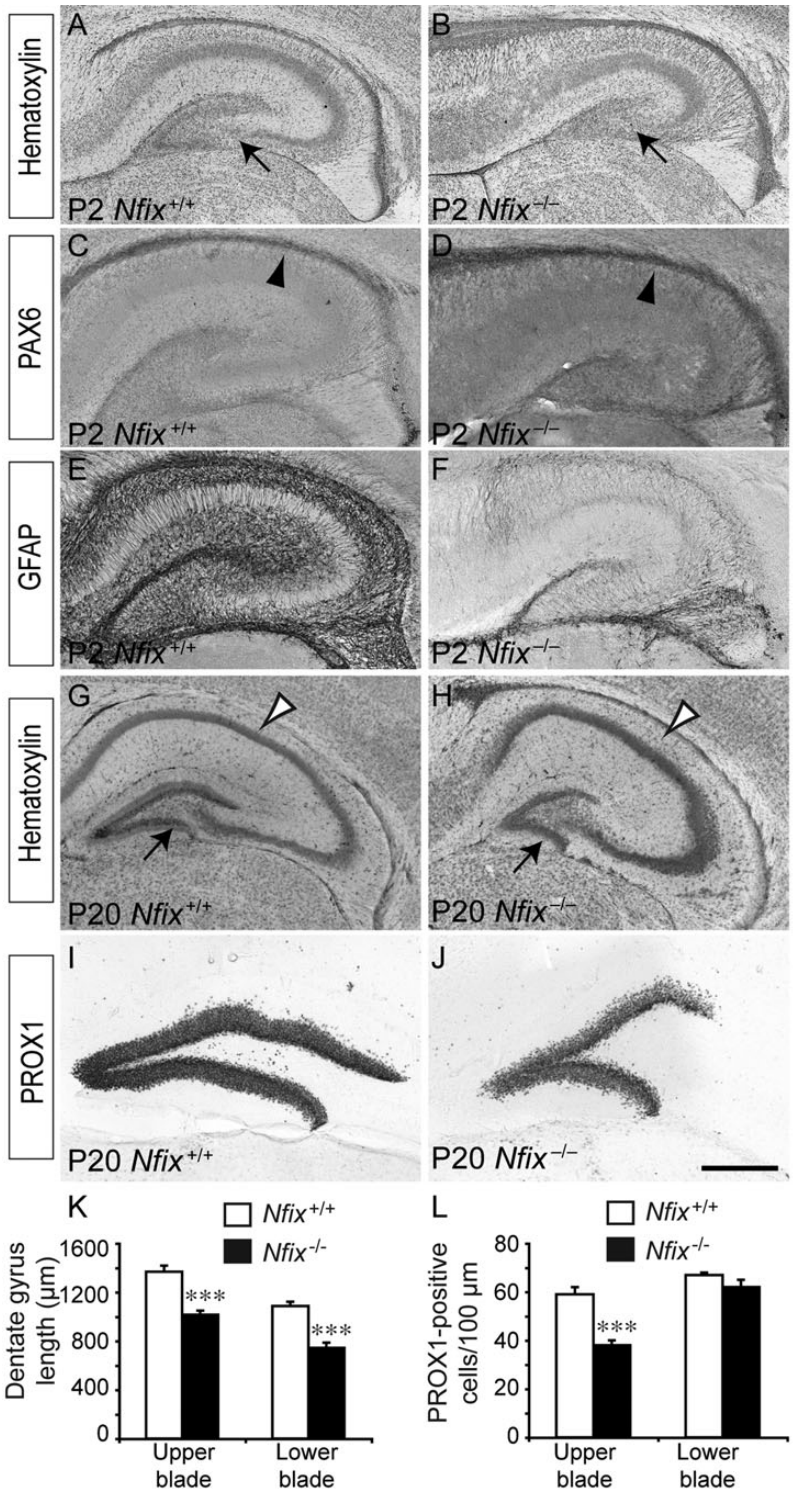

Figure 8. Abnormal hippocampal morphology in postnatal *Nfix*$^{-/-}$ mice. Coronal hippocampal sections of P2 (*A*–*F*) and P20 (*G*–*J*) wild-type and *Nfix*$^{-/-}$ mice. Hematoxylin staining revealed that, by P2, the dentate gyrus was evident within the hippocampus of both wild-type and *Nfix*$^{-/-}$ mice (arrows in *A* and *B*, respectively). The expression of PAX6 revealed that, in both wild-type (*C*) and *Nfix*$^{-/-}$ (*D*) mice, there were few remaining PAX6-expressing cells within the ventricular zone of the hippocampus (arrowheads in *C* and *D*). GFAP expression, however, was still markedly reduced in the hippocampus of *Nfix*$^{-/-}$ mice (*F*). (*G*) Hematoxylin staining of the hippocampus from a P20 wild-type brain. The dentate gyrus (arrow in *G*) and the CA regions (open arrowhead in *G*) were clearly evident. (*H*) In *Nfix*$^{-/-}$ mice, although the dentate gyrus (arrow in *H*) and CA (open arrowhead in *H*) regions were evident, their morphology was abnormal, being shortened along the mediolateral axis, and lengthened along the dorsoventral axis, respectively. (*I*, *J*) Expression of PROX1 within the dentate gyrus of wild-type (*I*) and *Nfix*$^{-/-}$ (*J*) mice. (*K*) The measurement of the lengths of the blades of the dentate gyrus revealed that both the upper and lower blades of the *Nfix* mutant were significantly shorter than those of their wild-type littermate controls. (*L*) Furthermore, there were also significantly fewer PROX1-positive dentate granule neurons per unit length within the upper blade of the dentate gyrus of *Nfix*$^{-/-}$ mice. ***$P < 0.001$, Student's *t*-test. Scale bar (in *J*): *A*–*F*, 350 μm; *G*–*J*, 650 μm.

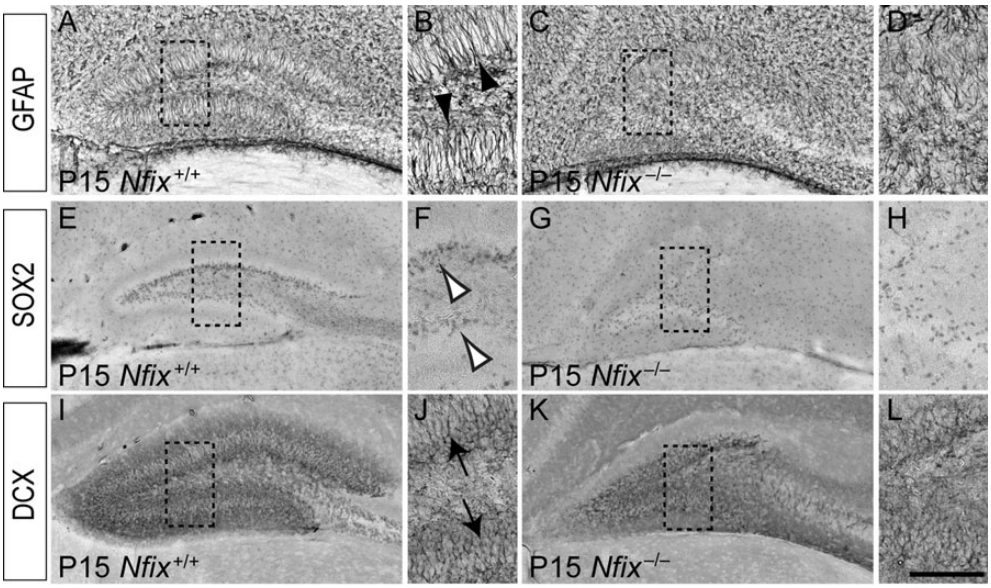

Figure 9. The subgranular zone is abnormal in the dentate gyrus of postnatal *Nfix*$^{-/-}$ mice. Expression of GFAP (*A–D*), SOX2 (*E–H*), and DCX (*I–L*) in the dentate gyrus of P15 wild-type (*A*, *B*, *E*, *F*, *I*, *J*) and *Nfix*$^{-/-}$ mice (*C*, *D*, *G*, *H*, *K*, *L*). (*A*) Expression of GFAP in the dentate gyrus of a P15 wild-type mouse. (*B*) Higher magnification view of the boxed region in *A*, showing the radially oriented, GFAP-positive fibers of subgranular zone neural progenitor cells (arrowheads in *B*). (*C*) Expression of GFAP in the dentate gyrus of a P15 *Nfix*$^{-/-}$ mouse. (*D*) Higher magnification view of the boxed region in *C*. There were fewer GFAP-expressing cells in the dentate gyrus of *Nfix* knockout mice that possessed a radially oriented fiber. (*E*) In the dentate gyrus of a P15 wild-type mouse, SOX2 was expressed by cells in the subgranular zone of the dentate gyrus. (*F*) Higher magnification view of the boxed region in *E*, showing SOX2-expressing progenitor cells within the subgranular zone (open arrowheads in *F*). (*G*) In *Nfix*$^{-/-}$ mice, SOX2-expressing progenitor cells did not align within the subgranular zone to the same extent as in wild-type mice. (*H*) Higher magnification view of the boxed region in *G*, revealing the disordered localization of progenitor cells within the dentate gyrus of *Nfix*$^{-/-}$ mice. (*I*, *J*) The expression of DCX within the dentate gyrus of wild-type mice revealed that immature neurons exhibited radially arrayed processes that extended into the granular zone (arrows in *J*). (*K*, *L*) In *Nfix*$^{-/-}$ mice, DCX-expressing cells exhibited a disordered morphology within the dentate gyrus. Panels*J* and *L* are higher magnification views of the boxed regions in *I* and *K*, respectively. Scale bar (in *L*): *A*, *C*, *E*, *G*, *I*, *K*, 500 μm; *B*, *D*, *F*, *H*, *J*, *L*, 100 μm.

this ordered array of DCX-expressing fibers, appearing instead disorganized within the dentate gyrus (Fig. 9*K*,*L*). These data from the dentate gyrus of postnatal animals suggest that *Nfix* plays an important role in the development of neural progenitor cells within this neurogenic niche of the adult brain, providing a significant advance in our understanding of the regulatory control of this process.

NFIX Represses Sox9 Expression During Embryonic Hippocampal Development

A salient feature emerging from our study to date was that, during embryogenesis, progenitor cell self-renewal was extended at the expense of differentiation, from which we inferred that *Nfix* acts, in part, via the repression of progenitor-specific genes. To gain a mechanistic insight into how NFIX acts to regulate neural progenitor cell differentiation, we performed a microarray screen of hippocampal tissue from littermate E16 *Nfix*$^{+/+}$ and *Nfix*$^{-/-}$ mice. This analysis identified over 1000 genes as being differentially expressed within the hippocampus of the mutant mice, using a significance level of $P < 0.05$ via ANOVA and a fold-change cut-off of 1.5 (Supplementary Table 1). In support of our findings relating to delayed neural progenitor cell differentiation, this analysis identified many neuronal-specific (*Prox1*, *Ka1*, and *Ncam1*) and glial-specific (*Gfap* and *Omg*) genes as being significantly downregulated within the hippocampus of *Nfix*$^{-/-}$ mice. Furthermore, functional annotation of genes downregulated in the hippocampus of the mutant mice identified the processes of neuron development, neuron projection development, and neuron differentiation as being enriched in the mutant (Fig. 10 and Table 1), further emphasizing that progenitor cell differentiation is delayed in the absence of *Nfix*. The expression of numerous genes was also significantly upregulated in the mutant hippocampus at E16, including a number previously implicated in progenitor cell self-renewal, such as the Notch pathway members *Dll1* and *Hey2* (Shimojo et al. 2008). Moreover, functional annotation of those genes upregulated in the hippocampus of *Nfix*$^{-/-}$ mice provided further evidence that the balance between progenitor cell differentiation and self-renewal was shifted toward self-renewal, with many processes involved in proliferation being evident, including cell division, cell cycle, DNA metabolic process, transcription, and mitotic cell cycle (Fig. 10). Taken together, these findings provide further support for the notion that progenitor cell maintenance is prolonged within *Nfix*$^{-/-}$ mice.

Interestingly, the analysis of the transcripts upregulated in the hippocampus of *Nfix*$^{-/-}$ mice at E16 (Table 2) revealed a variety of potential targets for transcriptional regulation by NFIX. Of particular interest was *Sox9*, a member of the *SoxE* family of transcription factors, which has recently been implicated in driving the induction and maintenance of cortical neural progenitor cells (Scott et al. 2010). Validation of the array results using qPCR confirmed that there were significantly elevated levels of *Sox9* mRNA in the hippocampus of *Nfix*$^{-/-}$ mice. Furthermore, using a SOX9-specific antibody, immunohistochemical analysis revealed significantly more SOX9-expressing neural progenitor cells within the hippocampal and neocortical ventricular zone of *Nfix*$^{-/-}$ mice (Fig. 11*A–D*; Supplementary Fig. 1). We therefore asked whether *Sox9* was a *direct* target for transcriptional control by NFIX. To do this, we first performed an in silico bioinformatic

A DAVID analysis: Functional annotation of genes downregulated in *Nfix*$^{-/-}$ hippocampal tissue

	Gene count	*P-value*
Regulation of synaptic transmission	10	1.16E-04
Neuron development	17	1.68E-04
Neurotransmitter transport	9	1.74E-04
Regulation of transmission of nerve impulse	10	2.00E-04
Neuron projection development	14	2.94E-04
Regulation of neurological system process	10	3.07E-04
Ion homeostasis	16	5.50E-04
Integrin-mediated signaling pathway	8	6.72E-04
Cellular chemical homeostasis	15	6.89E-04
Chemical homeostasis	18	6.96E-04
Cellular homeostasis	17	0.00108
Cell projection organization	16	0.00117
Cellular ion homeostasis	14	0.00168
Regulation of system process	12	0.00181
Behavior	18	0.00181
Neuron differentiation	18	0.00185

B DAVID analysis: Functional annotation of genes upregulated in *Nfix*$^{-/-}$ hippocampal tissue

	Gene count	*P-value*
Cell cycle	39	1.69E-07
DNA metabolic process	28	3.19E-06
Cell cycle phase	24	8.43E-06
Mitotic cell cycle	20	1.36E-05
DNA repair	18	3.99E-05
Protein amino acid phosphorylation	34	4.69E-05
Cell cycle process	25	5.39E-05
Cellular response to stress	25	7.63E-05
Phosphorylation	36	7.89E-05
Response to DNA damage stimulus	20	1.09E-04
Interphase of mitotic cell cycle	8	1.88E-04
Interphase	8	2.45E-04
Transcription	67	2.54E-04
Cell division	19	2.70E-04
Cell fate commitment	13	2.77E-04
Phosphorus metabolic process	39	3.59E-04
Phosphate metabolic process	39	3.59E-04
DNA recombination	9	4.52E-04
Regulation of transcription	78	5.83E-04

C DAVID analysis: Pathways downregulated in *Nfix*$^{-/-}$ hippocampal tissue

	Gene count	*P-value*
Calcium signaling pathway	14	2.75E-05
Dilated cardiomyopathy	7	0.00615
Long-term potentiation	6	0.00853
Long-term depression	6	0.00962
Focal adhesion	10	0.01002
Arrhythmogenic right ventricular cardiomyopathy	6	0.01143
Hypertrophic cardiomyopathy	6	0.01734
ECM-receptor interaction	6	0.01734
Amyotrophic lateral sclerosis	5	0.019
Viral myocarditis	6	0.019
Tight junction	7	0.03428
Neuroactive ligand-receptor interaction	10	0.04628

D DAVID analysis: Pathways upregulated in *Nfix*$^{-/-}$ hippocampal tissue

	Gene count	*P-value*
Pathways in cancer	22	1.68E-05
Wnt signaling pathway	13	1.70E-04
Homologous recombination	6	3.08E-04
Cell cycle	11	5.84E-04
Basal cell carcinoma	7	0.00179

Figure 10. Microarray and functional classification reveals diverse genes misregulated within the hippocampus of E16 *Nfix*$^{-/-}$ mice. Microarray analysis was performed on E16 wild-type and *Nfix*$^{-/-}$ hippocampal tissue. Genes were annotated using the functional annotation tool of DAVID, revealing key biological processes that were downregulated (*A*) and upregulated (*B*) in the hippocampus of *Nfix*$^{-/-}$ mice. Biological pathways involving mRNAs that were downregulated (*C*) or upregulated (*D*) in the hippocampus of *Nfix*$^{-/-}$ mice were also generated within DAVID.

Table 1
Key examples of transcripts downregulated in the hippocampus of *Nfix*$^{-/-}$ mice at E16

Functional classification (DAVID)	Downregulated genes
Neuron differentiation	*Fezf1; doublecortin; cholecystokinin; MAP2; Slit3; Sema3A; Sema5A*
Regulation of synaptic transmission	*calcium channel, voltage-dependent, P/Q type, alpha 1A subunit; dopamine receptor D1A; glutamate receptor, ionotropic, NMDA2B; glutamate receptor, ionotropic, kainate 1; glutamate receptor, metabotropic 5; alpha synuclein*
Neurotransmitter transport	*Solute carrier family 25 (mitochondrial carrier, adenine nucleotide translocator); solute carrier family 6 (neurotransmitter transporter, GABA), member 1; solute carrier family 6 (neurotransmitter transporter, GABA), member 11; synaptotagmin I*
Integrin-mediated signaling pathway	*Integrin alpha 11; integrin alpha 8; integrin alpha V; integrin beta 5; calcium and integrin binding family member 2*

Table 2
Key examples of transcripts upregulated in the hippocampus of *Nfix*$^{-/-}$ mice at E16

Functional classification (DAVID)	Upregulated genes
Transcription	***Sox9***; *Sox5, E2F6; FoxL2; Foxo4; neurogenin 2; TATA bix binding protein; Eya1; Eya3*
Cell division	*Anillin, actin binding protein; cell division cycle 2 homolog A; cell division cycle associated 7; Wnt3A; polo-like kinase 1; protein regulator of cytokinesis 1*
DNA metabolic process	*Cyclin E2; cyclin O; exonuclease 1; ligase I, DNA, ATP-dependent; topioisomerase (DNA) I; uracil DNA glycosylase*
Mitotic cell cycle	*Aurora kinase A; aurora kinase B; centromere protein F; cyclin D2; cyclin-dependent kinase 2; Nedd9; checkpoint kinase homolog 1*

screen of the *Sox9* promoter to search for putative NFI consensus DNA-binding sites. The NFI motif DNA-binding site was derived from a recent report that used ChIP sequencing to identify NFI binding sites in vivo (Pjanic et al. 2011). Using this motif, we scanned the region around the TSS of *Sox9* (see Materials and methods) and identified multiple putative NFI binding sites within this region, 2 of which were upstream of the TSS, and 2 of which were downstream of the TSS, including 1 within the first exon of the *Sox9* gene (+598; Fig. 11*E*). Although not common, transcription factor-binding sites have been identified in silico within the exonic region of many genes (Gotea et al. 2012). Moreover, the first exon of the *elastin* gene has been shown to possess a regulatory element that facilitates the expression of this gene (Pierce et al. 2006), while the transcription factor GATA-1 binds to a regulatory region in exon 1 of the *C–C chemokine receptor type 3*

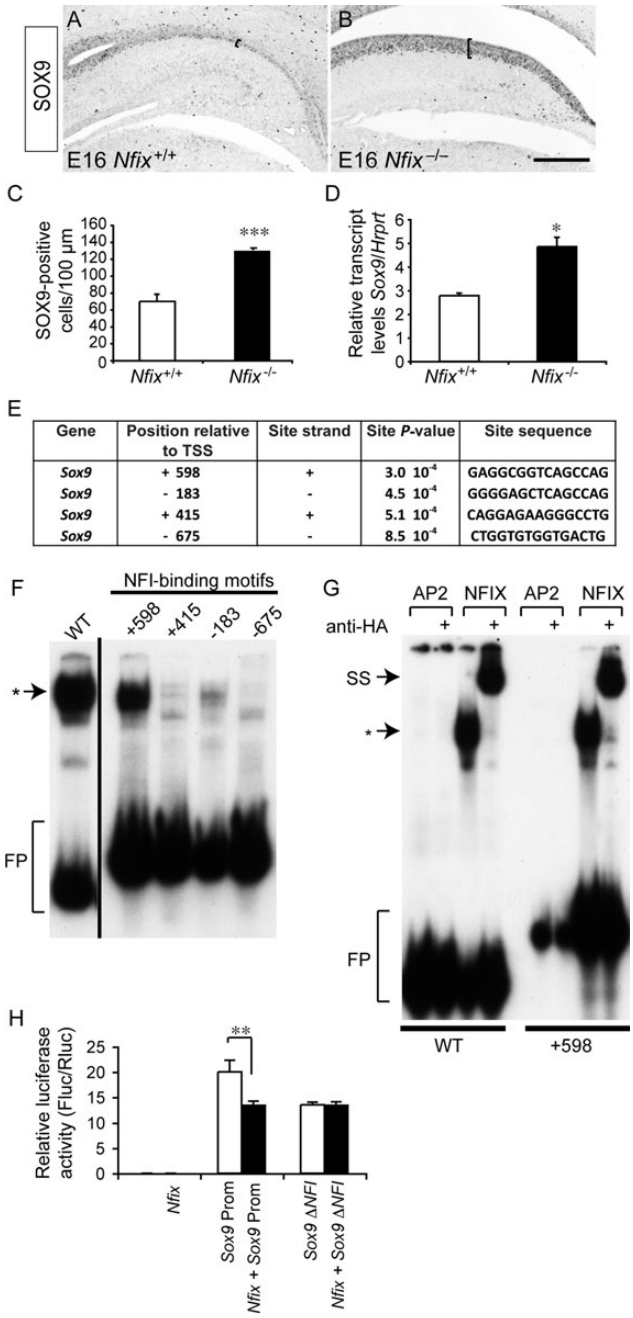

Gene	Position relative to TSS	Site strand	Site *P*-value	Site sequence
Sox9	+ 598	+	$3.0\ 10^{-4}$	GAGGCGGTCAGCCAG
Sox9	- 183	-	$4.5\ 10^{-4}$	GGGGAGCTCAGCCAG
Sox9	+ 415	+	$5.1\ 10^{-4}$	CAGGAGAAGGGCCTG
Sox9	- 675	-	$8.5\ 10^{-4}$	CTGGTGTGGTGACTG

Figure 11. Upregulation of SOX9 expression in *Nfix* mutants. (*A*, *B*) Coronal sections of E16 wild-type (*A*) and *Nfix*$^{-/-}$ (*B*) hippocampi, showing the expression of SOX9. There were significantly more SOX9-positive cells in the ventricular zone of the *Nfix* mutant than within the control (*C*; also compare brackets in *A* and *B*). (*D*) qPCR revealed significantly elevated levels of *Sox9* mRNA in the hippocampus of *Nfix*$^{-/-}$ mice compared with wild-type controls. (*E*) Potential NFI binding sites reported by FIMO around the *Sox9* TSS. We report the position in bases of each potential site relative to the TSS, the strand of the potential site, the *P*-value of the motif match, and the site sequence. (*F*) EMSA. E18 mouse brain nuclear extracts were incubated with radiolabeled probes for NFI control (lane 1), +598 (lane 2), +495 (lane 3), −183 (lane 4), and −675 (lane 5) consensus sites. Only the control and the +598 probes exhibited significant binding to the nuclear extract (asterisk). FP, free probe. (*G*) Supershift assay using nuclear extracts from COS cells expressing an HA-tagged NFIX expression construct. For the control probe (lane 3) and the +598 probe (lane 7), an NFIX complex was produced (asterisk) when the nuclear extract was incubated with either probe. However, the addition of a specific anti-HA antibody to the binding reaction depleted this complex and produced a supershifted complex (SS; lanes 4 and 8). A nonspecific transcription factor, AP2, did not demonstrate any specific binding to either oligonucleotide probe (lanes 1, 2, 5, and 6). (*H*) Reporter gene assay in NSC-34 cells. Transfection of an *Nfix* expression vector (*Nfix* pCAGIG) elicited no luciferase activity, whereas transfection of a luciferase construct under the control of the *Sox9* promoter elicited robust induction of the reporter gene. Cotransfection of *Nfix* with the *Sox9* promoter reporter yielded a significantly reduced level of luciferase activity. However, mutation of the putative +598 NFI binding site within the *Sox9* promoter (*Sox9ΔNFI*) abolished NFI-mediated repression of luciferase expression. $^{*}P < 0.05$, $^{***}P < 0.001$, Student's *t*-test; $^{**}P < 0.01$, ANOVA. Scale bar (in *B*): 250 µm.

gene (Zimmermann et al. 2005). In sum, our array data and in silico-binding site predictions provide support for the regulation of *Sox9* gene transcription by NFIX.

To determine which of these predicted sites were functionally relevant, we next performed electrophoretic mobility shift assays using oligonucleotide probes designed to encompass each of the putative NFI binding sites (−695, −183, +415, and +598). First, using E18 mouse cortex nuclear extracts, we showed that only the +598 oligonucleotide probe exhibited significant binding to the nuclear extract derived from the E18 mouse cortex, although the −183 probe also exhibited low levels of binding (Fig. 11*F*). We next performed supershift assays to determine whether the mobility shift we observed with respect to the +598 probe was due to NFIX. To do this, we transfected an HA-tagged NFIX expression construct into COS cells and isolated nuclear extracts 48 h later. Subsequent electrophoretic mobility shift assays with these nuclear extracts revealed supershifting of the +598 probe when an anti-HA antibody was present (Fig. 11*G*). A nonspecific transcription factor, AP2, did not exhibit any binding to the +598 probe. These data suggest that NFIX can directly interact with the +598 binding site within exon 1 of the *Sox9* gene.

To formally address whether NFIX was capable of regulating *Sox9* promoter-driven transcriptional activity, we employed a reporter gene assay, whereby the expression of the luciferase gene was under the control of a 250-bp region from the *Sox9* gene containing the +598 site. This analysis revealed that NFIX was able to directly repress luciferase expression driven by the *Sox9* promoter (Fig. 11*H*). Moreover, mutagenesis of the +598 site abolished repression of the luciferase gene, indicating the importance of this site for NFIX-mediated repression of *Sox9* expression (Fig. 11*H*). Taken together, these data suggest that NFIX promotes progenitor cell differentiation within the embryonic hippocampus through the direct transcriptional repression of *Sox9*.

Overexpression of NFIX Drives Precocious Gliogenesis In Vivo

Our data to date suggested that NFIX plays a pivotal role during development of the dorsal telencephalon, driving progenitor cell differentiation in part via direct repression of *Sox9* transcription. Given this, we posited that the overexpression of NFIX in vivo would culminate in precocious progenitor cell differentiation. To test this hypothesis, we used in utero electroporation to transfect neural progenitor cells in vivo with an NFIX expression construct (*Nfix* pCAGIG IRES GFP). As NFIX has been shown to regulate glial development in vitro (Cebolla and Vallejo 2006; Brun et al. 2009; Piper et al. 2011), we used the expression of the mature glial marker GFAP as our read-out of progenitor cell differentiation. Moreover, given that NFIX also regulates neocortical neural progenitor cell differentiation (Supplementary Figs 1–4) and that the

expression of GFAP within the neocortex is minimal before E16 (Shu, Butz, et al. 2003; Shu, Puche, et al. 2003), we chose to electroporate neocortical neural progenitor cells at E13 and to analyze GFAP expression 3 days later at E16, reasoning that this would allow the visualization of precocious gliogenesis without the potential confounding presence of endogenous gliogenesis. Electroporation of the vector only control into the neocortical ventricular zone at E13 did not result in precocious gliogenesis within the neocortex at E16 (Fig. 12*A–D*). However, the overexpression of NFIX at E13 did indeed result in the precocious expression of GFAP within the neocortex at E16 (Fig. 12*E–H*), demonstrating that NFIX plays a key role in driving the differentiation of neural progenitor cells in vivo.

Discussion

Many factors have been shown to act in concert to regulate the balance between neural progenitor cell self-renewal and differentiation during development. For example, members of the SOX family of transcription factors, such as SOX2, are known to promote the maintenance of progenitor cell identity during development of the embryonic cortex, and within the neurogenic niches of the adult brain (Bani-Yaghoub et al. 2006; Suh et al. 2007). Another member of the SOX family implicated in progenitor cell self-renewal during corticogenesis is SOX9, which has been shown to act downstream of SHH to induce and maintain neural progenitor cell identity (Scott et al. 2010). How SOX9 expression within cortical neural progenitor cells is regulated remains unclear, and indeed, whether or not the regulation of SOX9 by SHH is direct or indirect remains unresolved. Moreover, how SOX9 expression is downregulated to enable progenitor cell differentiation remains unknown. Here, we demonstrate that the transcription factor NFIX plays a key role in this process, promoting the differentiation of hippocampal neural progenitor cells in part via transcriptional repression of *Sox9*. Using *Nfix*$^{-/-}$ mice, we demonstrate that ventricular zone progenitor cells in the embryonic hippocampus are retained in the progenitor state for longer in the absence of *Nfix*, which leads to delays in both neuronal and glial differentiation. Furthermore, we identify multiple potential NFI binding sites in the basal promoter of the *Sox9* gene and demonstrate the ability of NFIX to repress *Sox9* promoter-driven gene expression. These findings provide a mechanistic insight into how the differentiation of neural progenitor cells within the hippocampus is orchestrated during development and highlight the importance of NFIX in regulating this process.

Although the NFI family were first isolated over 2 decades ago (Rupp et al. 1990; Kruse et al. 1991), the mechanisms by which they drive embryonic development, including that of the nervous system, remain only partially understood. However, work conducted both in vitro and in vivo has begun to reveal the role these transcription factors play during development, and importantly, to identify their downstream transcriptional targets. Expression studies have demonstrated that *Nfix* mRNA is expressed within the developing mouse telencephalon from approximately E11.5 (Chaudhry et al. 1997). Furthermore, in vitro studies have shown that NFIX drives the expression of astrocyte-specific genes, including *Gfap*, *Sparcl1*, *brain fatty acid-binding protein*, and *YKL-40* in various cell lines derived from human glioblastomas (Gopalan et al. 2006; Brun et al. 2009; Singh et al. 2011). Despite this, the role of *Nfix* during nervous system development remains poorly understood. Gene-specific knockout mice are now

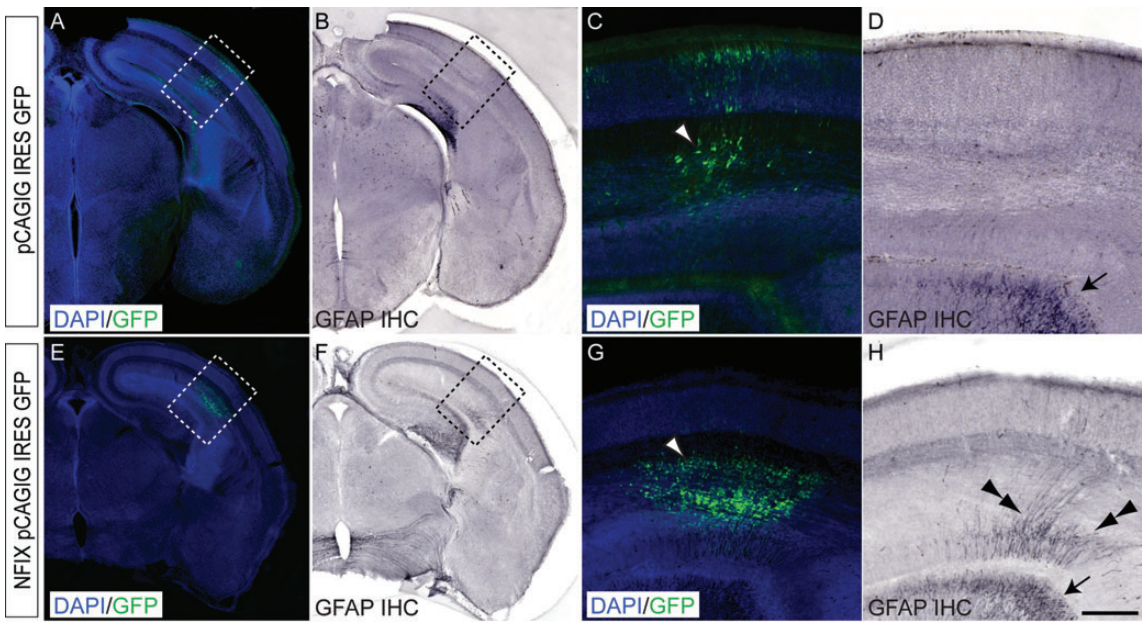

Figure 12. Overexpression of NFIX drives gliogenesis in vivo. Overexpression of a vector only control (pCAGIG IRES GFP; *A–D*) or NFIX (*Nfix* pCAGIG IRES GFP; *E–H*) into the neocortex of wild-type CD-1 mice at E13 using in utero electoporation. At E16, brains were fixed and sectioned, then processed for immunofluorescence (*A*, *C*, *E*, *G*), followed by immunohistochemistry (IHC) using an anti-GFAP antibody (*B*, *D*, *F*, *H*). Panels *A* and *B* show the same section with fluorescence (*A*) and brightfield (*B*) microscopy, respectively, as do panels *E* and *F*. In the control, expression of GFP can be seen within the neocortex (*A*, arrowhead in *C*). However, no GFAP immunoreactivity is present within the neocortex at this time (*B*, *D*), although GFAP expression can be seen in the hippocampus (arrow in *D*). In those embryos electroporated with the NFIX expression construct, expression of GFP can also be seen within the neocortex (*E*, arrowhead in *G*). However, as well as GFAP expression being evident within the hippocampus (arrow in *H*), ectopic expression of this glial marker is also evident within the neocortex (double arrowheads in *H*). Panels *C*, *D*, *G* and *H* are higher magnification views of the boxed regions in *A*, *B*, *E*, and *F*, respectively. Scale bar (in *H*): *A*, *B*, *E*, *F*, 600 μm; *C*, *D*, *G*, *H*, 150 μm.

providing important insights into the role of *Nfix* during nervous system development, with knockouts exhibiting a range of neurological abnormalities, including malformation of the hippocampal dentate gyrus, expansion of the cingulate cortex, and increased brain weight (Driller et al. 2007; Campbell et al. 2008). Mechanistically, we have recently shown that NFIX regulates the expression of *Gfap* during cerebellar development (Piper et al. 2011), but how NFIX acts in neural progenitor cells in vivo was not addressed in this study. Our current findings therefore provide a conceptual advance in our understanding of how *Nfix* drives neural progenitor cell differentiation during development, revealing an important role for this transcription factor in the repression of the stem cell maintenance gene, *Sox9*.

The SOX family of transcription factors play a variety of roles during the development of many organs (Stolt and Wegner 2010). Studies have shown that SOX8, SOX9, and SOX10, which comprise a subfamily of the SOX group known as the SOXE family (Bowles et al. 2000), are important determinants of progenitor cell differentiation (Stolt and Wegner 2010). For instance, *Sox9* is expressed by ventricular zone progenitor cells within the spinal cord at the time at which gliogenesis is initiated within this structure, and deletion of this gene culminates in deficits in both astrocyte and oligodendrocyte formation (Stolt et al. 2003). Furthermore, SOX10 is also expressed by oligodendrocyte progenitors within the developing spinal cord (Stolt et al. 2002), and compound loss of both *Sox9* and *Sox10* leads to a more severe phenotype with regard to oligodendrocyte formation than loss of *Sox9* alone (Stolt et al. 2003), highlighting the role of these genes in the formation of the oligodendrocyte lineage.

These findings indicate that SOXE family members are key determinants of promoting the gliogenic fate switch within the developing spinal cord (Stolt and Wegner 2010). However, the extent to which they reflect the development of other structures within the nervous system remains unclear. The function of SOX9 provides a pertinent example of this, as this transcription factor appears to play a distinct role during corticogenesis. SOX9 is expressed very early during cortical development, from approximately E10.5, when neural progenitor cells are undergoing the transition to radial glial cells (Scott et al. 2010). This is much earlier than the onset of gliogenesis, which is initiated at approximately E14 within the mouse forebrain (Shu, Butz, et al. 2003; Shu, Puche, et al. 2003). Both loss- and gain-of-function experiments have suggested that SOX9 plays a central role downstream of SHH in the induction and maintenance of cortical neural progenitor cells (Scott et al. 2010). This implies that SOX9 fulfils a different role during cortical development as opposed to spinal cord development, acting to promote progenitor cell self-renewal instead of acting in the switch toward glial fate determination. Interestingly, differences in the activity of the *Nfi* genes between the developing cortex and spinal cord are also evident. For instance, *Nfia*, which acts downstream of Notch signaling to induce gliogenesis within the cortex (Namihira et al. 2009), has been shown to downregulate Notch pathway activity within the telencephalon via the repression of the Notch effector *Hes1* (Piper et al. 2010), while in the developing spinal cord, *Nfia* is required for *Hes5* expression (Deneen et al. 2006). These findings highlight the important differences between the development of the cortex and spinal cord, and more broadly emphasize that the function of such transcription factors is influenced by the cellular and molecular context in which they act during embryogenesis.

Our data advance our understanding of how the self-renewal gene *Sox9* is regulated during hippocampal formation, as, to date, little has been known regarding its transcriptional control during forebrain development. Indeed, much of our understanding of *Sox9* regulation has been gleaned from studies within other organ systems. For example, male sex determination is coordinated via the synergistic action of *Sry* and *Sf1* on *Sox9* enhancer elements within developing Sertoli cells (Sekido and Lovell-Badge 2008). *Lhx2* has also been shown to regulate *Sox9* expression within hair follicle stem cells (Mardaryev et al. 2011), whereas *Notch1* signaling promotes *Sox9* expression during chondrogenesis (Haller et al. 2011). During cortical development, SHH too has been shown to induce *Sox9* expression, although whether this effect is direct or indirect remains unclear (Scott et al. 2010). Our data clearly indicate that *Nfix* plays an important role during the differentiation of embryonic hippocampal neural progenitor cells, repressing *Sox9* expression to promote the differentiation of progenitors at the expense of self-renewal. When considered in light of the role of *Nfix* in driving astrocyte-specific genes (Gopalan et al. 2006; Brun et al. 2009), this reveals that NFIX exerts multifactorial control during neural development. It remains likely, however, that other factors also act to regulate *Sox9* expression in addition to SHH and NFIX. LHX2 and Notch1 are likely candidates for contributing to the regulation of *Sox9* expression during forebrain development, given their previously reported roles in regulating the development of this structure (Mizutani et al. 2007; Subramanian et al. 2011). Interestingly, a recent report has also linked *Sox9* and another *Nfi* family member, *Nfia*, in co-operatively regulating astrogliogenesis within the spinal cord. SOX9 was shown to induce *Nfia* expression during spinal cord development, and these transcription factors were revealed to then form a transcriptional complex that coregulated the expression of *Apcdd1* and *Mmd2* (Kang et al. 2012). It remains unclear whether SOX9 forms active transcriptional complexes with NFIA, or with other NFI family members, within the developing telencephalon, and, moreover, we did not find evidence for the misregulation of either *Apcdd1* or *Mmd2* within the hippocampus of $Nfix^{-/-}$ (this study) or $Nfia^{-/-}$ mice (Piper et al. 2010), again indicating context-dependent differences exist in the actions of these transcription factors within the spinal cord and forebrain.

The findings we present here also provide an insight into the development of the subgranular zone of the dentate gyrus. Both the $Nfia^{-/-}$ and $Nfib^{-/-}$ lines die at birth (Shu, Butz, et al. 2003; Shu, Puche, et al. 2003; Steele-Perkins et al. 2005), and as such, the $Nfix^{-/-}$ line provides an opportunity to study *Nfi* gene function in postnatal hippocampal development. Here we reveal that, although the dentate gyrus does eventually form soon after birth in *Nfix* mutant mice, the morphology of this structure is aberrant, with neural progenitor cells exhibiting abnormal morphologies, and PROX1-expressing dentate granule neurons being found in significantly smaller numbers. These findings demonstrate that NFIX is important for both the architectural development of the dentate gyrus and the formation of the subgranular zone neurogenic niche. Unfortunately, *Nfix* mutants on a C57Bl/6J background die at weaning, precluding investigations aimed at determining whether these hippocampal abnormalities

culminate in functional deficits with regard to hippocampal function. The development of a conditional floxed *Nfix* allele may provide one avenue to address this issue.

Another interesting finding arising from these and other recent studies is the phenotypic similarity between mice lacking *Nfia*, *Nfib*, or *Nfix* (Barry et al. 2008; Piper et al. 2010; Heng et al. 2012). In each of these knockout lines, the astroglial development arising from progenitor cells within the ammonic neuroepithelium is delayed, suggesting that *Nfi* genes act in a common pathway to drive gliogenesis. Our data from postnatal $Nfix^{-/-}$ mice support the idea that NFI family members may act co-operatively in the gliogenic pathway, as gliogenesis within the hippocampus (Fig. 9) and neocortex (Supplementary Fig. 5) does eventually occur in the absence of *Nfix*. This finding is further supported by studies performed in human glioblastoma cell lines, which indicate that *Nfia* and *Nfib* act early during gliogenesis, whereas *Nfic* and *Nfix* act later in this process (Wilczynska et al. 2009). However, the extent to which individual NFI proteins act in either common or divergent pathways remains unresolved. Although the data generated both in vitro and from mouse models indicate that *Nfi* genes contribute to the expression of astrocyte-specific genes, it is unknown whether each family member targets a specific suite of downstream factors during development. However, the structure of the NFI proteins themselves provides insights into this issue. Each NFI has a highly conserved N-terminal DNA-binding domain, and a less well conserved C-terminal domain involved in protein–protein interactions (Mason et al. 2009). The inference from such structural separation between the N- and C-termini is that individual isoforms can potentially act in concert with different binding partners to regulate gene expression. Support for this is provided by the fact that we did not find evidence for the dysregulation of *Sox9* in microarrays of hippocampal tissue from $Nfia^{-/-}$ mice (Piper et al. 2010), or for the dysregulation of *Hes1*, a target for repression by *Nfia* and *Nfib* within $Nfix^{-/-}$ mice (Supplementary Table 1). Looking forward, comparative gene expression analyses of different *Nfi* knockouts in distinct spatial and temporal windows should provide valuable insights into the unique transcriptional signature of each NFI family member during development, thereby clarifying the extent to which these transcription factors act via common or divergent mechanisms throughout development. Such methods will also highlight the similarities and differences in the activities of the NFI proteins within different developmental contexts, such as the developing hippocampus and the developing spinal cord.

Supplementary Material

Supplementary material can be found at: http://www.cercor.oxfordjournals.org/.

Funding

This work was supported by National Health and Medical Research Council (NHMRC) project grants (grant number 1003462 to M.P., grant number 569504 to L.J.R.) and by National Institute of Health and NYSTEM grants (grant numbers HL080624 and C026429 to R.M.G.). The following authors were supported by NHMRC fellowships: M.P. (Biomedical Career Development Fellowship); L.J.R. (Principal Research Fellowship). Y.H.E.H. was supported by a University of Queensland International scholarship.

Notes

We thank Rowan Tweedale for critical analysis of the manuscript, and Drs. Peter Koopman, Robert Hevner, Shubha Tole, Andre Goffinet, and Niels Danbolt for kindly providing reagents. *Conflict of Interest*: None declared.

References

Avilion AA, Nicolis SK, Pevny LH, Perez L, Vivian N, Lovell-Badge R. 2003. Multipotent cell lineages in early mouse development depend on SOX2 function. Genes Dev. 17:126–140.

Bailey TL, Boden M, Buske FA, Frith M, Grant CE, Clementi L, Ren J, Li WW, Noble WS. 2009. MEME SUITE: tools for motif discovery and searching. Nucleic Acids Res. 37:W202–W208.

Bani-Yaghoub M, Tremblay RG, Lei JX, Zhang D, Zurakowski B, Sandhu JK, Smith B, Ribecco-Lutkiewicz M, Kennedy J, Walker PR *et al.* 2006. Role of Sox2 in the development of the mouse neocortex. Dev Biol. 295:52–66.

Barry G, Piper M, Lindwall C, Moldrich R, Mason S, Little E, Sarkar A, Tole S, Gronostajski RM, Richards LJ. 2008. Specific glial populations regulate hippocampal morphogenesis. J Neurosci. 28:12328–12340.

Bettler B, Boulter J, Hermans-Borgmeyer I, O'Shea-Greenfield A, Deneris ES, Moll C, Borgmeyer U, Hollmann M, Heinemann S. 1990. Cloning of a novel glutamate receptor subunit, GluR5: expression in the nervous system during development. Neuron. 5:583–595.

Bielle F, Griveau A, Narboux-Neme N, Vigneau S, Sigrist M, Arber S, Wassef M, Pierani A. 2005. Multiple origins of Cajal-Retzius cells at the borders of the developing pallium. Nat Neurosci. 8:1002–1012.

Bowles J, Schepers G, Koopman P. 2000. Phylogeny of the SOX family of developmental transcription factors based on sequence and structural indicators. Dev Biol. 227:239–255.

Brun M, Coles JE, Monckton EA, Glubrecht DD, Bisgrove D, Godbout R. 2009. Nuclear factor I regulates brain fatty acid-binding protein and glial fibrillary acidic protein gene expression in malignant glioma cell lines. J Mol Biol. 391:282–300.

Campbell CE, Piper M, Plachez C, Yeh YT, Baizer JS, Osinski JM, Litwack ED, Richards LJ, Gronostajski RM. 2008. The transcription factor Nfix is essential for normal brain development. BMC Dev Biol. 8:52.

Cashman NR, Durham HD, Blusztajn JK, Oda K, Tabira T, Shaw IT, Dahrouge S, Antel JP. 1992. Neuroblastoma x spinal cord (NSC) hybrid cell lines resemble developing motor neurons. Dev Dyn. 194:209–221.

Cebolla B, Vallejo M. 2006. Nuclear factor-I regulates glial fibrillary acidic protein gene expression in astrocytes differentiated from cortical precursor cells. J Neurochem. 97:1057–1070.

Chaudhry AZ, Lyons GE, Gronostajski RM. 1997. Expression patterns of the four nuclear factor I genes during mouse embryogenesis indicate a potential role in development. Dev Dyn. 208:313–325.

Dahlstrand J, Lardelli M, Lendahl U. 1995. Nestin mRNA expression correlates with the central nervous system progenitor cell state in many, but not all, regions of developing central nervous system. Brain Res Dev Brain Res. 84:109–129.

Deneen B, Ho R, Lukaszewicz A, Hochstim CJ, Gronostajski RM, Anderson DJ. 2006. The transcription factor NFIA controls the onset of gliogenesis in the developing spinal cord. Neuron. 52:953–968.

Driller K, Pagenstecher A, Uhl M, Omran H, Berlis A, Grunder A, Sippel AE. 2007. Nuclear Factor One X deficiency causes brain malformation and severe skeletal defects. Mol Cell Biol. 27:3855–3867.

Eckenhoff MF, Rakic P. 1988. Nature and fate of proliferative cells in the hippocampal dentate gyrus during the life span of the rhesus monkey. J Neurosci. 8:2729–2747.

Englund C, Fink A, Lau C, Pham D, Daza RA, Bulfone A, Kowalczyk T, Hevner RF. 2005. Pax6, Tbr2, and Tbr1 are expressed sequentially by radial glia, intermediate progenitor cells, and postmitotic neurons in developing neocortex. J Neurosci. 25:247–251.

Frantz GD, Bohner AP, Akers RM, McConnell SK. 1994. Regulation of the POU domain gene SCIP during cerebral cortical development. J Neurosci. 14:472–485.

Frotscher M, Haas CA, Forster E. 2003. Reelin controls granule cell migration in the dentate gyrus by acting on the radial glial scaffold. Cereb Cortex. 13:634–640.

Fujita PA, Rhead B, Zweig AS, Hinrichs AS, Karolchik D, Cline MS, Goldman M, Barber GP, Clawson H, Coelho A *et al.* 2011. The UCSC Genome Browser database: update 2011. Nucleic Acids Res. 39:D876–D882.

Garcia-Moreno F, Lopez-Mascaraque L, De Carlos JA. 2007. Origins and migratory routes of murine Cajal-Retzius cells. J Comp Neurol. 500:419–432.

Gleeson JG, Lin PT, Flanagan LA, Walsh CA. 1999. Doublecortin is a microtubule-associated protein and is expressed widely by migrating neurons. Neuron. 23:257–271.

Gopalan SM, Wilczynska KM, Konik BS, Bryan L, Kordula T. 2006. Nuclear factor-1-X regulates astrocyte-specific expression of the alpha1-antichymotrypsin and glial fibrillary acidic protein genes. J Biol Chem. 281:13126–13133.

Gotea V, Visel A, Westlund JM, Nobrega MA, Pennacchio LA, Ovcharenko I. 2012. Homotypic clusters of transcription factor binding sites are a key component of human promoters and enhancers. Genome Res. 20:565–577.

Gotz M, Huttner WB. 2005. The cell biology of neurogenesis. Nat Rev Mol Cell Biol. 6:777–788.

Gotz M, Stoykova A, Gruss P. 1998. Pax6 controls radial glia differentiation in the cerebral cortex. Neuron. 21:1031–1044.

Grant CE, Bailey TL, Noble WS. 2011. FIMO: scanning for occurrences of a given motif. Bioinformatics. 27:1017–1018.

Guillery RW. 2002. On counting and counting errors. J Comp Neurol. 447:1–7.

Haller R, Schwanbeck R, Martini S, Bernoth K, Kramer J, Just U, Rohwedel J. 2011. Notch1 signaling regulates chondrogenic lineage determination through Sox9 activation. Cell Death Differ. 19:461–469.

Hebert JM, Mishina Y, McConnell SK. 2002. BMP signaling is required locally to pattern the dorsal telencephalic midline. Neuron. 35:1029–1041.

Heng YH, Barry G, Richards LJ, Piper M. 2012. Nuclear factor I genes regulate neuronal migration. Neurosignals. 20:159–167.

Huang da W, Sherman BT, Lempicki RA. 2009. Systematic and integrative analysis of large gene lists using DAVID bioinformatics resources. Nat Protoc. 4:44–57.

Ihrie RA, Alvarez-Buylla A. 2008. Cells in the astroglial lineage are neural stem cells. Cell Tissue Res. 331:179–191.

Imayoshi I, Sakamoto M, Yamaguchi M, Mori K, Kageyama R. 2010. Essential roles of Notch signaling in maintenance of neural stem cells in developing and adult brains. J Neurosci. 30:3489–3498.

Kang P, Lee HK, Glasgow SM, Finley M, Donti T, Gaber ZB, Graham BH, Foster AE, Novitch BG, Gronostajski RM *et al.* 2012. Sox9 and NFIA coordinate a transcriptional regulatory cascade during the initiation of gliogenesis. Neuron. 74:79–94.

Kent J, Wheatley SC, Andrews JE, Sinclair AH, Koopman P. 1996. A male-specific role for SOX9 in vertebrate sex determination. Development. 122:2813–2822.

Komada M, Saitsu H, Kinboshi M, Miura T, Shiota K, Ishibashi M. 2008. Hedgehog signaling is involved in development of the neocortex. Development. 135:2717–2727.

Kruse U, Qian F, Sippel AE. 1991. Identification of a fourth nuclear factor I gene in chicken by cDNA cloning: NFI-X. Nucleic Acids Res. 19:6641.

Lendahl U, Zimmerman LB, McKay RD. 1990. CNS stem cells express a new class of intermediate filament protein. Cell. 60:585–595.

Manzini MC, Walsh CA. 2011. What disorders of cortical development tell us about the cortex: one plus one does not always make two. Curr Opin Genet Dev. 21:333–339.

Mardaryev AN, Meier N, Poterlowicz K, Sharov AA, Sharova TY, Ahmed MI, Rapisarda V, Lewis C, Fessing MY, Ruenger TM *et al.* 2011. Lhx2 differentially regulates Sox9, Tcf4 and Lgr5 in hair follicle stem cells to promote epidermal regeneration after injury. Development. 138:4843–4852.

Mason S, Piper M, Gronostajski RM, Richards LJ. 2009. Nuclear factor one transcription factors in CNS development. Mol Neurobiol. 39:10–23.

Mizutani K, Yoon K, Dang L, Tokunaga A, Gaiano N. 2007. Differential Notch signalling distinguishes neural stem cells from intermediate progenitors. Nature. 449:351–355.

Namihira M, Kohyama J, Semi K, Sanosaka T, Deneen B, Taga T, Nakashima K. 2009. Committed neuronal precursors confer astrocytic potential on residual neural precursor cells. Dev Cell. 16:245–255.

Pierce RA, Moore CH, Arikan MC. 2006. Positive transcriptional regulatory element located within exon 1 of elastin gene. Am J Physiol Lung Cell Mol Physiol. 291:L391–L399.

Piper M, Barry G, Hawkins J, Mason S, Lindwall C, Little E, Sarkar A, Smith AG, Moldrich RX, Boyle GM *et al.* 2010. NFIA controls telencephalic progenitor cell differentiation through repression of the Notch effector Hes1. J Neurosci. 30:9127–9139.

Piper M, Dawson AL, Lindwall C, Barry G, Plachez C, Richards LJ. 2007. Emx and Nfi genes regulate cortical development and axon guidance in the telencephalon. Novartis Found Symp. 288:230–242; discussion 242–235, 276–281.

Piper M, Harris L, Barry G, Heng YH, Plachez C, Gronostajski RM, Richards LJ. 2011. Nuclear factor one X regulates the development of multiple cellular populations in the postnatal cerebellum. J Comp Neurol. 519:3532–3548.

Piper M, Moldrich RX, Lindwall C, Little E, Barry G, Mason S, Sunn N, Kurniawan ND, Gronostajski RM, Richards LJ. 2009. Multiple non-cell-autonomous defects underlie neocortical callosal dysgenesis in Nfib-deficient mice. Neural Dev. 4:43.

Piper M, Plachez C, Zalucki O, Fothergill T, Goudreau G, Erzurumlu R, Gu C, Richards LJ. 2009. Neuropilin 1-Sema signaling regulates crossing of cingulate pioneering axons during development of the corpus callosum. Cereb Cortex. 19(Suppl 1):i11–i21.

Pjanic M, Pjanic P, Schmid C, Ambrosini G, Gaussin A, Plasari G, Mazza C, Bucher P, Mermod N. 2011. Nuclear factor I revealed as family of promoter binding transcription activators. BMC Genomics. 12:181.

Plachez C, Lindwall C, Sunn N, Piper M, Moldrich RX, Campbell CE, Osinski JM, Gronostajski RM, Richards LJ. 2008. Nuclear factor I gene expression in the developing forebrain. J Comp Neurol. 508:385–401.

Pleasure SJ, Anderson S, Hevner R, Bagri A, Marin O, Lowenstein DH, Rubenstein JL. 2000. Cell migration from the ganglionic eminences is required for the development of hippocampal GABAergic interneurons. Neuron. 28:727–740.

Pleasure SJ, Collins AE, Lowenstein DH. 2000. Unique expression patterns of cell fate molecules delineate sequential stages of dentate gyrus development. J Neurosci. 20:6095–6105.

Rash BG, Lim HD, Breunig JJ, Vaccarino FM. 2011. FGF signaling expands embryonic cortical surface area by regulating Notch-dependent neurogenesis. J Neurosci. 31:15604–15617.

Rickmann M, Amaral DG, Cowan WM. 1987. Organization of radial glial cells during the development of the rat dentate gyrus. J Comp Neurol. 264:449–479.

Rupp RA, Kruse U, Multhaup G, Gobel U, Beyreuther K, Sippel AE. 1990. Chicken NFI/TGGCA proteins are encoded by at least three independent genes: NFI-A, NFI-B and NFI-C with homologues in mammalian genomes. Nucleic Acids Res. 18:2607–2616.

Sahara S, O'Leary DD. 2009. Fgf10 regulates transition period of cortical stem cell differentiation to radial glia controlling generation of neurons and basal progenitors. Neuron. 63:48–62.

Sauvageot CM, Stiles CD. 2002. Molecular mechanisms controlling cortical gliogenesis. Curr Opin Neurobiol. 12:244–249.

Schmid CD, Bucher P. 2010. MER41 repeat sequences contain inducible STAT1 binding sites. PLoS One. 5:e11425.

Scott CE, Wynn SL, Sesay A, Cruz C, Cheung M, Gomez Gaviro MV, Booth S, Gao B, Cheah KS, Lovell-Badge R *et al.* 2010. SOX9

induces and maintains neural stem cells. Nat Neurosci. 13:1181–1189.
Sekido R, Lovell-Badge R. 2008. Sex determination involves synergistic action of SRY and SF1 on a specific Sox9 enhancer. Nature. 453:930–934.
Seri B, Garcia-Verdugo JM, Collado-Morente L, McEwen BS, Alvarez-Buylla A. 2004. Cell types, lineage, and architecture of the germinal zone in the adult dentate gyrus. J Comp Neurol. 478:359–378.
Seri B, Garcia-Verdugo JM, McEwen BS, Alvarez-Buylla A. 2001. Astrocytes give rise to new neurons in the adult mammalian hippocampus. J Neurosci. 21:7153–7160.
Shibata T, Yamada K, Watanabe M, Ikenaka K, Wada K, Tanaka K, Inoue Y. 1997. Glutamate transporter GLAST is expressed in the radial glia-astrocyte lineage of developing mouse spinal cord. J Neurosci. 17:9212–9219.
Shimojo H, Ohtsuka T, Kageyama R. 2008. Oscillations in notch signaling regulate maintenance of neural progenitors. Neuron. 58:52–64.
Shu T, Butz KG, Plachez C, Gronostajski RM, Richards LJ. 2003. Abnormal development of forebrain midline glia and commissural projections in Nfia knock-out mice. J Neurosci. 23:203–212.
Shu T, Puche AC, Richards LJ. 2003. Development of midline glial populations at the corticoseptal boundary. J Neurobiol. 57:81–94.
Sievers J, Hartmann D, Pehlemann FW, Berry M. 1992. Development of astroglial cells in the proliferative matrices, the granule cell layer, and the hippocampal fissure of the hamster dentate gyrus. J Comp Neurol. 320:1–32.
Singh SK, Bhardwaj R, Wilczynska KM, Dumur CI, Kordula T. 2011. A complex of nuclear factor I-X3 and STAT3 regulates astrocyte and glioma migration through the secreted glycoprotein YKL-40. J Biol Chem. 286:39893–39903.
Smith AG, Brightwell G, Smit SE, Parsons PG, Sturm RA. 1998. Redox regulation of Brn-2/N-Oct-3 POU domain DNA binding activity and proteolytic formation of N-Oct-5 during melanoma cell nuclear extraction. Melanoma Res. 8:2–10.
Steele-Perkins G, Plachez C, Butz KG, Yang G, Bachurski CJ, Kinsman SL, Litwack ED, Richards LJ, Gronostajski RM. 2005. The transcription factor gene Nfib is essential for both lung maturation and brain development. Mol Cell Biol. 25:685–698.
Stolt CC, Lommes P, Sock E, Chaboissier MC, Schedl A, Wegner M. 2003. The Sox9 transcription factor determines glial fate choice in the developing spinal cord. Genes Dev. 17:1677–1689.
Stolt CC, Rehberg S, Ader M, Lommes P, Riethmacher D, Schachner M, Bartsch U, Wegner M. 2002. Terminal differentiation of myelin-forming oligodendrocytes depends on the transcription factor Sox10. Genes Dev. 16:165–170.
Stolt CC, Wegner M. 2010. SoxE function in vertebrate nervous system development. Int J Biochem Cell Biol. 42:437–440.
Subramanian L, Sarkar A, Shetty AS, Muralidharan B, Padmanabhan H, Piper M, Monuki ES, Bach I, Gronostajski RM, Richards LJ *et al*. 2011. Transcription factor Lhx2 is necessary and sufficient to suppress astrogliogenesis and promote neurogenesis in the developing hippocampus. Proc Natl Acad Sci USA. 108:E265–E274.
Suh H, Consiglio A, Ray J, Sawai T, D'Amour KA, Gage FH. 2007. In vivo fate analysis reveals the multipotent and self-renewal capacities of Sox2+ neural stem cells in the adult hippocampus. Cell Stem Cell. 1:515–528.
Wang TW, Stromberg GP, Whitney JT, Brower NW, Klymkowsky MW, Parent JM. 2006. Sox3 expression identifies neural progenitors in persistent neonatal and adult mouse forebrain germinative zones. J Comp Neurol. 497:88–100.
Wang W, Mullikin-Kilpatrick D, Crandall JE, Gronostajski RM, Litwack ED, Kilpatrick DL. 2007. Nuclear factor I coordinates multiple phases of cerebellar granule cell development via regulation of cell adhesion molecules. J Neurosci. 27:6115–6127.
Wilczynska KM, Singh SK, Adams B, Bryan L, Rao RR, Valerie K, Wright S, Griswold-Prenner I, Kordula T. 2009. Nuclear factor I isoforms regulate gene expression during the differentiation of human neural progenitors to astrocytes. Stem Cells. 27:1173–1181.
Zhou CJ, Zhao C, Pleasure SJ. 2004. Wnt signaling mutants have decreased dentate granule cell production and radial glial scaffolding abnormalities. J Neurosci. 24:121–126.
Zimmermann N, Colyer JL, Koch LE, Rothenberg ME. 2005. Analysis of the CCR3 promoter reveals a regulatory region in exon 1 that binds GATA-1. BMC Immunol. 6:7.

CHAPTER 4

To determine the cell-type specific expression of NFIX within the SVZ, RMS and olfactory bulb

4.0 Aims of chapter

Neurogenesis persists within the rodent SVZ and SGZ throughout postnatal ages and into adulthood. Within the SVZ, neural progenitors proliferate and give rise to neuroblasts that migrate along the RMS into the olfactory bulb, where they differentiate and mature into interneurons. *Nfi* genes have been previous shown to regulate similar roles in other regions of the brain, including progenitor cell self-renewal (Namihira M et al. 2009; Piper M et al. 2010) and gliogenesis within the hippocampus (Deneen B et al. 2006; Barry G et al. 2008; Heng YH et al. 2014), as well as neuronal differentiation and migration within the cerebellum (Wang W et al. 2007). Furthermore, preliminary studies have shown that NFIX is expressed within the SVZ of postnatal mice, and that in the absence of this transcription factor, mice display an aberrant SVZ structure, with excessive PAX6 expressing cell within the SVZ (Campbell CE et al. 2008). These data suggest that NFIX regulates the development of the SVZ. Despite this knowledge, the expression of NFIX within the olfactory bulb, SVZ and RMS during development, postnatally and in adulthood has not yet been studied in detail, and in particular our understanding of which specific cellular populations express NFIX within these regions is limited. Thus, in the next chapter, I analysed the cell-type specific expression of NFIX within the SVZ, RMS and olfactory bulb of embryonic, postnatal and adult mice.

With regards to the data presented in this chapter, the findings have been incorporated into a manuscript along with the description of the SVZ phenotype of *Nfix*$^{-/-}$ mice, which has recently been published in *Cerebral Cortex* (Heng YHE et al. 2014). I did majority of the experiments for this manuscript, as well as preparing the Figures and writing the first draft of the manuscript. The work that was performed by other collaborators that contributed to this manuscript is detailed below:

- **Figure 4.2, 4.3 and 4.7**. The immunofluorescence analysis and confocal imaging were performed together with Dr. Kathleen Cato and Dr. Michael Piper (SBMS, University of Queensland).

- **Figure 4.6**. The immunofluorescence analysis and confocal imaging was performed by Mr Lachlan Harris (PhD student under the supervisor Dr. Michael Piper, SBMS, University of Queensland).

- **Table 4.1.** Putative NFI binding sites within the promoters of genes central to SVZ progenitor and periglomerular interneuron function were identified by Dr. Michael Piper (SBMS, University of Queensland) and Dr. Timothy Bailey (IMB, University of Queensland).

4.1 Abstract

The nuclear factor one (*Nfi*) genes encode a family of site-specific transcription factors. This family consists of four members in the vertebrates, namely *Nfia*, *Nfib*, *Nfic* and *Nfix*. *Nfia, Nfib* and *Nfix* are widely expressed in the developing mouse brain, and have been shown to play a critical role in the development of key structures including the pons, cerebellum, hippocampus, neocortex and spinal cord. NFIA and NFIB are also expressed within the developing and adult olfactory bulb, but the expression of NFIX within this structure is unknown. Here we analysed the expression of NFIX within this structure, as well as within the SVZ and RMS. In contrast to NFIA and NFIB, we found that NFIX was not expressed within the embryonic olfactory bulb, with expression in this region only becoming evident within the postnatal brain. NFIX was also expressed within the SVZ and RMS of the postnatal and adult brain. Furthermore, immunofluorescence analysis using cell-type specific markers revealed that NFIX was expressed by astrocytes and periglomerular neurons within the olfactory bulb, by migrating neuroblasts and astrocytes within the RMS, and by neural progenitor cells and ependymal cells within the SVZ. Collectively, these data demonstrate that NFIX is expressed widely within the postnatal and adult olfactory systems, suggesting that this transcription factor serves an important role in the function of this region of the brain.

4.2 Background

The rodent olfactory bulb contains two main populations of excitatory projection neurons, the mitral and tufted cells. These neurons are derived from progenitor cells within the ventricular zone of the embryonic olfactory bulb (Bayer SA 1983). In contrast, olfactory bulb interneurons are predominantly derived after birth from progenitor cells located within the SVZ lining the lateral ventricles. Throughout postnatal life, the progenitors within the SVZ neurogenic niche give rise to neuroblasts that migrate along the RMS to the olfactory bulb, where they ultimately differentiate into interneurons such as granule cells and periglomerular cells (Luskin MB 1993; Whitman MC and CA Greer 2009). As such, processes including neural progenitor cell differentiation and neuroblast migration play a central role in both the development and the maintenance of the structure of the mature olfactory bulb.

Recent research has shown that the *Nfi* family of transcription factors plays a central role in neural progenitor cell differentiation, as well as neuronal migration and differentiation (Mason S et al. 2009; Heng YH et al. 2012; Kilpatrick DL et al. 2012). For example, NFI transcription factors, which bind as either hetero- or homodimers to the dyad symmetric consensus sequence TTGGC(N5)GCCAA on double stranded DNA with high affinity or with lower affinity to half sites (TTGGC or GCCAA) (Gronostajski RM et al. 1985), have been implicated in the regulation of neural progenitor cell differentiation within the embryonic spinal cord (Deneen B et al. 2006), neocortex (Shu T et al. 2003; Namihira M et al. 2009; Piper M et al. 2009) and hippocampus (Barry G et al. 2008; Piper M et al. 2010). At a mechanistic level, NFIX has been shown to regulate the differentiation of neocortical and hippocampal neural progenitor cells via the repression of the progenitor cell maintenance factor *Sox9* (Heng YH *et al.* 2014). NFI proteins have also been shown to mediate neuronal differentiation and migration within the postnatal cerebellum (Wang W et al. 2007; Wang W et al. 2010), and mice lacking NFIX display defects in cerebellar morphology (Piper M et al. 2011).

Given the importance of NFIX for regulating neural progenitor cell differentiation and neuronal migration within other areas of the brain, we sought to analyze the expression of this factor in the olfactory bulb, SVZ and RMS, as the development and maintenance of these brain regions are predicated on these processes. Previous reports have indicated that mRNAs for all *Nfi* family members are expressed within the olfactory neuroepithelium (Baumeister H et al. 1999), and we have previously shown that NFIA and NFIB are expressed within the SVZ, RMS and olfactory bulb (Plachez C et al. 2012). However, the expression of NFIX at a cell-type specific resolution within these areas is unknown. Here we demonstrate that, unlike NFIA and NFIB, NFIX is not expressed within the embryonic olfactory bulb, with its expression only becoming evident postnatally and ultimately being confined to astrocytes and periglomerular cells within the adult olfactory bulb. NFIX is also expressed by SVZ progenitor cells, and by astrocytes and neuroblasts within the RMS. Collectively these findings suggest that NFIX is involved in the regulation of multiple aspects of the development of the mature olfactory bulb.

4.3 Results

4.3.1 NFIX expression in the developing and adult olfactory bulb

Using immunohistochemistry with an anti-NFIX antibody, we analysed the expression pattern of NFIX in the developing, postnatal and adult olfactory bulb. The specificity of the antibody was demonstrated by immunohistochemical staining of *Nfix*$^{-/-}$ tissue; we observed no labeling with this antibody within the olfactory bulb of P20 *Nfix*$^{-/-}$ mice (Appendix. 6). We next analysed the expression of NFIX within the embryonic, postnatal and adult olfactory bulb via immunohistochemistry. Unlike the expression of NFIA and NFIB, we did not observe expression of NFIX within the embryonic olfactory bulb between E14 and E18 (Figure. 4.1A and data not shown). At P5, NFIX was weakly expressed within the subependymal layer of the olfactory bulb (Figure. 4.1B), but by P10 there was evidence of extensive expression of NFIX within the olfactory bulb. Cells immunoreactive for NFIX were observed within the subependymal layer; these cells are likely SVZ-derived neuroblasts (Figure. 4.1C). Expression of NFIX was also detected within cells comprising the laminae of the olfactory bulb, including cells within the glomerular cell layer and the granule cell layer (Figure. 4.1C, D). By P20, NFIX was strongly expressed within the olfactory bulb, particularly by cells within the subependymal layer and the glomerular layer, but also by scattered cells within the other laminae of the olfactory bulb (Figure. 4.1E, F). This expression pattern was maintained within the adult olfactory bulb (Figure. 4.1G, H).

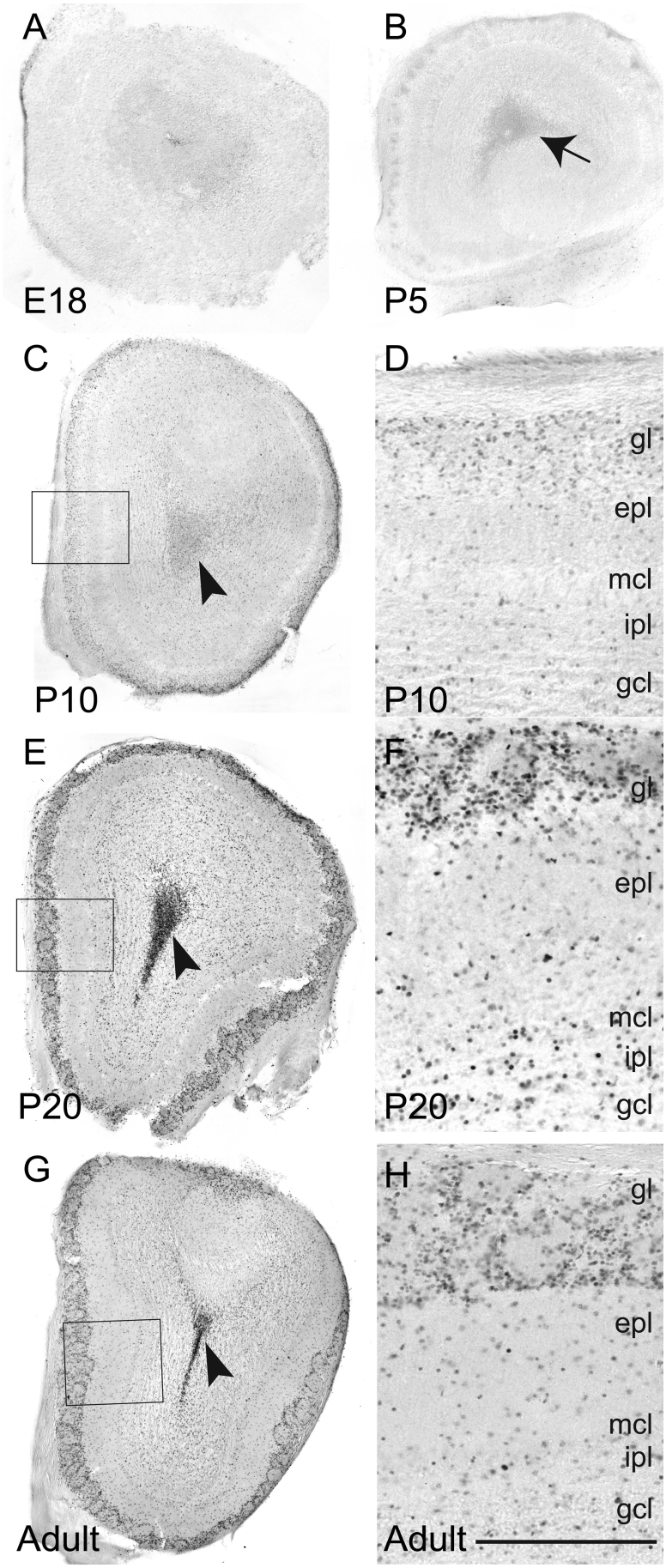
A
E18
B
P5
C
P10
D
gl
epl
mcl
ipl
gcl
P10
E
P20
F
gl
epl
mcl
ipl
gcl
P20
G
Adult
H
gl
epl
mcl
ipl
gcl
Adult

Figure 4.1. **NFIX expression within the postnatal and adult olfactory bulb.**

Coronal sections of the olfactory bulb from E18 (***A***), P5 (***B***), P10 (***C, D***), P20 (***E, F***) and adult (***G, H***) mice, showing expression of NFIX. ***(A)*** At E18, we could not detect any specific expression of NFIX within the olfactory bulb. ***(B)*** By P5, weak expression of NFIX was evident within the subependymal layer of the olfactory bulb (arrow in ***B***). ***(C)*** Expression of NFIX was more pronounced within the olfactory bulb at P10, including by cells within the subependymal layer (arrowhead in ***C***). ***(D)*** Higher magnification view of the boxed region in ***C***, revealing expression of NFIX by cells within the glomerular layer, as well as by other scattered cells within other laminae of the olfactory bulb. (***E-H***) At P20 and within the adult olfactory bulb, neuroblasts entering the olfactory bulb from the RMS were strongly immunoreactive for NFIX (arrowheads ***E, G***). Furthermore, cells within the glomerular layer displayed expression of this transcription factor. NFIX expression was also seen in scattered cells within other laminae of the olfactory bulb (***F, H***). Panels ***F*** and ***H*** are higher magnification views of the boxed regions in ***E*** and ***G*** respectively. gcl, granule cell layer; ipl, internal plexiform layer; mcl, mitral cell layer; epl, external plexiform layer; gl, glomerular layer. Scale bar in ***H***; 650 μm for ***A***; 500 μm for ***B;*** 450 μm for ***C***; 150 μm for ***D***; 250 μm for ***E, G***; 75 μm for ***G, H***.

4.3.2 Cell-type specific expression of NFIX within the adult olfactory bulb

Our expression analysis had indicated that many cells within the postnatal and adult olfactory bulb express NFIX (Figure. 4.1). To determine which specific cell types express this transcription factor within the adult olfactory bulb, we performed coimmunofluorescence labelling. To do this, we analysed the expression of NFIX in a strain of mice expressing GFP under the control of the *Gad67* promoter (*Gad67*- GFP) ((Tamamaki N et al. 2003). GAD67 is one of the principal enzymes used during the production of the inhibitory neurotransmitter γ-aminobutyric acid (GABA). Within the olfactory bulb, GFP expression within this transgenic line is seen within periglomerular cells and granule cells, as these cells are the principal GABA-ergic cells of the olfactory bulb (Parrish-Aungst S et al. 2007). Confocal microscopic analysis of olfactory bulb sections from adult *Gad67*-GFP mice revealed that NFIX was likely expressed by multiple cell types within this structure. GFP-positive neuroblasts within the subependymal layer expressed NFIX (Figure. 4.2B). However, although there were scattered cells within the granule cell layer, the mitral cell layer and the inner and outer plexiform layers that were immunoreactive for NFIX, they did not express GFP (Figure. 4.2C-E). However, *Gad67*-GFP-expressing neurons within the glomerular layer expressed NFIX (Figure. 4.2F), indicating that periglomerular interneurons do express this transcription factor.

To determine the identity of the scattered NFIX-expressing cells within the inner laminae of the olfactory bulb, we analysed expression of the microtubule marker Tuj1, which is expressed by neuronal cells such as mitral cells (Leo JM et al. 2000). This revealed that Tuj1-expressing neurons, including mitral cells, did not express NFIX (Figure. 4.3A). The olfactory bulb also contains glial cells in addition to neuronal populations. Given the well-documented role of NFI proteins in driving glial-specific gene expression *in vitro* (Cebolla B and M Vallejo 2006; Brun M et al. 2009; Wilczynska KM et al. 2009) and astrocytogenesis *in vivo* (Piper M et al. 2009; Heng YH et al. 2014) we analysed the expression of NFIX within mature astrocytes within the olfactory bulb via labelling with GFAP. Interestingly, cells

expressing NFIX within the granule cell layer and mitral cell layer were indeed surrounded by GFAP-positive fibres, suggesting that olfactory bulb astrocytes are likely to express this transcription factor (Figure. 4.3), although, given that NFIX expression is nuclear, and GFAP expression is cytoplasmic, we cannot definitively determine co-localisation using these two markers. Collectively, these data suggest that NFIX is likely expressed in distinct cell types, including astrocytes and periglomerular interneurons, indicating that NFIX plays multiple, context-dependent roles within the adult olfactory bulb.

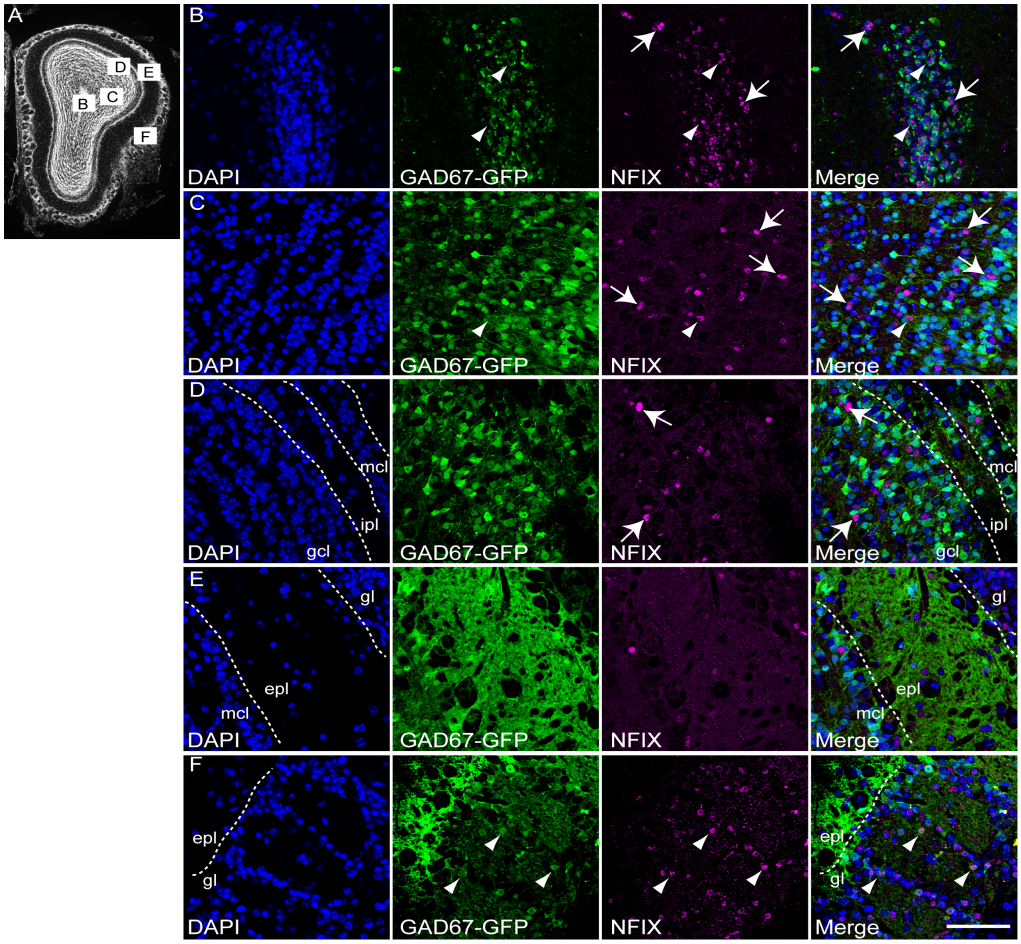

Figure 4.2. Periglomerular interneurons express NFIX within the adult olfactory bulb.

Coronal sections through the olfactory bulb of adult *Gad67*-GFP mice Panel ***A*** shows a low power image of a representative olfactory bulb section labeled with DAPI. The boxed regions indicate the location within the olfactory bulb from which the higher magnification images were obtained. Co immunofluorescence labeling and confocal microscopy (2 µm optical sections) were used to determine the cell-type specific expression of NFIX (magenta) within the adult olfactory bulb. Cell nuclei were labelled with DAPI (blue). ***(B***) Within the core of the olfactory bulb, NFIX-positive nuclei were often surrounded by cytoplasm containing GFP (arrowheads), suggesting that *Gad67*-GFP-expressing neuroblasts within the subependymal layer likely express NFIX. However, there were also some cells present that were immunoreactive for NFIX, but not GFP (arrows). (***C***) Within the granule cell layer (gcl), there were scattered NFIX-expressing cells, but these were mostly GFP-negative (arrows), although we did locate a small number of cells in which NFIX-expressing nuclei were surrounded by GFP-positive cytoplasm (arrowheads). (***D***) Similarly, we observed scattered NFIX-expressing cells within the internal plexiform layer (ipl) and mitral cell layer (mcl) (arrows), but these cells did not express GFP. (***E***) Within the external plexiform layer we saw very few NFIX-expressing cells, and these cells did not express GFP. (***F)*** Within the glomerular layer (gl), we observed numerous GFP-expressing cells that were also immunoreactive for NFIX (arrowheads), suggesting that periglomerular interneurons express NFIX. Scale bar in ***F***; 250 µm for ***A***; 40 µm for ***B-F***.

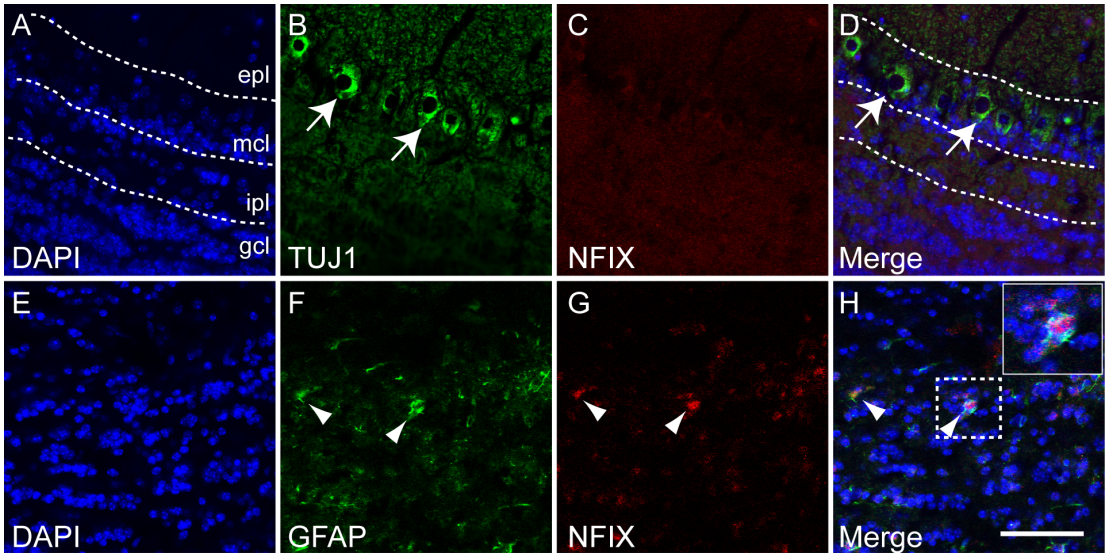

Figure 4.3. **Astrocytes within the adult olfactory bulb express NFIX.**

Coronal sections through the olfactory bulb of wild type mice. Coimmunofluroescence labelling and confocal microscopy (2 µm optical sections) were used to determine cell type specific expression of NFIX (red) within the adult olfactory bulb. Cell nuclei were labelled with DAPI (blue). (***A***) Expression of NFIX within the olfactory bulb was not coincident with Tuj1 expression by mitral cells (arrows in ***A***). (***B***) The fibers of GFAP-expressing astrocytes were seen to encompass the nuclei of NFIX expressing cells (arrowheads in ***B***), suggesting that olfactory bulb astrocytes likely express this transcription factor. A higher power view of an NFIX-expressing nucleus surrounded by GFAP-expressing fibres is shown within the inset of the merged panel on the lower right. gcl, granule cell layer; ipl, internal plexiform layer; mcl, mitral cell layer; epl, external plexiform layer. Scale bar in ***B***; 40 µm for ***A, B***.

4.3.3 NFIX is expressed in the developing and adult RMS and SVZ

Olfactory interneuron production begins during late embryogenesis and continues throughout adulthood in mice (Alvarez-Buylla A and DA Lim 2004). These cells are derived from neural progenitor cells located in the SVZ lining the walls of the lateral ventricles, which differentiate into neuroblasts that migrate along the RMS to the olfactory bulb (Whitman MC and CA Greer 2009). Here they ultimately mature into interneurons. We have previously described defects within the SVZ and RMS of *Nfix*$^{-/-}$ mice, suggestive of a role for NFIX in the normal development of these structures (Campbell CE et al. 2008). Given the SVZ phenotype of *Nfix*$^{-/-}$ mice and expression of NFIX by *Gad67*-GFP positive neuroblasts within the subependymal layer of the olfactory bulb (Fig. 4.2B), we next sought to assess the expression of NFIX within these regions of the developing and adult olfactory system.

Analysis of coronal sections of E18 wild type mouse brains at the level of the corpus callosum demonstrated that NFIX was expressed within the cortical plate of the forebrain, as previously described (Campbell CE et al. 2008). NFIX was also expressed by cells within the emerging SVZ and by cells within the nascent RMS (data not shown). By P5, this expression pattern had become more apparent, with NFIX expression evident within the caudal and rostral SVZ, and within the RMS (data not shown). By P20, the expression of NFIX within the olfactory system was clearly demonstrated through the analysis of sagittal sections of wild type brains. NFIX expression was evident within the hippocampal dentate gyrus (Figure. 4.4A) and within the SVZ, RMS and olfactory bulb (Figure. 4.4A-G). Expression of NFIX by cells within the SVZ and RMS was also recapitulated within the adult brain (Figure. 4.5A-F).

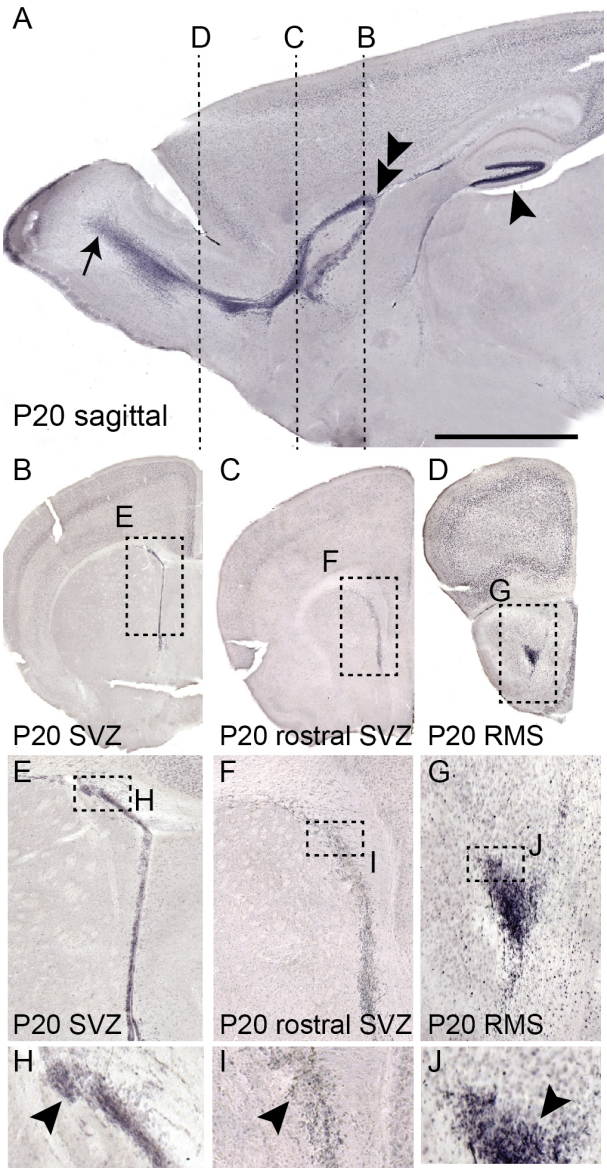

Figure 4.4 Expression of NFIX within the P20 SVZ and RMS.

Sagittal (***A***) and coronal (***B-J***) sections of P20 wild type brains. **A:** A mid-sagittal section of the P20 brain reveals the extensive expression of NFIX within the SVZ, RMS and olfactory bulb. The lines indicate the position of the coronal sections portrayed in panels ***B-D***. NFIX expression is also observed within the hippocampal dentate gyrus (arrowhead in ***A***). Coronal sections at the level of the SVZ (***B***), rostral SVZ (***C***) and RMS (***D***) demonstrate the expression of NFIX. Higher magnification images clearly reveal the expression of NFIX by cells within the SVZ (arrowheads in ***E, F***) and the RMS (arrowhead in ***G***). Panels ***E, F*** and ***G*** are higher magnification views of the boxed regions in ***B, C*** and ***D***, respectively. Panel ***H, I, J*** are higher power view of the boxed regions in ***E, F, G***, respectively, showing NFIX expression within the SVZ and RMS at P20. Scale bar in ***A***: 300 μm for ***B-D***; 100 μm for ***E-G***.

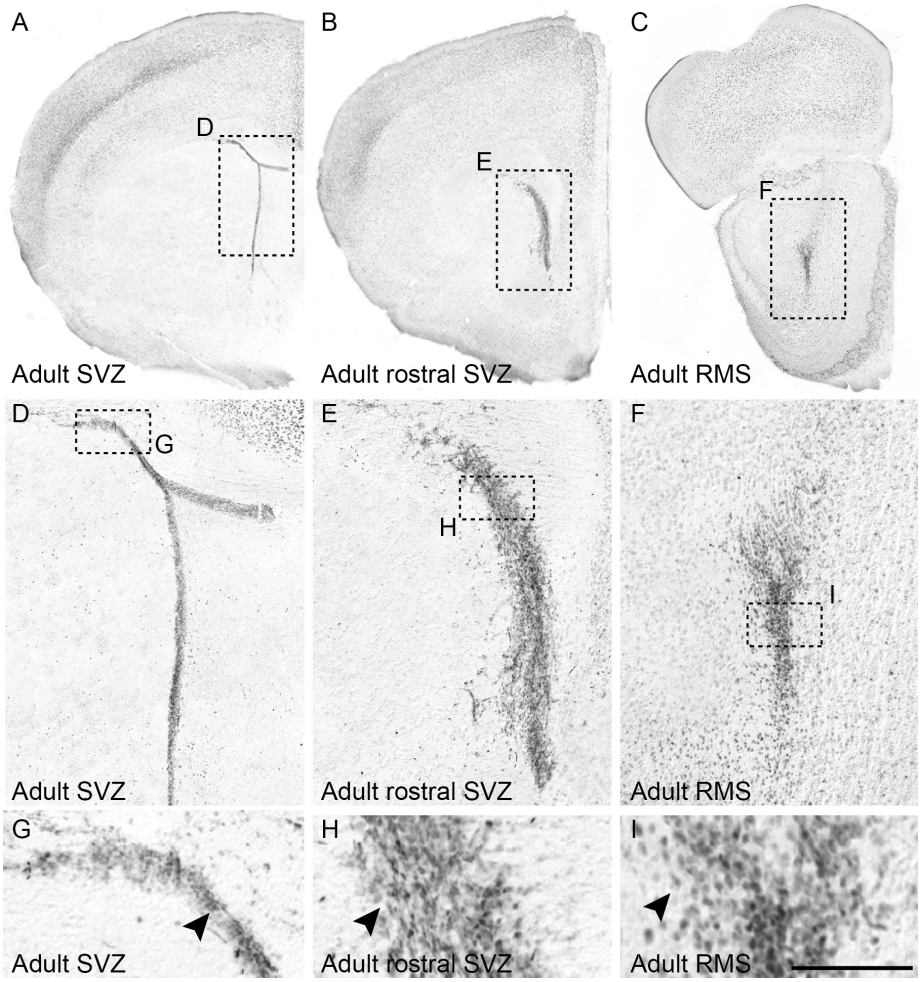

Figure 4.5 Continued expression of NFIX within the adult SVZ and RMS.

Coronal sections of adult wild-type brains. NFIX expression was evident within the SVZ (***A***, ***B***) and the RMS (***C***). Higher magnification images clearly demonstrate the expression of NFIX by cells within the SVZ (arrowheads in ***D***, ***E***) and the RMS (arrowhead in ***F***). Panels ***D***, ***E*** and ***F*** are higher magnification views of the boxed regions in ***A***, ***B*** and ***C***, respectively. Panel ***G, H, I*** are higher power view of the boxed regions in ***E, F, G***, respectively, showing that NFIX continue to be expressed by individual cells within the adult SVZ and RMS Scale bar in ***F;*** 300 μm for ***A***-***C***; 100 μm for ***D***-***F***.

4.3.4 Cell-type specific expression of NFIX within the adult SVZ and RMS

To identify the specific cell types within the SVZ and RMS that were expressing NFIX, we first analysed the expression of NFIX within the SVZ of a strain of mice expressing GFP under the control of the neural stem cell-specific *Hes5* promoter. Co-labelling of the SVZ of adult *Hes5*-GFP mice with antibodies against another neural stem cell marker, GFAP, and NFIX revealed that cells expressing both *Hes5*-GFP and GFAP also expressed NFIX (Fig. 4.6A-E). Interestingly, many cells were immunopositive for NFIX, but not for GFP. These are likely to be ependymal cells, as s100β-expressing ependymal cells lining the lateral ventricles were also immunopositive for NFIX (data not shown).

Within the SVZ and RMS, migrating neuroblasts express the microtubule-associated protein DCX and GAD67. To determine if neuroblasts within the adult brain express NFIX, we analysed the expression of this transcription factor in a strain of mice expressing GFP under the control of the *Dcx* promoter (*Dcx*-GFP). GFP-expressing neuroblasts within the SVZ and RMS were seen to express NFIX (Figure 4.7). Furthermore, this result was supported by findings in a line of mice expressing GFP under the control of the *Gad67* promoter (Tamamaki N et al. 2003) (Figure 4.7). However, although all neuroblasts within the RMS expressed NFIX, there were also cells surrounding the RMS that were immunoreactive for NFIX, but not for GFP (Figure 4.7). These cells could be RMS astrocytes, which comprise the glial tube through which SVZ-derived neuroblasts migrate *en route* to the olfactory bulb (Peretto P et al. 1997). Co-immunofluorescence labelling with anti-GFAP antibodies supported this supposition, with confocal microscopic analyses revealing that there were some cells expressing both GFAP and NFIX along the periphery of the RMS (Figure 4.7), though again, given that NFIX is nuclear, and GFAP cytoplasmic, we cannot definitively demonstrate co-localisation with this technique. Collectively, these findings suggest that NFIX is also expressed by multiple cellular populations within the adult SVZ and RMS.

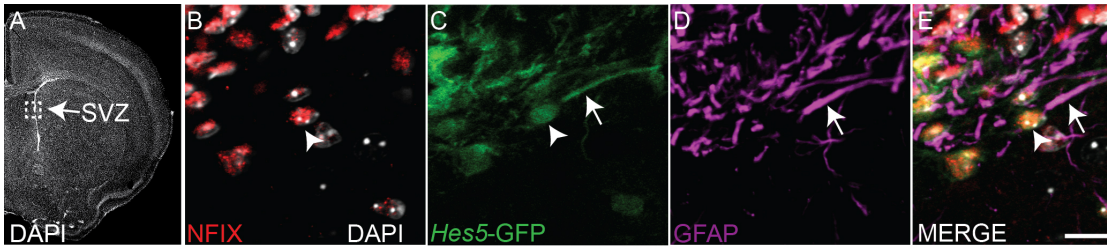

Figure 4.6. Neural progenitor cells and ependymal cells express NFIX within the adult SVZ.

Coronal sections through the SVZ of adult wild-type (***A, B, D, E***) and *Hes5*-GFP (***C***) mice. Panel ***A*** shows a low power image of a representative section labelled with DAPI. The boxed region indicates the approximate location within the SVZ from which the higher magnification images of other sections were obtained. Co-immunofluorescence labelling and confocal microscopy (2 µm optical section) were used to determine the cell-type specific expression of NFIX within the adult SVZ. Cell nuclei were labelled with DAPI (white). Within the SVZ of *Hes5*-GFP mice, GFP-expressing expressing neural stem cells (green, ***C***) express GFAP (magenta) and NFIX (red). The neural stem cell indicated demonstrates co-expression of GFP and NFIX within the nucleus (arrowheads in ***B, E***), as well as co-localisation of GFP and GFAP within the cytoplasm of this cell (arrow in ***D, E***). Scale bar (in ***E***); 300 µm for **A**; 25 µm for ***B-E***.

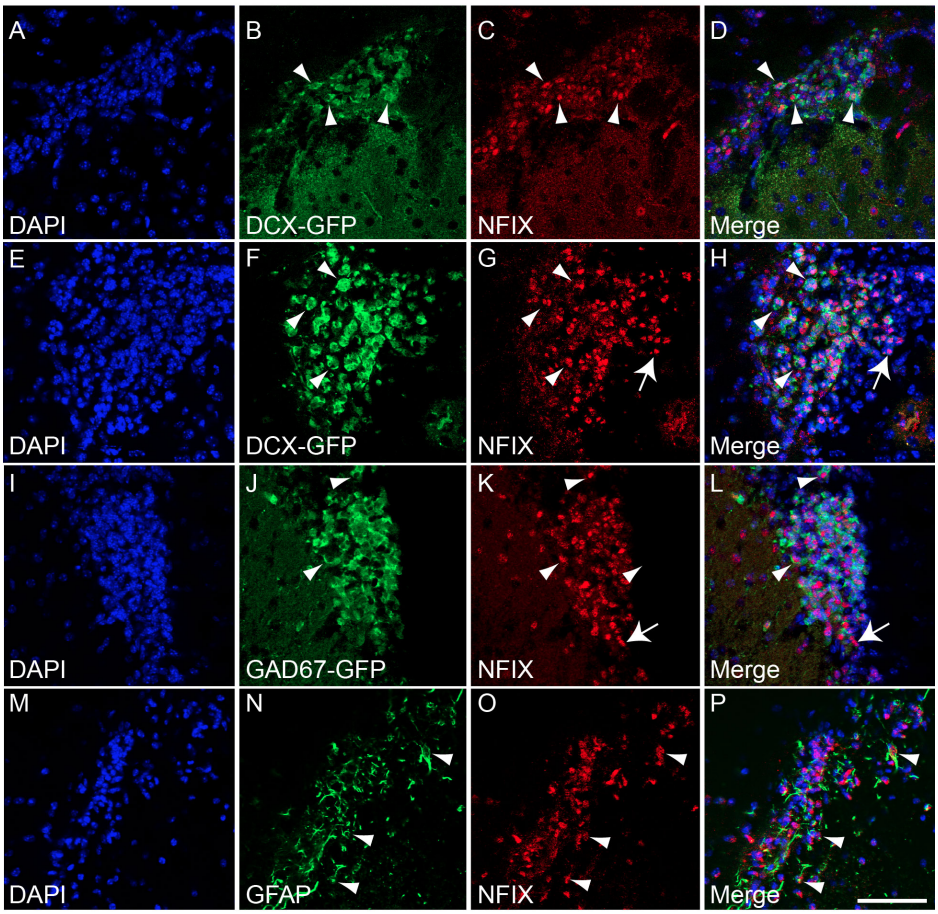

Figure 4.7. Cell-type specific expression of NFIX within the SVZ and RMS of adult mice. Coronal sections through the SVZ (***A-D***) and RMS (***E-P***) of adult wild-type (***M-P***), *Dcx*-GFP (***A-H***) and *Gad67*-GFP (***I-L***) mice. Co-immunofluorescence labelling and confocal microscopy (2 µm optical sections) were used to determine the cell-type specific expression of NFIX (red) within the adult SVZ and RMS. Cell nuclei were labelled with DAPI (blue). Within the SVZ and RMS of *Dcx*-GFP mice, NFIX expression was seen within GFP-expressing neuroblasts (arrowheads in ***B-D*** and ***F-H***). Similarly, within the RMS of *Gad67*-GFP mice (***J***), GFP-expressing neuroblasts expressed NFIX (arrowheads in ***J-L***). However, within the RMS of both strains of mice, there were NFIX-expressing cells on the periphery of the RMS that were GFP negative (arrows in ***G, H, K, L***). Within the RMS of adult wild-type mice (***M***), we observed NFIX-immunopositive cells on the periphery of the RMS that were surrounded by GFAP-positive fibers (arrowheads in ***N-P***), indicating that RMS astrocytes express NFIX. Scale bar (in ***P***); 40 µm.

4.4.6 Potential targets of NFIX within the olfactory system.

The DNA-binding consensus for NFI proteins has been well characterised from *in vitro* binding assays (Gronostajski RM et al. 1985) and a more recent paper used a chromatin immunoprecipitation sequencing approach with a pan-NFI antibody to refine the NFI binding consensus for this family *in vivo* (Pjanic M et al. 2011). We have previously used this newly refined motif to identify potential NFI binding sites within the promoters of genes implicated in neuroblast migration through the RMS, including *Slit1*, *Dcx*, *Cdk5*, and *Ncam1* (Plachez C et al. 2008). Here we extended this analysis to identify other potential NFI target genes within the olfactory system, based on the presence of a putative NFI binding site close to the transcription start site of the respective genes (Table 4.1). Within the SVZ these included *tenascin C, s100β, Egfr, Fgf2, Fgfr1, Fgfr2, plexin B2, Shh* and *Gli1*, all of which have been implicated in neurogenesis or stem cell maintenance within this niche (Palma V et al. 2005; Peretto P et al. 2005; Frinchi M et al. 2008; Lindberg OR et al. 2012; Saha B et al. 2012). For genes expressed within the olfactory bulb we also identified NFI binding sites in the promoters of *calretinin, glutamate decarboxylase 1 (Gad67)* and *glutamate decarboxylase 2 (Gad65)*, each of which has been implicated in the biology of periglomerluar neurons (Parrish-Aungst S et al. 2007; Kiyokage E et al. 2010). This analysis suggests that NFIX is likely to regulate multiple transcriptional programs within the olfactory system.

TABLE 4.1. Putative NFI binding sites within the promoters of genes central to SVZ progenitor and periglomerular interneuron function.

All potential NFI binding sites with *p*-values ≤ 10-4 were reported in the region of -3000 base pairs to +200 base pairs relative to the transcription start site (TSS) of the selected genes.

Gene	UCSC identifier	Position relative to TSS	Site *p*-value	Site sequence
Tenascin C	uc008thk.2	-98	2.4×10^{-5}	CAGGCGCGCCGCCAG
Tenascin C	uc008thk.2	-288	7.3×10^{-5}	CAGGCGCGCCGCCAG
Tenascin C	uc008thk.2	-2010	2.3×10^{-6}	TGGGAAGGGGGCCAG
Plexin B2	uc011zxs.1	196	6.4×10^{-5}	GTGGCCAGGTCCCTA
Plexin B2	uc011zxs.1	-503	5.3×10^{-5}	CTGGGGTGCATCCAA
Plexin B2	uc011zxs.1	-1336	1.3×10^{-5}	TTGGCAAGGTGCCCT
Plexin B2	uc011zxs.1	-1353	2.6×10^{-5}	GTGGCTGGCACCCAG
Plexin B2	uc011zxs.1	-2162	7.7×10^{-5}	CTGGCAGATTTCCCA
Plexin B2	uc011zxs.1	-2162	6.9×10^{-6}	TGGGAAATCTGCCAG
Plexin B2	uc011zxs.1	-2207	2.6×10^{-5}	CTGGGCAGGTTCCCG
s100β	uc007fuc.2	-213	5.8×10^{-6}	TTGGAACTGGGCCAA
s100β	uc007fuc.2	-1867	3.8×10^{-5}	GTGGACAGCAGACAG
s100β	uc007fuc.2	-2789	4.6×10^{-5}	CAGGGCCAGGGCCAG
Shh	uc008wua.2	-1221	1.5×10^{-5}	TGGGAGAAAAGCCAG
Gli1	uc007hjh.1	178	5.8×10^{-6}	AGGGCTGGGGGCCAG
Gli1	uc007hjh.1	-323	6.8×10^{-5}	CTGGCCTACAGACCA
Gli1	uc007hjh.1	-2941	4.0×10^{-5}	GTGGGTGGAGGCCAA
Fgf2	uc012cox.1	91	5.3×10^{-5}	GAGGCTGGCAGCCCG
Fgf2	uc012cox.1	60	5.2×10^{-6}	TGGGCTGGGAGCCCG
Fgf2	uc012cox.1	-335	4.8×10^{-6}	CGGGCTGGGTGCCCA

Fgf2	uc012cox.1	-405	5.6×10^{-5}	CAGGGCAAGCGCCAG
Fgf2	uc012cox.1	-1517	9.8×10^{-5}	CAGGCTGGCCTCCAA
Fgfr1	uc009lge.1	-2112	2.4×10^{-5}	TGGGGTGGAAGCCAG
Fgfr1	uc009lge.1	-2956	3.3×10^{-5}	AAGGGAAGGAGCCAG
Fgfr2	uc012fux.1	-232	1.7×10^{-5}	AAGGCCAAAAGCCAG
Fgfr2	uc012fux.1	-2873	1.8×10^{-5}	TGGGCCTGGCTCCAG
Fgfr2	uc012fux.1	-2946	3.8×10^{-5}	ATGGTCCACAGCCAG
Egfr	uc007ibo.1	160	6.4×10^{-5}	CTGGACGCGAGCCTG
Egfr	uc007ibo.1	111	8.7×10^{-5}	CTGGATCGAGTCCCG
Egfr	uc007ibo.1	-834	6.4×10^{-5}	GAGGCAAATTGCCAA
Egfr	uc007ibo.1	-1153	8.2×10^{-5}	CAGGGCTGCTGCCCA
Calretinin	uc009nko.1	-24	8.2×10^{-5}	GTGGCGCGCAGCCCC
Calretinin	uc009nko.1	-2117	9.2×10^{-7}	CTGGGAGGGAGCCAG
Calretinin	uc009nko.1	-2983	9.2×10^{-5}	GAGGCCTAGGTCCAG
Gad1 (Gad67)	uc008jzk.1	-2653	9.2×10^{-5}	TTGGACGGACGACAA
Gad2 (Gad65)	uc008ink.1	14	3.5×10^{-5}	GTGGAAAGGGCCCAA
Gad2 (Gad65)	uc008ink.1	-419	7.7×10^{-5}	TGGGGAAGGAACCAA

4.5 Discussion

Our results reveal that the expression of NFIX within the developing and adult olfactory bulb, RMS and SVZ is dynamic, with this transcription factor being expressed by multiple cellular populations in these regions of the olfactory system. Within the SVZ and RMS, NFIX is expressed by neural progenitor cells, ependymal cells, neurobasts and astrocytes. Within the adult olfactory bulb, the expression of NFIX is limited to neuroblasts, astrocytes and periglomerular cells. Collectively, these data suggest that NFIX plays multiple, context-dependent roles within the developing and adult olfactory system.

One interesting finding of our study was the distinct differences with respect to the expression of NFIX in the olfactory bulb when compared to other NFI family members. NFIX was not expressed within the olfactory bulb embryonically, and within the adult its expression was confined to neuroblasts, astrocytes and periglomerular interneurons. NFIA and NFIB, however, have been shown to be expressed within the ventricular zone of the embryonic olfactory bulb, and by astrocytes (NFIA) and mitral cells (NFIB) within the adult olfactory bulb (Plachez C et al. 2012). These differences highlight the fact that our understanding of how *Nfi* isoforms are regulated, both transcriptionally and post-transcriptionally, is very limited. However, there are studies that have begun to address the regulation of *Nfi* genes; these too are suggestive of the differential control of individual *Nfi* isoform expression by distinct regulatory programs. For instance, microarray studies performed on cultured neurospheres have suggested that EMX2 may repress the expression of *Nfia* (Gangemi RM et al. 2006), whereas a recent subtractive hybridisation study implicated *Nfib* downstream of Neurogenin 2 (Mattar P et al. 2004). More recently, the stem cell maintenance factor SOX9 has been shown to induce the expression of *Nfia* within the spinal cord to initiate gliogenesis (Kang P et al. 2012). At a post-transcriptional level, *Nfia* and *Nfib* have previously been shown to be regulated by miR223 (Zardo G et al. 2012) and miRs372/373 (Guo H et al. 2011) respectively, again demonstrating the likely existence of isoform-specific patterns of regulatory control for the *Nfi* family. Future studies aimed at elucidating the differential

control of *Nfi* family gene expression will enable us to parse the distinct programs regulating their expression, both within the olfactory bulb and throughout the nervous system.

Our research also reveals that within the SVZ a different situation is present, with NFIX (this study) and NFIA and NFIB (Plachez C et al. 2012) shown to be expressed by progenitor cells within this neurogenic niche. This suggests that NFI proteins may co-operate to regulate neural progenitor cell activity within the adult SVZ. Evidence to support this comes from studies that have shown that NFI isoforms can heterodimerise and regulate gene transcription (Liu Y et al. 1997; Chaudhry AZ et al. 1998), and from a recent finding indicating that a coordinated program of *Nfi* gene family expression is required to execute differentiation in cultured neuronal progenitor cells (Wilczynska KM et al. 2009). It is also possible that while being coexpressed, NFI isoforms regulate distinct genetic programs. Microarray studies performed in the hippocampus of *Nfia*$^{-/-}$ and *Nfix*$^{-/-}$ mice support this suggestion, as many genes were identified as being differentially misregulated within the two knockout strains in these studies (Piper M et al. 2010; Heng YH et al. 2014). The most parsimonious scenario, however, is that while NFI proteins co-operatively regulate some suites of genes, they act individually to regulate others. The analysis of individual *Nfix*$^{-/-}$ mice supports this, as, although *Nfia*$^{-/-}$, *Nfib*$^{-/-}$ and *Nfix*$^{-/-}$ mice all exhibit similar hippocampal phenotypes that are characterized by delayed gliogenesis and reduced dentate gyrus morphogenesis, they are not identical (Shu T et al. 2003; Piper M et al. 2010; Heng YH et al. 2014). For example, the development of hippocampal glia from both the ammonic neuroepithelium and fimbrioglial epithelium is delayed in *Nfia*$^{-/-}$ and *Nfix*$^{-/-}$ mice (Heng et al., 2012b, Piper et al., 2010), whereas *Nfib*$^{-/-}$ mice appear to have normal gliogenesis arising from the fimbrioglial epithelium (Barry G et al. 2008). Moreover, *Nfib*$^{-/-}$ mice display delayed formation of the basilar pons that is not evident within *Nfia*$^{-/-}$ or *Nfix*$^{-/-}$ mice (Kumbasar A et al. 2009); both *Nfia*$^{-/-}$ and *Nfib*$^{-/-}$ mice maintained on a C57Bl/6J background also die at birth (Shu T et al. 2003; Steele-Perkins G et al. 2005), whereas *Nfix*$^{-/-}$ mice survive until weaning (Heng YH et al. 2014).

At this stage the mechanism by which NFIX regulates the biology of SVZ neural progenitor cells remains unclear. Within the developing neocortex and hippocampus, NFIX was recently shown to promote neural progenitor cell differentiation via the repression of the stem cell factor *Sox9* (Heng YH et al. 2014). Given the expression of Sox9 within this neurogenic niche of the adult brain (Cheng LC et al. 2009), it is possible that NFIX functions to regulate *Sox9* expression within the SVZ. NFIX has further been shown to drive the expression of genes implicated in glial differentiation, such as *brain fatty acid-binding* protein and *Gfap* (Brun M et al. 2009). However, the phenotype of *Nfix*$^{-/-}$ mice, in which there are a significantly higher number of DCX-expressing cells within the postnatal SVZ of the mutant, suggests that NFIX may instead act to maintain neural progenitor cell identity within this niche, and that in its absence, progenitor cells prematurely differentiate into neuroblasts destined for the olfactory bulb (Campbell CE et al. 2008).

While the precise role of NFIX within the olfactory system remains unclear, some insights into the roles played by this transcription factor within SVZ progenitors and neuroblasts can be gleaned from the analysis of the promoters of potential NFIX target genes. For example, we identified putative NFI binding sites in the proximal promoters of *tenascin C* and *s100β*. Evidence to support a role for NFI proteins in the regulation of tenascin C has come from recent findings that indicate that the level of tenascin C protein is downregulated in the developing hippocampus of mice lacking either *Nfia* (Piper M et al. 2010), *Nfib* (Barry G et al. 2008) or *Nfix* (Heng YH et al. 2014). Furthermore, we have shown that the level of *s100β* mRNA is reduced in *Nfia*$^{-/-}$ mice (Piper M et al. 2010). Further validation of these, and other targets, involved in the biology of this neurogenic niche will clarify the role of NFIX in adult neurogenesis. We also identified putative NFI binding sites in genes central to the periglomerular interneuron function, namely *calretinin, Gad65* and *Gad67*. We have previously reported a decrease in the level of *calretinin* mRNA in the developing hippocampus of *Nfia*$^{-/-}$ mice (Piper M et al. 2010). Interestingly, the development and

maturation of cerebellar granule neurons has been shown to be dependent on NFI proteins (Wang W et al. 2004; Wang W et al. 2007; Wang W et al. 2010), and more recent findings indicate that NFIs are critical downstream of calretinin signalling in promoting a voltage sensitive developmental switch in late maturing cerebellar neurons (Ding B et al. 2013).

These findings reveal that, in addition to their role in regulating neural progenitor cell differentiation and astrocyte differentiation, the *Nfi* genes are pivotal for neuronal function in distinct areas within the central nervous system. Although such *in silico* predictions do not provide molecular evidence of NFIX-mediated regulation of these genes, they do indicate that NFIX is likely to contribute to the regulation of key genes involved in the biology of the SVZ and olfactory bulb. Future experiments detailing the molecular regulation of these genes by NFIX are needed to confirm if these genes are indeed *bona fide* targets for transcriptional regulation by NFIX.

Given the expression of NFIX by different cells within the SVZ, RMS and olfactory bulb, a further point of consideration is how this protein can exert separate regulatory programs within varied cellular contexts, despite a common DNA-binding motif. One possibility is the presence of different protein-protein interactions within each cellular environment, which potentially provides cell-type specificity to DNA binding events. In support of this, NFIX has previously been shown to interact with NFIB within gel shift analyses (Liu Y et al. 1997), and with STAT 3 in glioma cell lines *in vitro* (Singh SK et al. 2011), as well as to form a complex with SP-1, Rb and HDAC-1 to regulate context-specific gene expression in metastatic breast cancer cells (Singh J et al. 2002). In the future, proteomic analyses of the olfactory system will enable a clearer understanding of the binding partners of NFIX within this system, and how these impart changes to DNA-binding dynamics and hence cellular-specific programs of NFIX-mediated gene expression.

CHAPTER 5

To determine whether NFIX is essential for the proliferation and differentiation of progenitor cells within the SVZ and for the migration of SVZ-derived neuroblasts to the olfactory bulb.

The data contained in the following chapter was published in 2014 in *Cerebral Cortex*

Yee Hsieh Evelyn Heng, Bo Zhou, Lachlan Harris, Tracey Harvey, Aaron Smith, Elise Horne, Ben Martynoga, Jimena Andersen, Angeliki Achimastou, Kathleen Cato, Linda J. Richards, Richard M. Gronostajski, Giles S. Yeo, Francois Guillemot, Timothy L. Bailey, Michael Piper. 2014. NFIX regulates proliferation and migration within the murine SVZ neurogenic niche.
Cerebral Cortex 2014; 1-21; doi:10.1093/cercor/bhu253

5.0 Aims of chapter

In the previous chapter, my work revealed that NFIX is expressed by multiple cellular populations within the SVZ, RMS and olfactory bulb. Furthermore, previous studies have demonstrated that *Nfix*$^{-/-}$ mice display multiple telencephalic defects, including expansion of the cingulate cortex and the entire brain along its dorsoventral axis and, critically, the accumulation of progenitor cells and neuroblasts within the SVZ of the postnatal brain (Campbell CE et al. 2008). The dramatic increase in progenitor cells within the SVZ of *Nfix*$^{-/-}$ mice suggests that *Nfix* may play a role in regulating progenitor cell proliferation within the neurogenic niche. In addition, the accumulation of neuroblasts within the SVZ, coupled with the role played by NFI factors in regulating neuronal migration (Wang W et al. 2007), suggests that *Nfix* may also play a role in regulating the migration of the SVZ-derived neuroblasts out of the SVZ toward the olfactory bulb. The goal of this chapter was, therefore, to investigate the hypothesis that NFIX regulates both SVZ progenitor cell proliferation, and neuroblast migration, within the postnatal SVZ.

With regards to the data presented in this chapter, the findings have been incorporated into a manuscript along with the expression of NFIX within the SVZ, RMS and olfactory bulb mice, which has recently published in *Cerebral Cortex* (Heng YHE et al. 2014). In which, I revealed that NFIX acts in a pleiotropic fashion within the postnatal SVZ, regulating neural progenitor cell proliferation, while also mediating the migration of SVZ-derived neuroblasts to the olfactory bulb. Moreover, we revealed that *Gdnf* is a target for transcriptional activation by NFIX within the RMS. This work revealed a heretofore novel role for NFIX in mediating the transcription of *Gdnf*, which has previously been identified as an attractant for SVZ-derived neuroblasts. I did majority of the experiments for this manuscript, as well as preparing the Figures and writing the first draft of the manuscript. Work that was performed by other collaborators that contributed to this manuscript is detailed below:

- Figure 5.8A-F- Ki67 and DCX immunofluroscence and cell counts of wild type and *Nfix*$^{-/-}$ SVZ were performed by Mr Lachlan Harris (PhD student under the supervisor of Dr Michael Piper, SBMS, University of Queensland).

- **Figure 5.9E, F**- EMSA and supershift assays were conducted by Dr Aaron Smith (SBMS, University of Queensland).

- **Figure 5.9C**- Microarray analyses were performed by Dr Michael Piper (SBMS, University of Queensland), and analysis using Ingenuity Pathway Analysis (IPA) was performed by Dr Giles Yeo (CIMR, Cambridge, UK).

- **Figure 5.9G-** Luciferase assays were conducted in association with Dr Tracey Harvey (SBMS, University of Queensland).

- **Table 5.3** Putative NFI binding sites within the promoters of genes misregulated in the SVZ of *Nfix*$^{-/-}$ mice were identified by Dr. Michael Piper (SBMS, University of Queensland) and Dr Timothy Bailey (IMB, University of Queensland).

OXFORD

Cerebral Cortex, 2014, 1–21

doi: 10.1093/cercor/bhu253
ORIGINAL ARTICLE

ORIGINAL ARTICLE

NFIX Regulates Proliferation and Migration Within the Murine SVZ Neurogenic Niche

Yee Hsieh Evelyn Heng[1], Bo Zhou[5], Lachlan Harris[1], Tracey Harvey[1], Aaron Smith[1], Elise Horne[1], Ben Martynoga[4], Jimena Andersen[4], Angeliki Achimastou[4], Kathleen Cato[1], Linda J. Richards[1,2], Richard M. Gronostajski[5], Giles S. Yeo[6], François Guillemot[4], Timothy L. Bailey[3], and Michael Piper[1,2]

[1]The School of Biomedical Sciences, [2]Queensland Brain Institute, [3]Institute for Molecular Bioscience, The University of Queensland, Brisbane, QLD 4072, Australia, [4]Division of Molecular Neurobiology, MRC-National Institute for Medical Research, London NW7 1AA, UK, [5]Department of Biochemistry, Programs in Neuroscience and Genetics, Genomics & Bioinformatics, Developmental Genomics Group, New York State Center of Excellence in Bioinformatics and Life Sciences, State University of New York at Buffalo, Buffalo, NY 14203, USA, and [6]MRC Metabolic Diseases Unit, University of Cambridge Metabolic Research Laboratories, Wellcome Trust-MRC Institute of Metabolic Science, Addenbrooke's Hospital, Cambridge CB2 0QQ, UK

Address correspondence to Michael Piper, The School of Biomedical Sciences and the Queensland Brain Institute, The University of Queensland, Brisbane 4072, Australia. Email: m.piper@uq.edu.au

Abstract

Transcription factors of the nuclear factor one (NFI) family play a pivotal role in the development of the nervous system. One member, NFIX, regulates the development of the neocortex, hippocampus, and cerebellum. Postnatal *Nfix*$^{-/-}$ mice also display abnormalities within the subventricular zone (SVZ) lining the lateral ventricles, a region of the brain comprising a neurogenic niche that provides ongoing neurogenesis throughout life. Specifically, *Nfix*$^{-/-}$ mice exhibit more PAX6-expressing progenitor cells within the SVZ. However, the mechanism underlying the development of this phenotype remains undefined. Here, we reveal that NFIX contributes to multiple facets of SVZ development. Postnatal *Nfix*$^{-/-}$ mice exhibit increased levels of proliferation within the SVZ, both in vivo and in vitro as assessed by a neurosphere assay. Furthermore, we show that the migration of SVZ-derived neuroblasts to the olfactory bulb is impaired, and that the olfactory bulbs of postnatal *Nfix*$^{-/-}$ mice are smaller. We also demonstrate that gliogenesis within the rostral migratory stream is delayed in the absence of *Nfix*, and reveal that *Gdnf* (glial-derived neurotrophic factor), a known attractant for SVZ-derived neuroblasts, is a target for transcriptional activation by NFIX. Collectively, these findings suggest that NFIX regulates both proliferation and migration during the development of the SVZ neurogenic niche.

Key words: neuroblast, nuclear factor one X, olfactory bulb, rostral migratory stream, subventricular zone

Introduction

The subventricular zone (SVZ) is one of the 2 neurogenic niches in the rodent brain that continuously generates neurons throughout adult life (Kriegstein and Alvarez-Buylla 2009). Within the SVZ, the division of neural stem cells produces transit-amplifying cells, and ultimately neuroblasts. These SVZ-derived neuroblasts migrate away from the SVZ anteriorly along a distinct pathway known as the rostral migratory stream (RMS) to the olfactory bulb. Here, they differentiate into interneurons that migrate radially within the olfactory bulb to either the granule cell layer or the glomerular layer (Sun et al. 2010). Neurogenesis within the SVZ has been linked to innate olfactory responses, with deficits in SVZ neurogenesis in rodent models leading to altered behavior when confronted with a predator-specific odor, and sex-specific deficits in fertility and nurturing (females) and aggression and sexual behavior (males) (Sakamoto et al. 2011).

Neural stem cells within the SVZ are derived from the neuroepithelial progenitor cells of the embryonic forebrain, the radial glia. Indeed, fate-mapping experiments in mice have demonstrated that all parts of the telencephalic neuroepithelium, including the lateral ganglionic eminence, cortex and medial ganglionic eminence, contribute to the adult SVZ progenitor pool (Merkle et al. 2004; Young et al. 2007). Moreover, this heterogeneity is reflected in their neuronal progeny. For example, descendants of radial glia within the embryonic cortex and lateral ganglionic eminence are responsible for generating tyrosine hydroxylase-expressing and calretinin-expressing interneurons within the olfactory bulb (Whitman and Greer 2009). Interestingly, many of the genes shown to regulate radial glial self-renewal and neuronal specification and differentiation have also been shown to be functionally important within the SVZ neurogenic niche, including *Hes1* (Imayoshi et al. 2010), *Ngn2* (Brill et al. 2009), *NeuroD1* (Gao et al. 2009), *Pax6* (Brill et al. 2008), *Tbr2* (Roybon et al. 2009) and *Sox2* (Andreu-Agullo et al. 2012). However, despite these advances, our understanding of the molecular hierarchy controlling SVZ neurogenesis remains incomplete.

The migration of SVZ-derived neuroblasts to the olfactory bulb is also critical for neuronal replacement within this structure. Many cell-autonomous and non-cell-autonomous factors have been shown to control neuroblast migration. For instance, cytoskeletal factors such as doublecortin (DCX) and nude neurodevelopment protein 1-like 1 are critical cell-intrinsic proteins that are required for the migration of neuroblasts (Gleeson et al. 1999; Hippenmeyer et al. 2010). Moreover, extrinsic guidance cues such as slit and netrin are expressed within the forebrain and olfactory bulb and are required to shape the trajectory of migration through the RMS (Murase and Horwitz 2002; Nguyen-Ba-Charvet et al. 2004). Neuroblasts also migrate through a specialized glial substrate called the glial tube, which develops postnatally (Bovetti et al. 2007). The migration of neuroblasts through this astrocytic tube is facilitated by chemoattractants, including glial-derived neurotrophic factor (GDNF; Paratcha et al. 2006), but again, the molecular determinants regulating the development of this specialized substrate remain poorly understood.

The transcription factor nuclear factor one X (NFIX) has previously been implicated in regulating radial glial proliferation and differentiation within the embryonic forebrain, and the migration of neurons within the postnatal cerebellum (Piper et al. 2011; Heng et al. 2014). Here we reveal that NFIX also plays an important role in regulating these processes within the postnatal SVZ/RMS. Through the analysis of postnatal *Nfix*$^{-/-}$ mice, we demonstrate abnormal development of the SVZ and RMS in the absence of this transcription factor. Specifically, *Nfix*$^{-/-}$ mice exhibit increased numbers of neural progenitor cells within the SVZ, a finding supported by the increased numbers of spheres formed by *Nfix*$^{-/-}$ SVZ tissue in vitro in a neurosphere assay. Despite the increased levels of SVZ proliferation, the olfactory bulbs of *Nfix*$^{-/-}$ mice are smaller, with reduced numbers of interneurons expressing PAX6, calbindin and calretinin. Birthdating experiments further reveal deficits in the migration of SVZ-derived neuroblasts to the olfactory bulb. Finally, we demonstrate that gliogenesis within the RMS is delayed and identify *Gdnf* as a target for transcriptional activation by NFIX. Thus, NFIX regulates both proliferation and migration within the postnatal mouse SVZ/RMS.

Materials and Methods

Mouse Strains

Wild-type and *Nfix*$^{-/-}$ littermate mice were used in this study. These mice were maintained on a C57Bl/6J background. Timed-pregnant females were obtained by placing *Nfix*$^{+/-}$ male and *Nfix*$^{+/-}$ female mice together overnight. The following day was designated as embryonic day (E) 0 if the female had a vaginal plug. Mice were genotyped by polymerase chain reaction (PCR; Campbell et al. 2008). Transgenic mice expressing green fluorescent protein (GFP) under control of the glutamic acid decarboxylase 67 (*Gad67*) promoter were also used (Tamamaki et al. 2003), as were mice expressing GFP under the control of the *Dcx* promoter (Walker et al. 2007). The former mice have GFP knocked into the *Gad67* locus, and expression of GFP has previously been shown to colocalize with GAD67 expression (Tamamaki et al. 2003). The latter strain (*Dcx*-GFP/bacterial artificial chromosome [BAC]) was originally obtained from the Mutant Mouse Regional Resource Center and the Gene Expression Nervous System Atlas BAC transgenic project. The pattern of GFP expression in these animals matches previously reported expression of DCX (Gleeson et al. 1999). Finally, we used another BAC transgenic line expressing GFP under the control of the *Hes5* promoter. These mice have been shown previously to express GFP in neural stem cells within the adult brain (Jhaveri et al. 2010). All animals were bred at The University of Queensland under approval from the Institutional Animal Ethics Committee, and were performed according to the Australian Code of Practice for the Care and Use of Animals for Scientific Purposes.

Hematoxylin Staining

Brains from wild-type or *Nfix*$^{-/-}$ mice were dissected from the skull, blocked in 3% noble agar (Difco), and sectioned coronally at 50 μm on a vibratome (Leica). Sections were mounted and stained with Mayer's hematoxylin using standard protocols.

Immunohistochemistry

Embryos, postnatal pups and adult mice were transcardially perfused with 0.9% saline, followed by 4% paraformaldehyde, and postfixed in 4% paraformaldehyde at 4 °C. Brains were removed and sectioned at 50 μm using a vibratome. Immunohistochemistry (IHC) using the chromogen 3,3′-diaminobenzidine (DAB) was performed as described previously (Piper et al. 2009). Biotin-conjugated goat anti-rabbit IgG (BA-1000, Vector Laboratories) and biotin-conjugated donkey anti-mouse IgG (715-065-150, Jackson Immunoresearch) secondary antibodies were used at 1/1000. To perform co-immunofluorescence (IF) labeling, sections were incubated overnight with the primary antibodies at 4 °C.

They were then washed and incubated in a solution containing the secondary antibodies, before being washed again and counterstained with 4′,6-diami-dino-2-phenylindole (DAPI). The secondary antibodies used in this study were goat anti-rabbit IgG AlexaFluor 594 and goat anti-mouse IgG AlexaFluor 488 (both 1/1000; Invitrogen). Sections were then mounted in 50% glycerol diluted in phosphate-buffered saline.

For all immunohistochemical and IF analyses, at least 5 brains were analyzed. Sections labeled with DAB were imaged using an upright microscope (Zeiss upright Axio-Imager Z1) fitted with an Axio-Cam HRc camera. Sections labeled with fluorescent antibodies were imaged with a confocal microscope (Zeiss LSM 510 META) using Zen software (Zeiss). The confocal images presented are 2 μm optical sections of the labeled tissue.

Antibody Parameters

Primary antibodies used for IHC and IF on floating sections were anti-NFIX (ab101341, rabbit polyclonal, 1/10 000 IHC, 1/50 IF, Abcam), anti-GFAP (Z0334, rabbit polyclonal, 1/15 000 IHC, Dako), anti-GFAP (MAB 360, mouse monoclonal, 1/100 IF, Millipore), anti-PAX6 (AB2237, rabbit polyclonal, 1 : 20 000 IHC, Millipore), anti-GFAP (131-17719, Invitrogen, chicken polyclonal, 1/600), anti-GFAP (ab4674, chicken polyclonal, 1/200 IF, Abcam), anti-phosphohistone H3 (PHH3; 06-570, rabbit polyclonal, 1/10 000 IHC, Millipore), anti-polysialylated-neural cell adhesion molecule (PSA-NCAM) (5A5, 1/500 IHC, Developmental Studies Hybridoma Bank), anti-calbindin (CB-38a, rabbit polyclonal, 1/50 000 IHC, SWANT); anti-calretinin (CR 7699/3H, rabbit polyclonal, 1/50 000 IHC, SWANT), anti-cleaved caspase 3 (9661, rabbit polyclonal, 1/5000 IHC, Cell Signaling Technology), anti-DCX (ab18723, 1/50 000 IHC, Abcam), anti-DCX (sc8066, goat polyclonal, 1/50 IF, Santa Cruz), anti-TBR2 (rabbit polyclonal, 1/10 000 IHC, 1/250 IF, a gift from Dr Robert Hevner, University of Washington, Seattle), anti-5-bromo-2′-deoxyuridine (BrdU; G3G4, mouse monoclonal, 1/5000 IHC, Developmental Studies Hybridoma Bank), anti-Ki67 (NCL-Ki67p, rabbit polyclonal, 1/200 IF, Novocastra), anti-Ki67 (550609, mouse monoclonal, 1/200 IF, BD Pharmingen), anti-Tuj1 (MAB1195, mouse monoclonal, 1/1000 IF, R&D Systems), anti-S100β (ab66028, mouse monoclonal, 1/200 IF, Abcam), anti-MASH1 (ab74065, rabbit polyclonal, 1/10 000 IHC, Abcam), anti-SOX2 (#2784, rabbit polyclonal, 1/200 IF, Cell Signaling Technology) and anti-SOX10 (SC-17342, goat polyclonal, 1/200 IF, Santa Cruz).

Quantification of SVZ Size and Cell Numbers

To measure the area of the SVZ and RMS in postnatal wild-type and *Nfix*$^{-/-}$ brains, coronal sections at equivalent rostro-caudal positions were either immunostained or hematoxylin-stained, and imaged with an upright microscope coupled to AxioVision software (Zeiss). The cross-sectional area of the SVZ, rostral SVZ, and RMS in both wild-type and knockout samples was then calculated. Similarly, to quantify the number of CC3-, PHH3-, MASH1, TBR2, SOX2, and BrdU-positive cells within the SVZ of postnatal day 10 (P10) wild-type and knockout mice, sections were immunolabeled with the respective antibodies, then imaged. The total number of immunopositive cells within the SVZ was counted and is presented here as immunopositive cells per unit area of the SVZ. To quantify proliferating neuroblasts within the SVZ of P20 wild-type and knockout sections, IF staining of the markers DCX and Ki67 was performed. Nuclei were also labeled with DAPI. Sections were then imaged using a confocal microscope at the level of the SVZ. For each frame, the total number of DCX-positive cells was quantified, as was the number of cells positive for both DCX and Ki67. Data are presented as the number of cells expressing both DCX and Ki67 as a proportion of the total number of cells expressing DCX. To quantify interneuron populations within the olfactory bulb, P20 wild-type and knockout olfactory bulbs were sectioned coronally on a vibratome, and immunostaining was used to identify interneurons expressing PAX6, calbindin or calretinin. Sections were then imaged and the number of immunopositive cells per 100 μm within the glomerular layer and granule cell layer was counted, using representative sections from lateral, medial, dorsal and ventral regions of the respective olfactory bulbs. In all cases, at least 5 wild-type and 5 knockout brains were used for quantification. Quantification was performed blind to the genotype of the sample, and statistical analyses were performed using a two-tailed unpaired *t*-test. Error bars represent the standard error of the mean.

In Situ Hybridization

P20 brains were collected and fixed as described above ($n = 5$ for both wild-type and knockout). In situ hybridization was performed using anti-sense probes as previously described (Piper et al. 2009) with minor modifications. The hybridization temperature was 70 °C. The color reaction solution was BM Purple (Roche). In situ probes were kindly provided by Dr Jane Johnson (*Mash1*; University of Texas, Dallas, TX, USA) and by Dr Ryoichiro Kageyama (*Hes1* and *Hes5*; Kyoto University, Kyoto, Japan).

In Vivo BrdU Incorporation Assay

P8 wild-type and *Nfix*$^{-/-}$ mice were injected intraperitoneally with BrdU (Invitrogen) at 100 mg/kg. After 5 days, the animals were transcardially perfused with 0.9% saline, followed by 4% paraformaldehyde, and then postfixed in 4% paraformaldehyde at 4°C. Brains were removed and sectioned coronally at 50 μm using a vibratome. Antigen retrieval was performed by incubating sections in 2 N HCl for 45 min. IHC was then performed as described above. To quantify BrdU-positive cells in the SVZ, RMS, and ependymal cell layer of the olfactory bulb, sections at equivalent rostro-caudal positions were imaged, and the total number of BrdU-positive cells in a 200 μm^2 region was counted for both wild-type and mutant mice. To quantify BrdU-positive cells in the glomerular layer of the olfactory bulb, the number of immunopositive cells per 200 μm within the glomerular layer was counted, using representative sections from lateral, medial, dorsal and ventral regions of the respective olfactory bulbs. In all cases, at least 5 wild-type and 5 knockout brains were used for quantification. Quantification was performed blind to the genotype of the sample, and statistical analyses were performed using a two-tailed unpaired *t*-test. Error bars represent the standard error of the mean.

Microarray Analysis

To collect SVZ/RMS tissue, brains of P20 littermate wild-type ($n = 3$) and *Nfix*$^{-/-}$ mice ($n = 3$) were dissected from the skull, the SVZ exposed by cutting the brains coronally at the level of the corpus callosum, and the SVZ/RMS isolated by pinching it out with a pair of fine forceps. Total RNA was extracted using a QIAGEN RNA isolation kit, and the microarray analysis was performed at the Australian Research Council Special Research Centre for Functional and Applied Genomics (The University of Queensland, Australia) as described previously (Piper et al. 2010). Labeled and amplified material (1.5 μg/sample) was hybridized to Illumina's MouseWG-6 v2.0 Expression BeadChip at 55 °C for 18 h according

to the Illumina BeadStation 500X™ protocol. Arrays were washed and then stained with 1 μg/mL of cyanine3-streptavidin (Amersham Biosciences). The Illumina BeadArray™ reader was used to scan the arrays according to the manufacturer's instructions. Samples were initially evaluated using the BeadStudio™ software from Illumina. Quality control reports were satisfactory for all samples. The raw data were then imported into GeneSpring GX v7.3 (Agilent). Data were initially filtered using GeneSpring normalization algorithms. Quality control data filtering was then performed using the Bead detection score *P*-value, and with expression values below background, as determined by the cross-gene error model. Differential expression was determined by the one-way ANOVA-Welch's approximate *t*-test without a multiple testing correction. A cutoff *P*-value of 0.05 was used for the mean difference between wild-type and *Nfix*$^{-/-}$ SVZ tissue. In addition, a 1.5-fold-change filter was imposed on the genes from the ANOVA dataset. Pathway analysis was performed using Ingenuity Pathway Analysis.

Bioinformatic Promoter Screen

The NFI-binding motif was generated as reported previously (Heng et al. 2012) from published chromatin immunoprecipitation-sequencing (ChIP-seq) data for NFI (pan-NFI antibody used) (Pjanic et al. 2011). The DNA-binding domains of all NFI proteins are highly similar (Mason et al. 2009). In brief, we performed motif discovery using the MEME algorithm (Bailey et al. 2009) on ChIP-seq peaks redeclared using the ChIP-Peak algorithm (Schmid and Bucher 2010) from the published ChIP-seq "tag" data for NFI. We then identified potential NFI-binding sites by scanning the complete mouse genome downloaded from the UCSC Genome Browser (mm9, July 2007) (Fujita et al. 2011) using the MEME-derived motif and the FIMO motif-scanning program (Grant et al. 2011). FIMO was run on the mouse genome (without repeat masking) using a 0-order background generated on the entire mouse genome, and a pseudocount of 0.1. All potential binding sites with a *P*-value of $\leq 10^{-4}$ were reported in the region of −3000 to +200 bp relative to the transcription start site (TSS). Putative NFI-binding sites near the promoters of genes were identified by viewing the FIMO output using the UCSC genome browser.

Neurosphere Assay

Brains of P15 wild-type and *Nfix*$^{-/-}$ mice were isolated from the skull and dissected manually on the coronal plane to expose the lateral ventricles at the level of the corpus callosum. The SVZ was carefully removed using forceps, then cut into fine pieces before enzymatic digestion was performed by incubation in 0.05% trypsin at 37 °C for 15 min, a process that culminated in a single cell suspension. After centrifugation at 110 × g for 5 min, cells were carefully dissociated and resuspended in 5 mL of pre-warmed neurosphere medium containing 20 ng/mL of epidermal growth factor (EGF), 10 ng/mL of basic fibroblast growth factor (bFGF) and 3.5 μg/mL of heparin. The cell suspension was then run through a 50 μm filter. The primary tissue was plated at a concentration of 2.5×10^5 cells in 5 mL of medium in a T-25 flask for 7 days. The total number of spheres that had formed was counted after 7 days. The neurospheres were then dissociated and passaged at a constant density of 2.5×10^5 cells in 5 mL of medium and then counted 7 days later. This was then repeated for another 4 more passages. Sphere diameter was also measured at each passage, and the data shown represent the combined results from all the passages.

Neuroblast Migration Assay

To evaluate the contribution of NFIX during neuroblast migration, neurospheres from passage 4 wild-type and *Nfix*$^{-/-}$ cohorts were seeded onto coverslips coated with poly-L-ornithine (10 mg/mL) and placed into a 6-well plates containing DMEM- F12 (with 5% fetal bovine serum and 1% penicillin and streptomycin). Spheres of approximately equal sizes (100–200 μm in diameter) were used for this assay. Spheres were cultured for 3 days at 37 °C. A set of spheres from either genotype were also cultured with bath-applied recombinant GDNF (120 ng/mL; R&D Systems, recombinant human GDNF) for the 3 days. Following this adherent neurospheres were fixed with 4% PFA, and DCX expression was analyzed using IF staining with an anti-DCX antibody (1 : 1000, Abcam, AB18723) and a fluorescent secondary antibody (AlexaFluor 488; 1/500). Cell nuclei were stained with DAPI. Cultures were imaged using a fluorescence microscope (Zeiss upright Axio-Imager Z1). The distance each DCX-positive cell had migrated from the edge of the adherent sphere was measured with ImageJ. Spheres isolated from $n = 5$ wild-type and $n = 5$ *Nfix*$^{-/-}$ mice were counted. Quantification was performed blind to the genotype of the sample, and statistical analyses were performed using a two-tailed unpaired *t*-test. Error bars represent the standard error of the mean.

Luciferase Assay

Our bioinformatic promoter screen identified 2 potential NFI-binding sites within the *Gdnf* promoter, at +44 bp relative to the TSS (chromosome 15: 7811055–7811069, GTGGCCCGAATCCCA) and at −5 bp relative to the TSS (chromosome 15: 7811006–7811020, CTGGGCGGGGCCCCG). The constructs used in the luciferase assay were full-length *Nfix*, *Nfia* and *Nfib* expression constructs (each in the vector pCAGIG-IRES-GFP) and a *Renilla* luciferase construct containing 575 bp of the upstream promoter region of the mouse *Gdnf* gene (*Gdnf* Prom: chromosome 15: 7810505–7811080). This luciferase construct was obtained from Switchgear Genomics. A truncated *Gdnf* promoter construct was also generated, which lacked the 2 putative NFI-binding sites. This construct contained 470 bp of the upstream promoter region of the mouse *Gdnf* gene (chromosome 15: 7810505–7810975). DNA was transfected into Neuro2A cells using FuGene (Invitrogen). *Cypridina* luciferase was added to each transfection as a normalization control. After 48 h, luciferase activity was measured using a dual luciferase system (Switchgear Genomics). Within each experiment, each treatment was replicated 6 times. Each experiment was also independently replicated a minimum of 3 times. The pCAGIG vector alone did not significantly alter *Gdnf* promoter-driven luciferase activity (data not shown). Statistical analyses were performed using an ANOVA. Error bars indicate the standard error of the mean.

Electrophoretic Mobility Shift Assay

Nuclear extracts were isolated from the cortex of E18 brains, and from COS cells overexpressing HA-tagged versions of either NFIX or an unrelated control transcription factor, AP2. Electrophoretic mobility shift assays (EMSAs) were performed using radiolabeled annealed oligonucleotides containing *Gdnf* consensus sites from our bioinformatics screen. EMSA reactions were carried out as described previously using 1 μg of nuclear extract (Piper et al. 2010). Oligonucleotide sequences were: *Gdnf* −5, 5′- CCGGGACCTTCTGG GCGGGGCCCCGCGCTCC -3′ (upper strand), 5′- CCGGGGAGCGCGG GGCCCCGCCCAGAAGGTC -3′ (lower strand); *Gdnf* +44, 5′- CCGGGCT

GGATGGGATTCGGGCCACTTGGAC -3′ (upper strand), 5′- CCGG GTCCAAGTGGCCCGAATCCCATCCAGC -3′ (lower strand).

Supershift assays were performed with an anti-HA antibody (Sigma; #H9658).

Reverse Transcription and Quantitative Real-time PCR

SVZ/RMS and olfactory bulb tissue from P20 wild-type and *Nfix*$^{-/-}$ mice were microdissected and immediately snap-frozen. Total RNA was extracted using a RNeasy Micro Kit (Qiagen). Reverse transcription was performed using Superscript III (Invitrogen) and qPCR was performed as described previously (Piper et al. 2010). Briefly, 0.5 µg total RNA was reverse-transcribed with random hexamers. qPCRs were carried out in a Rotor-Gene 3000 (Corbett Life Science) using the SYBR Green PCR Master Mix (Invitrogen). All the samples were diluted 1/100 with RNase/DNase free water and 5 µL of these dilutions were used for each SYBR Green PCR containing 10 µL of SYBR Green PCR Master Mix, 10 µM of each primer, and deionized water. The reactions were incubated for 10 min at 95 °C followed by 40 cycles with 15 s denaturation at 95 °C, 20 s annealing at 60 °C, and 30 s extension at 72 °C. The primer sequences used in this study can be found in Table 1.

qPCR Data Expression and Analysis

After completion of the PCR amplification, the data were analyzed with the Rotor-Gene software as described previously (Piper et al. 2009). When quantifying the mRNA expression levels, the housekeeping gene *glyceraldehyde 3-phosphate dehydrogenase* (*Gapdh*) was used as a relative standard. All the samples were tested in triplicate. For all qPCR analyses, RNA from 8 biological replicates for both wild-type and *Nfix*$^{-/-}$ mice were interrogated. Relative transcript levels were assessed using the $\Delta\Delta C_t$ method as described previously (Piper et al. 2014). Statistical analyses were performed using a two-tailed unpaired *t*-test. Error bars represent the standard error of the mean.

Results

NFIX Is Expressed Within the SVZ and RMS of Postnatal and Adult Mice

We showed previously that the transcription factor NFIX is expressed within the developing forebrain, with expression evident within the ventricular zone of the neocortex and hippocampus. Furthermore, NFIX is expressed within the adult neurogenic niches of the brain, including the SVZ (Campbell et al. 2008). However, the expression of NFIX within specific cell types of the SVZ, RMS and olfactory bulb has not been defined in detail. To address this, we analyzed NFIX expression in postnatal and adult mice using IHC. The specificity of the anti-NFIX antibody we used

Table 1 Primer sequences used in this study

Gene	Sequence
Gapdh For	GCACAGTCAAGGCCGAGAAT
Gapdh Rev	GCCTTCTCCATGGTGGTGAA
Gdnf For	TGAAGACCACTCCCTCGG
Gdnf Rev	GCTTGTTTATCTGGTGACCTTTTC
Dcx For	TGGAAGCATGGATGAACTGG
Dcx Rev	CATGTTGGCAGATGTCTTTACG
Pax6 For	CTCCTAGTCACATTCCTATCAGC
Pax6 Rev	GCAAAGCACTGTACGTGTTG
Gfap For	AGTGGTATCGGTCTAAGTTTG
Gfap Rev	CGATAGTCGTTAGCTTCGTG

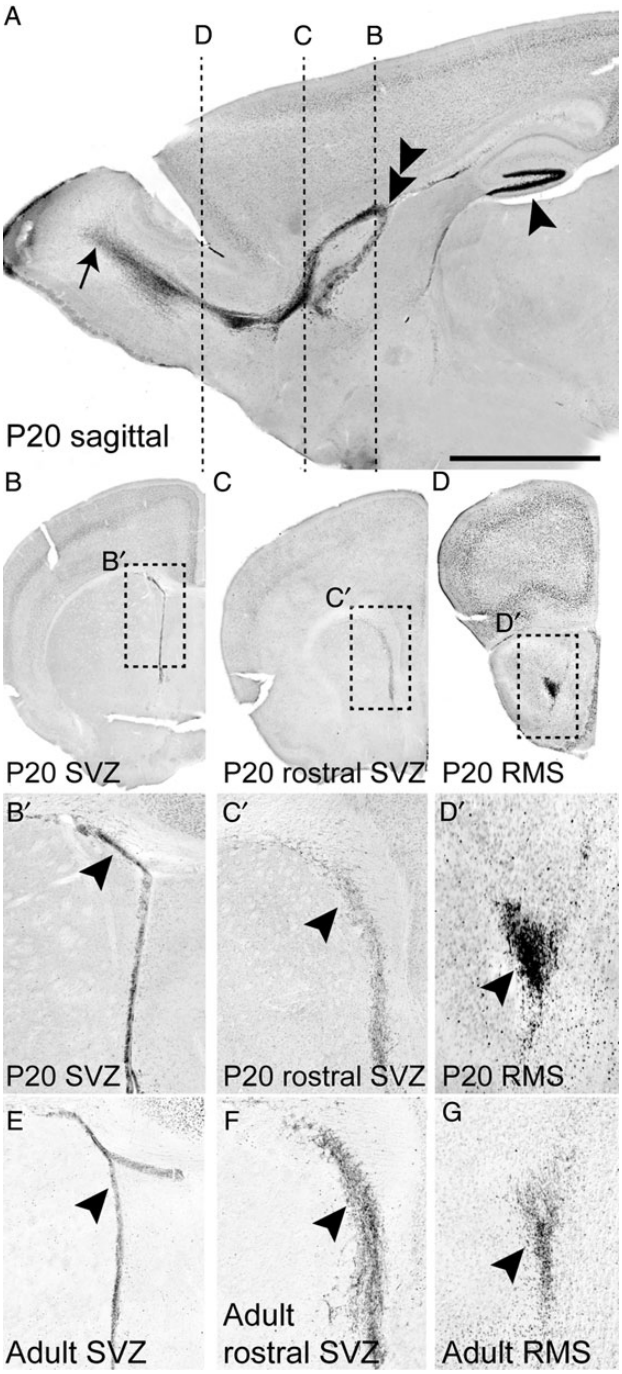

Figure 1. NFIX is expressed within the postnatal and adult SVZ. Expression of NFIX in sagittal (*A*) and coronal (*B–G*) sections of P20 (*A–D*) and adult (*E–G*) mice. (*A*) At P20, NFIX expression was observed within the hippocampus (arrowhead), the SVZ (double arrowhead) and olfactory bulb (arrow). The dotted lines in A indicate the rostro-caudal position from which panels (*B–D*) are taken. At the level of the corpus callosum, NFIX expression was evident within the SVZ (*B*, arrowhead in *B′*). Similarly, within the rostral SVZ (*C*, arrowhead in *C′*) and RMS (*D*, arrowhead in *D′*), NFIX expression was clearly seen. Within the adult brain, NFIX expression was also observed within the SVZ (arrowheads in *E,F*) and RMS (arrowhead in *G*). Scale bar (in *A*): *A–D*, 600 µm; *B′–D′* and *E–G*, 150 µm.

has been previously demonstrated (Harris et al. 2013); moreover, we observed no specific staining within the olfactory bulb of P20 *Nfix*$^{-/-}$ mice (Supplementary Fig. 1*A*,*B*). In wild-type mice, NFIX expression was observed within the germinal ventricular zone at E18 (Supplementary Fig. 1*C*,*D*). NFIX expression was also detected within the emerging SVZ and RMS at P5 and P10 (data not shown). By P20, the expression of NFIX within the SVZ and RMS was clearly seen in both sagittal and coronal sections from wild-type mice (Fig. 1*A*–*D*). Expression of NFIX was also observed in the olfactory bulb and the hippocampus (Fig. 1*A*). Using co-IF labeling, coupled with confocal microscopy, on the SVZ from P12 mice, we investigated the cell type-specific expression of NFIX within this developing postnatal neurogenic niche. At this age, nearly all neural stem cells (defined as cells expressing GFAP, but not s100β) were immunopositive for NFIX (Table 2). Similarly, proliferating progenitor cells in this niche (Ki67 +ve, DCX –ve; encompassing dividing stem cells and transit-amplifying cells), ependymal cells (cells immediately adjacent to the lateral ventricle expressing both GFAP and s100β), and neuroblasts (DCX +ve cells) were predominantly immunopositive for NFIX (Table 2). Interestingly, at this age, SVZ astrocytes (defined as cells not adjacent to the lateral ventricle that expressed GFAP and s100β) and cells of the oligodendrocyte lineage (SOX10 +ve) did not express NFIX. These findings demonstrate that NFIX is expressed by neural progenitor cells, transit-amplifying cells and neuroblasts within the postnatal SVZ neurogenic niche.

In the adult brain, NFIX expression was also clearly evident within the SVZ and RMS (Fig. 1*E*–*G*). To determine cell type-specific expression of NFIX within the adult SVZ and RMS, we again used co-IF labeling and confocal microscopy. First, we analyzed the expression of NFIX within the SVZ of a strain of mice expressing GFP under the control of the neural stem cell-specific *Hes*5 promoter. Co-labeling of the SVZ of adult *Hes*5-GFP mice with antibodies against another neural stem cell marker, GFAP, and NFIX, revealed that cells expressing both *Hes*5-GFP and GFAP also expressed NFIX (Fig. 2*A*–*E*). Interestingly, many cells were immunopositive for NFIX, but not for GFP. Some of these cells are likely to be ependymal cells, as s100β-expressing ependymal cells lining the lateral ventricles were also immunopositive for NFIX (Fig. 2*F*–*I*).

Within the SVZ and RMS, migrating neuroblasts express the microtubule-associated protein DCX, and GAD67, one of the principal enzymes used during the production of the inhibitory neurotransmitter γ-aminobutyric acid (GABA). To determine whether neuroblasts within the adult brain express NFIX, we analyzed the expression of this transcription factor in a strain of mice expressing GFP under the control of the DCX promoter (*Dcx*-GFP). GFP-expressing neuroblasts within the SVZ and RMS were seen to express NFIX (Supplementary Fig. 2*A*–*H*). Similarly,

Table 2 Cell type-specific of NFIX expression within the postnatal SVZ

Marker expression	Cellular population	Number of population expressing NFIX
GFAP +ve; s100β –ve	Neural progenitor cell	289/290
GFAP +ve; s100β +ve	Mature astrocyte	0/35
GFAP +ve; s100β +ve (adjacent to the LV)	Ependymal cell	115/115
Ki67 +ve; DCX –ve	Proliferating cell (neural progenitor cells and transit-amplifying cells)	112/112
Ki67 +ve; DCX +ve	Dividing neuroblast	64/64
Ki67 –ve; DCX +ve	Non-dividing neuroblast	77/100
SOX10 +ve	Oligodendrocytes and oligodendrocyte precursor cells	0/48

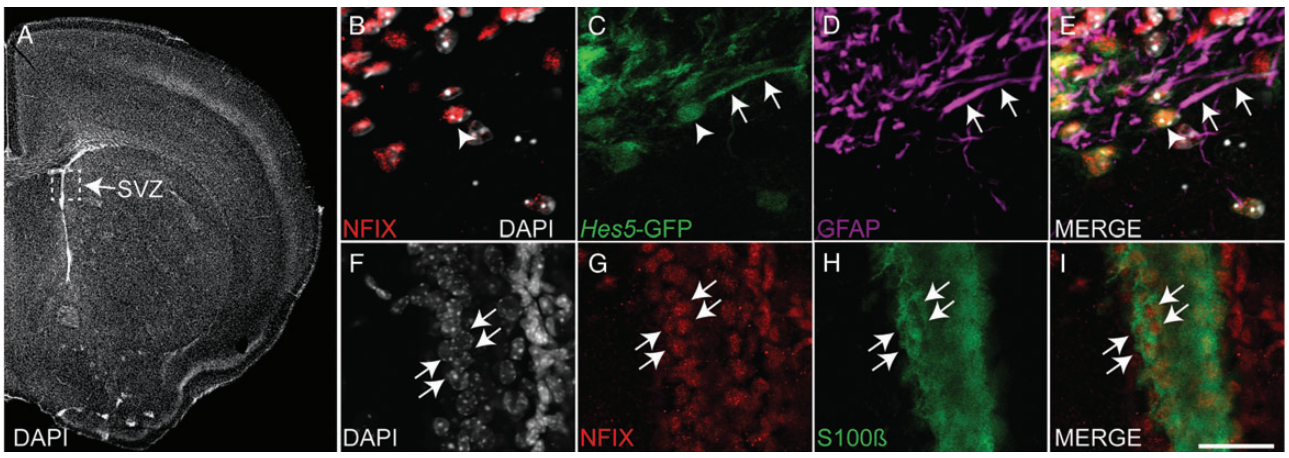

Figure 2. Neural progenitor cells and ependymal cells express NFIX within the adult SVZ. Coronal sections through the SVZ of adult wild-type (*A*, *F*–*I*) and *Hes*5-GFP (*B*–*E*) mice. (*A*) A low power image of a representative section labeled with DAPI. The boxed region indicates the approximate location within the SVZ from which the higher magnification images of other sections were obtained. Co-IF labeling and confocal microscopy were used to determine the cell type-specific expression of NFIX within the adult SVZ. Cell nuclei were labeled with DAPI (white). Within the SVZ of *Hes*5-GFP mice, GFP-positive neural stem cells (green, *C*) co-expressed GFAP (magenta) and NFIX (red). The neural stem cell indicated demonstrates the expression of GFP and NFIX within the nucleus (arrowheads in *B* and*E*), as well as colocalization of GFP and GFAP within the cytoplasm (arrows in *D* and *E*). Within the SVZ of wild-type mice (*F*), ependymal cells (arrows *F*–*I*) express s100β (green, *H* and *I*) and NFIX (red; *G* and *I*). Scale bar (in *I*); 300 μm for *A*; 25 μm for *B*–*I*.

Gad67-GFP-expressing neuroblasts within the RMS (Tamamaki et al. 2003) also co-expressed NFIX (Supplementary Fig. 2*I–L*). However, although all neuroblasts within the RMS expressed NFIX, there were also cells surrounding the RMS that were immunoreactive for NFIX, but not for GFP (Supplementary Fig. 2*H*,*L*). These cells could be RMS astrocytes, which comprise the glial tube through which SVZ-derived neuroblasts migrate en route to the olfactory bulb (Peretto et al. 1997). Co-IF labeling with anti-GFAP antibodies supported this hypothesis, with confocal microscopic analyses revealing that there were some cells

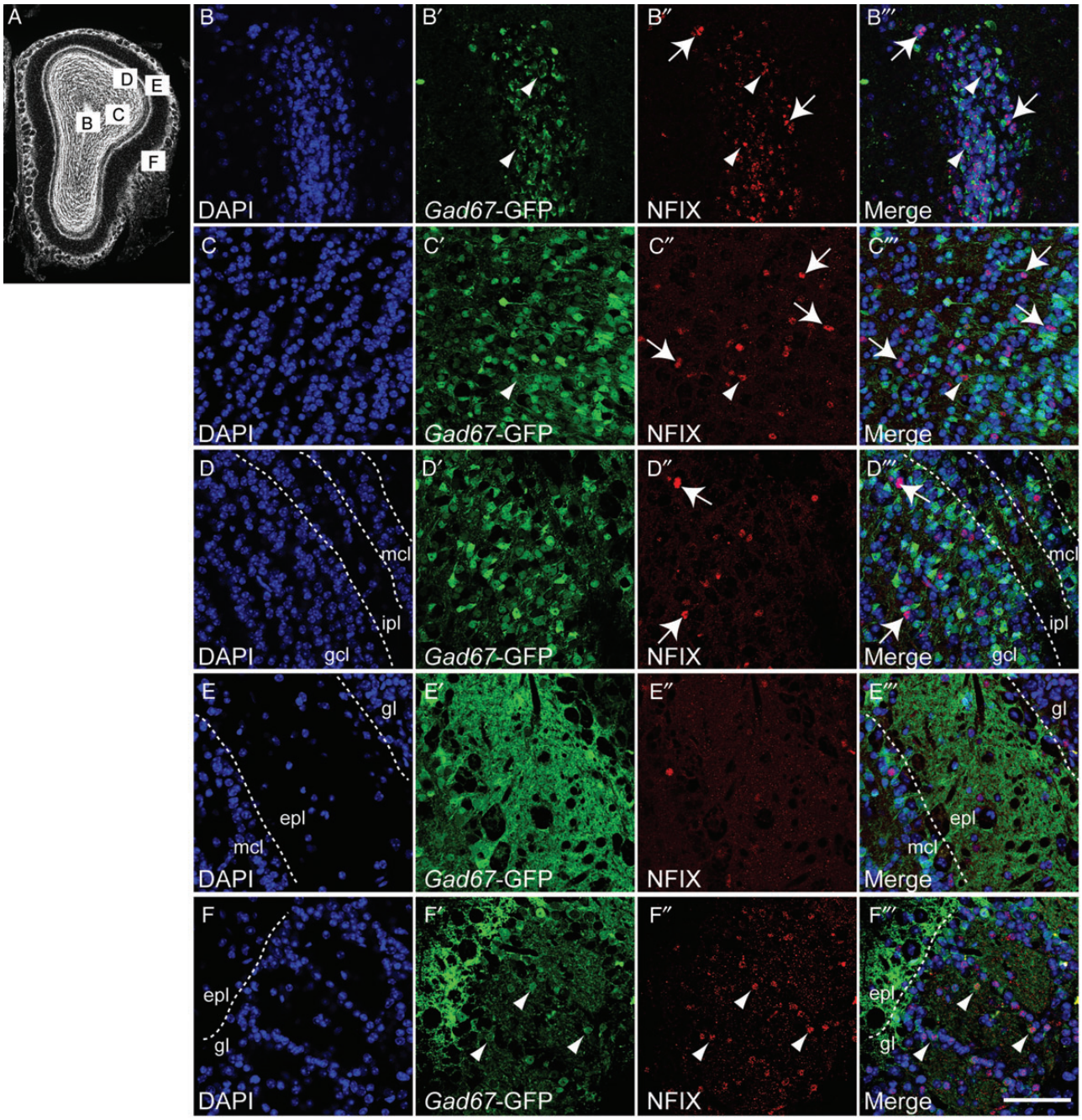

Figure 3. Cell type-specific expression of NFIX within the olfactory bulb of adult *Gad67*-GFP mice. Coronal sections through the olfactory bulb of adult *Gad67*-GFP mice. (*A*) A low power image of a representative olfactory bulb section labeled with DAPI. The boxed regions indicate the location within the olfactory bulb from which the higher magnification images were obtained. Co-IF labeling and confocal microscopy were used to determine the cell type-specific expression of NFIX (red) within the adult olfactory bulb. Cell nuclei were labeled with DAPI (blue). (*B*) Within the core of the olfactory bulb, expression of NFIX coincided with that of GFP within neuroblasts (arrowheads, *B′–B‴*). However, there were also some cells present that were immunoreactive for NFIX, but not for GFP (arrows, *B″–B‴*). (*C*) Within the granule cell layer (gcl), there were scattered NFIX-expressing cells, but these were mostly GFP-negative (arrows, *C″–C‴*), although we did locate a small number of cells expressing both GFP and NFIX (arrowheads, *C′–C‴*). (*D*) Similarly, we observed scattered NFIX-expressing cells within the internal plexiform layer (ipl) and mitral cell layer (mcl) (arrows in *D″–D‴*), but these cells did not express GFP. (*E*) Within the external plexiform layer, we saw very few NFIX-expressing cells, and these cells did not express GFP. (*F*) Within the glomerular layer (gl), we observed numerous GFP-expressing cells that were also immunoreactive for NFIX (arrowheads in *F′–F‴*). Scale bar (in *F‴*); 250 μm for *A*; 40 μm for remaining panels.

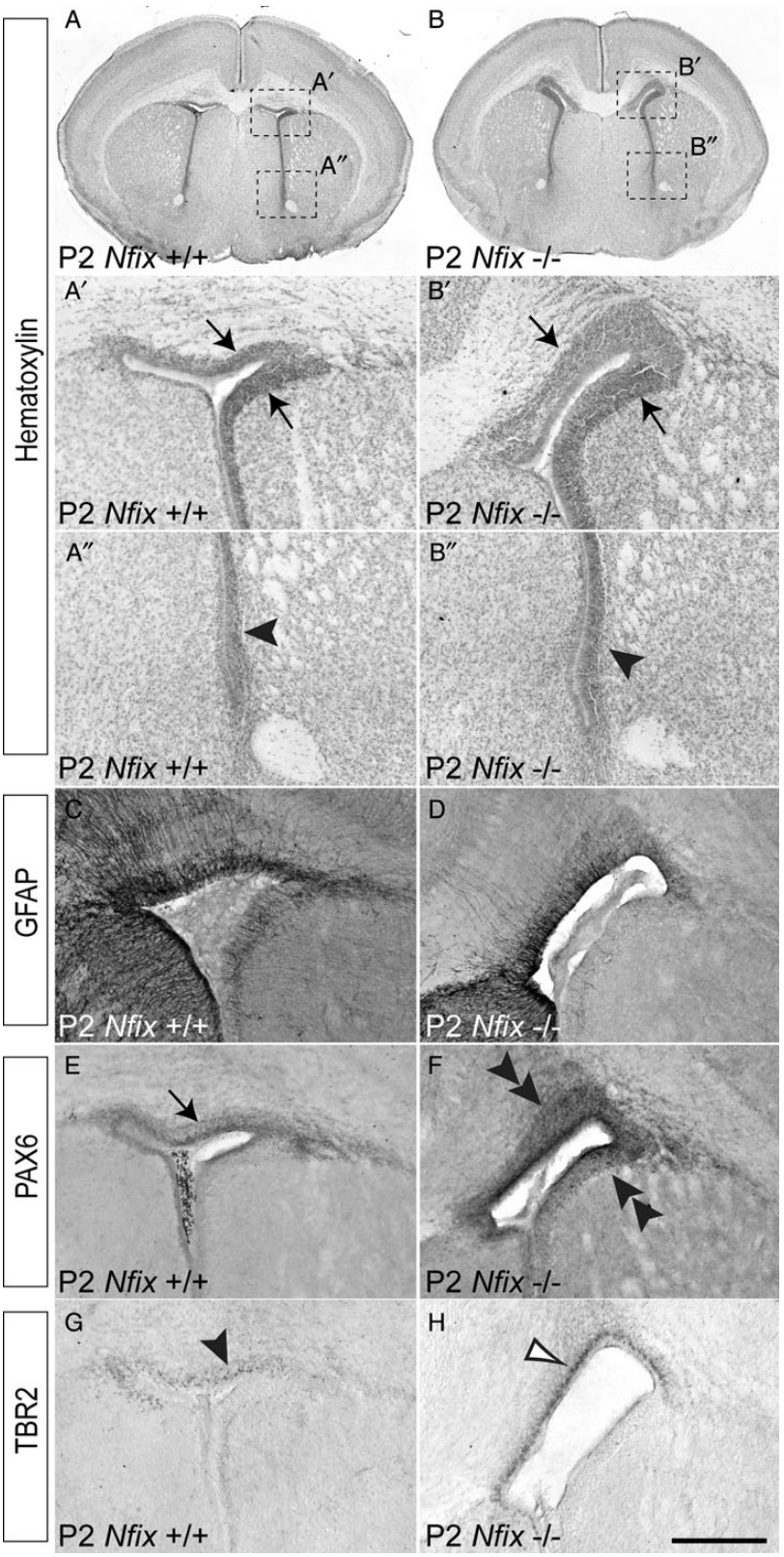

Figure 4. Deficits in SVZ structure within the early postnatal period of *Nfix*$^{-/-}$ mice. Coronal sections of P2 *Nfix*$^{+/+}$ (*A*, *C*, *E* and *G*) and *Nfix*$^{-/-}$ (*B*, *D*, *F* and *H*) mice at the level of the corpus callosum. Hematoxylin staining of wild-type and *Nfix*$^{-/-}$ sections revealed that the SVZ of mutant mice had become thickened by this age compared with the wild type. Higher magnification views of the dorsal (*A*′ and *B*′) and ventral (*A*″ and *B*″) lateral ventricles indicated that the dorsolateral SVZ of the mutant was thickened in comparison with the control (compare arrows in *A*′ and *B*′), whereas the ventral SVZ appeared normal (compare arrowheads in *A*″ and *B*″). Expression of GFAP at the cortical midline of the mutant (*D*) was still markedly lower than that seen in the control (*C*). Interestingly, there were more cells expressing PAX6 in the mutant (double arrowheads in *F*) than in the control (arrow in *E*). Similarly, TBR2 expression within the SVZ was elevated in *Nfix*$^{-/-}$ mice (compare open arrowhead in *H* with the arrowhead in *G*). Scale bar (in *H*): 600 μm for *A* and *B*; 150 μm for *A*′, *A*″, *B*′, *B*″ and *C*–*H*.

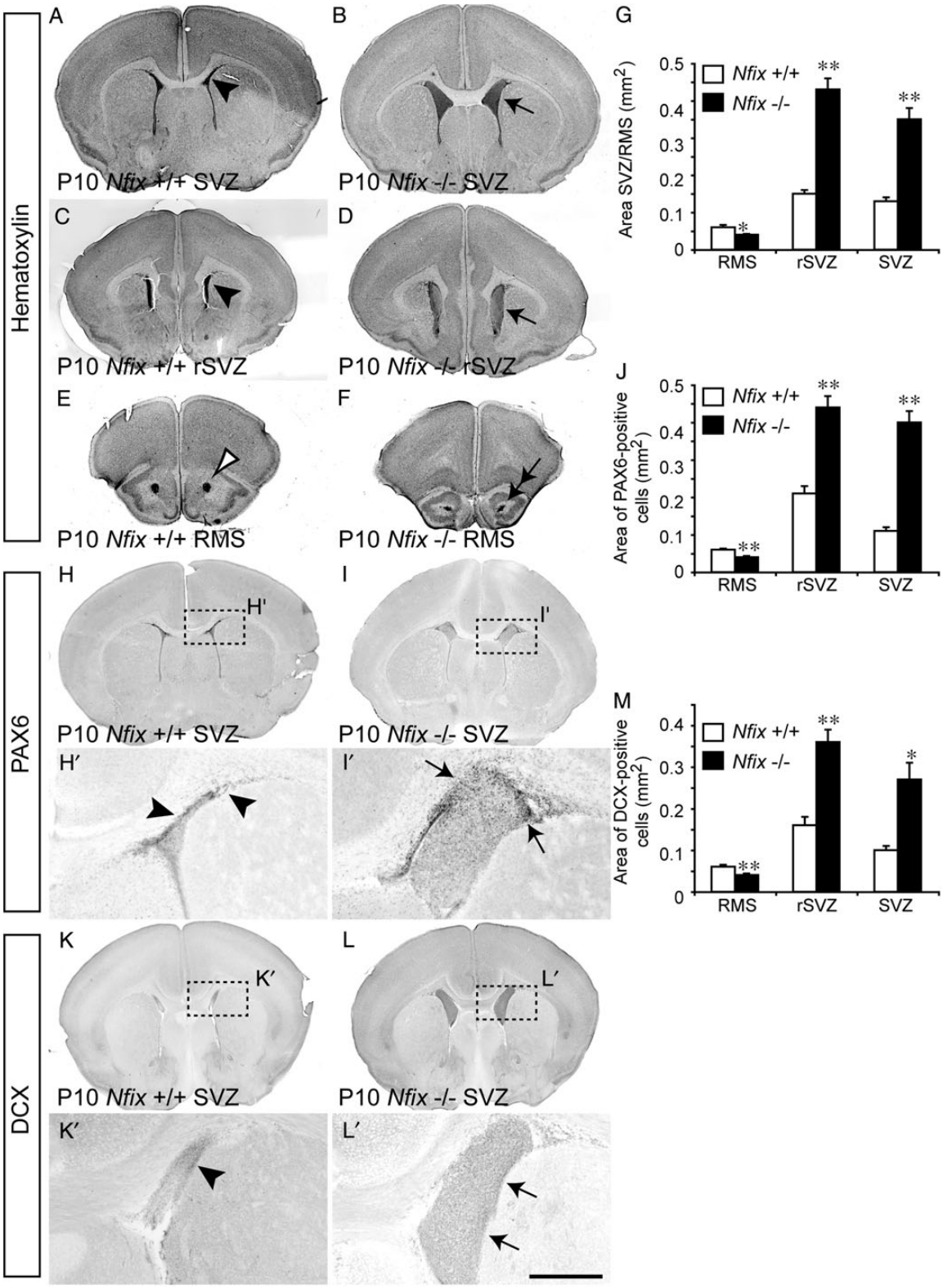

Figure 5. Expansion of the SVZ in mice lacking *Nfix*. Coronal sections of P10 *Nfix*$^{+/+}$ (*A*, *C*, *E*, *H* and *K*) and *Nfix*$^{-/-}$ (*B*, *D*, *F*, *I*, *L*) mice at the level of the corpus callosum (*A*, *B*, *H*, *I*, *K*, *L*), rostral SVZ (rSVZ—immediately rostral to the corpus callosum; *C* and *D*) and RMS (*E* and *F*). Hematoxylin staining revealed a dramatically expanded SVZ within the mutant mice (arrows in *B* and *D*) compared with controls (arrowheads *A* and *C*). The cross-sectional area of the RMS, however, was reduced in the mutant (compare the open arrowhead in *E* with the double-headed arrow in *F*). *G* represents quantification of the cross-sectional area of the SVZ in the mutant, which was significantly larger, and the RMS, which was significantly reduced, relative to the wild-type controls. Expression of the stem cell marker PAX6 (*H*, *H*′, *I* and *I*′) and the neuroblast marker DCX (*K*, *K*′, *L* and *L*′) also revealed markedly more cells expressing these factors within the SVZ of *Nfix*$^{-/-}$ mice than in comparison with the controls (compare arrowheads in *H*′ and *K*′ with the arrows in *I*′ and *L*′), whereas the RMS within the mutant was smaller (*J* and *M*). $^{*}P < 0.05$, $^{**}P < 0.01$, *t*-test. Scale bar (in *L*′): 600 μm.

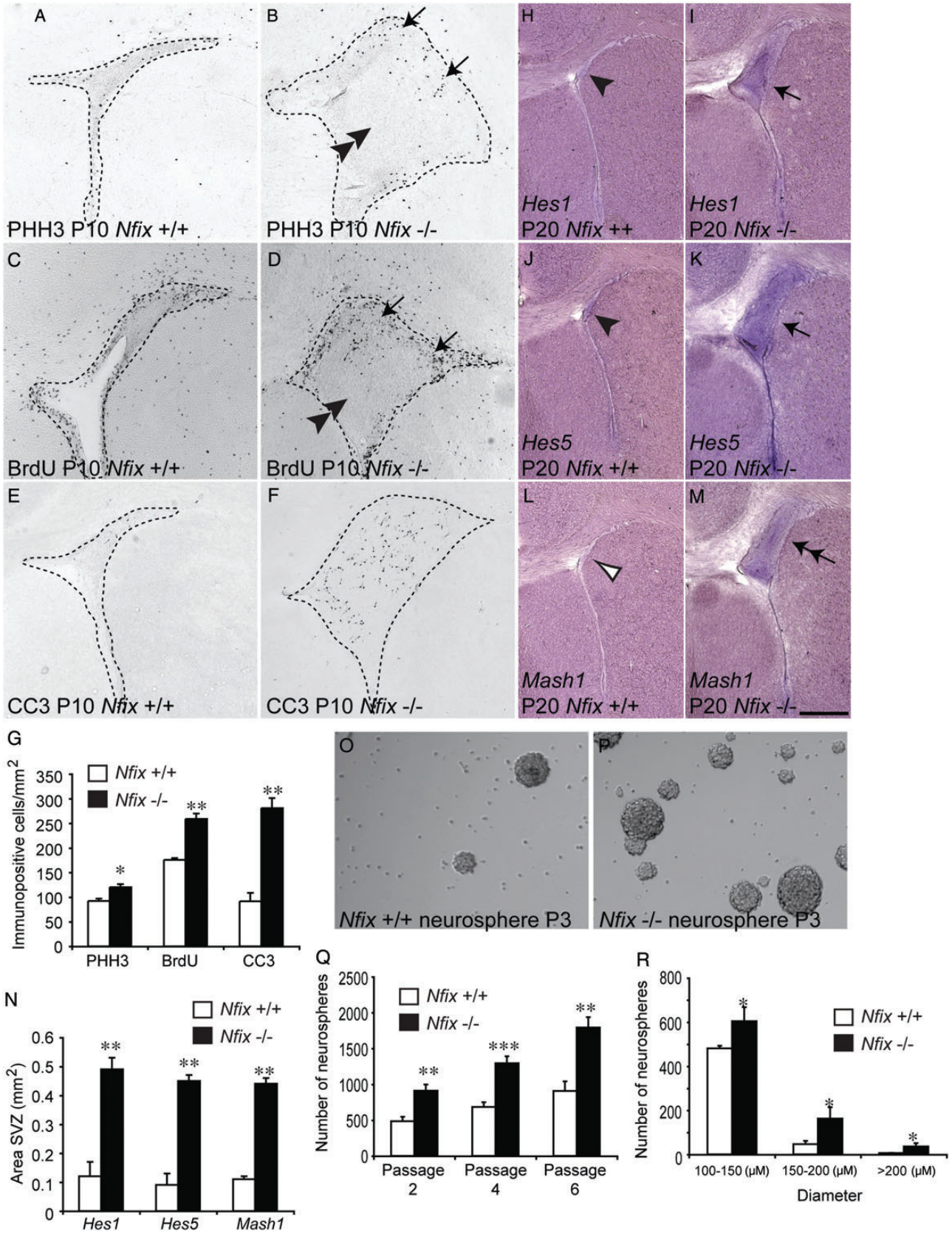

Figure 6. Increased proliferation within the SVZ of postnatal *Nfix*$^{-/-}$ mice. Coronal sections at the level of the corpus callosum through P10 (A–F) and P20 (*H–M*) *Nfix*$^{+/+}$ (A, *C*, *E*, *H*, *J* and *L*) and *Nfix*$^{-/-}$ (*B*,*D*, *F*, *I*, *K* and *M*) mice. There were significantly more PHH3-positive, BrdU-positive (BrdU administered 2 h prior to sacrifice), and cleaved caspase 3-positive (CC3) cells per unit area of the mutant SVZ than the wild-type (*A–G*). Interestingly, with both PHH3 and BrdU labeling in the mutant, the proliferative cells were observed on the periphery of the SVZ (arrows in *B* and *D*), but to a lesser extent in the center of the SVZ (double arrowheads, *B* and *D*). At P20, expression of the neural stem

expressing both GFAP and NFIX along the periphery of the RMS (Supplementary Fig. 2M–P). Collectively, these findings indicate that NFIX is expressed by multiple cellular populations within the adult SVZ and RMS.

Expression of NFIX Within the Developing and Adult Olfactory Bulb

Given that NFIX is expressed within the olfactory bulb at P20 (Fig. 1A), we examined NFIX expression within this structure in more detail. NFIX was not expressed within the olfactory bulb of embryonic or early postnatal mice (data not shown). At P10, expression of NFIX became apparent, with weak expression within the subependymal layer; these cells are likely to be SVZ-derived neuroblasts (Supplementary Fig. 3A). Low expression of NFIX was also detected within cells within the laminae of the olfactory bulb, including cells within the glomerular layer and the granule cell layer (Supplementary Fig. 3B). By P20, NFIX was strongly expressed within the olfactory bulb, particularly by cells within the subependymal layer and the glomerular layer, but also by scattered cells within the other laminae of the olfactory bulb (Supplementary Fig. 3C,D). This expression pattern was maintained within the adult olfactory bulb (Supplementary Fig. 3E,F). Within the adult olfactory bulb, we used the *Gad67*-GFP line to assess cell type-specific expression of NFIX. These analyses revealed that *Gad67*-GFP-expressing neuroblasts within the subependymal layer and periglomerular interneurons express NFIX within the adult olfactory bulb (Fig. 3). Moreover, co-IF staining for GFAP and NFIX showed that olfactory bulb astrocytes express NFIX (Supplementary Fig. 4E–H).

Development of the SVZ Is Aberrant in Postnatal *Nfix*$^{-/-}$ Mice

The expression of NFIX in neural stem cells within the postnatal SVZ suggests a role for this transcription factor in regulating the development of this neurogenic niche. In support of this, we reported previously that P16 *Nfix*$^{-/-}$ mice exhibit more PAX6-expressing cells within the SVZ than littermate controls (Campbell et al. 2008). However, when this phenotype first becomes evident is unclear. We therefore analyzed the germinal zones around the lateral ventricles of wild-type and *Nfix*$^{-/-}$ mice at E18 (Supplementary Fig. 5A,B). Hematoxylin staining revealed an enlarged cingulate cortex in *Nfix*$^{-/-}$ mice, in line with previous reports (Campbell et al. 2008), as well as a smaller corpus callosum, and IHC further revealed reduced GFAP expression at the cortical midline (Supplementary Fig. 5G,H). We have previously reported that neural progenitor cells within the dorsal telencephalon are delayed in their differentiation in the absence of NFIX (Heng et al. 2014), and the analysis of both the radial glial marker PAX6 and the intermediate progenitor cell marker TBR2 within the germinal zones surrounding the lateral ventricles supported this finding, with more cells expressing these markers within the germinal zones of the mutant. However, this phenotype appeared subtle at the level of the corpus callosum at E18 (Supplementary Fig. 5C–F).

By P2, however, the germinal zones around the ventricles of *Nfix*$^{-/-}$ mice were appreciably different from those of wild-type littermate controls. Hematoxylin staining revealed that the region lining the lateral ventricles of *Nfix*$^{-/-}$ mice was thickened dorso-laterally, although it appeared normal ventrally (Fig. 4A, B). Expression of GFAP within the mutant at this age was still diminished, but the expression of both PAX6 and TBR2 was elevated in comparison with controls (Fig. 4C–H). This phenotype was even more pronounced at P10, where hematoxylin staining and PAX6 IHC revealed that the SVZ of *Nfix*$^{-/-}$ mice was significantly larger in area than that of controls (Fig. 5A–D,G–J). Interestingly, this situation was reversed when we analyzed the cross-sectional area of the RMS, which was significantly reduced in mice lacking *Nfix* (Fig. 5E–G). Staining with the neuroblast marker DCX supported this finding, revealing significantly more DCX +ve cells within the SVZ of mutant mice, but a reduced cross-sectional area of the RMS (Fig. 5K–M). These findings indicate that, although proliferation in the SVZ of mutant mice is likely to be increased, there are fewer cells migrating to the olfactory bulb, suggesting that migration through the RMS is impaired in these mice. This phenotype was recapitulated at P20, with increased numbers of cells expressing PAX6, DCX, and another neuroblast marker, PSA-NCAM, within the SVZ of *Nfix*$^{-/-}$ mice (Supplementary Fig. 6). These findings demonstrate that the SVZ in *Nfix*$^{-/-}$ mice begins to develop significant abnormalities in the early postnatal period, and suggest that deficits in both proliferation and neuroblast migration are responsible for the SVZ phenotype within these mice.

Elevated Proliferation Within the SVZ of Postnatal *Nfix*$^{-/-}$ Mice

To assess the contribution of NFIX to proliferation within the SVZ/RMS, we analyzed proliferation via the expression of the mitotic marker PHH3 at P10. As anticipated, there were significantly more PHH3 +ve cells per unit area in the mutant when compared with littermate controls (Fig. 6A,B,G). Similarly, labeling cells in S-phase with BrdU 2 h prior to sacrifice revealed significantly more proliferating cells within the SVZ of *Nfix*$^{-/-}$ mice (Fig. 6C,D,G). Interestingly, there were also more apoptotic cells per unit area of the mutant SVZ (Fig. 6E–G). Analysis of the expression of the Notch effector genes *Hes1* and *Hes5*, both markers for SVZ neural stem cells, by in situ hybridization further revealed elevated levels of expression of these factors within the SVZ of *Nfix*$^{-/-}$ mice. Similarly, *Mash1*, a marker for transit-amplifying cells (Kim et al. 2011), was more highly expressed within the mutant SVZ (Fig. 6H–N). Finally, cell counts performed on the SVZ of P10 wild-type and *Nfix*$^{-/-}$ mice revealed significantly more cells per unit area expressing the neural stem cell marker SOX2 (Andreu-Agullo et al. 2012) and also more transit-amplifying cells expressing MASH1 in the mutant in comparison with the control (Fig. 7A–D,G).

These findings are suggestive of increased proliferation within the SVZ of mice lacking *Nfix*. To probe this further, we isolated neural progenitor cells from the SVZ of P15 *Nfix*$^{-/-}$ and wild-type littermate mice, and cultured them in vitro for 6 passages using a

cell markers *Hes1* and *Hes5* was increased within the mutant SVZ (compare arrows in I and K with arrowheads in H and J). Similarly, the expression of *Mash1*, which labels transit-amplifying cells within the SVZ neurogenic niche, was elevated within *Nfix*$^{-/-}$ mice (compare double-headed arrow in M with open arrowhead in L). (N) Quantification revealed a significantly larger SVZ region expressing *Hes1*, *Hes5* and *Mash1* within *Nfix*$^{-/-}$ mice. (O–Q) Culturing SVZ-derived cells in an in vitro neurosphere assay resulted in significantly higher numbers of neurospheres (Q) in tissue isolated from *Nfix*$^{-/-}$ mice (P) when compared with wild-type controls (O). Neurospheres derived from *Nfix*$^{-/-}$ tissue were also significantly larger than those isolated from wild-type controls (R). Panels O and P are neurospheres from passage 3 (P3). *$P < 0.05$, **$P < 0.01$, ***$P < 0.001$ t-test. Scale bar (in M): 100 μm for A–F; 125 μm for H–M; 100 μm for O and P.

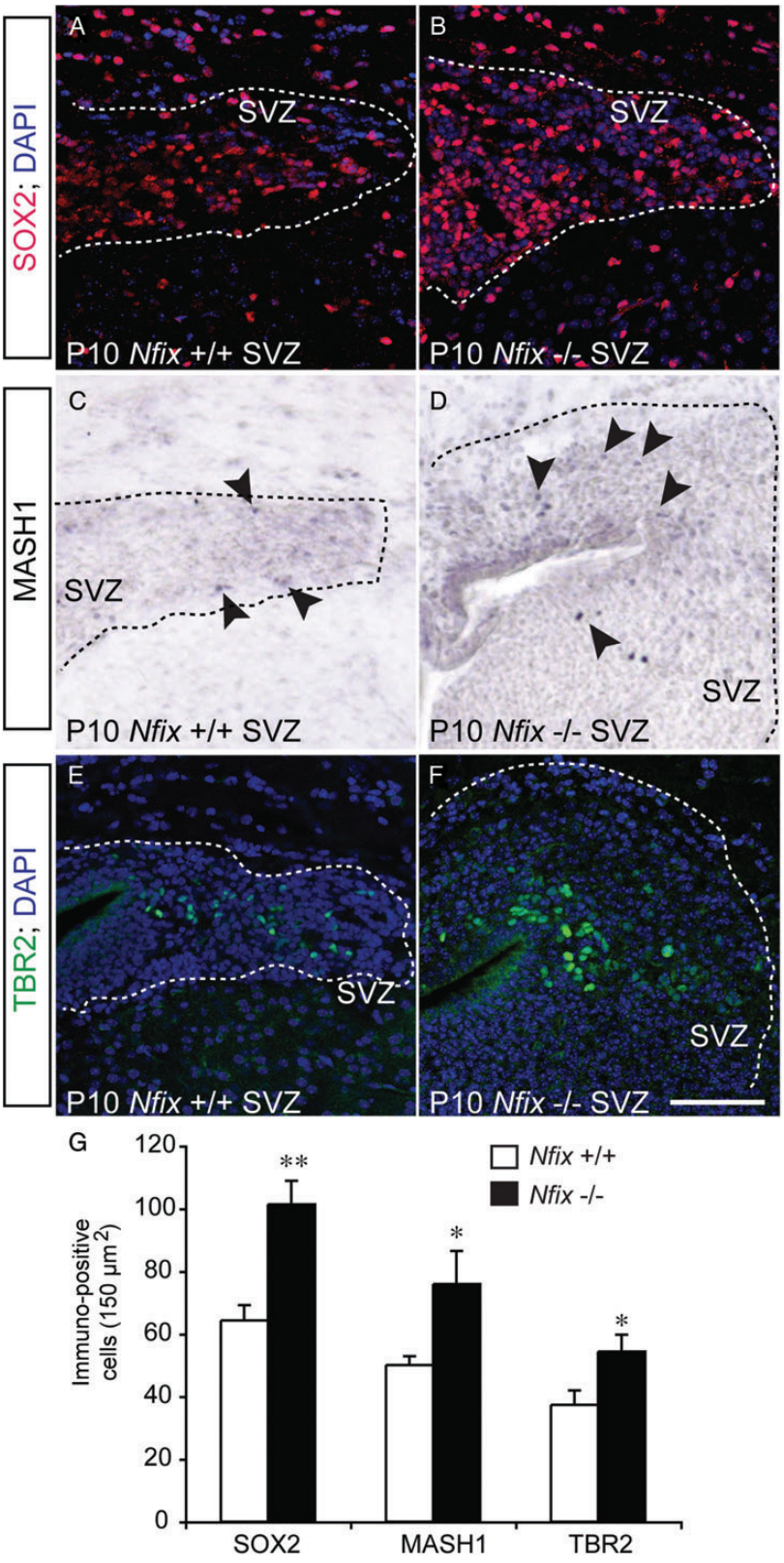

Figure 7. Increased numbers of neural stem cells and transit-amplifying cells in the SVZ of *Nfix* mutant mice. Coronal sections of P10 $Nfix^{+/+}$ and $Nfix^{-/-}$ mice revealing expression of the neural stem cell marker SOX2 (*A* and *B*), the transit-amplifying cell marker MASH1 (*C* and *D*) and of TBR2, a marker for a subpopulation of SVZ-derived neuroblasts (*E* and *F*) within the SVZ. The SVZ is delineated by the dashed lines in each image. There were significantly more cells expressing SOX2, MASH1 and TBR2 in the mutant in comparison with the control (*G*). $^{*}P < 0.05$, $^{**}P < 0.01$, *t*-test. Scale bar (in *F*): 100 µm.

neurosphere assay. This analysis revealed the presence of significantly more neurospheres at each passage in tissue isolated from *Nfix*$^{-/-}$ mice (Fig. 6O–Q). Moreover, there were significantly larger neurospheres in those cultures derived from the SVZ of *Nfix*$^{-/-}$ mice, indicative of elevated levels of proliferation. Collectively, these findings reveal that the proliferation of neural progenitor cells within the SVZ of postnatal *Nfix*$^{-/-}$ mice is elevated, suggestive of a role for this transcription factor in the repression of progenitor cell proliferation within this neurogenic niche.

Neuroblast Migration to the Olfactory Bulb Is Diminished in the Absence of NFIX

Interestingly, despite the increased levels of proliferation within the SVZ of *Nfix*$^{-/-}$ mice, both the RMS and olfactory bulbs of mutant mice were smaller than in their littermate controls (Figs 5E–G and 8A,B; Supplementary Fig. 7A–E). This, coupled with the large accumulation of neuroblasts expressing the markers DCX (Fig. 5) and TBR2 (Brill et al. 2009; Fig. 7E–G), within the SVZ of these mice, suggests that neuroblasts are unable to migrate normally through the RMS to the olfactory bulb in the absence of this transcription factor. Analysis of sagittal sections of P20 brains provided further support for this. In wild-type mice, hematoxylin-stained sections clearly revealed the trajectory of the RMS (Fig. 8A), and neuroblasts, characterized by the expression of PSA-NCAM and DCX, were readily visualized within the RMS (Fig. 8C,E). In the mutant, however, the RMS was smaller, there were fewer DCX-positive cells within the RMS, and the expression of PSA-NCAM within the RMS was almost absent (Fig. 8B,D,F).

To further investigate the migration of SVZ-derived neuroblasts, we performed a pulse-chase experiment with BrdU. *Nfix*$^{+/+}$ and *Nfix*$^{-/-}$ mice were administered an injection of BrdU (100 mg/kg) at P8, and the location of labeled cells was analyzed 5 days later at P13. In line with our previous findings relating to proliferation, we saw significantly more BrdU-positive cells per unit area of the SVZ in the mutant than in the control. However, there were significantly fewer BrdU-positive cells within the RMS and the ependymal layer and the glomerular layer of the olfactory bulb (Fig. 8G–Q), suggesting that neuroblasts derived from SVZ progenitors labeled at P8 had not migrated as far as those from the control cohort. To further investigate the migration of SVZ-derived neuroblasts, we performed a migration assay by enabling cultured neurospheres from wild-type and mutant mice to adhere to coverslips and to differentiate, through the removal of the mitogenic growth factors EGF and bFGF. Three days later, the distance migrated from parental spheres by DCX-expressing cells was quantified, revealing that wild-type neuroblasts had migrated, on average, significantly further than those from *Nfix*$^{-/-}$ mice (Fig. 9). This finding suggests that the cell-autonomous migration of SVZ-derived neuroblasts is abnormal in the absence of *Nfix*.

As they migrate from the SVZ through the RMS towards the olfactory bulb, neuroblasts proliferate, then exit the cell cycle, and stop expressing proliferative markers such as Ki67 (Smith and Luskin 1998). Our SVZ expression analysis (Table 2) had shown that all of the proliferating neuroblasts investigated, and the majority of those that were no longer proliferating, expressed NFIX. If the migration of neuroblasts was indeed impaired in *Nfix*$^{-/-}$ mice, we hypothesized that proportionally fewer DCX-expressing cells would be labeled with proliferative markers in the mutant, due to the fact that they would exit the cell cycle within the SVZ, rather than later in their migratory trajectory. In support of this, co-IF labeling of the SVZ of P20 wild-type and mutant mice with DCX and Ki67 revealed that, although there were more DCX-expressing cells within the mutant SVZ (Supplementary Fig. 6I–L), the proportion of proliferating neuroblasts was significantly smaller than that of controls (Fig. 10A–G), suggestive of the majority of these neuroblasts exiting the cell cycle within the SVZ, not within the RMS.

Reduced Interneuron Numbers in the Olfactory Bulb of *Nfix*$^{-/-}$ Mice

Given the deficits in migration of neuroblasts through the RMS within *Nfix*$^{-/-}$ mice, we investigated whether this phenotype culminated in reduced interneuron numbers within the olfactory bulb. SVZ progenitors located in different regions of the SVZ produce distinct neuronal progeny, with progenitors in the dorsal SVZ producing tyrosine hydroxylase-expressing periglomerular cells and superficial granule cells, those in the RMS and anterior SVZ generating calretinin-expressing periglomerular cells and granule cells, and those in the ventral SVZ producing calbindin-expressing periglomerular cells and deep granule cells (Young et al. 2007). PAX6 is expressed by both dopaminergic periglomerular cells and by a subpopulation of granule cells in wild-type mice (Brill et al. 2008). At P20 in the absence of *Nfix*, we observed significantly fewer PAX6-expressing cells within the glomerular and granule cell layer (Fig. 10H,K,N). Similarly, we observed significantly fewer calbindin- and calretinin-expressing cells within the glomerular layer of the mutant olfactory bulb (Fig. 10I,J,L,M,O,P). Given that the expansion in the SVZ only manifested dorsally in mutant mice, yet reductions in the numbers of multiple populations of interneurons derived from across the SVZ germinal zones were observed, these findings are illustrative of a global deficit in neuroblast migration from the SVZ to the olfactory bulb in the absence of *Nfix* and likely underlies the reduced size of the olfactory bulbs in these mutant mice.

Nfix$^{-/-}$ Mice Display Reduced Gliogenesis Within the RMS

The environmental context through which neuroblasts navigate the RMS is also critical. Glial tubes, which form in the postnatal period, form a conduit via which neuroblasts migrate through the RMS to the olfactory bulb. Given the previously described role for NFI factors in mediating gliogenesis (Brun et al. 2009; Whitman and Greer 2009; Singh, Bhardwaj, et al. 2011; Singh, Wilczynska, et al. 2011), we analyzed the expression of the glial marker, GFAP, within sagittal sections of P20 wild-type and *Nfix*$^{-/-}$ mice. In wild-type mice, GFAP-positive fibers clearly delineated the RMS (Fig. 11A). In the mutant, however, the expression of GFAP was markedly lower within the RMS and olfactory bulb (Fig. 11B), suggesting that gliogenesis is reduced within these regions of *Nfix*$^{-/-}$ mice. This finding is analogous to previous reports within the postnatal hippocampus (Heng et al. 2014), and suggests that a deficit in glial tube genesis may be the underlying mechanism responsible, at least in part, for the migratory phenotype seen in these mice.

Gdnf Is a Target for Transcriptional Activation by NFIX Within the RMS

NFIX has previously been shown to regulate gliogenesis, and the expression of glial-specific markers such as GFAP expression in vitro (Brun et al. 2009; Singh, Wilczynska, et al. 2011). To identify additional novel targets of NFIX during development of the SVZ and RMS, we performed a microarray on microdissected SVZ/RMS tissue from P20 wild-type and *Nfix*$^{-/-}$ mice. This analysis identified over 800 genes as being misregulated in the mutant,

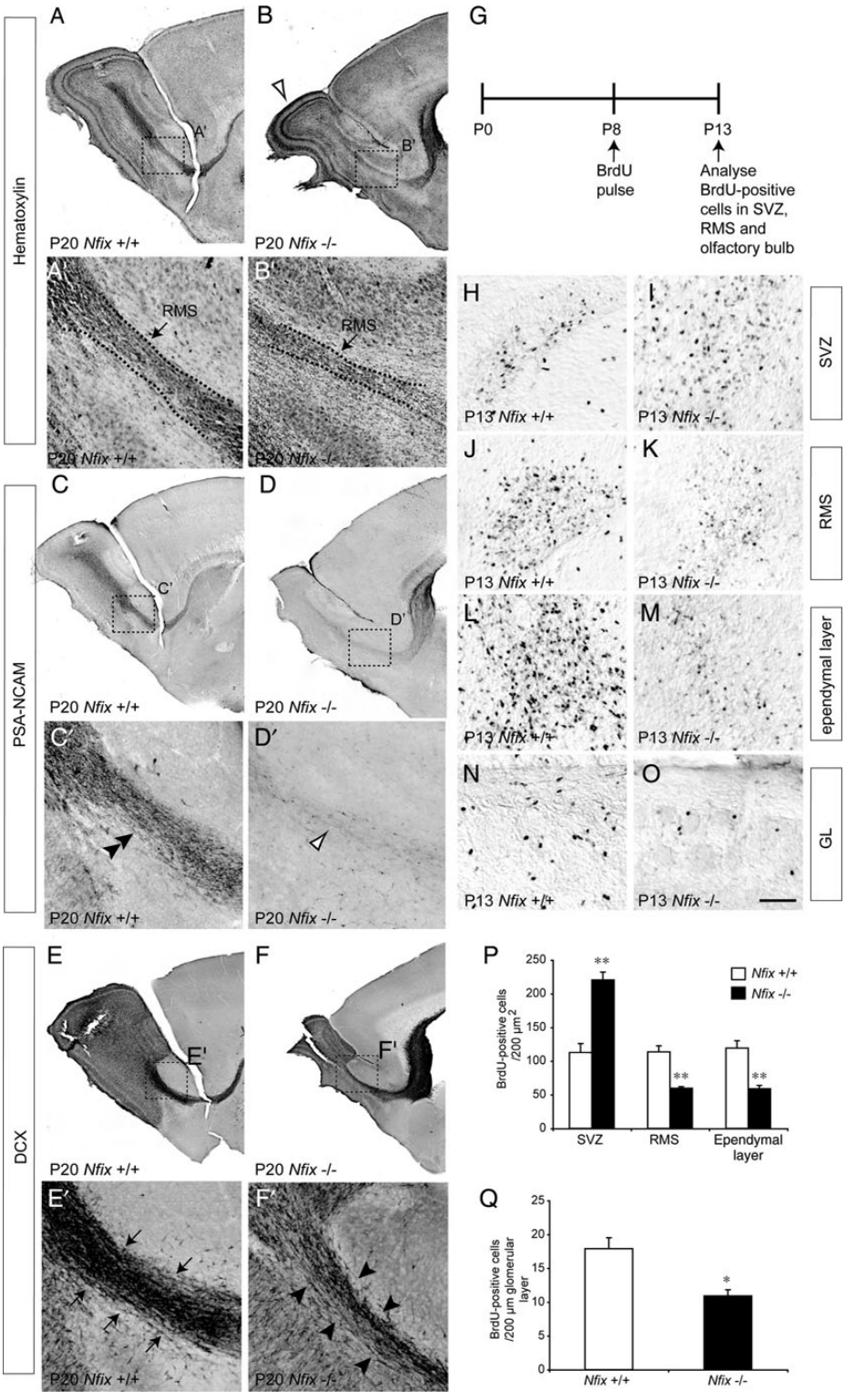

Figure 8. Abnormal migration through the RMS in postnatal mice lacking *Nfix*. (*A*–*F*) Sagittal sections through *Nfix*$^{+/+}$ (*A*, *C* and *E*) and *Nfix*$^{-/-}$ (*B*, *D* and *F*) mice. Hematoxylin staining of wild-type mice (*A*) revealed a well-demarcated RMS (dashed lines in *A*′). The RMS of *Nfix*$^{-/-}$ mice (*B*) was markedly smaller (dashed lines in *B*′), as was the olfactory bulb (open arrowhead in *B*). The expression of PSA-NCAM was also reduced within the RMS of mutant mice (compare double arrowhead in *C*′ with the open arrowhead in *D*′). Similarly, expression of DCX in the wild-type RMS (*E*, arrows encompass the RMS in *E*′) was more extensive than within the mutant RMS (*F*, arrowheads encompass the RMS in *F*′). (*G*) Experimental protocol for BrdU-pulse labeling experiment. (*H*–*O*) Coronal sections of *Nfix*$^{+/+}$ and *Nfix*$^{-/-}$ mice at the level of the SVZ (*H* and *I*), RMS (*J* and *K*), ependymal layer of the olfactory bulb (*L* and *M*), and glomerular layer (GL) of the olfactory bulb (*N* and *O*), revealing BrdU-labeled cells. There were significantly more BrdU-labeled cells within the SVZ, but significantly fewer labeled cells within the RMS and olfactory bulb, of mutant mice in comparison with wild-type controls (*P* and *Q*). *$P < 0.05$, **$P < 0.01$, *t*-test. Scale bar (in *O*): 600 µm for *A*–*F*; 100 µm for *A*′–*F*′; 75 µm for *H*–*O*.

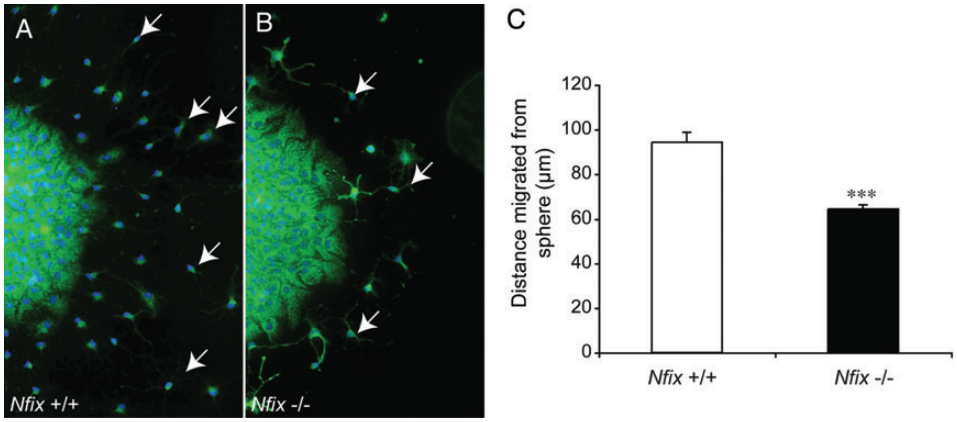

Figure 9. Reduced migration of *Nfix*$^{-/-}$ neuroblasts in vitro. Wild-type (*A*) and *Nfix*$^{-/-}$ (*B*) SVZ-derived neurospheres of similar dimensions were cultured for 72 h in the absence of mitogenic growth factors. The expression of DCX (green) was used to reveal migratory neuroblasts (arrows in *A* and *B*). (*C*) Neuroblasts isolated from the SVZ of wild-type mice migrated, on average, significantly further than those from *Nfix*$^{-/-}$ mice. Cell nuclei are labeled with DAPI (blue). ***$P < 0.005$, *t*-test. Scale bar (in *B*): 100 μm.

using a significance value of $P < 0.05$ via ANOVA and a fold-change cutoff of 1.5. Functional annotation of these transcripts using Ingenuity Pathway Analysis identified many processes as being misregulated in the mutant, including cellular development nervous system development and function, cellular movement and neurobiological disease (Supplementary Fig. 8). Key transcripts upregulated in the mutant SVZ included the progenitor cell markers *Hes1*, *Dlx1* and *Dlx2* (Fig. 11C and Table 3). We have previously demonstrated regulation of *Hes1* by NFI family members (Piper et al. 2010) and Notch signaling is critical for the maintenance of the SVZ neurogenic niche (Imayoshi et al. 2010); thus, it seems likely that the proliferative phenotype we observed in the SVZ of *Nfix*$^{-/-}$ mice (Figs 5–7) stems, at least in part, from misregulation of the Notch signaling pathway. Downregulated transcripts included the guidance receptors *Plxnd1* and *Unc5b*, as well as *Flt1*, the receptor for vascular endothelial growth factor (VEGF) (Fig. 11C and Table 4). Interestingly, *Gdnf*, which has previously been shown to promote migration through the RMS (Paratcha et al. 2006), was also downregulated in the mutant (Fig. 11C and Table 4). Validation of the array results using qPCR confirmed that levels of *Gdnf* mRNA were significantly lower in the mutant SVZ/RMS and olfactory bulb (Fig. 11*D*). In line with our immunohistochemical data, levels of *Dcx* mRNA were significantly higher in the mutant SVZ/RMS, but lower in the olfactory bulb of the mutant, and the levels of *Gfap* and *Pax6* mRNA were significantly lower in the olfactory bulb of *Nfix*$^{-/-}$ mice (Fig. 11*D*).

These array and qPCR findings suggested that diminished *Gdnf* expression within the RMS of *Nfix*$^{-/-}$ mice may underlie part of the phenotype exhibited by these mice. To determine whether *Gdnf* is a direct target for transcriptional control by NFIX, we screened the *Gdnf* promoter in silico for potential NFI-binding sites (see Materials and Methods) and identified 2 putative NFI motifs close to the *Gdnf* TSS (−5 and +44). Furthermore, NFIX was able to bind to an oligonucleotide probe containing the −5 sequence in vitro in an electrophoretic mobility shift assay (Fig. 11*E*,*F*). Finally, we used a reporter gene assay to investigate whether NFIX could activate *Gdnf* promoter-driven transcriptional activity. A fragment of the *Gdnf* promoter containing the putative NFI-binding site was able to significantly activate reporter gene expression in a luciferase assay conducted in Neuro2A cells, and this reporter gene expression was significantly increased by the co-expression of NFIX, as well as by the co-expression of the other NFI family members reported to be expressed within the adult SVZ, NFIA and NFIB (Plachez et al. 2012; Fig. 11*G*). Moreover, luciferase expression driven by a truncated version of the *Gdnf* promoter lacking the NFI-binding site was unable to be enhanced by NFIX, indicative of this site being critical for NFI-mediated activation of *Gdnf* promoter-mediated transcription. Finally, we sought to determine whether *Nfix*$^{+/+}$ and *Nfix*$^{-/-}$ neuroblasts were similarly responsive to GDNF in vitro, by culturing wild-type and mutant spheres with 120 ng/mL of bath-applied GDNF in the neuroblast migration assay (Fig. 9). Interestingly, both wild-type and mutant cells were similarly responsive to GDNF. Wild-type cells cultured in the presence of GDNF migrated 30.4% further than wild-type cells cultured without GDNF, whereas mutant cells cultured with GDNF migrated 29.3% further than mutant cells cultured without GDNF ($P < 0.05$, ANOVA). Taken together, our data suggest that NFIX is involved in the activation of *Gdnf* transcription within the olfactory bulb and RMS, and that, in the absence of *Nfix*, the reduction in *Gdnf* expression is responsible for at least part of the decreased migration of SVZ-derived neuroblasts within these mice.

Discussion

Unlike the postnatal human SVZ, in which the birth of olfactory neurons diminishes rapidly after 18 months of age (Sanai et al. 2011; Wang et al. 2011; Bergmann et al. 2012), neurogenesis within the SVZ niche continues throughout life in rodents such as mice (Alvarez-Buylla and Garcia-Verdugo 2002). The ongoing production of olfactory bulb interneurons within the postnatal and adult rodent brain relies upon both the proliferation of neural progenitor cells within the SVZ and the migration of their progeny through the RMS to the olfactory bulb, where they differentiate and mature into granule and periglomerular cells (Kriegstein and Alvarez-Buylla 2009). This intricate process relies on a host of factors, both cell-intrinsic and cell-extrinsic to the progenitor cells and neuroblasts, that must work in concert to ensure the generation of the requisite number of interneurons required for replacement within the olfactory bulb (Whitman and Greer 2009). Here, we identify the transcription factor NFIX as a vital contributor to the development of the postnatal SVZ/RMS, with abnormalities in both proliferation and migration evident within this neurogenic niche in mice lacking this gene.

Studies into the development of other regions of the brain have also highlighted a central role for NFIX in the control of neural progenitor cell proliferation and the migration of their progeny (Heng et al. 2012; Harris et al. 2014). With relation to the

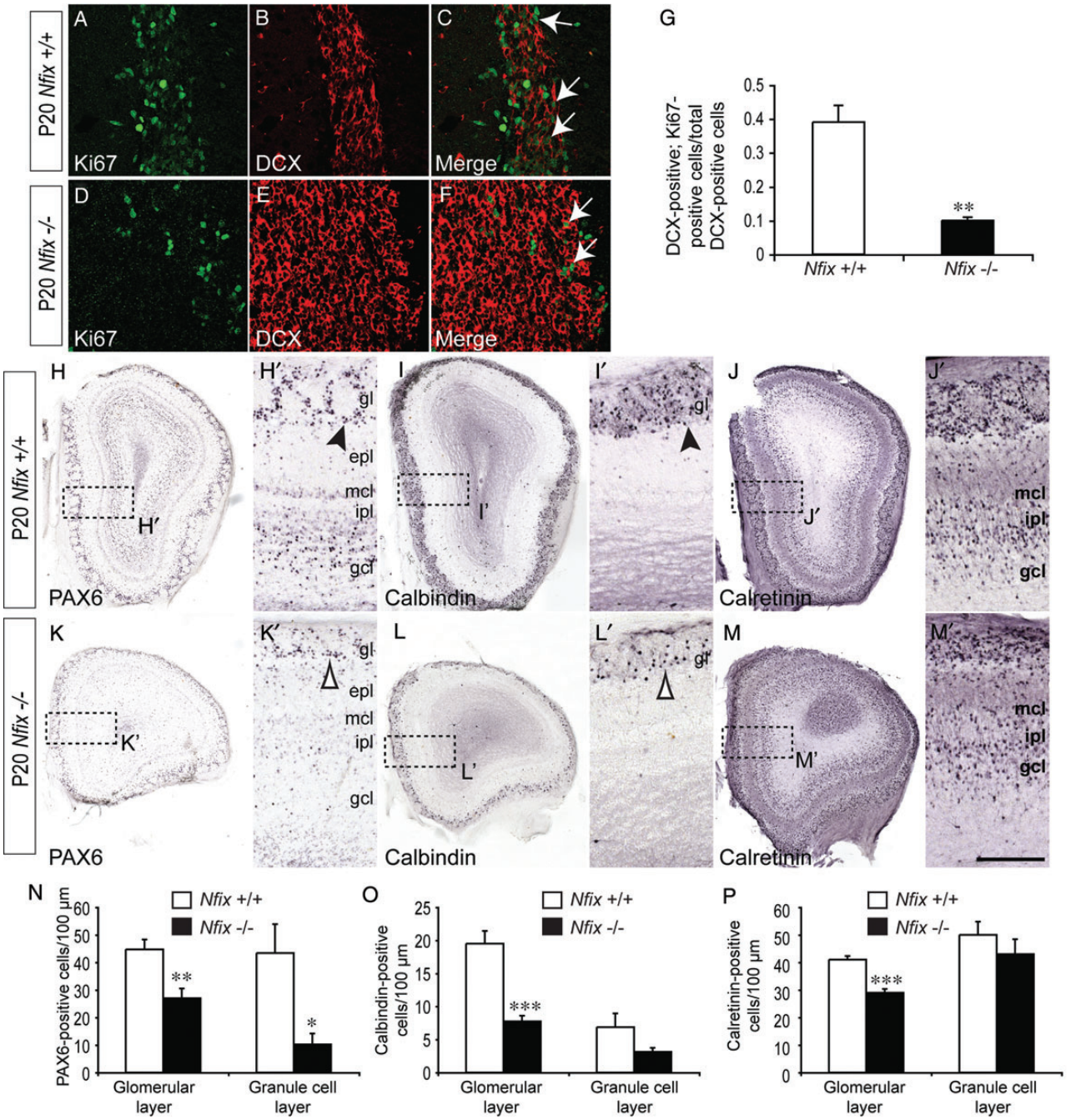

Figure 10. Decreased populations of interneurons within the olfactory bulb of *Nfix*$^{-/-}$ mice. Coronal sections through the SVZ (*A–F*) and olfactory bulb (*H–M*) of *Nfix*$^{+/+}$ and *Nfix*$^{-/-}$ mice. (*A–F*) Confocal sections through the SVZ of *Nfix*$^{+/+}$ (*A–C*) and *Nfix*$^{-/-}$ (*D–F*) mice revealing the expression of Ki67 (green) and DCX (red). Arrows in *C* and *F* indicate cells expressing both DCX and Ki67. Quantification reveals that a significantly greater proportion of DCX-positive cells in the wild-type retain Ki67 expression than within the mutant (*G*). (*H–M*) Expression of the interneuron markers PAX6 (*H* and *K*), calbindin (*I* and *L*) and calretinin (*J* and *M*) within the olfactory bulbs of *Nfix*$^{+/+}$ and *Nfix*$^{-/-}$ mice. There were significantly fewer PAX6-expressing cells within the glomerular layer (compare arrowhead in *H′* with the open arrowhead in *K′*) and granule cell layer of the mutant mice at this age (*N*). Similarly, there were fewer calbindin-expressing neurons (compare arrowhead in *I′* with the open arrowhead in *L′*) and calretinin-expressing neurons (*J* and *M*) in the mutant in comparison with the control (*O* and *P*). gl, glomerular layer; epl, external plexiform layer, mcl, mitral cell layer; ipl, internal plexiform layer; gcl, granule cell layer. *P<0.05, **P<0.01, ***P<0.001, *t*-test. Scale bar (in *M′*): 75 µm for *A–F* and *H′–M′*; 300 µm for *H–M*.

control of self-renewal and cell cycle exit, NFIX acts to promote the differentiation of neural progenitor cells within the developing neocortex and hippocampus, in part via the transcriptional repression of Sox9 (Heng et al. 2014), a factor pivotal for the induction and maintenance of cortical neural progenitors (Scott et al. 2010). Indeed, NFI transcription factors have been shown to regulate neural progenitor cell differentiation through a variety of different mechanisms, including the repression of stem cell self-renewal genes (Piper et al. 2010; Piper et al. 2014), the activation of differentiation-specific programs of gene expression (Cebolla and Vallejo 2006), and through the epigenetic control of DNA methylation (Namihira et al. 2009).

We have also recently reported a role for NFIX in the development (Heng et al. 2014) and function (Harris et al. 2013) of the

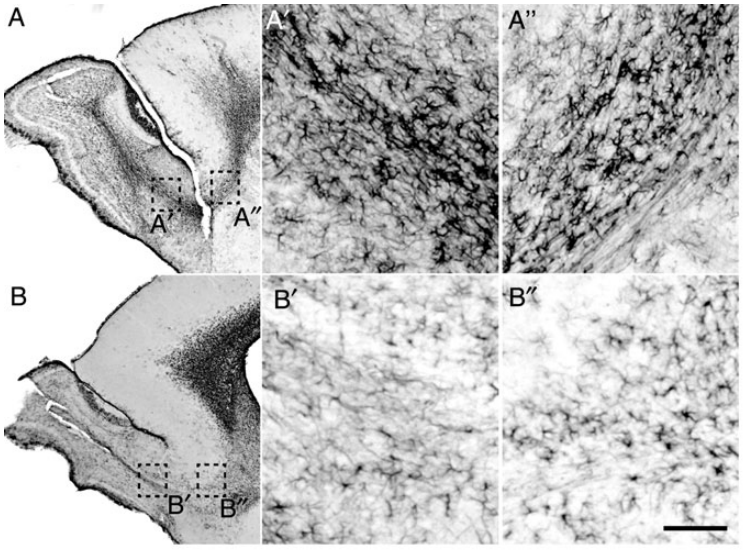

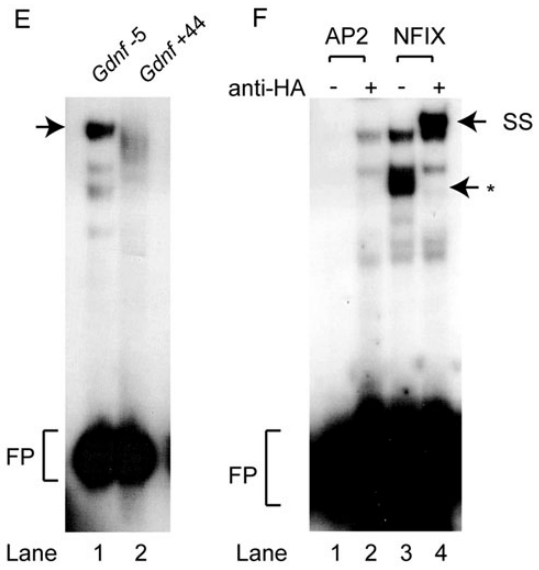

C

Downregulated	Fold change	Function
Gdnf	-2.02	Neurotrophic factor
Unc5b	-1.69	Axon guidance receptor
Flt1	-1.63	Vascular endothelial growth factor receptor
Pxnd1	-1.61	Axon guidance receptor
Upregulated	**Fold change**	**Function**
Calb	2.76	Calcium-binding protein
Dcx	2.16	Microtubule-associated protein
Hes1	1.84	Notch pathway
Th	1.82	Enzyme in dopamine biosynthetic pathway

D

Gene	Source	Relative mRNA level in control	Relative mRNA level in KO	*P* value
Gdnf	SVZ/RMS	0.8	0.55	0.03
Gdnf	OB	0.44	0.16	0.01
Dcx	SVZ/RMS	27	52.8	0.01
Dcx	OB	146	98.7	0.003
Gfap	OB	29.3	13.8	0.002
Pax6	OB	13.7	10.5	0.04

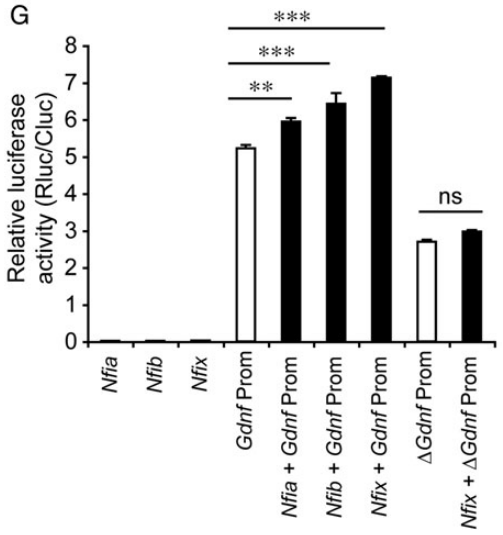

Figure 11. *Gdnf* is a direct target for transcriptional activation by NFIX. (*A* and *B*) Sagittal sections through *Nfix*$^{+/+}$ (*A*) and *Nfix*$^{-/-}$ (*B*) mice at P20. The expression of GFAP within the RMS of wild-type mice at this age is extensive (*A*′ and *A*″), but is markedly reduced in the mutant RMS (*B*′ and *B*″). (*C*) Microarray analyses revealed transcripts that were downregulated or upregulated in the SVZ/RMS of *Nfix*$^{-/-}$ mice at P20. (*D*) qPCR validation revealed that the level of *Gdnf* mRNA was significantly lower within both the SVZ/RMS and olfactory bulb (OB) of the mutant in comparison with the control at P20. Mutant mice also exhibited elevated levels of *Dcx* mRNA within the SVZ/RMS, but reduced levels of *Dcx*, *Gfap* and *Pax6* mRNAs within the olfactory bulb. (*E* and *F*) Results of EMSA. (*E*) E18 mouse cortical nuclear extracts were incubated with radiolabeled probes for the −5 (lane 1) and +44 (lane 2) consensus sites. A factor from the nuclear extract bound to the −5 probe (arrow). FP, free probe. (*F*) Nuclear extracts from COS cells expressing HA-tagged versions of the transcription factors AP2 (lanes 1 and 2) or NFIX (lanes 3 and 4) were incubated with radiolabeled probes for the −5 consensus site. There was no specific binding in the lanes containing the nuclear extracts from the AP2-expressing cells (lanes 1 and 2). A factor from the nuclear extract containing the NFIX expression construct did bind to the probe (*; lane 3). Inclusion of an anti-HA antibody into the binding reaction caused a supershift in this band (SS, lane 4). (*G*) Luciferase reporter gene assay performed in Neuro2A cells. Expression of NFIA, NFIB or NFIX elicited negligible luciferase activity, whereas transfection of a *Gdnf* promoter-driven luciferase reporter construct elicited reporter gene induction. Co-transfection of the *Nfix* expression construct and the *Gdnf* promoter resulted in a significantly increased level of luciferase activity. Similarly, co-transfection of *Nfia* or *Nfib* also significantly increased luciferase expression. However, *Nfix* was unable to enhance the activity of a truncated *Gdnf* promoter construct (Δ*Gdnf* prom) lacking the putative NFI-binding site. $^{**}P < 0.01$, $^{***}P < 0.001$, ANOVA. ns, not significant. Scale bar (in *B*″): 600 μm for *A* and *B*; 100 μm for *A*′ and *B*″.

other main neurogenic niche within the brain, the subgranular zone of the dentate gyrus, showing that NFIX mediates progenitor cell differentiation within this niche (Heng et al. 2014). Here, we extend our earlier description of the SVZ of *Nfix*$^{-/-}$ mice (Campbell et al. 2008), revealing that NFIX is also important for proliferation within the postnatal SVZ. Our studies demonstrate an increase in proliferation within the *Nfix*$^{-/-}$ postnatal SVZ, with significantly more proliferative cells in this region, as well as increased expression of progenitor cell markers including PAX6, SOX2, *Hes1* and *Hes5*, as well as MASH1, a marker for transit-amplifying cells. While it is likely that these findings reflect elevated proliferation within the SVZ, one potential caveat to this interpretation is that neuroblasts continue to proliferate within the SVZ/RMS. When considered in light of the diminished migration within these mutant mice, the attribution of the increased proliferation within the *Nfix*$^{-/-}$ SVZ solely to enhanced proliferation of

Table 3 Key examples of transcripts upregulated in the SVZ/RMS of *Nfix*$^{-/-}$ mice at P20

Functional classification (Ingenuity)	Upregulated genes
Cellular growth and proliferation	*Hes1*, *Dicer 1*, *Sox4*, *Igfbp6*, *Igfbp3*, *E2f1*, *Igfbp4*, *Socs2*, *Cntfr*
Nervous system development and function	*Map1b*, *Sfrp2*, *Grik5*, *Dlx1*, *Dlx2*, *Dcx*, *Gad1*, *Nrxn2*
Cellular function and maintenance	*Sema4A*, *Sox4*, *Mtor*, *Cebpb*, *Ifngr2*, *Sgk1*
Cancer	*Stra13*, *Flh2*, *Xpa*, *Chst8*, *Chic2*

Table 4 Key examples of transcripts downregulated in the SVZ/RMS of *Nfix*$^{-/-}$ mice at P20

Functional classification (Ingenuity)	Downregulated genes
Nervous system development and function	*Gdnf*, *Grik*, *Chat*, *Foxo1*, *Adam17*, *Gas7*, *Kcn2*, *Slc5a4*
Neurological disease	*Slit3*, *Flt1*, *Spock 3*, *Dock4*, *Kifib*, *Itgb4*, *Msx1*, *Slc5a7*, *Plxnd1*, *Scn2b*
Cell cycle	*E2f6*, *Rarres 2*, *Bcl2*, *Kit*, *Rarb*, *Gas7*
Cellular movement	*Unc5b*, *Fgf10*, *Akap9*, *Alcam*, *Gab1*, *Klf2*

neural progenitor cells becomes problematic. However, our in vitro neurosphere assay clearly demonstrated enhanced proliferation of SVZ tissue isolated from *Nfix*$^{-/-}$ mice over multiple passages. Furthermore, many of the neuroblasts within the mutant SVZ had in fact exited the cell cycle, and were no longer proliferative. Collectively, these data are strongly indicative of increased numbers of proliferating neural progenitor cells in the SVZ of mice lacking *Nfix*.

Indeed, recent reports have shown that NFIX is an important regulator of both proliferation of stem cells and of their subsequent differentiation, both within and outside the central nervous system. For example, within the hematopoietic system, NFIX was recently identified as being expressed by stem and progenitor cells, and was shown to promote their survival in vivo (Holmfeldt et al. 2013). Moreover, NFIX has been demonstrated to be instrumental for differentiation within the developing skeletal musculature, driving the switch from embryonic-specific to fetal-specific programs of gene expression (Messina et al. 2010). By what means then, does NFIX regulate proliferation within the SVZ? Numerous genes have been shown to control proliferation within this neurogenic niche, including members of the Notch signaling pathway (Imayoshi et al. 2010), *Sox2* (Andreu-Agullo et al. 2012), *Sox9* (Cheng et al. 2009), *Pax6* (Brill et al. 2009), and *Dlx1* and *Dlx2* (Brill et al. 2008). Given previous reports of modulation of Notch pathway signaling by NFI family members (Deneen et al. 2006; Piper et al. 2010), as well as regulation of *Sox9* by NFIX (Heng et al. 2014), it is likely that NFIX can regulate the transcription of at least a subset of these genes, a supposition supported by the presence of putative NFI-binding sites within the promoters of many of the genes implicated within these pathways (Table 5). Thus, NFIX may act to suppress the proliferation of stem cells and transit-amplifying cells within the SVZ during postnatal development. However, another alternative explanation could be that the loss of *Nfix* culminates in a shift in the balance between stem cell quiescence and active cell division.

Table 5 Putative NFI-binding sites within the promoters of genes misregulated in the SVZ of *Nfix*$^{-/-}$ mice

Gene	UCSC identifier	Position relative to TSS	Site *P*-value	Site sequence
Dab1	uc008txv.1	−386	2.8×10^{-5}	GTGGCGGGCTCCCAG
Dab1	uc008txv.1	−489	3.9×10^{-6}	CGGGCGCAGAGCCAA
Dab1	uc008txu.1	−1912	8.2×10^{-5}	TTGGGCAAATGCCAT
Dab1	uc008txv.1	−2618	6.8×10^{-5}	TGGGAAGAGAACCAA
Dlx1	uc008kau.1	−601	1.4×10^{-5}	CTGGCCAGACCCCAG
Dlx1	uc008kau.1	−2946	8.7×10^{-5}	GAGGATCAGGGCCAG
Fscn1	uc009ajl.1	−304	8.4×10^{-6}	TTGGAGATCAGCCAA
Fscn1	uc009ajl.1	−814	8.2×10^{-5}	ATGGCACAGCCCCAA
Fscn1	uc009ajl.1	−1003	1.7×10^{-5}	CTGGGGTAGGGCCAG
Fscn1	uc009ajl.1	−1033	1.1×10^{-5}	AGGGCCAGGGGCCCA
Gdnf	uc007vee.1	44	4.3×10^{-5}	GTGGCCCGAATCCCA
Gdnf	uc007vee.1	−5	9.8×10^{-5}	CTGGGCGGGGCCCCG
Pax6	uc008lla.1	−242	2.1×10^{-5}	CTGGTGCAGAGCCAG
Pax6	uc008lla.1	−716	5.3×10^{-5}	CTGGGAAGAAGACAG
Pax6	uc008lky.1	−937	2.1×10^{-5}	AGGGATGAGAGCCAG
Pax6	uc008lla.1	−1069	6.4×10^{-5}	CTGGCGCGAGGCCCC
Pax6	uc008lku.1	−1095	4.3×10^{-6}	CTGGGAGACAGCCAG
Pax6	uc008lku.1	−1454	1.8×10^{-5}	TTGGATAGGTCCCAA
Pax6	uc008lku.1	−1771	7.7×10^{-5}	GAGGCCCAGGGCCCA
Pax6	uc008llc.1	−2861	6.8×10^{-5}	GTGGGAAGGCTCCAG
Plxnd1	uc009djn.1	102	6.0×10^{-5}	CGGGGGGGGGGCCCG
Plxnd1	uc009djn.1	−162	1.7×10^{-6}	CTGGCCAGGAACCAG
Plxnd1	uc009djn.1	−488	6.0×10^{-5}	GGGGACTGTGGCCAG
Plxnd1	uc009djn.1	−1281	4.6×10^{-5}	AGGGCTCAGAGCCCA
Plxnd1	uc009djn.1	−1311	1.9×10^{-5}	TGGGGTGGGGGCCAG
Plxnd1	uc009djn.1	−2738	7.3×10^{-5}	CTGGACAGTGGCCAT
Sox2	uc008oxu.1	−2065	8.7×10^{-5}	AGGGAAGGCGGCCAC
Sox2	uc008oxu.1	−2411	9.8×10^{-5}	GTGGCGCGCGGACAA
Unc5b	uc007ffe.1	−95	9.8×10^{-5}	CGGGGGCGGAGCCAC
Unc5b	uc007ffd.1	−217	6.8×10^{-5}	GTGGAAAGTGGCCCA
Unc5b	uc007ffd.1	−1613	4.6×10^{-5}	GAGGCGCAGGGCCAG
Unc5b	uc007ffe.1	−2324	3.3×10^{-5}	TGGGAAAGGAGACAG
Unc5b	uc007ffd.1	−2743	4.9×10^{-5}	CAGGAAAGAGGCCCA

Note: All potential NFI-binding sites with *P*-values $\leq 10^{-4}$ were reported in the region of −3000 to +200 bp relative to the TSS of the selected genes.

Within the adult SVZ, neural progenitor cells predominantly exist in a quiescent state, dividing rarely to ensure that the progenitor pool does not become depleted. How stem cell quiescence is maintained remains unclear, although neural activity has been implicated in the regulation of this process within the adult dentate gyrus (Song et al. 2012). Intriguingly, NFIX has recently been shown to contribute to the regulation of quiescence in neural stem cells in vitro (Martynoga et al. 2013). Could the enlarged SVZ in *Nfix*$^{-/-}$ mice reflect a diminution of the quiescent progenitor cell pool and an increase in the dividing pool in these mutants? Given that we begin to see a thickened SVZ at P2, well before the mature SVZ neurogenic niche becomes established, it seems unlikely that aberrant exit from quiescence underlies the phenotype observed here.

In addition to regulating the proliferation of neural progenitor cells, NFIX has also been implicated in the regulation of post-mitotic cell migration within the hippocampus (Heng et al. 2014), cerebellum (Piper et al. 2011) and RMS (this study). The contribution of NFIs to cellular migration within the nervous system has been most extensively investigated with respect to postnatal formation of the cerebellum (Kilpatrick et al. 2010). NFIs, which are expressed by post-mitotic migrating cerebellar granule neurons,

regulate a diverse set of target genes, including *Tag-1*, *ephrin B1*, and *N-cadherin* (Wang et al. 2007, 2010), all of which ensure the efficient migration of newborn granule cells from the germinal external granule layer to the internal granule cell layer.

How could NFIX mediate migration through the nascent RMS to the olfactory bulb? Given the expression of NFIX by both neuroblasts within the adult SVZ and RMS, and by GFAP-positive glia surrounding the RMS, it is likely that factors both intrinsic and extrinsic to migrating neuroblasts are controlled by this transcription factor. There are numerous examples of mouse mutants that exhibit abnormal neuroblast migration, leading to an accumulation of neuroblasts within the SVZ and proximal RMS, and a smaller olfactory bulb. For example, the ablation of cell-autonomous factors within neuroblasts, such as the reelin receptors ApoER2/VLDL, the adaptor protein Dab1 (Andrade et al. 2007), the actin-bundling protein fascin (Sonego et al. 2013) and cyclin-dependent kinase 5 (Hirota et al. 2007), all result in aberrant migration of neuroblasts. Another critical cell-autonomous factor required for neuroblast migration is PSA-NCAM, which facilitates chain migration of neuroblasts through the RMS (Ono et al. 1994; Hu et al. 1996). The reduction in PSA-NCAM expression within the RMS at P20 is indicative of potential regulation of this cell adhesion molecule by NFIX during development. DCX is also important for neuroblast migration within the RMS (Koizumi et al. 2006). We have previously reported numerous potential sites for NFI binding within the promoters of *cyclin-dependent kinase 5*, *Ncam1* and *Dcx* (Plachez et al. 2012), and have also identified potential NFI-binding sites in the proximal promoters of many other of the aforementioned genes (Table 5), a finding that points to NFIX regulating multiple cell-autonomous aspects of neuroblast migration during development.

Our data also indicate that NFIX may regulate neuroblast migration via non-cell-autonomous mechanisms during development. Although neuroblasts begin migrating to the olfactory bulb during late gestation, well before the glial tube develops (Sun et al. 2010), the glial tube has formed by P20, and this structure plays a crucial part in facilitating ongoing neuroblast migration. The dramatic reduction in GFAP-expressing glia within the RMS and olfactory bulb of mutant mice is indicative of delayed glial development, findings supported by the reported roles for NFI family members, including NFIX, in promoting gliogenesis both in vitro (Brun et al. 2009; Singh, Bhardwaj, et al. 2011) and in vivo (Shu et al. 2003; Deneen et al. 2006). Here, we reveal *Gdnf* as a potential direct target for transcriptional activation by NFIX, suggesting a mechanism by which this chemoattractant for neuroblasts (Paratcha et al. 2006) is transcriptionally activated during development. Our array and bioinformatics findings also point to further targets for transcriptional regulation by NFIX in the non-cell-autonomous regulation of neuroblast migration, including *Flt1*, which encodes one of the VEGF receptors. Given the integral role played by the vasculature in supporting and guiding neuroblast migration (Snapyan et al. 2009), these findings provide insights into additional avenues through which NFIX may regulate the development of the RMS.

Taken together, our findings provide a comprehensive insight into how NFIX modulates the development of the postnatal SVZ neurogenic niche, migration within the RMS, as well as the consequences of aberrant formation of these structures with regard to interneuron populations within the olfactory bulb. The diverse genetic programs and identification of further direct transcriptional targets controlled by NFIX within the SVZ and RMS, as well as the role of NFIX expression within mature interneuron populations within the olfactory bulb, remain open questions for future studies.

Supplementary Material

Supplementary material can be found at: http://www.cercor.oxfordjournals.org/

Funding

This work was supported by National Health and Medical Research Council (NHMRC) project grants (grant nos 1003462, 1057751, and 1022308 to M.P. and 569504 to L.J.R.) and by the National Institute of Health and NYSTEM grants (grant nos HL080624, C026714, and C026429 to R.M.G.). The following authors were supported by fellowships: M.P. (Australian Research Council Future Fellowship; FT120100170) and L.J.R. (NHMRC Principal Research Fellowship). Y.H.E.H. was supported by an University of Queensland International Scholarship and L.H. was supported by an Australian Postgraduate Award.

Notes

We thank Chantelle Reid and Erica Little for technical assistance, Prof. Perry Bartlett (Queensland Brain Institute) for provision of the *Dcx*-GFP and *Hes5*-GFP mice, Prof. Pankaj Sah (Queensland Brain Institute) and Prof. Yuchio Yanagawa (Gunma University Graduate School of Medicine, Japan) for provision of the *Gad67*-GFP mice, Rowan Tweedale for critical analysis of the manuscript, and Profs Jane Johnson, Robert Hevner and Ryoichiro Kageyama for kindly providing reagents. *Conflict of Interest*: None declared.

References

Alvarez-Buylla A, Garcia-Verdugo JM. 2002. Neurogenesis in adult subventricular zone. J Neurosci. 22:629–634.

Andrade N, Komnenovic V, Blake SM, Jossin Y, Howell B, Goffinet A, Schneider WJ, Nimpf J. 2007. ApoER2/VLDL receptor and Dab1 in the rostral migratory stream function in postnatal neuronal migration independently of Reelin. Proc Natl Acad Sci USA. 104:8508–8513.

Andreu-Agullo C, Maurin T, Thompson CB, Lai EC. 2012. Ars2 maintains neural stem-cell identity through direct transcriptional activation of Sox2. Nature. 481:195–198.

Bailey TL, Boden M, Buske FA, Frith M, Grant CE, Clementi L, Ren J, Li WW, Noble WS. 2009. MEME SUITE: tools for motif discovery and searching. Nucleic Acids Res. 37:W202–W208.

Bergmann O, Liebl J, Bernard S, Alkass K, Yeung MS, Steier P, Kutschera W, Johnson L, Landen M, Druid H, et al. 2012. The age of olfactory bulb neurons in humans. Neuron. 74:634–639.

Bovetti S, Bovolin P, Perroteau I, Puche AC. 2007. Subventricular zone-derived neuroblast migration to the olfactory bulb is modulated by matrix remodelling. Eur J Neurosci. 25:2021–2033.

Brill MS, Ninkovic J, Winpenny E, Hodge RD, Ozen I, Yang R, Lepier A, Gascon S, Erdelyi F, Szabo G, et al. 2009. Adult generation of glutamatergic olfactory bulb interneurons. Nat Neurosci. 12:1524–1533.

Brill MS, Snapyan M, Wohlfrom H, Ninkovic J, Jawerka M, Mastick GS, Ashery-Padan R, Saghatelyan A, Berninger B, Gotz M. 2008. A dlx2- and pax6-dependent transcriptional code for periglomerular neuron specification in the adult olfactory bulb. J Neurosci. 28:6439–6452.

Brun M, Coles JE, Monckton EA, Glubrecht DD, Bisgrove D, Godbout R. 2009. Nuclear factor I regulates brain fatty acid-

binding protein and glial fibrillary acidic protein gene expression in malignant glioma cell lines. J Mol Biol. 391:282–300.
Campbell CE, Piper M, Plachez C, Yeh YT, Baizer JS, Osinski JM, Litwack ED, Richards LJ, Gronostajski RM. 2008. The transcription factor Nfix is essential for normal brain development. BMC Dev Biol. 8:52.
Cebolla B, Vallejo M. 2006. Nuclear factor-I regulates glial fibrillary acidic protein gene expression in astrocytes differentiated from cortical precursor cells. J Neurochem. 97:1057–1070.
Cheng LC, Pastrana E, Tavazoie M, Doetsch F. 2009. miR-124 regulates adult neurogenesis in the subventricular zone stem cell niche. Nat Neurosci. 12:399–408.
Deneen B, Ho R, Lukaszewicz A, Hochstim CJ, Gronostajski RM, Anderson DJ. 2006. The transcription factor NFIA controls the onset of gliogenesis in the developing spinal cord. Neuron. 52:953–968.
Fujita PA, Rhead B, Zweig AS, Hinrichs AS, Karolchik D, Cline MS, Goldman M, Barber GP, Clawson H, Coelho A, et al. 2011. The UCSC Genome Browser database: update 2011. Nucleic Acids Res. 39:D876–D882.
Gao Z, Ure K, Ables JL, Lagace DC, Nave KA, Goebbels S, Eisch AJ, Hsieh J. 2009. Neurod1 is essential for the survival and maturation of adult-born neurons. Nat Neurosci. 12:1090–1092.
Gleeson JG, Lin PT, Flanagan LA, Walsh CA. 1999. Doublecortin is a microtubule-associated protein and is expressed widely by migrating neurons. Neuron. 23:257–271.
Grant CE, Bailey TL, Noble WS. 2011. FIMO: scanning for occurrences of a given motif. Bioinformatics. 27:1017–1018.
Harris L, Dixon C, Cato K, Heng YH, Kurniawan ND, Ullmann JF, Janke AL, Gronostajski RM, Richards LJ, Burne TH, et al. 2013. Heterozygosity for nuclear factor one X affects hippocampal-dependent behaviour in mice. PloS ONE. 8:e65478.
Harris L, Genovesi LA, Gronostajski RM, Wainwright BJ, Piper M. Forthcoming 2014. Nuclear factor one transcription factors: divergent functions in developmental versus adult stem cell populations. Dev Dynamics; doi:10.1002/dvdy.24182.
Heng YH, Barry G, Richards LJ, Piper M. 2012. Nuclear factor I genes regulate neuronal migration. Neurosignals. 20:159–167.
Heng YH, McLeay RC, Harvey TJ, Smith AG, Barry G, Cato K, Plachez C, Little E, Mason S, Dixon C, et al. 2014. NFIX regulates neural progenitor cell differentiation during hippocampal morphogenesis. Cereb Cortex. 24:261–279.
Hippenmeyer S, Youn YH, Moon HM, Miyamichi K, Zong H, Wynshaw-Boris A, Luo L. 2010. Genetic mosaic dissection of Lis1 and Ndel1 in neuronal migration. Neuron. 68:695–709.
Hirota Y, Ohshima T, Kaneko N, Ikeda M, Iwasato T, Kulkarni AB, Mikoshiba K, Okano H, Sawamoto K. 2007. Cyclin-dependent kinase 5 is required for control of neuroblast migration in the postnatal subventricular zone. J Neurosci. 27:12829–12838.
Holmfeldt P, Pardieck J, Saulsberry AC, Nandakumar SK, Finkelstein D, Gray JT, Persons DA, McKinney-Freeman S. 2013. Nfix is a novel regulator of murine hematopoietic stem and progenitor cell survival. Blood. 122:2987–2996.
Hu H, Tomasiewicz H, Magnuson T, Rutishauser U. 1996. The role of polysialic acid in migration of olfactory bulb interneuron precursors in the subventricular zone. Neuron. 16:735–743.
Imayoshi I, Sakamoto M, Yamaguchi M, Mori K, Kageyama R. 2010. Essential roles of Notch signaling in maintenance of neural stem cells in developing and adult brains. J Neurosci. 30:3489–3498.
Jhaveri DJ, Mackay EW, Hamlin AS, Marathe SV, Nandam LS, Vaidya VA, Bartlett PF. 2010. Norepinephrine directly activates adult hippocampal precursors via beta3-adrenergic receptors. J Neurosci. 30:2795–2806.
Kilpatrick DL, Wang W, Gronostajski R, Litwack ED. 2010. Nuclear factor I and cerebellar granule neuron development: an intrinsic-extrinsic interplay. Cerebellum. 11:41–49.
Kim EJ, Ables JL, Dickel LK, Eisch AJ, Johnson JE. 2011. Ascl1 (Mash1) defines cells with long-term neurogenic potential in subgranular and subventricular zones in adult mouse brain. PloS ONE. 6:e18472.
Koizumi H, Higginbotham H, Poon T, Tanaka T, Brinkman BC, Gleeson JG. 2006. Doublecortin maintains bipolar shape and nuclear translocation during migration in the adult forebrain. Nat Neurosci. 9:779–786.
Kriegstein A, Alvarez-Buylla A. 2009. The glial nature of embryonic and adult neural stem cells. Annu Rev Neurosci. 32:149–184.
Martynoga B, Mateo JL, Zhou B, Andersen J, Achimastou A, Urban N, van den Berg D, Georgopoulou D, Hadjur S, Wittbrodt J, et al. 2013. Epigenomic enhancer annotation reveals a key role for NFIX in neural stem cell quiescence. Genes Dev. 27:1769–1786.
Mason S, Piper M, Gronostajski RM, Richards LJ. 2009. Nuclear factor one transcription factors in CNS development. Mol Neurobiol. 39:10–23.
Merkle FT, Tramontin AD, Garcia-Verdugo JM, Alvarez-Buylla A. 2004. Radial glia give rise to adult neural stem cells in the subventricular zone. Proc Natl Acad Sci USA. 101:17528–17532.
Messina G, Biressi S, Monteverde S, Magli A, Cassano M, Perani L, Roncaglia E, Tagliafico E, Starnes L, Campbell CE, et al. 2010. Nfix regulates fetal-specific transcription in developing skeletal muscle. Cell. 140:554–566.
Murase S, Horwitz AF. 2002. Deleted in colorectal carcinoma and differentially expressed integrins mediate the directional migration of neural precursors in the rostral migratory stream. J Neurosci. 22:3568–3579.
Namihira M, Kohyama J, Semi K, Sanosaka T, Deneen B, Taga T, Nakashima K. 2009. Committed neuronal precursors confer astrocytic potential on residual neural precursor cells. Dev Cell. 16:245–255.
Nguyen-Ba-Charvet KT, Picard-Riera N, Tessier-Lavigne M, Baron-Van Evercooren A, Sotelo C, Chedotal A. 2004. Multiple roles for slits in the control of cell migration in the rostral migratory stream. J Neurosci. 24:1497–1506.
Ono K, Tomasiewicz H, Magnuson T, Rutishauser U. 1994. N-CAM mutation inhibits tangential neuronal migration and is phenocopied by enzymatic removal of polysialic acid. Neuron. 13:595–609.
Paratcha G, Ibanez CF, Ledda F. 2006. GDNF is a chemoattractant factor for neuronal precursor cells in the rostral migratory stream. Mol Cell Neurosci. 31:505–514.
Peretto P, Merighi A, Fasolo A, Bonfanti L. 1997. Glial tubes in the rostral migratory stream of the adult rat. Brain Res Bull. 42:9–21.
Piper M, Barry G, Harvey TJ, McLeay R, Smith AG, Harris L, Mason S, Stringer BW, Day BW, Wray NR, et al. 2014. NFIB-mediated repression of the epigenetic factor Ezh2 regulates cortical development. J Neurosci. 34:2921–2930.
Piper M, Barry G, Hawkins J, Mason S, Lindwall C, Little E, Sarkar A, Smith AG, Moldrich RX, Boyle GM, et al. 2010. NFIA controls telencephalic progenitor cell differentiation through repression of the Notch effector Hes1. J Neurosci. 30:9127–9139.
Piper M, Harris L, Barry G, Heng YH, Plachez C, Gronostajski RM, Richards LJ. 2011. Nuclear factor one X regulates the development of multiple cellular populations in the postnatal cerebellum. J Comp Neurol. 519:3532–3548.

Piper M, Plachez C, Zalucki O, Fothergill T, Goudreau G, Erzurumlu R, Gu C, Richards LJ. 2009. Neuropilin 1-Sema signaling regulates crossing of cingulate pioneering axons during development of the corpus callosum. Cereb Cortex. 19 (Suppl 1):i11–i21.

Pjanic M, Pjanic P, Schmid C, Ambrosini G, Gaussin A, Plasari G, Mazza C, Bucher P, Mermod N. 2011. Nuclear factor I revealed as family of promoter binding transcription activators. BMC Genomics. 12:181.

Plachez C, Cato K, McLeay RC, Heng YH, Bailey TL, Gronostasjki RM, Richards LJ, Puche AC, Piper M. 2012. Expression of nuclear factor one A and -B in the olfactory bulb. J Comp Neurol. 520:3135–3149.

Roybon L, Deierborg T, Brundin P, Li JY. 2009. Involvement of Ngn2, Tbr and NeuroD proteins during postnatal olfactory bulb neurogenesis. Eur J Neurosci. 29:232–243.

Sakamoto M, Imayoshi I, Ohtsuka T, Yamaguchi M, Mori K, Kageyama R. 2011. Continuous neurogenesis in the adult forebrain is required for innate olfactory responses. Proc Natl Acad Sci USA. 108:8479–8484.

Sanai N, Nguyen T, Ihrie RA, Mirzadeh Z, Tsai HH, Wong M, Gupta N, Berger MS, Huang E, Garcia-Verdugo JM, et al. 2011. Corridors of migrating neurons in the human brain and their decline during infancy. Nature. 478:382–386.

Schmid CD, Bucher P. 2010. MER41 repeat sequences contain inducible STAT1 binding sites. PloS ONE. 5:e11425.

Scott CE, Wynn SL, Sesay A, Cruz C, Cheung M, Gomez Gaviro MV, Booth S, Gao B, Cheah KS, Lovell-Badge R, et al. 2010. SOX9 induces and maintains neural stem cells. Nat Neurosci. 13:1181–1189.

Shu T, Butz KG, Plachez C, Gronostajski RM, Richards LJ. 2003. Abnormal development of forebrain midline glia and commissural projections in Nfia knock-out mice. J Neurosci. 23:203–212.

Singh SK, Bhardwaj R, Wilczynska KM, Dumur CI, Kordula T. 2011. A complex of nuclear factor I-X3 and STAT3 regulates astrocyte and glioma migration through the secreted glycoprotein YKL-40. J Biol Chem. 286:39893–39903.

Singh SK, Wilczynska KM, Grzybowski A, Yester J, Osrah B, Bryan L, Wright S, Griswold-Prenner I, Kordula T. 2011. The unique transcriptional activation domain of nuclear factor-I-X3 is critical to specifically induce marker gene expression in astrocytes. J Biol Chem. 286:7315–7326.

Smith CM, Luskin MB. 1998. Cell cycle length of olfactory bulb neuronal progenitors in the rostral migratory stream. Dev Dynamics. 213:220–227.

Snapyan M, Lemasson M, Brill MS, Blais M, Massouh M, Ninkovic J, Gravel C, Berthod F, Gotz M, Barker PA, et al. 2009. Vasculature guides migrating neuronal precursors in the adult mammalian forebrain via brain-derived neurotrophic factor signaling. J Neurosci. 29:4172–4188.

Sonego M, Gajendra S, Parsons M, Ma Y, Hobbs C, Zentar MP, Williams G, Machesky LM, Doherty P, Lalli G. 2013. Fascin regulates the migration of subventricular zone-derived neuroblasts in the postnatal brain. J Neurosci. 33:12171–12185.

Song J, Zhong C, Bonaguidi MA, Sun GJ, Hsu D, Gu Y, Meletis K, Huang ZJ, Ge S, Enikolopov G, et al. 2012. Neuronal circuitry mechanism regulating adult quiescent neural stem-cell fate decision. Nature. 489:150–154.

Sun W, Kim H, Moon Y. 2010. Control of neuronal migration through rostral migration stream in mice. Anat Cell Biol. 43:269–279.

Tamamaki N, Yanagawa Y, Tomioka R, Miyazaki J, Obata K, Kaneko T. 2003. Green fluorescent protein expression and colocalization with calretinin, parvalbumin, and somatostatin in the GAD67-GFP knock-in mouse. J Comp Neurol. 467:60–79.

Walker TL, Yasuda T, Adams DJ, Bartlett PF. 2007. The doublecortin-expressing population in the developing and adult brain contains multipotential precursors in addition to neuronal-lineage cells. J Neurosci. 27:3734–3742.

Wang C, Liu F, Liu YY, Zhao CH, You Y, Wang L, Zhang J, Wei B, Ma T, Zhang Q, et al. 2011. Identification and characterization of neuroblasts in the subventricular zone and rostral migratory stream of the adult human brain. Cell Res. 21:1534–1550.

Wang W, Crandall JE, Litwack ED, Gronostajski RM, Kilpatrick DL. 2010. Targets of the nuclear factor I regulon involved in early and late development of postmitotic cerebellar granule neurons. J Neurosci Res. 88:258–265.

Wang W, Mullikin-Kilpatrick D, Crandall JE, Gronostajski RM, Litwack ED, Kilpatrick DL. 2007. Nuclear factor I coordinates multiple phases of cerebellar granule cell development via regulation of cell adhesion molecules. J Neurosci. 27:6115–6127.

Whitman MC, Greer CA. 2009. Adult neurogenesis and the olfactory system. Prog Neurobiol. 89:162–175.

Young KM, Fogarty M, Kessaris N, Richardson WD. 2007. Subventricular zone stem cells are heterogeneous with respect to their embryonic origins and neurogenic fates in the adult olfactory bulb. J Neurosci. 27:8286–8296.

CHAPTER 6

Discussion

Although NFI proteins have emerged in the last 10 years as critical regulators of central nervous system development, relatively little work had been done on the role of NFIX within the developing brain. Instead, most of our understanding of how NFI transcription factors regulate cortical development had been obtained by studying mice lacking either *Nfia* or *Nfib* (Shu T et al. 2003; Barry G et al. 2008; Plachez C et al. 2008; Heng YH et al. 2012). My thesis has provided a number of conceptual advances to the field, providing significant insights into the role of NFIX as a mediator of neural stem cell biology within the nascent hippocampus (Heng YH et al. 2014) and the SVZ (Heng YHE et al., 2014) of the postnatal lateral ventricles. Moreover, I contributed to a recent study revealing NFIX is also important for the normal formation of the cerebellum during the postnatal period in mice (Piper M et al. 2011), and a further study demonstrating that NFIX is important for hippocampal-specific learning and memory within adult mice (Harris L et al. 2013). Collectively, these findings highlight the central role played by NFIX in diverse regions of the nervous system, and further serve as a platform upon which future investigations into nervous system development can be launched using NFIX as a probe to study stem cell biology, as well as to further elucidate the transcriptional regulation of mature cell types within the brain, including neurons and glia.

6.0. NFIX regulates development of the hippocampus

The first significant finding of my research was to demonstrate that NFIX plays an important role in mediating neural stem cell differentiation during the development of the embryonic hippocampus, in part via mediating the transcriptional repression of the stem cell maintenance factor, *Sox9* (Heng YH et al. 2014). In the absence of *Nfix*, the differentiation of stem cells within the hippocampal primordium was delayed, culminating in a morphologically abnormal hippocampus in the early postnatal period. Moreover, there were significantly fewer neural stem cells localised to the postnatal dentate gyrus, indicative of NFIX being potentially important for neurogenesis within this neurogenic niche of the adult brain, a finding

supported by recent investigations into hippocampal-dependent learning and memory deficits in heterozygous *Nfix* mice (Harris L et al. 2013).

One question raised by my findings is how similar are the regulatory programs controlled by NFI family members during development? NFI proteins members display overlapping expression patterns within neural stem and progenitor cell populations in diverse regions of the brain during development (Chaudhry AZ et al. 1997). For example, within the postnatal cerebellum, NFIA, NFIB and NFIX are all expressed progenitor cells within the external granule cell layer (Wang W et al. 2007). Similarly, NFIA, NFIB and NFIX are also expressed by radial glia within the developing neocortex and hippocampus (Shu T et al. 2003; Steele-Perkins G et al. 2005; Plachez C et al. 2008). At a functional level, NFI family members also appear to play similar roles in the developing and postnatal brain. Within the developing cerebellum, NFIA, NFIB and NFIX play a similar role in regulating the differentiation and migration of progenitor cells within the external granule cell layer (Wang W et al. 2007; Wang W et al. 2010; Piper M et al. 2011). Furthermore, within the developing hippocampus, *Nfia*, *Nfib* and *Nfix* knockout mice all exhibit similar phenotypes, including an expansion of the progenitor cell population within the VZ, as well as delayed glial and neuronal differentiation (Piper M et al. 2010; Heng YH et al. 2014). These similar phenotypes suggest that NFIs regulate progenitor cell proliferation and differentiation within this structure in a mechanistically similar fashion (Heng YH et al. 2014). However, despite these similarities, NFI members appear able to play different roles within the nascent hippocampus. For example, unlike NFIA and NFIX, NFIB does not appear to regulate the development of glia arising from the fimbrioglial neuroepithelium within the hippocampus, as this glial population develops normally in *Nfib* knockout mice (Barry G et al. 2008).

These subtle differences between individual *Nfi* knockout strains suggest that each *Nfi* family member is not equivalent, and that, while they do regulate similar processes, they exhibit some distinct functions. Indeed, whether NFIs regulate similar sets of genes within the

developing the brain remains unclear. Published microarray studies performed on E16 hippocampi from either *Nfia, Nfib* or *Nfix* knockout mice indicate that, whereas some genes, such as *Gfap*, are misregulated in all knockout mice (Cebolla B and M Vallejo 2006; Barry G et al. 2008), there are many gene and pathways that are only misregulated in individual knockouts. For instance, *Nfib* mutant mice exhibit misregulation of many genes implicated in chromatin modification (Piper M et al. 2014), whereas these pathways are not over-represented in *Nfia* and *Nfix* mutant mice. How then could we identify exactly which genes are commonly regulated by individual NFI family members, and perhaps more interestingly, which genes are differentially regulated by the NFIs during development? Perhaps the most efficient way to determine this for a particular tissue would be to perform ChIP-sequencing using antibodies specific to each NFI family member. Although this technique has been used previously to study NFI function (Martynoga B et al. 2013), to date researchers have only performed this technique using pan-NFI antibodies that do not discriminate between individual family members. This has limited the ability to parse the functions of each NFI family member from the others. However, we are now currently collaborating with the group of Prof. Matthew Scott (Stanford, USA), whose group has been able to perform ChIP-sequencing on progenitor cells isolated from the external granule cell layer of the developing cerebellum with antibodies specific to NFIA, NFIB and NFIX. We are now analyzing these data to determine similarities and differences with regards to NFI function within the postnatal cerebellum. Validation of the interaction between NFI members and their target genes will be done using gel shift assays and luciferase assays as described within this thesis. These studies, which we also aim to perform in the developing cortex and adult neurogenic niches, will definitively reveal the overlapping and distinct roles played by individual NFI family members within the brain, as well as identifying further potential direct targets of NFI factors during development.

6.1. Normal development of the SVZ neurogenic niche requires NFIX

The second significant finding of my thesis was to demonstrate that NFIX plays pleiotropic roles during the development of the second neurogenic niche of the adult cortex, namely the SVZ. My work revealed that NFIX regulates the proliferation of neural progenitor cells within the postnatal SVZ, and that in its absence, proliferation of stem cells is dramatically increased. Additionally, NFIX was also shown to regulate the migration of SVZ-derived neuroblasts to the olfactory bulb in both cell-autonomous and non-cell-autonomous mechanisms. Finally, I revealed that *Gdnf*, a chemoattractant for SVZ-derived neuroblasts, is a target for transcriptional activation by NFIX within astrocytes located in the developing rostral migratory stream. Collectively, this work highlights that NFIX plays multiple roles during SVZ development and neuroblast migration.

One pertinent aspect of this work was to reveal that NFIX is expressed by multiple cells types within the developing and adult SVZ, RMS and olfactory bulb. As previously discussed (Discussion, Chapter 4), this brings into question how this protein can exert separate regulatory programs within varied cellular contexts. One possibility is the presence of different protein-protein interactions within each cellular environment, which potentially provides cell-type specificity to DNA binding events. Indeed, NFI proteins are modular, and contain a DNA-binding N-terminal domain, and a C-terminal protein-protein interaction domain. It is through different binding interactions with the latter that specificity to NFIX transcriptional regulation could be achieved in different cellular contexts. Although few studies have identified binding partners for NFIX factors, NFIX has previously been shown to interact with NFIB within gel shift analyses (Liu Y et al. 1997), and with STAT 3 in glioma cell lines *in vitro* (Singh SK et al. 2011), as well as to form a complex with SP-1, Rb and HDAC-1 to regulate context-specific gene expression in metastatic breast cancer cells (Singh J et al. 2002). These findings highlight that NFIX can co-operate with divergent proteins, and suggest that interactions with other binding partners may indeed provide specificity to NFIX transcriptional control. A second way in which this may occur is simply through availability

of DNA binding sites, which may be modulated via global chromatin accessibility. This mechanism, which may work in tandem with the previous idea, would similarly enable NFIX to mediate different targets by the simple expedient of enabling access to distinct DNA domains controlled by epigenetic DNA modification. In future, proteomic and epigenetic analyses of the olfactory system will enable a clearer understanding of the role of NFIX within this system, and the mechanisms underlying how cellular-specific programs of NFIX-mediated gene expression are mediated.

Another point of interest arising from my findings was the demonstration of NFIX expression by neural stem cells within the SVZ of the adult cortex. This finding is suggestive of an ongoing role for NFIX in mediating the biology of these cells within the mature brain. However, whether or not NFIX plays a functionally similar role in the adult brain as compared to the developing brain (promoting stem cell differentiation) is at this stage unclear. One point germane to this consideration is that stem cells in the adult brain are different to embryonic stem cells. Whereas those stem cells within the developing brain are continuously proceeding through the cell cycle to either self-renew or differentiate, the vast majority of neural stem cells within the adult brain exist in a quiescent state outside the cell cycle (G_0). This state is thought to minimise the metabolic stresses of division that these cells would otherwise encounter over the course of a lifetime. Could NFIX potentially be involved in the regulation of adult neural stem cell quiescence?

Preliminary findings suggest that this may indeed be the case. In a recent collaborative study, our laboratory found that NFIX is expressed by quiescent adult neural stem cells within the hippocampus and that NFIX plays an important role in regulating neural stem cell quiescence *in vitro* (Martynoga B et al. 2013). These findings suggest that NFIX may indeed be playing a functionally different role in embryonic versus adult neural stem cells. However, the majority of this study was performed using cultured neural stem cells derived from embryonic stem cells, making direct comparisons to adult neural stem cells *in vivo* difficult to make with any

great confidence. The future direction of this work is to study the role of NFIX *in vivo* within the adult neurogenic niches, to ascertain if indeed it is involved in the regulation of adult neural stem cell quiescence. Moreover, using techniques such as ChIP-sequencing, the targets of NFIX in adult neural stem cells could be assayed and investigated in further detail. Such studies will greatly increase our understanding of the molecular programs regulating neural stem cell quiescence, providing springboard to analyse how stem cell quiescence can be modulated, perhaps in time to provide stem cell activation to ameliorate neurodegenerative disorders such as Parkinson's disease. Moreover, similar analyses could be performed in other regions of the adult body to determine if NFIs also mediate quiescence in other contexts. With this in mind, NFIX was recently shown to also play an important role in regulating hematopoietic progenitor and stem cell survival (Holmfeldt P et al. 2013), and to regulate stem cell quiescence within the stem cell niches of hair follicles in mammals (Chang CY et al. 2013). This suggests that NFIs do indeed play an important role in regulating progenitor cell quiescence within multiple organs in the body. This appears to be a fruitful area for further research especially given the importance of stem cell misregulation in diseases such as cancer.

6.2. Future Directions

Our laboratory, and those of others, has revealed that NFIs play important roles in the development of many regions of the body, both within the CNS, and without. However, one limitation of many of these studies has been that they have been performed with total gene knockouts, which has meant that the interpretation of any phenotypes has needed to be very careful to reflect the fact that phenotypic abnormalities may have had their root indirectly through deficits in other developmental domains. Moreover, apart from *Nfic*$^{-/-}$ mice, *Nfi* knockout mice die at birth or at weaning, precluding the investigation of their roles within the adult brain using these models (das Neves L et al. 1999; Steele-Perkins G et al. 2005; Campbell CE et al. 2008). Looking forwards, unravelling the role of *Nfi* genes in the adult brain will require the use of conditional knockout lines couples with cre lines that can confer

temporal and spatial control of gene ablation. Fortunately, conditional lines are now becoming available, with both *Nfib* (Hsu YC et al. 2011) and *Nfix* (Messina G et al. 2010) conditional alleles having been described recently. The Piper laboratory now has a breeding colony of the *Nfix* conditional line, and is crossing this to lines expressing cre recombinase under the control of different stem cell specific promoters (nestin Cre ER^{T2} and GLAST Cre ER^{T2}) as well as neuroblast-specific promoters (DCX Cre ER^{T2}). Conditional ablation of *Nfix* from adult neural stem cells will enable the role of this transcription factor in cellular quiescence to be investigated in isolation from any potential developmental deficits arising during embryogenesis. Similarly, removal of *Nfix* from within migratory neuroblasts will enable the cell-autonomous role of *Nfix* in mediating neuroblast migration to be assessed. We will also be able to couple these studies to behavioural analyses of conditional knockout mice, using techniques that test adult neural stem cell function within the hippocampus (e.g. Morris water maze) and the SVZ/olfactory bulb (odour discrimination tests). Moreover, we now have access to conditional alleles for *Nfia* and *Nfib*, which will further enable us to dissect the roles of these genes in the adult brain, and to enable us to compare and contrast the roles of these factors within the adult brain. Collectively, these studies are crucial if we are to appreciate the ongoing role of NFI proteins within the adult.

6.3. Are these studies relevant for human biology?

Although this thesis focused entirely on mice as model system to study CNS development, they also provide insights into human congential disorders that arise from mutation or deletion of NFI genes. For instance, *NFIX* deletions or nonsense mutations have been identified as one of the causative factors for multiple cases of Sotos-like overgrowth and Marshall-Smith syndrome, which are conditions in humans. They are characterized by advanced bone age, overgrowth, musculoskeletal abnormalities and abnormal behaviour, as well as learning difficulties (Malan V et al. 2010; Priolo M et al. 2012; Yoneda Y et al. 2012). Magnetic resonance imaging analyses revealed that these patients display hypoplasia of the corpus callosum and ventricular dilation (Malan V et al. 2010; Priolo M et al. 2012; Yoneda

Y et al. 2012), similar to what is observed in *Nfix* mutant mice (Campbell CE et al. 2008). Furthermore, *NFIA* haploinsufficiency, due to chromosomal translocation or deletion, has also been identified as one of the factors that result in human syndrome that involves both CNS and urinary tract defects (Lu W et al. 2007). Patients with this condition display CNS malformations consisting of a thin, hypoplastic, or absent corpus callosum, and hydrocephalus or ventriculomegaly, phenotypes that are also recapitulated within *Nfia* mutant mice. Furthermore, majority of patients with *NFIA* mutations also exhibit chiari type 1 malformation, tethered spinal cord and urinary tract defects (Lu W et al. 2007). Collectively, these data highlight the important roles played by the *Nfi* transcription factor family in the development of multiple systems within the human body. As such understanding the role played by NFIs within animal models such as rodents will likely provide important insights into the underlying basis of the neurological disorders in humans, and will hopefully contribute toward development of therapies for these disorders.

Appendices

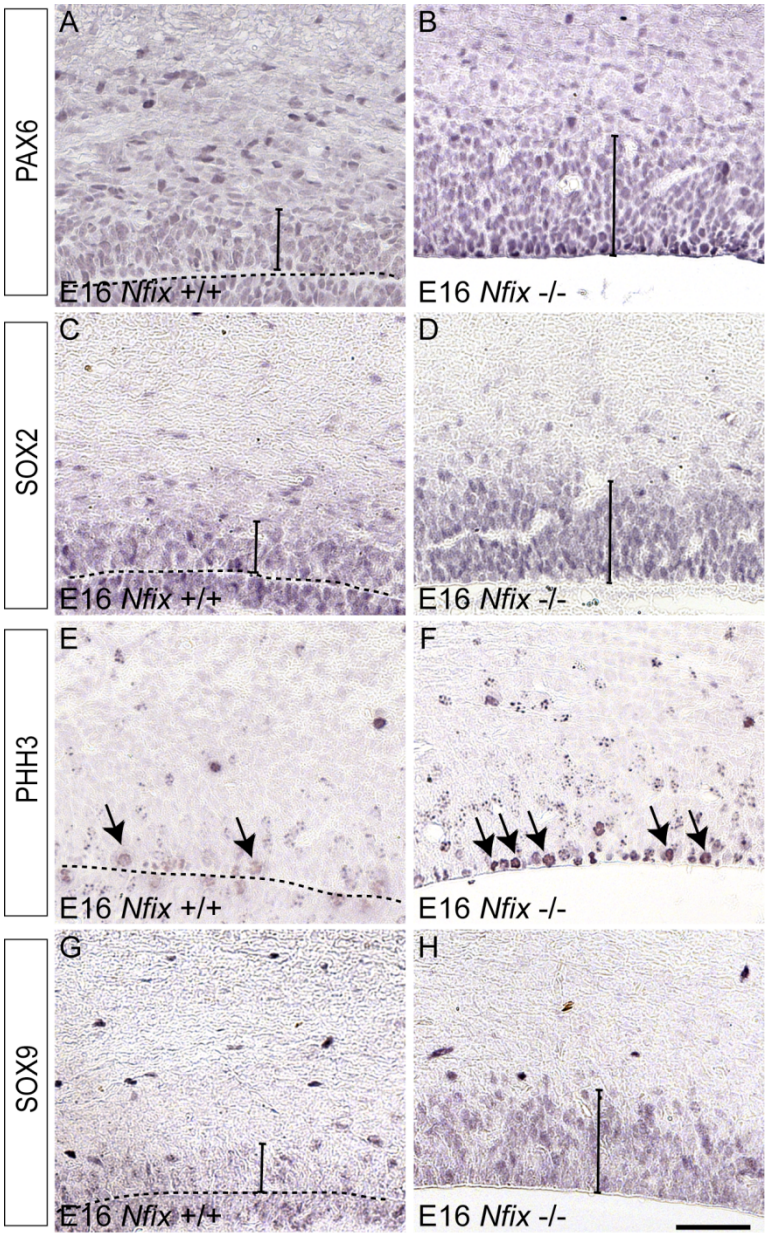

Appendix 1. Delayed differentiation of ventricular zone progenitor cells in the neocortex of *Nfix*$^{-/-}$ mice.

A-H Coronal paraffin sections of the neocortex of E16 wild type and *Nfix*$^{-/-}$ mice. The brackets delineate the ventricular zone. The dotted lines represent the ventricular space separating the hippocampal and neocortical ventricular zones. Immunostaining of the progenitor cell markers PAX6 (***A, B***) and SOX2 (***C, D***), the mitotic marker phosphohistone H3 (PHH3, ***E, F***) and SOX9 (***G, H***) is shown. The width of the neocortical ventricular zone was greater in the mutants compared to controls, as evidenced by the larger number of ventricular zone progenitor cells in the mutant labeled with either PAX6, SOX2 or SOX9 (***B, D, H***). Moreover, there were more mitotically active cells (arrows in ***E*** and ***F***) in the ventricular zone of the *Nfix*$^{-/-}$ mice neocortex. Scale bar (in ***H***): 250 μm.

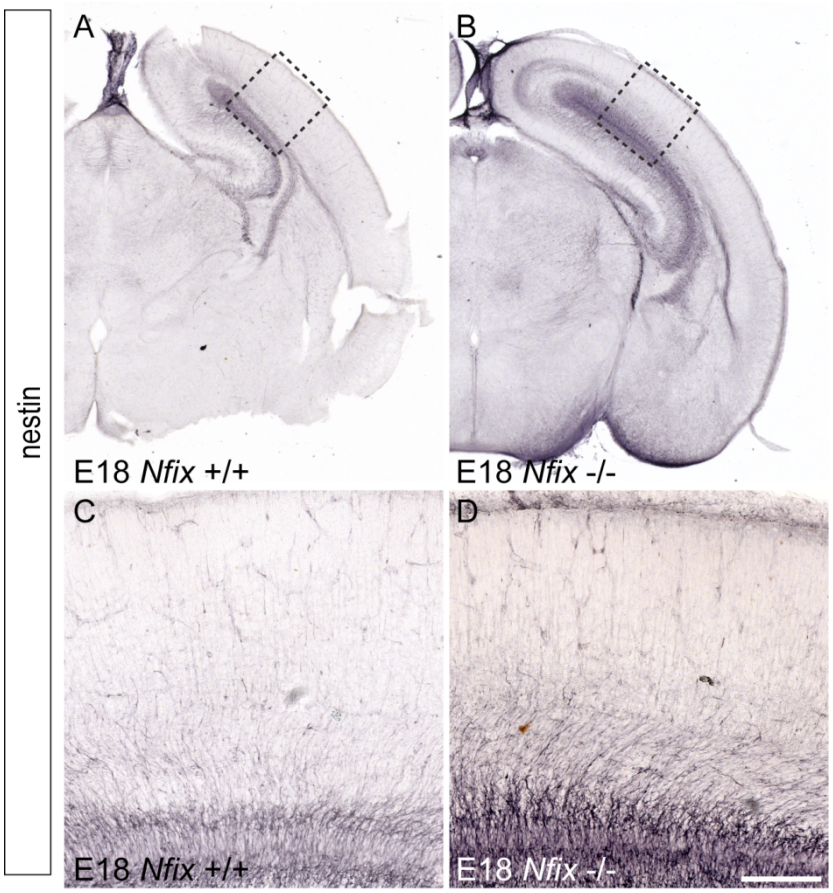

Appendix 2. Increased expression of nestin in the neocortex of E18 *Nfix*$^{-/-}$ mice.

A-D Coronal sections of E18 wild type and *Nfix*$^{-/-}$ brains immunostained with antibodies against the radial progenitor marker nestin. Nestin immunoreactivity within the neocortex was higher in the mutant in comparison to the wild-type control. Panels ***C*** and ***D*** are higher magnification views of the boxed regions in ***A*** and ***B*** respectively. Scale bar (in ***D***): ***A, B,*** 600 μm; ***C, D*** 200 μm.

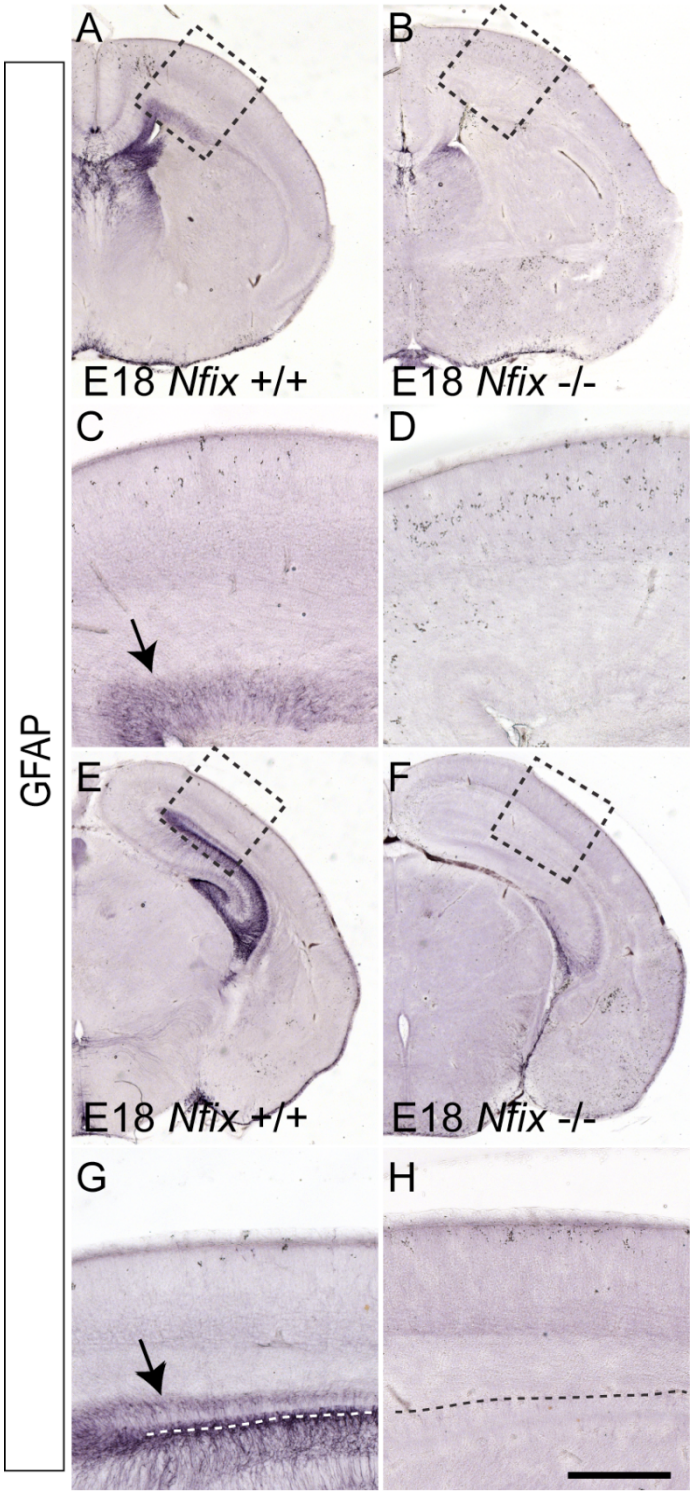

Appendix 3. Decreased expression of GFAP in the neocortex of E18 *Nfix*$^{-/-}$ mice.

A-H Coronal sections of E18 wild type (***A, C, E, G***) and *Nfix*$^{-/-}$ (***B, D, F, H***) mice at the level of the corpus callosum (***A-D***) and the hippocampus (***E-H***). Neocortical expression of GFAP was evident in the wild type (arrows in ***C*** and ***G***), but not in the mutant. Panels ***C***, ***D, G*** and ***H*** are higher magnification views of the boxed regions in ***A, B***, ***E*** and ***F*** respectively. Scale bar (in ***D***): ***A, B,*** 600 μm; ***C, D*** 250 μm.

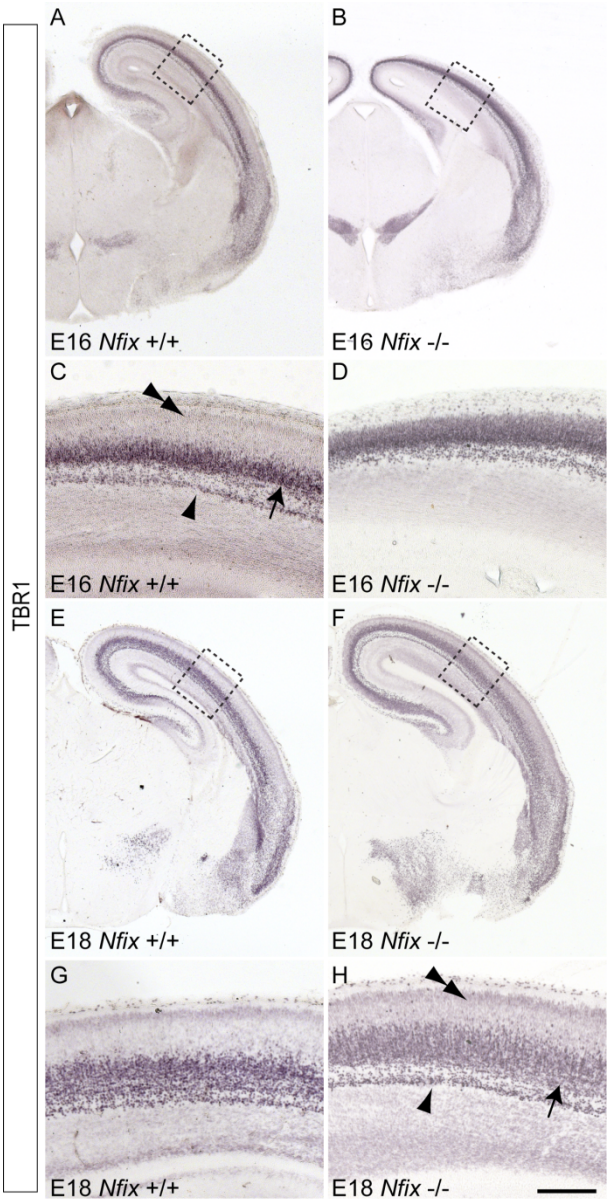

Appendix 4. Neuronal development is delayed in the neocortex of *Nfix*$^{-/-}$ mice.

Expression of the neuronal marker TBR1 in coronal sections of wild type (***A, C, E, G***) and *Nfix*$^{-/-}$ (***B, D, F, H***) mice. At E16, expression of TBR1 in wild type mice was evident within the cells of the subplate (arrowhead in ***C***) and layer VI of the cortical plate (arrow in ***C***). Neurons within the upper layers of the cortical plate did not exhibit TBR1 immunoreactivity (double arrowhead in ***C***). A similar pattern of expression in the wild type was evident at E18 (***E, G***). In the mutant at E16, however, expression of TBR1 within the neocortex appeared delayed (***B, D***). By E18, expression of TBR1 within the neocortex of *Nfix*$^{-/-}$ mice was evident within the cells of the subplate (arrowhead in ***H***) and layer VI of the cortical plate (arrow in ***H***), but not within the superficial cortical plate (double arrowhead in ***H***), in a pattern similar to that observed in the E16 wild type neocortex (compare panels ***C*** and ***H***). Scale bar (in ***H***): ***A, B, E, F*** 600 μm; ***C, D, G, H*** 250 μm.

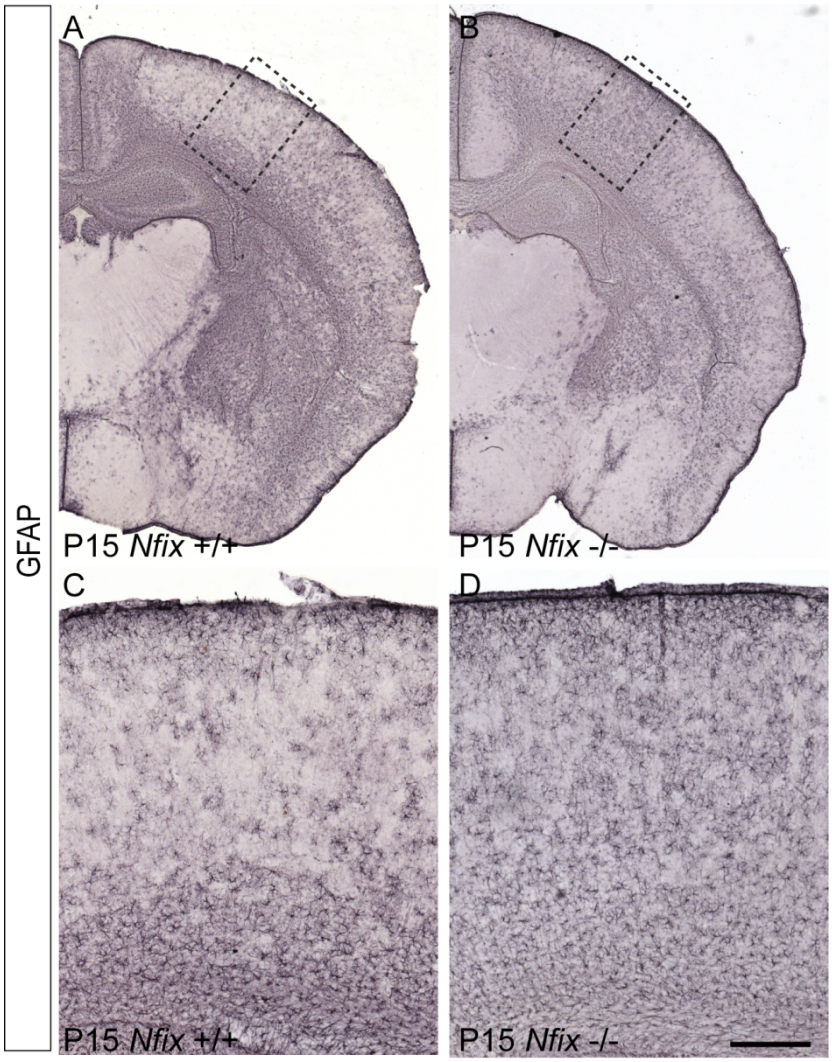

Appendix 5. Expression of GFAP in the neocortex of postnatal *Nfix* wild type and *Nfix*$^{-/-}$ mice.

Expression of the astrocytic marker, GFAP, in the neocortex of P15 wild type (***A, C***) and *Nfix*$^{-/-}$ (***B, D***) mice. By this age, the expression of GFAP in the mutant neocortex was no longer reduced in comparison to that seen within wild type littermate controls. Panels ***C*** and ***D*** are higher magnification views of the boxed regions in ***A*** and ***B*** respectively. Scale bar (in ***D***): ***A, B*** 1 mm; ***C, D*** 150 μm.

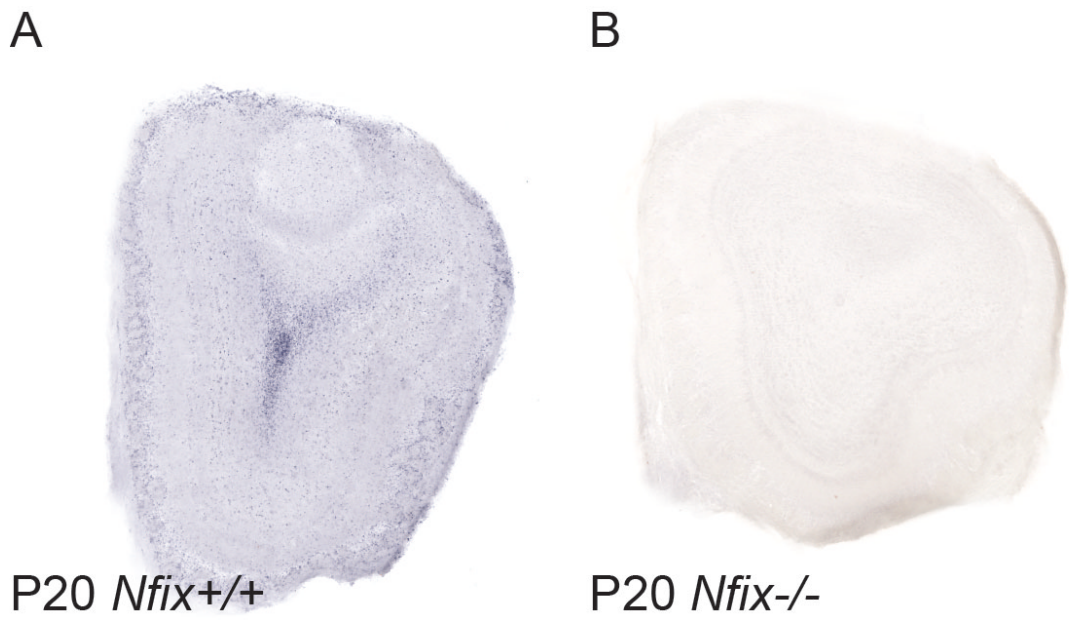

Appendix 6. Anti-NFIX antibody specificity

(A-B) Immunohistochemical staining of P20 coronal sections of the olfactory bulb from wild type (*Nfix*$^{+/+}$) (***A***) and *Nfix*$^{-/-}$ (***B***) mice. Whereas NFIX expression was clearly apparent in the wild-type olfactory bulb, there was no specific staining in the *Nfix*$^{-/-}$ mice, indicating that the anti-NFIX antibody specifically recognises the NFIX protein *in vivo*.

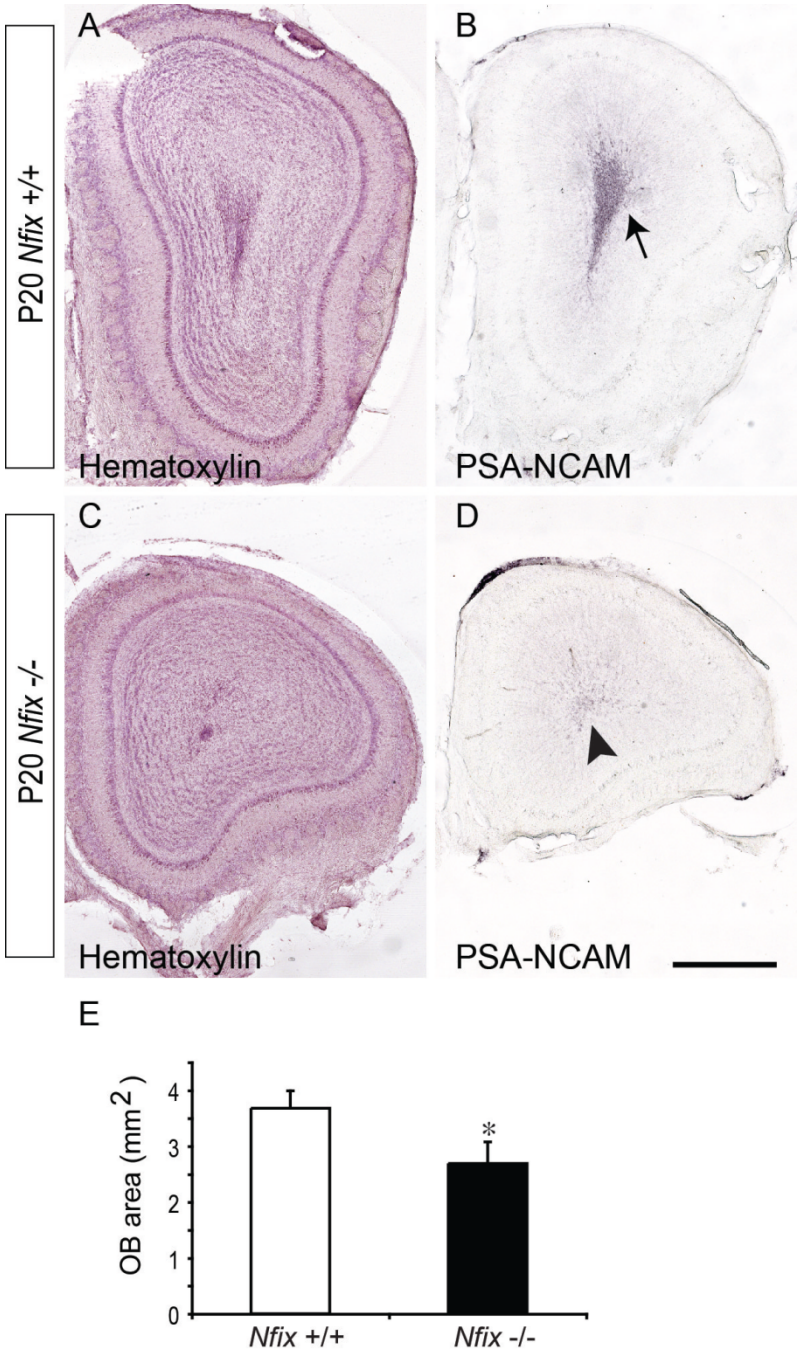

Appendix 7. Reduction in the size of olfactory bulbs in mice lacking *Nfix*.

Coronal sections of P20 wild type (***A, B***) and *Nfix*$^{-/-}$ (***C, D***) mice at the level of the olfactory bulb. Hematoxylin staining performed on olfactory bulbs from wild type (***A***) and *Nfix*$^{-/-}$ (***C***) mice revealed that the cross-sectional area of the olfactory bulb was significantly reduced in the absence of this transcription factor (***E***). Immunohistochemistry against PSA-NCAM demonstrated that, whereas there were many PSA-NCAM-expressing neuroblasts within the ependymal layer of the wild-type (arrow in ***B***), there were far fewer PSA-NCAM-expressing cells in the mutant (arrowhead in ***C***). * $p < 0.05$, *t*-test.Scale bar (in ***D***): 100 µm.

A Ingenuity analysis: Functional annotation of genes upregulated in *Nfix*$^{-/-}$ SVZ tissue

Category	No. of molecules	*p*-value
Neurological Disease	100	7.73E-07
Cell Death	75	2.48E-06
Developmental Disorder	34	1.39E-05
Cellular Development	64	3.34E-05
Cell-To-Cell Signaling and Interaction	28	3.70E-05
Nervous System Development and Function	40	3.70E-05
Cellular Growth and Proliferation	90	4.08E-05
Cancer	86	4.61E-05
Cellular Movement	43	6.28E-05
Amino Acid Metabolism	14	6.78E-05
Protein Synthesis	3	6.78E-05
Small Molecule Biochemistry	42	6.78E-05
Cell Morphology	28	9.55E-05
Cellular Function and Maintenance	28	9.55E-05
Cardiovascular System Development and Function	6	9.73E-05

B Ingenuity analysis: Functional annotation of gen downregulated in *Nfix*$^{-/-}$ SVZ tissue

Category	No. of molecules	*p*-
Genetic Disorder	188	1.3
Neurological Disease	125	1.3
Skeletal and Muscular Disorders	106	1.3
Behavior	29	2.2
Organismal Functions	16	5.3
Cell Death	89	7.2
Gastrointestinal Disease	73	2.1
Inflammatory Disease	92	2.1
Cancer	98	2.4
Reproductive System Disease	41	2.4
Cell Cycle	42	4.5
Nervous System Development and Function	46	5.9

C Ingenuity analysis: Pathways upregulated in *Nfix*$^{-/-}$ SVZ tissue

Ingenuity Canonical Pathways	No. of molecules	*p*-value
Type I Diabetes Mellitus Signaling	7	**1.41E-03**
Virus Entry via Endocytic Pathways	6	**2.51E-03**
IGF-1 Signaling	6	**2.82E-03**
Breast Cancer Regulation by Stathmin1	9	**2.95E-03**
Neuroprotective Role of THOP1 in Alzheimer's Disease	4	**3.16E-03**
Caveolar-mediated Endocytosis Signaling	5	**5.37E-03**
Dopamine Receptor Signaling	5	**5.37E-03**
VDR/RXR Activation	5	**6.76E-03**
CCR3 Signaling in Eosinophils	6	**8.32E-03**
Prostate Cancer Signaling	5	**9.12E-03**
PI3K/AKT Signaling	6	**0.01**
OX40 Signaling Pathway	5	**0.01**
TR/RXR Activation	5	**0.01**
IL-1 Signaling	5	**0.01**
Cellular Effects of Sildenafil (Viagra)	6	**0.02**
Insulin Receptor Signaling	6	**0.02**
AMPK Signaling	6	**0.02**
JAK/Stat Signaling	4	**0.02**
Relaxin Signaling	6	**0.02**
Taurine and Hypotaurine Metabolism	2	**0.02**
Antigen Presentation Pathway	3	**0.02**
Antiproliferative Role of Somatostatin Receptor 2	4	**0.03**
Role of Tissue Factor in Cancer	5	**0.03**
Integrin Signaling	7	**0.03**
Melanoma Signaling	3	**0.03**
Cyclins and Cell Cycle Regulation	4	**0.03**
Graft-versus-Host Disease Signaling	3	**0.03**
Type II Diabetes Mellitus Signaling	5	**0.03**
Autoimmune Thyroid Disease Signaling	3	**0.03**
Hereditary Breast Cancer Signaling	5	**0.04**
Cytotoxic T Lymphocyte-mediated Apoptosis of Target Cells	4	**0.04**
Lipid Antigen Presentation by CD1	2	**0.04**
Cdc42 Signaling	6	**0.04**
Allograft Rejection Signaling	4	**0.04**
Pentose and Glucuronate Interconversions	3	**0.04**
Sulfur Metabolism	2	**0.04**
CNTF Signaling	3	**0.04**
ATM Signaling	3	**0.04**
Î±-Adrenergic Signaling	4	**0.05**
Calcium Signaling	6	**0.05**
Androgen and Estrogen Metabolism	4	**0.05**
IL-8 Signaling	6	**0.05**
G Beta Gamma Signaling	4	**0.05**
Crosstalk between Dendritic Cells and Natural Killer Cells	4	**0.05**
Role of NFAT in Regulation of the Immune Response	6	**0.05**
CREB Signaling in Neurons	6	**0.05**
Role of BRCA1 in DNA Damage Response	3	**0.05**
Cell Cycle: G1/S Checkpoint Regulation	3	**0.05**

D Ingenuity analysis: Pathways downregulated in *Nfix*$^{-/-}$ SVZ tissue

Ingenuity Canonical Pathways	No. of molecules	*p*-va
Cyclins and Cell Cycle Regulation	6	**3.3**
Mitotic Roles of Polo-Like Kinase	5	**4.9**
Cardiac Î²-adrenergic Signaling	7	**9.7**
Relaxin Signaling	7	0
CREB Signaling in Neurons	8	0
Synaptic Long Term Depression	7	0
Cell Cycle: G1/S Checkpoint Regulation	4	0
Axonal Guidance Signaling	13	0
G Protein Signaling Mediated by Tubby	3	0
Î±-Adrenergic Signaling	5	0
VEGF Signaling	5	0
Breast Cancer Regulation by Stathmin1	8	0
G Beta Gamma Signaling	5	0
Phenylalanine Metabolism	3	0
Glycerophospholipid Metabolism	6	0
CCR5 Signaling in Macrophages	4	0
IL-8 Signaling	7	0
Antiproliferative Role of Somatostatin Receptor 2	4	0
Dopamine Receptor Signaling	4	0
fMLP Signaling in Neutrophils	5	0
Role of NFAT in Cardiac Hypertrophy	7	0
VDR/RXR Activation	4	0

Appendix 8. Microarray and functional classification reveals diverse genes misregulated within the SVZ/RMS of P20 *Nfix*$^{-/-}$ mice.

Microarray analysis was performed on tissue isolated from the SVZ/RMS of P20 wild type and *Nfix*$^{-/-}$ mice. Genes were annotated using Ingenuity Pathway Analysis, revealing key biological categories that were upregulated (***A***) and downregulated (***B***) in the within the SVZ/RMS of *Nfix*$^{-/-}$ mice. Biological pathways involving mRNAs that were upregulated (***C***) or downregulated (***D***) in the SVZ/RMS of *Nfix*$^{-/-}$ mice were also generated within Ingenuity Pathway Analysis.

References

Abrous DN, Koehl M, Le Moal M. 2005. Adult neurogenesis: from precursors to network and physiology. Physiol Rev 85(2): 523-69

Altman J. 1969. Autoradiographic and histological studies of postnatal neurogenesis. IV. Cell proliferation and migration in the anterior forebrain, with special reference to persisting neurogenesis in the olfactory bulb. J Comp Neurol 137:433-457.

Altman J, Bayer SA. 1990. Migration and distribution of two populations of hippocampal granule cell precursors during the perinatal and postnatal periods. J Comp Neurol 301:365-381.

Alvarez-Buylla A, Lim DA. 2004. For the long run: maintaining germinal niches in the adult brain. Neuron 41:683-686.

Andreu-Agullo C, Maurin T, Thompson CB, Lai EC. 2012. Ars2 maintains neural stem-cell identity through direct transcriptional activation of Sox2. Nature 481:195-198.

Angevine JB, Jr. 1965. Time of neuron origin in the hippocampal region. An autoradiographic study in the mouse. Exp Neurol Suppl:Suppl 2:1-70.

Apt D, Liu Y, Bernard HU. 1994. Cloning and functional analysis of spliced isoforms of human nuclear factor I-X: interference with transcriptional activation by NFI/CTF in a cell-type specific manner. Nucleic Acids Res 22:3825-3833.

Bailey TL, Boden M, Buske FA, Frith M, Grant CE, Clementi L, Ren J, Li WW, Noble WS. 2009. MEME SUITE: tools for motif discovery and searching. Nucleic Acids Res 37:W202-208.

Barry G, Piper M, Lindwall C, Moldrich R, Mason S, Little E, Sarkar A, Tole S, Gronostajski RM, Richards LJ. 2008. Specific glial populations regulate hippocampal morphogenesis. J Neurosci 28:12328-12340.

Baumeister H, Gronostajski RM, Lyons GE, Margolis FL. 1999. Identification of NFI-binding sites and cloning of NFI-cDNAs suggest a regulatory role for NFI transcription factors in olfactory neuron gene expression. Brain Res Mol Brain Res 72:65-79.

Bayer SA. 1983. 3H-thymidine-radiographic studies of neurogenesis in the rat olfactory bulb. Exp Brain Res 50:329-340.

Brun M, Coles JE, Monckton EA, Glubrecht DD, Bisgrove D, Godbout R. 2009. Nuclear factor I regulates brain fatty acid-binding protein and glial fibrillary acidic protein gene expression in malignant glioma cell lines. J Mol Biol 391:282-300.

Campbell CE, Piper M, Plachez C, Yeh YT, Baizer JS, Osinski JM, Litwack ED, Richards LJ, Gronostajski RM. 2008. The transcription factor Nfix is essential for normal brain development. BMC Dev Biol 8:52.

Cashman NR, Durham HD, Blusztajn JK, Oda K, Tabira T, Shaw IT, Dahrouge S, Antel JP. 1992. Neuroblastoma x spinal cord (NSC) hybrid cell lines resemble developing motor neurons. Dev Dyn 194:209-221.

Cebolla B, Vallejo M. 2006. Nuclear factor-I regulates glial fibrillary acidic protein gene expression in astrocytes differentiated from cortical precursor cells. J Neurochem 97:1057-1070.

Chang CY, Pasolli HA, Giannopoulou EG, Guasch G, Gronostajski RM, Elemento O, Fuchs E. 2013. NFIB is a governor of epithelial-melanocyte stem cell behaviour in a shared niche. Nature 495:98-102.

Chaudhry AZ, Lyons GE, Gronostajski RM. 1997. Expression patterns of the four nuclear factor I genes during mouse embryogenesis indicate a potential role in development. Dev Dyn 208:313-325.

Chaudhry AZ, Vitullo AD, Gronostajski RM. 1998. Nuclear factor I (NFI) isoforms differentially activate simple versus complex NFI-responsive promoters. J Biol Chem 273:18538-18546.

Cheng LC, Pastrana E, Tavazoie M, Doetsch F. 2009. miR-124 regulates adult neurogenesis in the subventricular zone stem cell niche. Nat Neurosci 12:399-408.

Chenn A, McConnell SK. 1995. Cleavage orientation and the asymmetric inheritance of Notch1 immunoreactivity in mammalian neurogenesis. Cell 82:631-641.

das Neves L, Duchala CS, Tolentino-Silva F, Haxhiu MA, Colmenares C, Macklin WB, Campbell CE, Butz KG, Gronostajski RM. 1999. Disruption of the murine nuclear factor I-A gene (Nfia) results in perinatal lethality, hydrocephalus, and agenesis of the corpus callosum. Proc Natl Acad Sci U S A 96:11946-11951.

Deneen B, Ho R, Lukaszewicz A, Hochstim CJ, Gronostajski RM, Anderson DJ. 2006. The transcription factor NFIA controls the onset of gliogenesis in the developing spinal cord. Neuron 52:953-968.

Ding B, Wang W, Selvakumar T, Xi HS, Zhu H, Chow CW, Horton JD, Gronostajski RM, Kilpatrick DL. 2013. Temporal regulation of nuclear factor one occupancy by calcineurin/NFAT governs a voltage-sensitive developmental switch in late maturing neurons. J Neurosci 33:2860-2872.

Driller K, Pagenstecher A, Uhl M, Omran H, Berlis A, Grunder A, Sippel AE. 2007. Nuclear factor I X deficiency causes brain malformation and severe skeletal defects. Mol Cell Biol 27:3855-3867.

Duan X, Kang E, Liu CY, Ming GL, Song H. 2008. Development of neural stem cell in the adult brain. Curr Opin Neurobiol 18:108-115.

Elder GA, Liang Z, Snyder SE, Lazzarini RA. 1992. Multiple nuclear factors interact with the promoter of the human neurofilament M gene. Brain Res Mol Brain Res 15:99-107.

Eriksson PS, Perfilieva E, Bjork-Eriksson T, Alborn AM, Nordborg C, Peterson DA, Gage FH. 1998. Neurogenesis in the adult human hippocampus. Nature medicine 4:1313-1317.

Ferri AL, Cavallaro M, Braida D, Di Cristofano A, Canta A, Vezzani A, Ottolenghi S, Pandolfi PP, Sala M, DeBiasi S, Nicolis SK. 2004. Sox2 deficiency causes neurodegeneration and impaired neurogenesis in the adult mouse brain. Development 131:3805-3819.

Fletcher CF, Jenkins NA, Copeland NG, Chaudhry AZ, Gronostajski RM. 1999. Exon structure of the nuclear factor I DNA-binding domain from C. elegans to mammals. Mamm Genome 10:390-396.

Frinchi M, Bonomo A, Trovato-Salinaro A, Condorelli DF, Fuxe K, Spampinato MG, Mudo G. 2008. Fibroblast growth factor-2 and its receptor expression in proliferating precursor cells of the subventricular zone in the adult rat brain. Neurosci Lett 447:20-25.

Fujita PA, Rhead B, Zweig AS, Hinrichs AS, Karolchik D, Cline MS, Goldman M, Barber GP, Clawson H, Coelho A, Diekhans M, Dreszer TR, Giardine BM, Harte RA, Hillman-Jackson J, Hsu F, Kirkup V, Kuhn RM, Learned K, Li CH, Meyer LR, Pohl A, Raney BJ, Rosenbloom KR, Smith KE, Haussler D, Kent WJ. 2011. The UCSC Genome Browser database: update 2011. Nucleic Acids Res 39:D876-882.

Furukawa T, Mukherjee S, Bao ZZ, Morrow EM, Cepko CL. 2000. rax, Hes1, and notch1 promote the formation of Muller glia by postnatal retinal progenitor cells. Neuron 26:383-394.

Gangemi RM, Daga A, Muzio L, Marubbi D, Cocozza S, Perera M, Verardo S, Bordo D, Griffero F, Capra MC, Mallamaci A, Corte G. 2006. Effects of Emx2 inactivation on the gene expression profile of neural precursors. Eur J Neurosci 23:325-334.

Gleeson JG, Lin PT, Flanagan LA, Walsh CA. 1999. Doublecortin is a microtubule-associated protein and is expressed widely by migrating neurons. Neuron 23:257-271.

Gong S, Yang XW, Li C, Heintz N. 2002. Highly efficient modification of bacterial artificial chromosomes (BACs) using novel shuttle vectors containing the R6Kgamma origin of replication. Genome Res 12:1992-1998.

Gotz M, Huttner WB. 2005. The cell biology of neurogenesis. Nature reviews Molecular cell biology 6:777-788.

Graham V, Khudyakov J, Ellis P, Pevny L. 2003. SOX2 functions to maintain neural progenitor identity. Neuron 39:749-765.

Grant CE, Bailey TL, Noble WS. 2011. FIMO: scanning for occurrences of a given motif. Bioinformatics 27:1017-1018.

Grant SG, O'Dell TJ, Karl KA, Stein PL, Soriano P, Kandel ER. 1992. Impaired long-term potentiation, spatial learning, and hippocampal development in fyn mutant mice. Science (New York, NY) 258:1903-1910.

Gronostajski RM. 1986. Analysis of nuclear factor I binding to DNA using degenerate oligonucleotides. Nucleic Acids Res 14:9117-9132.

Gronostajski RM. 2000. Roles of the NFI/CTF gene family in transcription and development. Gene 249:31-45.

Gronostajski RM, Adhya S, Nagata K, Guggenheimer RA, Hurwitz J. 1985. Site-specific DNA binding of nuclear factor I: analyses of cellular binding sites. Mol Cell Biol 5:964-971.

Grove EA, Tole S. 1999. Patterning events and specification signals in the developing hippocampus. Cereb Cortex 9:551-561.

Grunder A, Ebel TT, Mallo M, Schwarzkopf G, Shimizu T, Sippel AE, Schrewe H. 2002. Nuclear factor I-B (Nfib) deficient mice have severe lung hypoplasia. Mechanisms of development 112:69-77.

Guo H, Liu H, Mitchelson K, Rao H, Luo M, Xie L, Sun Y, Zhang L, Lu Y, Liu R, Ren A, Liu S, Zhou S, Zhu J, Zhou Y, Huang A, Wei L, Guo Y, Cheng J. 2011. MicroRNAs-372/373 promote the expression of hepatitis B virus through the targeting of nuclear factor I/B. Hepatology 54:808-819.

Harris L, Dixon C, Cato K, Heng YH, Kurniawan ND, Ullmann JF, Janke AL, Gronostajski RM, Richards LJ, Burne TH, Piper M. 2013. Heterozygosity for nuclear factor one x affects hippocampal-dependent behaviour in mice. PLoS One 8:e65478.

Heng YH, Barry G, Richards LJ, Piper M. 2012. Nuclear factor I genes regulate neuronal migration. Neurosignals 20:159-167.

Heng YH, McLeay RC, Harvey TJ, Smith AG, Barry G, Cato K, Plachez C, Little E, Mason S, Dixon C, Gronostajski RM, Bailey TL, Richards LJ, Piper M. 2014. NFIX regulates neural progenitor cell differentiation during hippocampal morphogenesis. Cereb Cortex 24:261-279.

Heng YHE, Zhou B, Harris L, Harvey T, Smith A, Horn E, Martynoga B, Andersen J, Achimastou A, Cato K, Richards LJ, Gronostajski RM, Yeo GS, Guillemot F, Bailey TL, Piper M. 2014. NFIX regulates proliferation and migration within the murine SVZ neurogenic niche. Cereb Cortex. doi:10.1093/cercor/bhu253

Hinds JW. 1968. Autoradiographic study of histogenesis in the mouse olfactory bulb. I. Time of origin of neurons and neuroglia. J Comp Neurol 134:287-304.

Holmfeldt P, Pardieck J, Saulsberry AC, Nandakumar SK, Finkelstein D, Gray JT, Persons DA, McKinney-Freeman S. 2013. Nfix is a novel regulator of murine hematopoietic stem and progenitor cell survival. Blood 122:2987-2996.

Holmfeldt P, Pardieck J, Saulsberry AC, Nandakumar SK, Finkelstein D, Gray JT, Persons DA, McKinney-Freeman S. 2013. Nfix is a novel regulator of murine hematopoietic stem and progenitor cell survival. Blood 122:2987-2996.

Hsu YC, Osinski J, Campbell CE, Litwack ED, Wang D, Liu S, Bachurski CJ, Gronostajski RM. 2011. Mesenchymal nuclear factor I B regulates cell proliferation and epithelial differentiation during lung maturation. Dev Biol 354:242-252.

Huang da W, Sherman BT, Lempicki RA. 2009. Systematic and integrative analysis of large gene lists using DAVID bioinformatics resources. Nat Protoc 4:44-57.

Huttner WB, Brand M. 1997. Asymmetric division and polarity of neuroepithelial cells. Curr Opin Neurobiol 7:29-39.

Ihrie RA, Alvarez-Buylla A. 2011. Lake-front property: a unique germinal niche by the lateral ventricles of the adult brain. Neuron 70:674-686.

Imayoshi I, Sakamoto M, Yamaguchi M, Mori K, Kageyama R. 2010. Essential roles of Notch signaling in maintenance of neural stem cells in developing and adult brains. J Neurosci 30:3489-3498.

Inoue T, Tamura T, Furuichi T, Mikoshiba K. 1990. Isolation of complementary DNAs encoding a cerebellum-enriched nuclear factor I family that activates transcription from the mouse myelin basic protein promoter. J Biol Chem 265:19065-19070.

Jhaveri DJ, Mackay EW, Hamlin AS, Marathe SV, Nandam LS, Vaidya VA, Bartlett PF. 2010. Norepinephrine directly activates adult hippocampal precursors via beta3-adrenergic receptors. J Neurosci 30:2795-2806.

Kageyama R, Imayoshi I, Sakamoto M. 2012. The role of neurogenesis in olfaction-dependent behaviors. Behav Brain Res 227:459-463.

Kageyama R, Ohtsuka T, Hatakeyama J, Ohsawa R. 2005. Roles of bHLH genes in neural stem cell differentiation. Exp Cell Res 306:343-348.

Kageyama R, Ohtsuka T, Kobayashi T. 2007. The Hes gene family: repressors and oscillators that orchestrate embryogenesis. Development 134:1243-1251.

Kang P, Lee HK, Glasgow SM, Finley M, Donti T, Gaber ZB, Graham BH, Foster AE, Novitch BG, Gronostajski RM, Deneen B. 2012. Sox9 and NFIA coordinate a transcriptional regulatory cascade during the initiation of gliogenesis. Neuron 74:79-94.

Kempermann G, Jessberger S, Steiner B, Kronenberg G. 2004. Milestones of neuronal development in the adult hippocampus. Trends Neurosci 27:447-452.

Kent J, Wheatley SC, Andrews JE, Sinclair AH, Koopman P. 1996. A male-specific role for SOX9 in vertebrate sex determination. Development 122:2813-2822.

Kilpatrick DL, Wang W, Gronostajski R, Litwack ED. 2012. Nuclear factor I and cerebellar granule neuron development: an intrinsic-extrinsic interplay. Cerebellum 11:41-49.

Kiyokage E, Pan YZ, Shao Z, Kobayashi K, Szabo G, Yanagawa Y, Obata K, Okano H, Toida K, Puche AC, Shipley MT. 2010. Molecular identity of periglomerular and short axon cells. J Neurosci 30:1185-1196.

Kriegstein A, Alvarez-Buylla A. 2009. The glial nature of embryonic and adult neural stem cells. Annu Rev Neurosci 32:149-184.

Kriegstein AR, Noctor SC. 2004. Patterns of neuronal migration in the embryonic cortex. Trends Neurosci 27:392-399.

Kruse U, Qian F, Sippel AE. 1991. Identification of a fourth nuclear factor I gene in chicken by cDNA cloning: NFI-X. Nucleic Acids Res 19:6641.

Kruse U, Sippel AE. 1994. Transcription factor nuclear factor I proteins form stable homo- and heterodimers. FEBS Lett 348:46-50.

Kumar DU, Nagaraj R, Devaraj H. 2012. Immunolocalization of Notch1, Hes1, and Nf-Kb in the Murine Hippocampal Subgranular Zone (SGZ): Possible Role of the Notch Pathway in the Maintenance of the SGZ Neural Stem Cell Population. Neurophysiology 44:208-215.

Kumbasar A, Plachez C, Gronostajski RM, Richards LJ, Litwack ED. 2009. Absence of the transcription factor Nfib delays the formation of the basilar pontine and other mossy fiber nuclei. J Comp Neurol 513:98-112.

Law AK, Pencea V, Buck CR, Luskin MB. 1999. Neurogenesis and neuronal migration in the neonatal rat forebrain anterior subventricular zone do not require GFAP-positive astrocytes. Dev Biol 216:622-634.

Lemaire V, Tronel S, Montaron MF, Fabre A, Dugast E, Abrous DN. 2012. Long-lasting plasticity of hippocampal adult-born neurons. J Neurosci 32:3101-3108.

Lennington JB, Yang Z, Conover JC. 2003. Neural stem cells and the regulation of adult neurogenesis. Reprod Biol Endocrinol 1:99.

Leo JM, Devine AH, Brunjes PC. 2000. Focal denervation alters cellular phenotypes and survival in the developing rat olfactory bulb. J Comp Neurol 417:325-336.

Li G, Fang L, Fernandez G, Pleasure SJ. 2013. The ventral hippocampus is the embryonic origin for adult neural stem cells in the dentate gyrus. Neuron 78:658-672.

Li G, Pleasure SJ. 2005. Morphogenesis of the dentate gyrus: what we are learning from mouse mutants. Dev Neurosci 27:93-99.

Lindberg OR, Persson A, Brederlau A, Shabro A, Kuhn HG. 2012. EGF-induced expansion of migratory cells in the rostral migratory stream. PLoS One 7:e46380.

Liu Y, Bernard HU, Apt D. 1997. NFI-B3, a novel transcriptional repressor of the nuclear factor I family, is generated by alternative RNA processing. J Biol Chem 272:10739-10745.

Lu W, Quintero-Rivera F, Fan Y, Alkuraya FS, Donovan DJ, Xi Q, Turbe-Doan A, Li QG, Campbell CG, Shanske AL, Sherr EH, Ahmad A, Peters R, Rilliet B, Parvex P, Bassuk AG, Harris DJ, Ferguson H, Kelly C, Walsh CA, Gronostajski RM, Devriendt K, Higgins A, Ligon AH, Quade BJ, Morton CC, Gusella JF, Maas RL. 2007. NFIA haploinsufficiency is associated with a CNS malformation syndrome and urinary tract defects. PLoS Genet 3:e80.

Liu Y, Bernard HU, Apt D. 1997. NFI-B3, a novel transcriptional repressor of the nuclear factor I family, is generated by alternative RNA processing. J Biol Chem 272:10739-10745.

Lu W, Quintero-Rivera F, Fan Y, Alkuraya FS, Donovan DJ, Xi Q, Turbe-Doan A, Li QG, Campbell CG, Shanske AL, Sherr EH, Ahmad A, Peters R, Rilliet B, Parvex P, Bassuk AG, Harris DJ, Ferguson H, Kelly C, Walsh CA, Gronostajski RM, Devriendt K, Higgins A, Ligon AH, Quade BJ, Morton CC, Gusella JF, Maas RL. 2007. NFIA haploinsufficiency is associated with a CNS malformation syndrome and urinary tract defects. PLoS Genet 3:e80.

Luskin MB. 1993. Restricted proliferation and migration of postnatally generated neurons derived from the forebrain subventricular zone. Neuron 11:173-189.

Luskin MB. 1998. Neuroblasts of the postnatal mammalian forebrain: their phenotype and fate. J Neurobiol 36:221-233.

Ma DK, Marchetto MC, Guo JU, Ming GL, Gage FH, Song H. 2010. Epigenetic choreographers of neurogenesis in the adult mammalian brain. Nat Neurosci 13:1338-1344.

Malan V, Rajan D, Thomas S, Shaw AC, Louis Dit Picard H, Layet V, Till M, van Haeringen A, Mortier G, Nampoothiri S, Puseljic S, Legeai-Mallet L, Carter NP, Vekemans M, Munnich A, Hennekam RC, Colleaux L, Cormier-Daire V. 2010. Distinct effects of allelic NFIX mutations on nonsense-mediated mRNA decay engender either a Sotos-like or a Marshall-Smith syndrome. Am J Hum Genet 87:189-198.

Martynoga B, Mateo JL, Zhou B, Andersen J, Achimastou A, Urban N, van den Berg D, Georgopoulou D, Hadjur S, Wittbrodt J, Ettwiller L, Piper M, Gronostajski RM, Guillemot F. 2013. Epigenomic enhancer annotation reveals a key role for NFIX in neural stem cell quiescence. Genes Dev 27:1769-1786.

Mason S, Piper M, Gronostajski RM, Richards LJ. 2009. Nuclear factor one transcription factors in CNS development. Mol Neurobiol 39:10-23.

Mattar P, Britz O, Johannes C, Nieto M, Ma L, Rebeyka A, Klenin N, Polleux F, Guillemot F, Schuurmans C. 2004. A screen for downstream effectors of Neurogenin2 in the embryonic neocortex. Dev Biol 273:373-389.

Meisterernst M, Gander I, Rogge L, Winnacker EL. 1988. A quantitative analysis of nuclear factor I/DNA interactions. Nucleic Acids Res 16:4419-4435.

Merkle FT, Tramontin AD, Garcia-Verdugo JM, Alvarez-Buylla A. 2004. Radial glia give rise to adult neural stem cells in the subventricular zone. Proc Natl Acad Sci U S A 101:17528-17532.

Messina G, Biressi S, Monteverde S, Magli A, Cassano M, Perani L, Roncaglia E, Tagliafico E, Starnes L, Campbell CE, Grossi M, Goldhamer DJ, Gronostajski RM, Cossu G. 2010. Nfix regulates fetal-specific transcription in developing skeletal muscle. Cell 140:554-566.

Ming GL, Song H. 2005. Adult neurogenesis in the mammalian central nervous system. Annu Rev Neurosci 28:223-250.

Ming GL, Song H. 2011. Adult neurogenesis in the mammalian brain: significant answers and significant questions. Neuron 70:687-702.

Miura M, Tamura T, Mikoshiba K. 1990. Cell-specific expression of the mouse glial fibrillary acidic protein gene: identification of the cis- and trans-acting promoter elements for astrocyte-specific expression. J Neurochem 55:1180-1188.

Mu Y, Lee SW, Gage FH. 2010. Signaling in adult neurogenesis. Curr Opin Neurobiol 20:416-423.

Murtagh J, Martin F, Gronostajski RM. 2003. The Nuclear Factor I (NFI) gene family in mammary gland development and function. J Mammary Gland Biol Neoplasia 8:241-254.

Nagata K, Guggenheimer RA, Enomoto T, Lichy JH, Hurwitz J. 1982. Adenovirus DNA replication in vitro: identification of a host factor that stimulates synthesis of the preterminal protein-dCMP complex. Proc Natl Acad Sci U S A 79:6438-6442.

Nagata K, Guggenheimer RA, Hurwitz J. 1983. Specific binding of a cellular DNA replication protein to the origin of replication of adenovirus DNA. Proc Natl Acad Sci U S A 80:6177-6181.

Namihira M, Kohyama J, Semi K, Sanosaka T, Deneen B, Taga T, Nakashima K. 2009. Committed neuronal precursors confer astrocytic potential on residual neural precursor cells. Dev Cell 16:245-255.

Noctor SC, Martinez-Cerdeno V, Kriegstein AR. 2008. Distinct behaviors of neural stem and progenitor cells underlie cortical neurogenesis. J Comp Neurol 508:28-44.

O'Leary DD, Sahara S. 2008. Genetic regulation of arealization of the neocortex. Curr Opin Neurobiol 18:90-100.

O'Rourke NA. 1996. Neuronal chain gangs: homotypic contacts support migration into the olfactory bulb. Neuron 16:1061-1064.

Ohtsuka T, Ishibashi M, Gradwohl G, Nakanishi S, Guillemot F, Kageyama R. 1999. Hes1 and Hes5 as notch effectors in mammalian neuronal differentiation. EMBO J 18:2196-2207.

Ohtsuka T, Sakamoto M, Guillemot F, Kageyama R. 2001. Roles of the basic helix-loop-helix genes Hes1 and Hes5 in expansion of neural stem cells of the developing brain. J Biol Chem 276:30467-30474.

Palma V, Lim DA, Dahmane N, Sanchez P, Brionne TC, Herzberg CD, Gitton Y, Carleton A, Alvarez-Buylla A, Ruiz i Altaba A. 2005. Sonic hedgehog controls stem cell behavior in the postnatal and adult brain. Development 132:335-344.

Park JC, Herr Y, Kim HJ, Gronostajski RM, Cho MI. 2007. Nfic gene disruption inhibits differentiation of odontoblasts responsible for root formation and results in formation of short and abnormal roots in mice. J Periodontol 78:1795-1802.

Parrish-Aungst S, Shipley MT, Erdelyi F, Szabo G, Puche AC. 2007. Quantitative analysis of neuronal diversity in the mouse olfactory bulb. J Comp Neurol 501:825-836.

Peretto P, Giachino C, Aimar P, Fasolo A, Bonfanti L. 2005. Chain formation and glial tube assembly in the shift from neonatal to adult subventricular zone of the rodent forebrain. J Comp Neurol 487:407-427.

Peretto P, Merighi A, Fasolo A, Bonfanti L. 1997. Glial tubes in the rostral migratory stream of the adult rat. Brain Res Bull 42:9-21.

Peretto P, Merighi A, Fasolo A, Bonfanti L. 1999. The subependymal layer in rodents: a site of structural plasticity and cell migration in the adult mammalian brain. Brain Res Bull 49:221-243.

Piper M, Barry G, Harvey TJ, McLeay R, Smith AG, Harris L, Mason S, Stringer BW, Day BW, Wray NR, Gronostajski RM, Bailey TL, Boyd AW, Richards LJ. 2014. NFIB-mediated repression of the epigenetic factor Ezh2 regulates cortical development. J Neurosci 34:2921-2930.

Piper M, Barry G, Hawkins J, Mason S, Lindwall C, Little E, Sarkar A, Smith AG, Moldrich RX, Boyle GM, Tole S, Gronostajski RM, Bailey TL, Richards LJ. 2010. NFIA

controls telencephalic progenitor cell differentiation through repression of the Notch effector Hes1. J Neurosci 30:9127-9139.

Piper M, Harris L, Barry G, Heng YH, Plachez C, Gronostajski RM, Richards LJ. 2011. Nuclear factor one X regulates the development of multiple cellular populations in the postnatal cerebellum. J Comp Neurol 519:3532-3548.

Piper M, Moldrich RX, Lindwall C, Little E, Barry G, Mason S, Sunn N, Kurniawan ND, Gronostajski RM, Richards LJ. 2009. Multiple non-cell-autonomous defects underlie neocortical callosal dysgenesis in Nfib-deficient mice. Neural Dev 4:43.

Piper M, Plachez C, Zalucki O, Fothergill T, Goudreau G, Erzurumlu R, Gu C, Richards LJ. 2009. Neuropilin 1-Sema signaling regulates crossing of cingulate pioneering axons during development of the corpus callosum. Cereb Cortex 19 Suppl 1:i11-21.

Pjanic M, Pjanic P, Schmid C, Ambrosini G, Gaussin A, Plasari G, Mazza C, Bucher P, Mermod N. 2011. Nuclear factor I revealed as family of promoter binding transcription activators. BMC Genomics 12:181.

Plachez C, Cato K, McLeay RC, Heng YH, Bailey TL, Gronostasjki RM, Richards LJ, Puche AC, Piper M. 2012. Expression of nuclear factor one A and -B in the olfactory bulb. J Comp Neurol 520:3135-3149.

Plachez C, Lindwall C, Sunn N, Piper M, Moldrich RX, Campbell CE, Osinski JM, Gronostajski RM, Richards LJ. 2008. Nuclear factor I gene expression in the developing forebrain. J Comp Neurol 508:385-401.

Priolo M, Grosso E, Mammi C, Labate C, Naretto VG, Vacalebre C, Caridi P, Lagana C. 2012. A peculiar mutation in the DNA-binding/dimerization domain of NFIX causes Sotos-like overgrowth syndrome: a new case. Gene 511:103-105.

Quinones-Hinojosa A, Sanai N, Soriano-Navarro M, Gonzalez-Perez O, Mirzadeh Z, Gil-Perotin S, Romero-Rodriguez R, Berger MS, Garcia-Verdugo JM, Alvarez-Buylla A. 2006. Cellular composition and cytoarchitecture of the adult human subventricular zone: a niche of neural stem cells. J Comp Neurol 494:415-434.

Rakic P. 2007. The radial edifice of cortical architecture: from neuronal silhouettes to genetic engineering. Brain Res Rev 55:204-219.

Rupp RA, Kruse U, Multhaup G, Gobel U, Beyreuther K, Sippel AE. 1990. Chicken NFI/TGGCA proteins are encoded by at least three independent genes: NFI-A, NFI-B and NFI-C with homologues in mammalian genomes. Nucleic Acids Res 18:2607-2616.

Saha B, Ypsilanti AR, Boutin C, Cremer H, Chedotal A. 2012. Plexin-B2 regulates the proliferation and migration of neuroblasts in the postnatal and adult subventricular zone. J Neurosci 32:16892-16905.

Sakamoto M, Imayoshi I, Ohtsuka T, Yamaguchi M, Mori K, Kageyama R. 2011. Continuous neurogenesis in the adult forebrain is required for innate olfactory responses. Proc Natl Acad Sci U S A 108:8479-8484.

Santoro C, Mermod N, Andrews PC, Tjian R. 1988. A family of human CCAAT-box-binding proteins active in transcription and DNA replication: cloning and expression of multiple cDNAs. Nature 334:218-224.

Schmid CD, Bucher P. 2010. MER41 repeat sequences contain inducible STAT1 binding sites. PLoS One 5:e11425.

Shu T, Butz KG, Plachez C, Gronostajski RM, Richards LJ. 2003. Abnormal development of forebrain midline glia and commissural projections in Nfia knock-out mice. J Neurosci 23:203-212.

Singh J, Murata K, Itahana Y, Desprez PY. 2002. Constitutive expression of the Id-1 promoter in human metastatic breast cancer cells is linked with the loss of NF-1/Rb/HDAC-1 transcription repressor complex. Oncogene 21:1812-1822.

Singh SK, Bhardwaj R, Wilczynska KM, Dumur CI, Kordula T. 2011. A complex of nuclear factor I-X3 and STAT3 regulates astrocyte and glioma migration through the secreted glycoprotein YKL-40. J Biol Chem 286:39893-39903.

Steele-Perkins G, Butz KG, Lyons GE, Zeichner-David M, Kim HJ, Cho MI, Gronostajski RM. 2003. Essential role for NFI-C/CTF transcription-replication factor in tooth root development. Mol Cell Biol 23:1075-1084.

Steele-Perkins G, Plachez C, Butz KG, Yang G, Bachurski CJ, Kinsman SL, Litwack ED, Richards LJ, Gronostajski RM. 2005. The transcription factor gene Nfib is essential for both lung maturation and brain development. Mol Cell Biol 25:685-698.

Strausberg RL, Feingold EA, Grouse LH, Derge JG, Klausner RD, Collins FS, Wagner L, Shenmen CM, Schuler GD, Altschul SF, Zeeberg B, Buetow KH, Schaefer CF, Bhat NK, Hopkins RF, Jordan H, Moore T, Max SI, Wang J, Hsieh F, Diatchenko L, Marusina K, Farmer AA, Rubin GM, Hong L, Stapleton M, Soares MB, Bonaldo MF, Casavant TL, Scheetz TE, Brownstein MJ, Usdin TB, Toshiyuki S, Carninci P, Prange C, Raha SS, Loquellano NA, Peters GJ, Abramson RD, Mullahy SJ, Bosak SA, McEwan PJ, McKernan KJ, Malek JA, Gunaratne PH, Richards S, Worley KC, Hale S, Garcia AM, Gay LJ, Hulyk SW, Villalon DK, Muzny DM, Sodergren EJ, Lu X, Gibbs RA, Fahey J, Helton E, Ketteman M, Madan A, Rodrigues S, Sanchez A, Whiting M, Young AC, Shevchenko Y, Bouffard GG, Blakesley RW, Touchman JW, Green ED, Dickson MC, Rodriguez AC, Grimwood J, Schmutz J, Myers RM, Butterfield YS, Krzywinski MI, Skalska U, Smailus DE, Schnerch A, Schein JE, Jones SJ, Marra MA. 2002. Generation and initial analysis of more than 15,000 full-length human and mouse cDNA sequences. Proc Natl Acad Sci U S A 99:16899-16903.

Suh H, Consiglio A, Ray J, Sawai T, D'Amour KA, Gage FH. 2007. In vivo fate analysis reveals the multipotent and self-renewal capacities of Sox2+ neural stem cells in the adult hippocampus. Cell Stem Cell 1:515-528.

Takahashi T, Nowakowski RS, Caviness VS, Jr. 1994. Mode of cell proliferation in the developing mouse neocortex. Proc Natl Acad Sci U S A 91:375-379.

Tamamaki N, Yanagawa Y, Tomioka R, Miyazaki J, Obata K, Kaneko T. 2003. Green fluorescent protein expression and colocalization with calretinin, parvalbumin, and somatostatin in the GAD67-GFP knock-in mouse. J Comp Neurol 467:60-79.

Tamura T, Miura M, Ikenaka K, Mikoshiba K. 1988. Analysis of transcription control elements of the mouse myelin basic protein gene in HeLa cell extracts: demonstration of a strong NFI-binding motif in the upstream region. Nucleic Acids Res 16:11441-11459.

Tatsunori Seki KS, Jack M. Parent, Arturo Alvarez-Buylla. 2011. Neurogenesis in the Adult Brain I: Neurobiology: Springer.

Walker TL, Yasuda T, Adams DJ, Bartlett PF. 2007. The doublecortin-expressing population in the developing and adult brain contains multipotential precursors in addition to neuronal-lineage cells. J Neurosci 27:3734-3742.

Wang W, Crandall JE, Litwack ED, Gronostajski RM, Kilpatrick DL. 2010. Targets of the nuclear factor I regulon involved in early and late development of postmitotic cerebellar granule neurons. J Neurosci Res 88:258-265.

Wang W, Mullikin-Kilpatrick D, Crandall JE, Gronostajski RM, Litwack ED, Kilpatrick DL. 2007. Nuclear factor I coordinates multiple phases of cerebellar granule cell development via regulation of cell adhesion molecules. J Neurosci 27:6115-6127.

Wang W, Stock RE, Gronostajski RM, Wong YW, Schachner M, Kilpatrick DL. 2004. A role for nuclear factor I in the intrinsic control of cerebellar granule neuron gene expression. J Biol Chem 279:53491-53497.

Waterston RH, Lindblad-Toh K, Birney E, Rogers J, Abril JF, Agarwal P, Agarwala R, Ainscough R, Alexandersson M, An P, Antonarakis SE, Attwood J, Baertsch R, Bailey J, Barlow K, Beck S, Berry E, Birren B, Bloom T, Bork P, Botcherby M, Bray N, Brent MR, Brown DG, Brown SD, Bult C, Burton J, Butler J, Campbell RD, Carninci P, Cawley S, Chiaromonte F, Chinwalla AT, Church DM, Clamp M, Clee C, Collins FS, Cook LL, Copley RR, Coulson A, Couronne O, Cuff J, Curwen V, Cutts T, Daly M, David R, Davies J, Delehaunty KD, Deri J, Dermitzakis ET, Dewey C, Dickens NJ, Diekhans M, Dodge S, Dubchak I, Dunn DM, Eddy SR, Elnitski L, Emes RD, Eswara P, Eyras E, Felsenfeld A, Fewell GA, Flicek P, Foley K, Frankel WN, Fulton LA, Fulton RS, Furey TS, Gage D, Gibbs RA, Glusman G, Gnerre S, Goldman N, Goodstadt L, Grafham D, Graves TA, Green ED, Gregory S, Guigo R, Guyer M, Hardison RC, Haussler D, Hayashizaki Y, Hillier LW, Hinrichs A, Hlavina W, Holzer T, Hsu F, Hua A, Hubbard T, Hunt A, Jackson I, Jaffe DB, Johnson LS, Jones M, Jones TA, Joy A, Kamal M, Karlsson EK, Karolchik D, Kasprzyk A, Kawai J, Keibler E, Kells C, Kent WJ, Kirby A, Kolbe DL, Korf I, Kucherlapati RS, Kulbokas EJ, Kulp D, Landers T, Leger JP, Leonard S, Letunic I, Levine R, Li J, Li M, Lloyd C, Lucas S, Ma B, Maglott DR, Mardis ER, Matthews L, Mauceli E, Mayer JH, McCarthy M, McCombie WR, McLaren S, McLay K, McPherson JD, Meldrim J, Meredith B, Mesirov JP, Miller W, Miner TL, Mongin E, Montgomery KT, Morgan M, Mott R, Mullikin JC, Muzny DM, Nash WE, Nelson JO, Nhan MN, Nicol R, Ning Z, Nusbaum C, O'Connor MJ, Okazaki Y, Oliver K, Overton-Larty E, Pachter L, Parra G, Pepin KH, Peterson J, Pevzner P, Plumb R, Pohl CS, Poliakov A, Ponce TC, Ponting CP, Potter S, Quail M, Reymond A, Roe BA, Roskin KM, Rubin EM, Rust AG, Santos R, Sapojnikov V, Schultz B, Schultz J, Schwartz MS, Schwartz S, Scott C, Seaman S, Searle S, Sharpe T, Sheridan A, Shownkeen R, Sims S, Singer JB, Slater G, Smit A, Smith DR, Spencer B, Stabenau A, Stange-Thomann N, Sugnet C, Suyama M, Tesler G, Thompson J, Torrents D, Trevaskis E, Tromp J, Ucla C, Ureta-Vidal A, Vinson JP, Von Niederhausern AC, Wade CM, Wall M, Weber RJ, Weiss RB, Wendl MC, West AP, Wetterstrand K, Wheeler R, Whelan S, Wierzbowski J, Willey D, Williams S, Wilson RK, Winter E, Worley KC, Wyman D, Yang S, Yang SP, Zdobnov EM, Zody MC, Lander ES. 2002. Initial sequencing and comparative analysis of the mouse genome. Nature 420:520-562.

Whitman MC, Greer CA. 2009. Adult neurogenesis and the olfactory system. Prog Neurobiol 89:162-175.

Wilczynska KM, Singh SK, Adams B, Bryan L, Rao RR, Valerie K, Wright S, Griswold-Prenner I, Kordula T. 2009. Nuclear factor I isoforms regulate gene expression during the differentiation of human neural progenitors to astrocytes. Stem Cells 27:1173-1181.

Yoneda Y, Saitsu H, Touyama M, Makita Y, Miyamoto A, Hamada K, Kurotaki N, Tomita H, Nishiyama K, Tsurusaki Y, Doi H, Miyake N, Ogata K, Naritomi K, Matsumoto N. 2012. Missense mutations in the DNA-binding/dimerization domain of NFIX cause Sotos-like features. J Hum Genet 57:207-211.